The American Mineralogist

Journal of the Mineralogical Society of America

UNIVERSITY OF ILLINOIS
LIBRARY
JUL 7 1959
CHICAGO

VOL. 44 MAY–JUNE, 1959 Nos. 5 and 6

Contents

Stability relations of cinnabar and metacinnabar . . . . . Frank W. Dickson and George Tunell 471
Hydromuscovite with $2M_2$ structure . . . . . I. M. Threadgold 488
X-ray and electron diffraction data for sepiolite . . . . . G. W. Brindley 495
Erionite from Cenozoic tuffaceous sediments . . . . . Kenneth S. Deffeyes 501
Comparative study of ten monazites . . . . . Martin W. Molloy 510
Hellyerite, a new nickel carbonate from Tasmania . . . . . K. L. Williams, I. M. Threadgold and A. W. Hounslow 533
Kyanite-garnet gedritite near Orofino, Idaho . . . . . Anna Hietanen 539
Uvarovite garnet and South African jade from Transvaal . . . . . J. J. Frankel 565
Identification of oriented inclusions in pyroxene crystals . . . . . M. C. Bown and P. Gay 592
Perthite formed by reorganization of albite . . . . . Forbes Robertson 603
Re-examination of "struverite" from Malaya . . . . . B. H. Flinter 620
Ningyoite, a new uranous phosphate from Japan . . . . . T. Muto, R. Meyrowitz, A. M. Pommer and T. Murano 633
Notes and News: Chromian antigorite from Lancaster Co., Pennsylvania . . . . . J. J. Glass, A. C. Vlisidis and N. C. Pearre 651
  Magmatic differentiation at Amboy Crater, California . . Ronald B. Parker 656
  Olivine-spinel inversion in fayalite . . . . . A. E. Ringwood 659
  X-ray emission and flame photometer determination of the K_2O content of potash feldspars . . . . . Donald O. Emerson 661
  Unit cell of carminite . . . . . Abraham Rosenzweig and Joseph J. Finney 663
  Substitution of Fe^{3+} for Al^{3+} in synthetic spessartite . . . . . S. Geller and C. E. Miller 665
  Macro point counting . . . . . Frank J. Fitch 667
  The rhombic amphibole holmquistite . . . . . Nils Sundius 669
  Inequilibrium modification of the corundum structure Davis M. Lapham 670

(*Continued on Cover 2*)

EDITOR: LEWIS S. RAMSDELL

BOARD OF ASSOCIATE EDITORS:

ROBERT GARRELS
D. JEROME FISHER
GEORGE W. BRINDLEY
JOSEPH MURDOCH (1957–59)
GEORGE T. FAUST (1958–60)
ADOLF PABST (1959–61)

Published bi-monthly by the Society

(*Contents continued*)

Magnetite in microcrystalline quartz, Lancaster Co., Pennsylvania. . . . . Davis M. Lapham 672
Differential thermal analysis of evaporites. . . . O. C. Kopp and P. F. Kerr 674
Refinement of the crystal structure of dolomite. H. Steinfink and F. J. Sans 679
Occurrence of jordanite in the Otavi Mountains, S. W. Africa. N. L. Markham 682
The pyrite-marcasite relation. A. Pabst 685
Book Review. 691
New Mineral Names. 692

Mineralogical Society of America

ASSOCIATED WITH THE GEOLOGICAL SOCIETY OF AMERICA

President: Ralph E. Grim, University of Illinois, Urbana, Illinois.
Vice-President: Joseph Murdoch, University of California at Los Angeles, Los Angeles, California.
Secretary: C. S. Hurlbut, Jr., Harvard University, Cambridge 38, Massachusetts.
Treasurer: Marjorie Hooker, U. S. Geological Survey, Washington 25, D. C.
Editor: Lewis S. Ramsdell, University of Michigan, Ann Arbor, Michigan.
Councilors: Alfred O. Woodford, Pomona College, Claremont, California.
Samuel S. Goldich, University of Minnesota, Minneapolis 14, Minnesota.
Brian H. Mason, American Museum of Natural History, New York 24, New York.
Richard H. Jahns, California Institute of Technology, Pasadena, California.
Charles Milton, U. S. Geological Survey, Washington 25, D. C.
Wilfrid R. Foster, Ohio State University, Columbus 10, Ohio.
Edward W. Nuffield, University of Toronto, Toronto 5, Ontario, Canada.
George E. Goodspeed, University of Washington, Seattle 5, Washington.

The enlarged issues of this journal for 1959 are made possible by a grant from the Penrose Fund of the Geological Society of America.

The American Mineralogist—Journal of the Mineralogical Society of America

The journal, containing articles on mineralogy, crystallography, and allied sciences, is issued every two months. Contributions are invited.

The general conduct of the journal is in the hands of the editor, Lewis S. Ram dell, Department of Mineralogy, University of Michigan, to whom all manuscrip should be submitted. To assist the editor, the Council of the Society has appointe the following Board of Associate Editors:

Robert M. Garrels, Harvard University, Cambridge 38, Massachusetts.
Joseph Murdoch, University of California at Los Angeles, Los Angeles, California.
D. Jerome Fisher, University of Chicago, Chicago 37, Illinois.
George T. Faust, U. S. Geological Survey, Washington 25, D. C.
George W. Brindley, Pennsylvania State University, University Park, Pennsylvania.
A. Pabst, University of California, Berkeley 4, California.

Authors are requested to submit two copies of each manuscript, typewritten on standard size paper, 8½×11 inches. Photographs submitted for cuts should be glossy prints.

Authors are entitled to 50 free reprints, without covers, of each article published.

Sent to all members and fellows of the Mineralogical Society of America. Membership dues $4.00 annually, fellowship dues $5.00 annually, which includes receipt of the American Mineralogist and GeoTimes, which is published by the American Geological Institute. Subscriptions for libraries, colleges, institutions, companies and similar organizations $6.00 annually.

Entered as second class matter at the post office at Menasha, Wis., under Act of March 3, 1879. Acceptance for mailing at the special rate of postage provided for in section 1103, Act of Oct. 3, 1917, paragraph 4 section 429 P. L. & R. authorized March 13, 1922.

Notice of change of address, orders, and remittances should be sent to Marjorie Hooker, c/o U. S. Geological Survey, Washington 25, D. C.

Printed by the George Banta Company, Inc., Menasha, Wisconsin
Printed in the United States of America

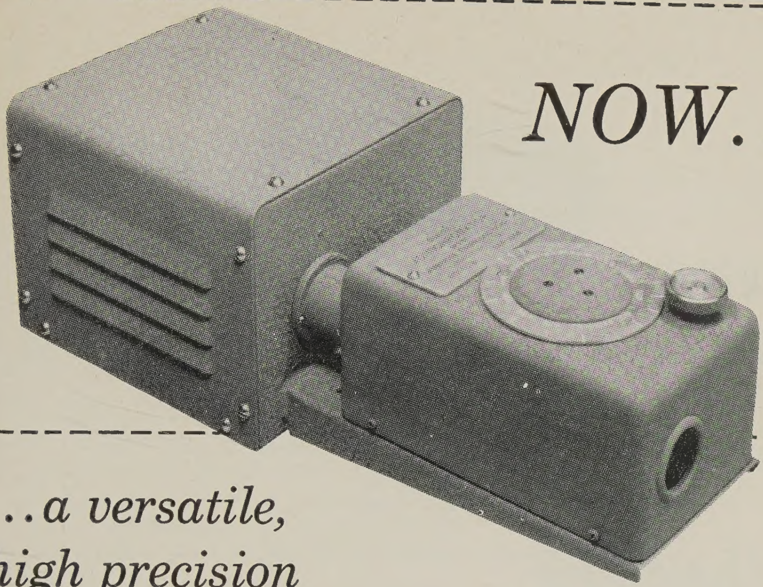

NOW...

...a versatile,
high precision

CAMBION® Monochromator with light source

- **Cold Intense 100 Watt Zirconium Arc Light**
- **Point Source — .08″ Diameter**
- **Convenient Circular Light Aperture**
- **Wide Range of Wavelengths — 4500A to 6400A**
- **Narrow Pass Band Width — 40A to 120A**

Iere's the ideal monochromator for op-
l crystallography determinations. Can be
d with both microscope and refractometer.
lizes the rotary dispersion of quartz to
vide a continuous selection of wave-
gths. Combines highest intensity light
rce with large aperture. Power source,
t, and lenses in compact, portable
t. Overall length 14″; height 5″;
th 6″. Crackle grey finish. Send
pon for complete details.

CAMBRIDGE THERMIONIC CORPORATION
CAMBION
The guaranteed electronic components

Cambridge Thermionic Corporation
503 Concord Avenue
Cambridge 38, Massachusetts

Please send complete details on
CAMBION Monochromator.

Name.........................

Title.........................

Address.........................

City........*Zone*....*State*.........

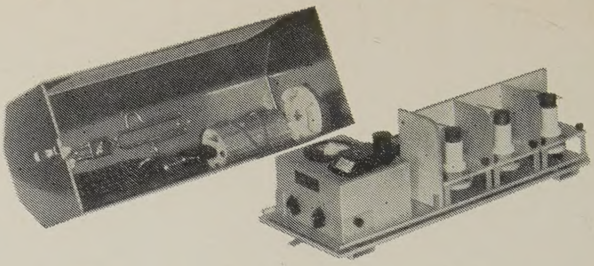

PORTABLE

DIFFERENTIAL THERMAL ANALYSIS APPARATUS

Certain mineralogical analyses can be performed on the apparatus which involves measuring and graphing the difference in temperature between the sample being examined and an inert substance as the two are heated rapidly. The temperature of the sample during a test is influenced by the reactions taking place. This portable apparatus operates from 115 volt A.C. or D.C. Request Bulletin 320 for complete information.

Eberbach
CORPORATION
P.O. Box 63 Ann Arbor, Michigan

MINERAL SPECIMENS

Large variety of crystals, crystal groups, rare minerals, and ore minerals for collectors, universities and museums.

Mineral Catalog 25¢, or sent free when requested on official letterhead.

Filer's are interested in buying or exchanging for good quality minerals, especially from foreign countries. Correspondence is invited.

FILER'S
P. O. Box 372, Redlands, California

Our Specialty is
SELECTED MINERAL SPECIMENS
FROM WORLD-WIDE LOCALITIES FOR COLLECTORS AND MUSEUMS
we also carry a complete line of
MINERALIGHTS, DETECTRON GEIGER COUNTERS, ESTWING PROSPECTOR PICKS, MINERALOGICAL BOOKS, ETC.
Send for free current bulletin
SCHORTMANN'S MINERALS
6 McKinley Avenue Easthampton, Massachusetts

For Mineralogists:

Index of Refraction Liquids

Range: 1.35 to 2.11 index; available in sets of limited range, or in sets with various intervals, or in any selection. Note that liquids 2.01 to 2.11 are now available.

See detailed price list of index liquids in our three-page advertisement in the July-August and September-October issues of the American Mineralogist. Or, write for Price List Nd-AM

Allen Reference Sets for Microscopical Studies in Mineralogy and Petrology

Six sets of Authentic materials for use as standards for refractive index, for standard materials mounted in balsam to be compared with unknowns, and for demonstration of typical optical characteristics under microscopical study.

Write for descriptive material A-AM

Text: Practical Refractometry by Means of the Microscope

By Roy M. Allen, D.Sc.

Describes the technique of the immersion method of microscopy, with particular reference to the identification of minerals. Written primarily for elementary instruction, but this text will be very useful also to advanced workers. Price $1.00. Copy will be sent on approval.

Heavy Liquids

Formulated especially for determination of specific gravity of minerals, but special formulations are being made to order for various procedures. If you have any special problem in this field of separation of minerals or other materials by differences in specific gravity, please write us about your problem. Or, just write for leaflet HL-AM.

Lovins Field Finder

For re-locating any point of interest on microscope slide. Same size as a 3″ x 1″ microscope slide; has 1012 1mm. squares, each square numbered and lettered, with sides graduated into tenths. A beautiful example of micro-photography.

Write for Leaflet LFF-AM

Gems, Testing For Identity and For Defects

The CARGILLE-ALLEN GEM TESTING SET is the title of our new book describing the properties of gems and also the equipment for certain identification of gems by a new simple procedure. Price $1.00; this amount applicable to purchase price of any of the items listed in the book.

R. P. Cargille Laboratories, Inc.
117 Liberty St., New York 6, N.Y.

Important McGraw-Hill Books

THE EARTH AND ITS GRAVITY FIELD

By W. A. HEISKANEN, Ohio State University; and F. A. VENING MEINESZ, University of Utrecht. *McGraw-Hill International Series in the Earth Sciences.* 470 pages, $12.50.

An advanced volume of great value to graduate students in geology, geophysics and related fields. It presents new conclusions of the earth's tendency towards equilibrium, and of the character and size of deviations from this equilibrium. The approach is entirely new, with the material based mainly on the authors' studies. Recent advances covered include the global significance of the pendulum apparatus of Vening Meinesz for gravity observations at sea.

MICROSCOPIC PETROGRAPHY

By E. WILLIAM HEINRICH. 292 pages, $6.50.

A complete treatment of the microscopic investigation of igneous, sedimentary and metamorphic rocks. All major types of rocks in each group are described, with emphasis on the employment of thin sections in their study. In addition, considerable material is provided on the interpretation of the genesis of the rocks based upon their mineralogies and textures. Here is all the up-to-date material in the field, including a discussion of the point counter in micrometric mineralogical analysis.

OPTICAL MINERALOGY

By PAUL F. KERR, Columbia University. New Third Edition. 442 pages, $8.50.

This book explains the use of the polarizing microscope in the study of transparent minerals. The optical properties of common minerals are given, and the optical principles are explained. Tables are provided to aid identification. The book is intended as a text for laboratory classes in optical mineralogy and as a useful reference book wherever the polarizing microscope is employed.

MINERALOGY: An Introduction to the Study of Minerals and Crystals

By EDWARD H. KRAUS, WALTER F. HUNT, and L. S. RAMSDELL, University of Michigan. New Fifth Edition. 686 pages, $9.00.

Here is a well-known college text used in geology departments and for reference by practicing geologists. It has always been popular for its extensive use of halftone cuts of crystal models to supplement the conventional line drawings of crystals which many students have difficulty in visualizing correctly. Photographs and short biographical sketches of distinguished mineralogists are another feature of this book.

Send for copies on approval

McGRAW-HILL BOOK COMPANY, INC.
330 WEST 42ND STREET, NEW YORK 18, N. Y.

WILEY • BOOKS

Employs the vector approach
in the solution of the phase problem

VECTOR SPACE

and its application in crystal-structure investigation

By MARTIN J. BUERGER, *Massachusetts Institute of Technology.*

Opens up the whole field of vector space . . .

The successful solution of Patterson syntheses for the approximate electron densities of crystals has, among other developments in the field, provided a significant break-through in the investigation of crystal-structures. Reviewing this progress, Buerger reports fully on the increased importance of using vector space as a relatively easy solution of the phase problem normally encountered in the study of the arrangement of atoms in crystals. Whereas the subject is described only briefly in general works on crystal-structure analysis or in widely scattered literature, this book is unique in that it deals exclusively with the theory of vector space and its application in crystallography.

Suitable for both academic and professional use . . .

Chapters containing the theory of vector space are self-contained and require no special technical or mathematical background. Crystallographers, mineralogists, physicists, chemists, and metallurgists interested in investigations of crystal-structure will find this book a valuable addition to their reference library. Graduate and undergraduate students can utilize it as an authoritative reference on vector space and its applications.

1959 **347 pages** **$12.00**

Send for an examination copy.

JOHN WILEY & SONS, Inc.
440 Fourth Avenue **New York 16, N.Y.**

MINERAL SPECIMENS *For Sale or Exchange*
MICROSCOPES BOOKS · GEOLOGICAL SUPPLIES
Catalog on request

SCOTT J. WILLIAMS
Mineralogist

2346 S. SCOTTSDALE ROAD · SCOTTSDALE, ARIZONA, U.S.A.

d. m. organist
PETROGRAPHIC LABORATORY
BOX 176 • NEWARK, DELAWARE

THIN SECTIONS OF
ROCKS, MINERALS, ORES, CERAMICS
PREPARED ROCK SECTIONS FOR STUDENT USE
GRAIN COUNTS • PETROGRAPHIC ANALYSIS

MINERALOGICAL SOCIETY OF AMERICA MEMBERSHIP INFORMATION

Membership: Membership in The Mineralogical Society of America is open to persons interested in the fields of mineralogy, petrography, crystallography and allied sciences. Prospective members should obtain an application blank from the Treasurer. Upon the return of the blank to the Treasurer, properly filled out and accompanied by a remittance of $4.00 for annual dues, his name will be added to the mailing and membership list. Membership includes receipt of the Society's journal, *The American Mineralogist.* Membership is effective as of January of each year and members receive all numbers of the journal for the year. Dues may be remitted directly to the Treasurer or through an agent, payable to The Mineralogical Society of America. No discount is allowed agents on membership dues. Memberships are personal and may not be held in order to obtain the lower rate for the journal for organization use.

MINERALOGICAL SOCIETY OF AMERICA
Marjorie Hooker, Treasurer
c/o U. S. Geological Survey, Washington 25, D.C.

THE AMERICAN MINERALOGIST
JOURNAL OF THE MINERALOGICAL SOCIETY OF AMERICA

Vol. 44 MAY–JUNE, 1959 Nos. 5 and 6

THE STABILITY RELATIONS OF CINNABAR AND METACINNABAR*

FRANK W. DICKSON AND GEORGE TUNELL, *University of California, Riverside and Los Angeles, California.*

ABSTRACT

The stability relations of cinnabar and metacinnabar have not been well understood. Metacinnabar, or black HgS, has been supposed to occur in nature as a metastable substance found in weathered portions of mercury ore deposits. Cinnabar, or red HgS, was considered to be the only stable modification of HgS. However, the results of the present study indicate that pure red HgS, cinnabar, inverts to black HgS, metacinnabar, at 344° C., at one atmosphere pressure. The inversion is comparatively rapid and is reversible for pure HgS. The presence of small amounts of iron, zinc, or selenium in the metacinnabar structure retards the inversion of metacinnabar to cinnabar at temperatures at which cinnabar is stable. In addition, the presence of iron or zinc in the metacinnabar depresses the inversion temperature: iron, to as low as 305° C.; and zinc, to as low as 240° C.

Studies of ores and protores containing both cinnabar and metacinnabar show that in general metacinnabar was deposited earlier than cinnabar. Metacinnabar does not appear to be an alteration product of cinnabar, but some cinnabar is the product of the inversion of metacinnabar. Conclusions from study of ores and protores are consistent with conclusions from the laboratory study of equilibrium relations of cinnabar and metacinnabar.

INTRODUCTION

The relationship of cinnabar, red HgS, to metacinnabar, black HgS, has been inadequately studied and has been poorly understood. Moore, who first described metacinnabar in 1872 (6), recognized that the metacinnabar in the specimens he studied had been deposited earlier than associated cinnabar, but he thought that metacinnabar was amorphous. Penfield first demonstrated that metacinnabar is crystalline and correctly assigned it to the sphalerite group (8, p. 452–453). Lindgren (5, p. 463) regarded metacinnabar as a supergene mineral found principally in altered mercury ore deposits. Lindgren's opinion was widely accepted, although later workers have observed that some metacinnabar is earlier than accompanying cinnabar (Ross, 10, p. 51; Bailey and Phoenix, 2, p. 137; and Eckel and Myers, 3, p. 97–98). Studies by the present authors indicate that metacinnabar is a hypogene mineral which in most instances was deposited earlier than associated cinnabar.

---

* Publication No. 101, Institute of Geophysics, University of California, Los Angeles 24, California.

Previous Experimental Work

Allen, Crenshaw, and Merwin (1) studied aspects of the chemical and thermal behavior of HgS, with the aim of determining the conditions under which cinnabar and metacinnabar are formed. Red HgS and black HgS were heated in evacuated vessels in the presence of substances such as ammonium sulfide and sulfuric acid, at temperatures ranging from 100° C. to 570° C., for times varying from one-half day to five days. After cooling the samples were examined under the microscope for evidences of inversion. Red HgS was reported to be unchanged, but black HgS was either partially or completely altered to red HgS. Allen, Crenshaw, and Merwin concluded that red HgS was stable at all temperatures up to 570° C. and that metacinnabar was not stable under any of the conditions of their experiments. They found the thermal behavior of HgS to be rather confusing, however. They reported that HgS, initially red, heated to 445° C. appeared black to the naked eye, but after the samples were ground fine and examined under the microscope they were seen to be made up mostly of cinnabar. The black color of the unground samples was apparently caused by a thin layer of metacinnabar on the cinnabar particles. No satisfactory explanation was presented for the appearance of black HgS, which had formed from red HgS in contradiction to their conclusion that red HgS was the stable phase at 445° C. The suggestion was offered that black HgS deposited from the vapor in the container when the container and contents were quenched.

The equilibrium pressures of the reaction $n\text{HgS}_{(\text{solid})} \rightarrow n\text{Hg}_{(\text{gas})} + \text{S}_{n(\text{gas})}$ were measured by Rinse at temperatures ranging from 331° C. to 651° C. (9, p. 28–32). HgS samples were heated in a sealed glass instrument, one end of which was a hollow glass spring which coiled or uncoiled in response to unbalanced pressure between the interior and exterior of the instrument. The internal pressure was estimated by measuring the external pressure required to bring the spring to a zero position. Table 1 presents Rinse's data.

Rinse noted that red HgS became black when heated above 400° C., and he showed that the HgS had acquired the specific gravity of metacinnabar. By the use of an undescribed method of plotting his data, he deduced that red HgS inverts to black HgS at $386 \pm 2°$ C. However, Rinse mentioned that HgS heated for three days at 347° C. became black and possessed a specific gravity intermediate between cinnabar and metacinnabar. He applied the theory of allotropy as expounded by Smits (11) to explain the appearance of metacinnabar below the supposed inversion

TABLE 1. RINSE'S VALUES FOR THE DISSOCIATION PRESSURES OF THE REACTION $n\mathrm{HgS}_{(\mathrm{solid})} \rightarrow n\mathrm{Hg}_{(\mathrm{gas})} + \mathrm{S}_{n(\mathrm{gas})}$ AS A FUNCTION OF TEMPERATURE

Red HgS		Black HgS			
Temp. in ° C.	Pressure in mm. Hg	Temp. in ° C.	Pressure in mm. Hg	Temp. in ° C.	Pressure in mm. Hg
333	1.1	331.5	1.45	440	34.0
345.5	1.95	351	2.7	447.5	40.7
351	2.1	357	3.35	457.5	53.0
356	2.8	359.5	3.7	472	73.8
360	3.1	365	4.2	479.5	86.4
362	3.3	373	5.35	491	115.3
371.5	4.7	378	6.4	501.5	147
378.5	5.95	383	7.4	521	221.5
		392.5	9.6	540	340
		395	10.55	564	526
		400	12.0	582	740
		409.5	15.4	599	983
		422.5	22.35	633	1766
		429	25.75	651	2385

temperature. From thermodynamical considerations, however, it appears most unlikely that metacinnabar could form from cinnabar as a result of a reaction in the solid state below the true inversion temperature. Therefore, Rinse's determination of the inversion temperature seems to be in error. Furthermore, inspection of his data, plotted in Fig. 1 as pressure versus temperature, shows no well defined intersection of the curve for cinnabar with the curve for metacinnabar. His measurements are not sufficiently reliable to permit an exact determination of the inversion temperature.

Treadwell and Schaufelberger (12, p. 1938) estimated the inversion temperature to be 400° C. by heating red HgS in capillary glass tubes for several hours at controlled temperatures. They noted that cinnabar heated at 375° to 385° C. became black, but x-ray examination revealed only a trace of metacinnabar. Treadwell and Schaufelberger theorized that the metacinnabar had deposited from the vapor phase during the quenching of the sample. They demonstrated the slowness of the inversion of metacinnabar to cinnabar under the stability conditions of cinnabar. For example, black HgS heated at 250° to 300° C. for 30 hours was only partially transformed to cinnabar.

Professor W. S. Fyfe, of the Department of Geology, University of California, Berkeley, California, noted that red HgS transformed to black HgS at 290° C. and 80 bars water pressure (oral communication).

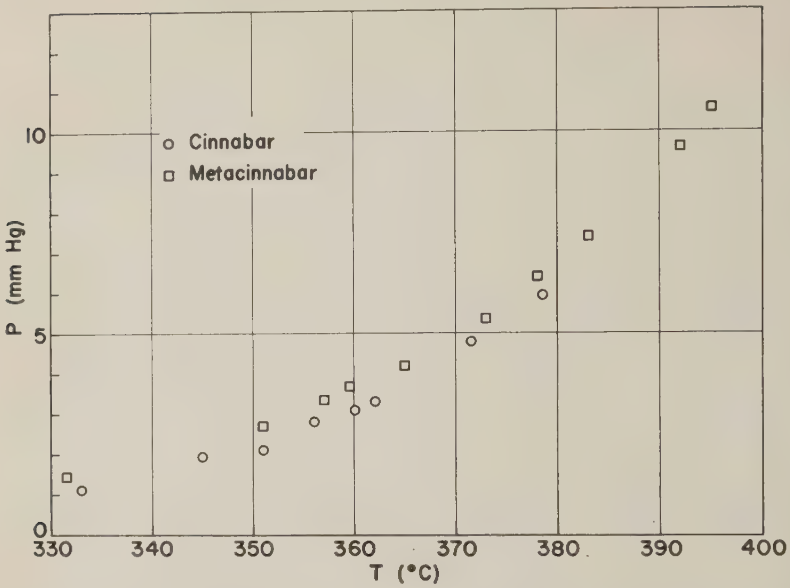

FIG. 1. A plot of a portion of Rinse's temperature-pressure determinations for the reactions $n\mathrm{HgS}_{(\mathrm{red})} \rightarrow n\mathrm{Hg}_{(\mathrm{gas})} + \mathrm{S}_{n(\mathrm{gas})}$ and $n\mathrm{HgS}_{(\mathrm{black})} \rightarrow n\mathrm{Hg}_{(\mathrm{gas})} + \mathrm{S}_{n(\mathrm{gas})}$.

However, Fyfe's experiments were carried out with natural cinnabar, which may have been impure, and he used steel containers to hold the experimental mixtures. Both of these factors may have had an effect on the inversion temperature (see p. 480–481, this paper).

PRESENT EXPERIMENTAL WORK

The solubilities of black HgS and red HgS in Na_2S solutions were determined by the authors at 25° C., 50° C., and 75° C. at one atmosphere pressure (3, p. 18). The solubility of black HgS, though greater than that of red HgS at all three temperatures, decreases more rapidly with increasing temperature than the solubility of red HgS (Fig. 2). Extrapolating the data to higher temperatures shows that at some temperature above those examined by us, the solubilities of the two forms can be expected to become equal. Inasmuch as the two forms would then be capable of coexisting in stable equilibrium in contact with the same solution at one temperature, that temperature would be the inversion temperature. The inversion temperature could not be determined accurately from the solubility data, however, because the angle of intersection of the extrapolated curves is small and small experimental errors greatly affect the location of the intersection.

The inversion temperature was therefore measured by more accurate

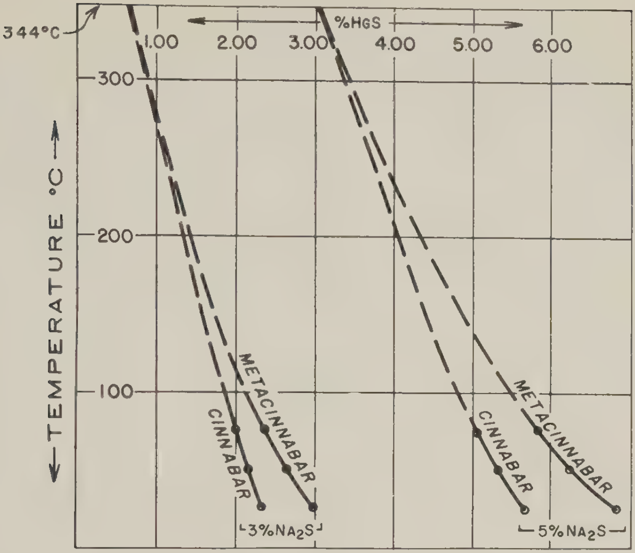

FIG. 2. The solubility of cinnabar (red HgS) and metacinnabar (black HgS) in 3% and 5% sodium sulfide solutions at 25° C., 50° C., and 75° C. as determined by Dickson and Tunell. Solid lines connect experimentally determined points, and broken lines represent curves extrapolated to intersect at the inversion temperature, 344° C.

direct methods. The first method involved heating Baker and Adamson reagent grade red HgS in a series of sealed evacuated glass tubes at controlled temperatures ranging from 320° C. to 380° C., each for a period of one week. The cooled samples were examined by the *x*-ray spectrometer to detect the presence of metacinnabar. The inversion temperature determined in this way is 344° C. ± 4° C. Attempts were made to measure the inversion temperature by heating black HgS, but the transformation of black HgS synthesized in the laboratory to red HgS proved to be so sluggish that runs of excessive duration would have been required to effect the inversion. For example, only a small part, perhaps 5%, of black HgS heated for three weeks at 330° C. was converted to red HgS.

A second method of determining the inversion temperature involved the use of a temperature gradient furnace designed by Kennedy and Dickson for the purpose of studying dissociation pressures of metal sulfide reactions. A capillary glass tube was filled with red HgS and heated in such a manner that a temperature gradient of about ten degrees per inch existed along the tube. The furnace used to establish the temperature gradient is illustrated in Fig. 3. The alundum core of the furnace was wound with three platinum wire coils: a rear coil (not used in our experiments) to maintain a constant temperature zone; a middle coil to estab-

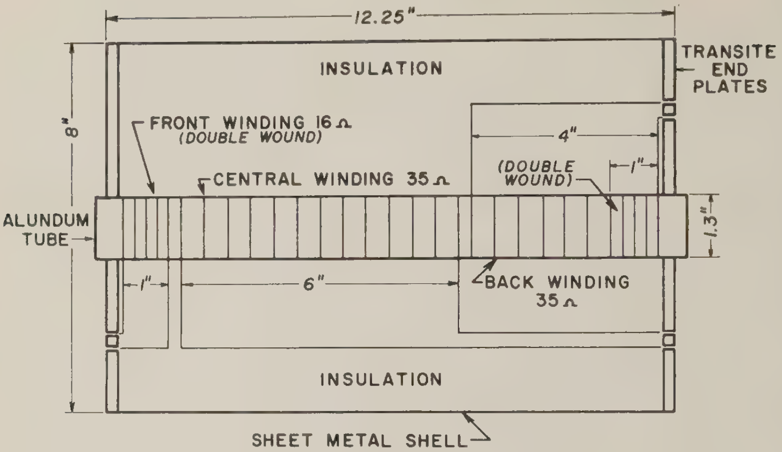

FIG. 3. Cross-section view of temperature-gradient furnace used to determine inversion temperatures. (Apparatus designed by Kennedy and Dickson.)

lish a temperature gradient over the central portion of the tube; and a front coil to allow manipulation of the temperature gradient. The power input to each of the coils was controlled by separate phase-shifting thyratron controllers. Inside the alundum core was a stainless steel tube (Fig. 4) which provided a thermal mass and smoothed the temperature distribution. Alumel-chromel thermocouples were precisely spaced at intervals along the steel tube, sunk in receptacles in holes in the steel which allowed placement of the thermocouples close to the glass tube. Temperatures along the steel tube could be adjusted by varying the power delivered to the separate heating coils.

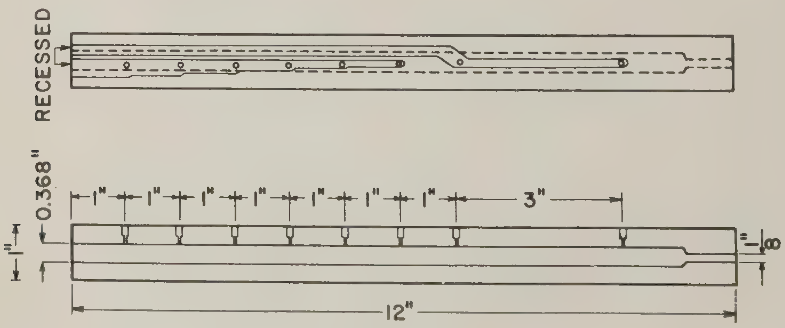

FIG. 4. Schematic diagram of stainless steel tube designed to fit in alundum tube of the temperature gradient furnace. Upper drawing is a plan view showing thermocouple wells and longitudinal grooves in which thermocouple leads were placed. Lower drawing is a cross-sectional view showing placement and shape of thermocouple wells.

The experimental procedure was to place a thick-walled capillary glass tube filled with red HgS in the stainless steel tube and to allow the glass to attain the temperature of the steel. The position of the boundary between unaltered red HgS and black HgS was observed at regular intervals of time. No migration of the boundary was observed after 24 hours of exposure to the temperature gradient, but to ensure complete reaction the capillary was left in the apparatus for four days. At the end of four days the capillary was withdrawn, air quenched, and the boundary between red and black HgS was located within one-tenth of an inch. The temperature which had existed at the boundary before removal of the capillary tube was obtained by thermocouple measurements of temperature made before the tube was withdrawn. An inversion temperature of 344° C. ± 2° C. was obtained in this way. The presence of metacinnabar in the darkened HgS was confirmed by *x*-ray examination.

Differential thermal analyses of red HgS, kindly carried out for us by Dr. J. F. Burst at the Shell Development Company, Houston, Texas, revealed that an endothermic reaction, presumably the inversion of red HgS to black HgS, was initiated at 355° C. and completed at 381° C. The differential thermal analyzer heats the sample rapidly, in this case at a rate of ten degrees Centigrade per minute. The inversion of red HgS to black HgS proceeds slowly at or near 344° C. and it is to be expected that the inversion temperature determined by such rapid heating would be higher than one obtained by slow heating.

Dr. R. A. Rowland, also of the Shell Development Company, Houston, Texas, measured for as atomic planar spacings of HgS at temperatures above 300° C. by use of the oscillating-heating *x*-ray diffractometer (13, p. 118–119). Temperatures were not measured accurately enough to permit a determination of the inversion temperature. However, Dr. Rowland confirmed the inversion of red HgS to black HgS at elevated temperatures, and further demonstrated that the crystalline phase actually existing at the elevated temperatures is metacinnabar.

That cinnabar inverts to metacinnabar on heating has therefore been experimentally well established. Why did such careful workers as Allen, Crenshaw, and Merwin fail to observe the inversion? The answer seems to be that black HgS produced by heating pure red HgS above 344° C. reverts rapidly to red HgS on cooling below 344° C. The actual process of reversion can be observed. Fine-grained HgS crystals, made by heating red HgS in a sealed evacuated glass tube at 350° C. were black when first cooled to room temperature, but on standing for about one-half hour changed to red. Grinding freshly-made black HgS appeared to accelerate the reversion to red HgS.

A further illustration of the reversion process was the behavior of freshly-made black HgS while being examined by the *x*-ray spectrometer. A diagnostic part of the 2θ region for cinnabar and metacinnabar (30° to 32°, copper Kα radiation) was scanned at two minute intervals and the peaks representing the diffracted *x*-ray beams were plotted on graph paper by means of a strip chart recorder (Fig. 5). The first scanning showed a metacinnabar peak and a cinnabar peak of about the same height; subsequent scannings showed progressively decreased heights of metacinnabar peaks and increased heights of cinnabar peaks. Peak heights are directly proportional to the amount of each phase in the sample and thus the ratio of the amount of cinnabar to the amount of metacinnabar increased with time. Presumably if the sample had been examined while still hot there would have been only a metacinnabar peak, as in the case of Dr. Rowland's experiment, but between the end of the heating process and the first scanning by the spectrometer there was about a 30 second delay owing to the time required to grind the sample and sediment it on a glass plate.

The fact that black HgS, formed by heating pure red HgS above 344° C., reverts rapidly to cinnabar on cooling probably explains why Allen, Crenshaw, and Merwin did not discover that cinnabar inverts to metacinnabar at high temperatures.

The rapidity with which pure black HgS reverts to red HgS on cooling in the laboratory raises another question: How is it possible for metacinnabar to persist at ordinary temperatures, as it does in nature, and in some cases in the laboratory? In an attempt to answer this question the effect of impurities in the system was investigated.

Analyses show that naturally occurring metacinnabar contains elements such as iron, zinc, and selenium, sometimes in major amounts. Table 2 presents analyses of metacinnabar taken from *Dana's System of Mineralogy, Seventh Edition* (7, p. 216); it is noteworthy that the specimens of metacinnabar contained in addition to mercury and sulfur at least one of the elements mentioned above and some contained two. Few reliable analyses of cinnabar have been reported in the literature, but several specimens analyzed by the writers contained less than 0.1% nonvolatile impurities. By contrast, homogeneous metacinnabar from the Mt. Diablo mine, California, contained 0.5% iron.

Samples of red HgS were heated in the presence of iron sulfide, zinc sulfide, and selenium, respectively. These substances acted to retard the reversion of metacinnabar to cinnabar; freshly formed metacinnabar made in this way did not revert to cinnabar, but remained unchanged after being kept for months at room temperature. The metacinnabar was only metastable, however, and could be converted to cinnabar by allowing it to stand in contact with sodium sulfide solutions.

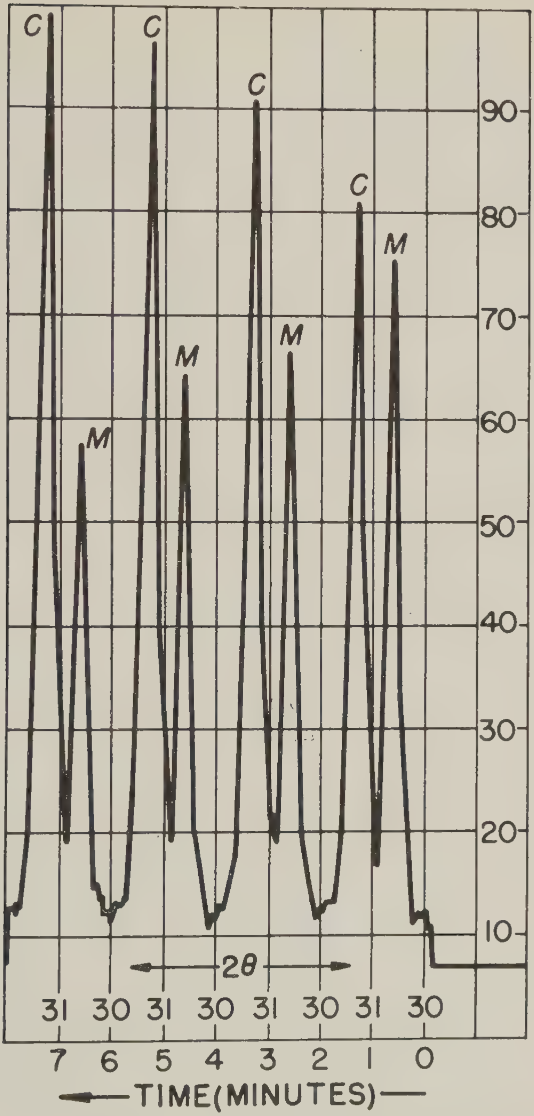

FIG. 5. X-ray spectrometer measurements of diffraction peaks of HgS heated previously above 344° C., the inversion temperature of red and black HgS. The 2θ region from 30° to 32° was scanned at two-minute intervals. Peaks labeled M represent the 2.92 Å spacing of black HgS, and peaks labeled C represent the 2.85 Å spacing of red HgS. The intensities of the diffracted beams are proportional to areas under the peaks, and are direct functions of the amounts of the phases present in the sample. Note the increase in the height of C and the decrease in the height of M with the passage of time. Cu Kα radiation was used.

Table 2. Analyses of Metacinnabar Listed in Dana's System of Mineralogy, 7th Edition, Page 216

	1	2	3	4	5	6
Weight % Hg	86.22	77.68	79.73	79.69	83.38	81.83
Weight % Fe		5.36	trace	1.04		
Weight % Zn			4.23	3.32	2.17	
Weight % Se			1.08			6.49
Weight % S	13.78	14.97	14.58	14.97	14.24	10.30
Rem.		1.41			0.52	
Total	100.00	99.42	99.62	99.02	100.31	98.12

1. Pure HgS.
2. Felsöbánya, Transylvania. Rem. is insoluble.
3. Guadalcazar, Mexico (guadalcazarite).
4. Pola de Lena, Spain.
5. Levigliani, Italy (leviglianite). Rem. is FeO.
6. San Onofre, Mexico (onofrite).

The amount of Fe or Zn needed to retard the reversion of metacinnabar was quite small, less than 0.3 per cent. Metacinnabar made by heating an intimately ground mixture of four parts of red HgS to one part of FeS_2 at 520° C. for 16 hours, contained slightly more than 0.1% iron. The metacinnabar formed a solid black cake, conforming in shape to the interior of the glass tube used to hold the sample. A powdery layer of excess FeS_2 remained on the upper surface of the cake. This FeS_2 was removed easily by scraping, however. Before analysis, to ensure that no FeS_2 was mechanically mixed with the metacinnabar the cake was ground fine and the powder was passed through a magnetic separator with sufficient magnetic flux to remove FeS_2. No iron-rich fraction separated. Under the microscope the material was observed to be uniformly black and homogeneous.

As a control (initially red) pure HgS was heated in a sealed evacuated glass tube for 16 hours at 520° C. in the oven alongside the tube containing the red HgS and FeS_2 mixture. A solid, homogeneous, deep red cake formed, similar in shape to the metacinnabar cake previously described. A dissimilar feature of the red cake was that it had fractured into polygonal columns oriented at right angles to the glass tube wall. It is likely that at 520° C. the HgS was metacinnabar, which on cooling inverted to cinnabar. The decrease in volume involved when the metacinnabar inverted to cinnabar probably caused the fragmentation.

As mentioned on page 475, unsuccessful attempts had been made by us to determine the inversion temperature by heating laboratory prepared metacinnabar. The sluggishness of the reaction was probably caused by the effect of small amounts of impurities introduced during the process used to synthesize the metacinnabar. The metacinnabar was made by precipitation from mercuric sulfide-sodium sulfide solutions. This method resulted in a fine-grained precipitate which probably absorbed impurities from the solution.

The small amount of black HgS which Allen, Crenshaw, and Merwin found in their heated red HgS samples may have resulted from the presence of traces of impurities in the red HgS. That only a small amount of metacinnabar persisted is evidence that their red HgS was quite pure.

In addition to retarding the inversion of metacinnabar to cinnabar, the presence of iron or zinc depresses the inversion temperature. FeS_2 lowers the inversion temperature to at least as low as 305° C., and ZnS to at least 240° C. These temperatures were determined by heating intimate mixtures of red HgS and amorphous iron and zinc sulfides in glass capillary tubes in the controlled temperature-gradient furnace for one week periods. It should be emphasized that the values obtained in this way are upper bounds only. Solid-solid reactions are involved which probably become slower at low temperatures, and the temperatures reported may be merely those at which the reactions become so slow as not to be detectable after one week.

It should be pointed out that the "pure" HgS used in the determination of the inversion temperature contained a very small amount of iron, of the order of 0.01%. Since even very small amounts of impurities may influence the temperature of inversion, the inversion temperature reported for HgS of this iron content may be slightly different from the true inversion temperature of pure HgS.

As mentioned earlier, Fyfe observed that natural cinnabar inverted to metacinnabar at 290° C., under water pressure in a steel bomb. The temperature was lower than 344° C. probably because of impurities, either existing in the original sample or, more likely, introduced from the metal walls of the bomb.

In summary, the laboratory study of the stability relations of cinnabar and metacinnabar has demonstrated that: (1) at one atmosphere pressure pure HgS exists in two stable modifications, cinnabar (red HgS) at or below 344° C. ± 2° C., and metacinnabar (black HgS) at or above the same temperature; (2) pure metacinnabar reverts rapidly to cinnabar below 344° C.; (3) the presence of Fe, Zn, or Se retards the reversion to cinnabar below the inversion temperature; and (4) the presence of FeS_2 depresses the inversion temperature to at least 305° C., and the presence of Zn depresses the inversion temperature to at least 240° C.

Petrographic Studies

Textural relations of cinnabar and metacinnabar were studied in ores and protores collected at numerous mercury mines and occurrences in California, Oregon, and Nevada. The mineral relations were studied by techniques involving the use of polished sections, thin sections, and polished surfaces. Examination of minerals in cavities by means of the binocular microscope proved to be most informative. Minerals were identified by *x*-ray methods whenever possible. The textures observed in ores and protores from some of the localities are described briefly in the following pages.

Senator mine and Mariposa Canyon prospect

The Senator mine and the Mariposa Canyon prospect, two neighboring localities in the Toquima Range, Nevada, had been examined previously by Bailey and Phoenix, who stated that at the Senator mine "Metacinnabar occurs as coarse crystals in a barite-quartz gangue. Cinnabar occurs as coatings on the metacinnabar, as small veinlets in barite and quartz, and as painty clouds in the kaolinized wall rocks" (2, p. 137). Although Bailey and Phoenix did not explicitly state the time relations involved, it seems apparent from their textural descriptions that they recognized that at least a part of the metacinnabar was earlier than cinnabar. In ore specimens examined by the present writers from both the Senator mine and the Mariposa prospect, mercuric sulfide commonly occurs as rounded grains embedded in a quartz-barite matrix in veins which transect altered granitic rocks. The mercuric sulfide grains are made up of a core of metacinnabar enveloped by a shell of cinnabar. This relation indicates continuous deposition of mercuric sulfide, with early metacinnabar followed by cinnabar. An unusual specimen from the Senator mine shows a clear euhedral barite crystal which contains euhedral crystals of metacinnabar and cinnabar on interior planar surfaces (phantom crystal faces), and on outer faces. The metacinnabar and cinnabar crystals in this specimen are not in contact, but are heterogeneously arranged, and in places are concentrated along lines which apparently represent former crystal edges. During the growth of the barite crystal metacinnabar and cinnabar crystals deposited either simultaneously or in alternation.

Aetna and Knoxville mines

Unequivocal evidence showing that metacinnabar crystals were deposited earlier than associated cinnabar crystals was observed in specimens from the Aetna and Knoxville mines, California. Equant, euhedral metacinnabar crystals in cavities in altered serpentine from both localities

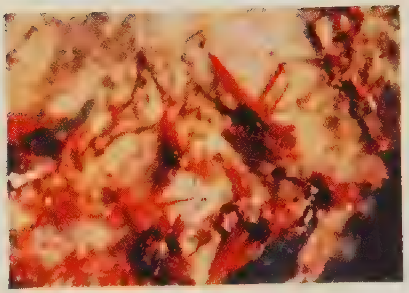

FIG. 6

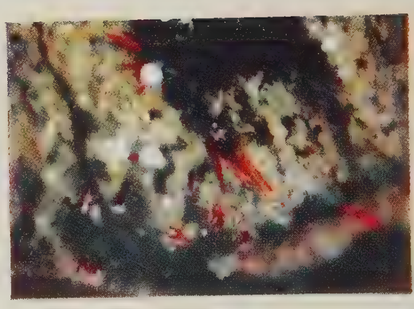

FIG. 7

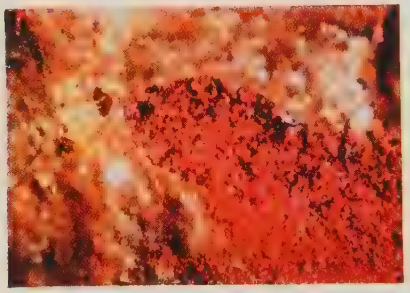

FIG. 8

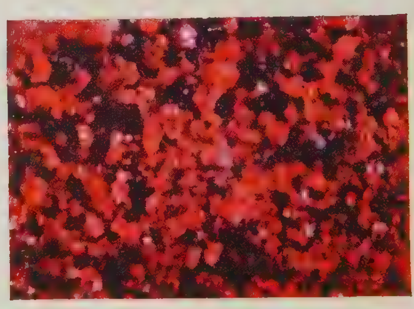

FIG. 9

FIG. 6. Metacinnabar crystals (black) overlain by elongate cinnabar crystals (red) in cavities in silicified serpentine from the Aetna mine, California. ×13.

FIG. 7. Metacinnabar crystals (black) overlain by elongate cinnabar crystals (red) in silicified serpentine, showing progressive darkening of cinnabar near the base of the crystals. Knoxville mine, California. ×13.

FIG. 8. Equant cinnabar (red) and metacinnabar (black) crystals in cavity in "silica-carbonate" rock from the Mt. Jackson mine, California. ×13.

FIG. 9. More highly magnified view of the central portion of the Mt. Jackson specimen pictured in Fig. 8, showing intimate mixture of cinnabar and metacinnabar crystals. ×47.

are coated with euhedral needle-like crystals of cinnabar which radiate outward from the surfaces of the metacinnabar crystals (Fig. 6). In some of the Knoxville specimens some elongate cinnabar crystals show near their bases color gradation from typical bright red, through dark red, to black at the junction with metacinnabar (Fig. 7). The cinnabar in these specimens clearly formed after the metacinnabar. The color change at the base of the cinnabar crystals is somewhat difficult to interpret; perhaps conditions during continuous deposition of mercuric sulfide changed rather abruptly from those favoring metacinnabar to those favoring cinnabar.

Some of the metacinnabar crystals in the Aetna specimens are altered to a reddish-black spongy residue about which unaltered cinnabar crystals are arranged in the same way that cinnabar crystals are arranged about unaltered metacinnabar crystals. The metacinnabar crystals apparently were less resistant to chemical attack than the cinnabar crystals. The preferential alteration and removal of metacinnabar suggests that at the time of the attack cinnabar was stable. A common laboratory method of removing small amounts of metacinnabar from cinnabar is to wash the mixture with dilute sodium sulfide solution which selectively dissolves the metacinnabar. Late solutions evidently acted on the metacinnabar and cinnabar crystals in some of the Aetna specimens in a similar way.

New Idria mine

In samples of ore collected at the New Idria mine several kinds of metacinnabar-cinnabar textures were observed which indicate early metacinnabar. For example, alternating thin layers of metacinnabar and dolomite adhere to fracture walls in brecciated sandstone. Overlying the metacinnabar and dolomite layers in the medial portions of the veins massive layers of cinnabar are commonly present. Scattered on other surfaces are small euhedral crystals of metacinnabar covered by layers of cinnabar. Eckel and Myers (3, p. 97–98) on the basis of examination of cinnabar-metacinnabar textures in rocks from the New Idria mine also concluded that the metacinnabar was earlier than the cinnabar.

Mt. Jackson mine

In samples of ore from the Mt. Jackson mine, California, the times of deposition of metacinnabar and cinnabar apparently overlapped. Tiny euhedral crystals of metacinnabar and cinnabar are mixed together in fractures and cavities in strongly silicified rocks. Commonly cinnabar crystals are perched on metacinnabar crystals and nearby in the same cavity metacinnabar crystals are perched on cinnabar (Figs. 8 and 9).

Mt. Diablo mine

C. P. Ross has pointed out that at the Mt. Diablo mine metacinnabar in general appears to have deposited earlier than cinnabar (10, p. 51). Our observations are in accord with those of Ross. Veinlets containing metacinnabar transected by cinnabar veinlets were noted by us, indicating that some metacinnabar is earlier than cinnabar. However, because of the complex mineral sequence in the rocks at Mt. Diablo, and the added difficulty that cinnabar and metacinnabar do not occur together in many of the specimens, the possibility that some or even much of the cinnabar is earlier than some metacinnabar cannot be ruled out.

Amedee Hot Springs, California, and Boiling Springs, Idaho

Metacinnabar and cinnabar occur as thin coatings on calcareous tufa and lake sediments in and about hot spring orifices at Amedee, California, near the east shore of Honey Lake. The rock surfaces over which the spring waters flow are coated by layers of fine-grained cinnabar as much as one-tenth of an inch thick. Overlying the cinnabar is a thinner layer of sooty metacinnabar. The mercuric sulfide forms aprons which extend about 25 feet down slope from the hot spring orifices. The thickness of the layer of mercuric sulfide and the proportion of cinnabar to metacinnabar decrease progressively away from the outlets. In the throats of the hottest vents nearly all the mercuric sulfide is in the form of cinnabar.

A few specimens from Amedee show wispy layers of metacinnabar alternating with thicker layers of cinnabar; in some of these specimens metacinnabar has partially altered to cinnabar, but for most of the cinnabar there is no evidence suggesting that it was not deposited as cinnabar.

A mercuric sulfide occurrence at Boiling Springs, Idaho, very similar to that at Amedee was described briefly by White (14, p. 124-125). Boiling Springs was visited by us during the summer of 1958 and specimens were taken for study. Specimens collected near the hot spring orifices showed layers of cinnabar coating the country rock, overlain in turn by thinner layers of metacinnabar.

The time relations at Amedee and Boiling Springs are the reverse of the usual relation seen elsewhere. Most of the metacinnabar was deposited later than associated cinnabar. The occurrences at Amedee and Boiling Springs are also unusual in that deposition has taken place at the earth's surface very recently, under relatively low conditions of temperature (near 100° C.) and pressure (approximately one atmosphere).

Summary of field and petrographic studies

The field and petrographic studies have demonstrated that: (1) metacinnabar is an earlier mineral than cinnabar as a general rule, although in exceptional circumstances it may be later; (2) in some cases mercuric sulfide was deposited continuously, with early metacinnabar giving way to later cinnabar; (3) in rare instances cinnabar and metacinnabar were deposited simultaneously or in alternation; and (4) metacinnabar was deposited from solutions as metacinnabar, and can not be considered to be an alteration product of cinnabar.

GEOLOGIC CONCLUSIONS

The conclusions resulting from the petrologic studies are in agreement with the determination of the stability relations of cinnabar and metacinnabar by laboratory experiments. That metacinnabar occurs as a hypogene mineral is supported by the petrologic evidence; the conclusion that it occurs as a hypogene mineral is furthermore in accord with the experimental fact that it is stable at high temperatures. The experimental evidence does not preclude the possibility that some metacinnabar in nature has formed metastably even though it was deposited by hypogene solutions.

That metacinnabar should be an earlier mineral than cinnabar appears to be expectable if deposition takes place along with falling temperatures. In this case a high temperature phase should be earlier than a low temperature phase of the same composition.

Textures indicating continuous deposition of mercuric sulfide, with metacinnabar giving way to cinnabar, can be explained in two ways. First, the mercuric sulfide might have been deposited continuously while the temperature dropped from a temperature above the inversion temperature to one below it; or second, deposition may have taken place at a constant temperature, with the concentration in the ore-carrying fluid of a substance such as iron decreasing continuously until at some concentration cinnabar became the stable phase. Probably it is more reasonable to explain continuous deposition of HgS by appealing to falling temperature; if variation in composition of the solutions from which the mercuric sulfide is being deposited commonly determined which phase was formed, reverse relations (early cinnabar and late metacinnabar) should be observed in more specimens than actually is the case.

Simultaneous deposition of cinnabar and metacinnabar could take place stably only if the temperature, pressure, and compositional conditions were precisely adjusted so that cinnabar and metacinnabar were in equilibrium. Such a delicate adjustment would be expected to occur infrequently in nature and, indeed, textures indicating simultaneous deposition of the two minerals are rare. It is possible, theoretically, for cinnabar and metacinnabar to precipitate together over a temperature interval if the composition of the system varied in such a way as to maintain equilibrium, but this does not appear very probable.

Mineral relationships indicating alternating deposition of cinnabar and metacinnabar imply that these minerals were deposited in an environment of fluctuating chemical and physical conditions. At a given temperature the concentration of substances such as iron or zinc may have fluctuated about certain critical concentrations, or for a given composition, the temperature may have varied above and below the inversion temperature.

The occurrences of HgS at Amedee Hot Springs, California, and Boiling Springs, Idaho, where metacinnabar was deposited later than cinnabar, were both unusual in that deposition has taken place at the earth's surface quite recently. Hot, supersaturated waters have deposited mercuric sulfide at the zone of maximum change in conditions, where temperature and pressure are changing sharply and where there is increased turbulence. The metacinnabar has apparently formed metastably as it does at ordinary temperatures and pressures in the laboratory, probably as a consequence of rapid deposition. Some cinnabar has been formed by the alteration of metacinnabar to cinnabar; it is possible that all of the cinnabar formed in this way, but textural evidences bearing on this point are meager. If some of the cinnabar was deposited as cinnabar, and, as appears likely, if the physical conditions have remained essentially the same during the period of deposition, chemical conditions must have varied to enable fluctuating deposition of cinnabar with metacinnabar.[1]

ACKNOWLEDGMENTS

The authors wish to express their appreciation to the National Science Foundation for financial support of this study. Our thanks are also extended to Professor G. C. Kennedy of the Institute of Geophysics, University of California, Los Angeles, for generously making available equipment and laboratory facilities. Dr. K. J. Hsu and Dr. D. V. Higgs of the Shell Development Company, Houston, Texas, and Professor

---

[1] This paper, being concerned chiefly with cinnabar-metacinnabar relations, has discussed extensively specimens containing both minerals. It should be emphasized, however, that although metacinnabar occurs more commonly than has been generally realized, nevertheless, in most mercury deposits cinnabar is the only mercury mineral present. In general, moreover, the textural evidences indicate that the cinnabar was deposited as such, not as metacinnabar which in turn inverted to cinnabar.

T. H. McCulloh of the University of California, Riverside, California, aided greatly by reading and constructively criticizing the manuscript.

BIBLIOGRAPHY

1. ALLEN, E. T., CRENSHAW, J. L., AND MERWIN, H. E. (1912), The sulphides of zinc, cadmium, and mercury; their crystalline forms and genetic conditions: *Am. Jour. Sci., Ser. 4,* **34** (whole no. 184), 341–396.
2. BAILEY, EDGAR H., AND PHOENIX, DAVID A. (1944), Quicksilver deposits in Nevada: *Univ. Nev. Bull.,* **38.**
3. DICKSON, FRANK W., AND TUNELL, GEORGE, (1955), Geochemical and petrographic aspects of mercury ore deposits: Final Report, Office of Naval Research Contract Nonr 233 (12), Project NR 081-74, 79 p.
4. ECKEL, EDWIN B., AND MYERS, W. B. (1946), Quicksilver deposits of the New Idria district, San Benito and Fresno Counties, California: *Calif. Jour. Mines and Geol.,* **42,** 81–124.
5. LINDGREN, WALDEMAR (1933), Mineral Deposits: McGraw-Hill Book Co., Inc. New York and London.
6. MOORE, GIDEON E. (1872), On the occurrence in nature of amorphous mercuric sulphide: *Am. Jour. Sci., Ser. 3,* **3** (whole no. 103), p. 36–43.
7. PALACHE, CHARLES, BERMAN, HARRY, AND FRONDEL, CLIFFORD (1952), Dana's System of Mineralogy, 7th Ed., v. 1: John Wiley and Sons, Inc., New York.
8. PENFIELD, SAMUEL L. (1885), Crystallized tiemannite and metacinnabarite: *Am. Jour. Sci., Ser. 3,* **24** (whole no. 129), p. 449–454.
9. RINSE J., (1928), The vapor pressure, dissociation and transition point of mercury sulfide: *Rec. Trav. Chim.,* **47,** p. 28–32.
10. ROSS, CLYDE P. (1940), Quicksilver deposits of the Mount Diablo district, Contra Costa County, California: *U. S. Geol. Survey Bull.* **922-B.**
11. SMITS, A. (1923), The Theory of Allotropy, translated from German by J. Smeath Thomas: Longmans, Green and Company, London.
12. TREADWELL, W. D., AND SCHAUFELBERGER, F. (1946), Zur Kenntnis der Löslichkeit des Quecksilbersulfids: *Helv. Chim. Acta,* **29,** 1936–1946.
13. WEISS, E. J., AND ROWLAND, RICHARDS, A. (1956), Oscillating-heating x-ray diffractometer studies of clay mineral dehydroxylation: *Am. Mineral.* **41,** 117–126.
14. WHITE, DONALD E. (1955), Thermal springs and epithermal ore deposits: *Econ. Geol.,* **50,** 99–154.

Manuscript received July 26, 1958.

THE AMERICAN MINERALOGIST, VOL. 44, MAY-JUNE, 1959

A HYDROMUSCOVITE WITH THE $2M_2$ STRUCTURE, FROM MOUNT LYELL, TASMANIA[1]

I. M. Threadgold, *Mineragraphic Investigations, C.S.I.R.O., Melbourne, Victoria.*

Abstract

A fine-grained mica from Mount Lyell, Western Tasmania, shown by chemical analysis to be a hydromuscovite, probably of metasomatic origin, gives an x-ray powder pattern similar to that of a $2M_2$ ($6M$) mica polymorph. This structure was previously only known to occur in lepidolites containing 4.0–5.1% Li_2O. A differential thermal analysis of the hydromuscovite has been carried out.

Introduction

Associated with the copper orebodies of the Mount Lyell field, in Western Tasmania, are foliated masses of extremely fine-grained green micaceous minerals. These minerals, which have been referred to collectively in the past as "batchelorite," following Petterd (1910), consist chiefly of muscovite (sericite), pyrophyllite and mixtures of these two minerals, with or without some admixed chlorite. The masses occur mainly at the contact of the ore with the enclosing schists and tend to be associated with the higher grade ore. They were particularly prominent in association with the rich sections of the North Lyell and Lyell Comstock orebodies. The North Lyell orebody consisted essentially of bornite, chalcopyrite, pyrite and quartz, with bornite the dominant copper mineral, in places almost to the exclusion of chalcopyrite. The Lyell Comstock orebody consisted of chalcopyrite and pyrite disseminated through schists, with small amounts of bornite locally in pockets and disseminations (Edwards, 1939).

In the course of examining a suite of specimens of these green micaceous minerals, one specimen,* from the No. 4 level of the Lyell Comstock Mine, was found to consist of hydromuscovite with the $2M_2$ structure.

Mount Lyell Hydromuscovite

Physical Properties

The hand specimen is similar to many of the other specimens of fine-grained micaceous minerals from Mount Lyell. It is dark emerald green in color, with a waxy luster, extremely fine-grained, foliated and is slightly greasy to the touch.

---

[1] Published by permission of the Commonwealth Scientific and Industrial Research Organization.

* Specimen labelled "batchelorite" in the collection of the Geology Department, University of Melbourne, Victoria (Reg. No. 2900).

Scattered through the specimen are numerous specks of sulphide. A polished section reveals that these specks are ragged particles of pyrite ranging from about 0.50 mm. to 0.01 mm. across. Occasional particles contain small inclusions of chalcopyrite up to about 0.02 mm. across.

Chemical Composition

The chemical analysis, given in Table 1, is similar to that of the well characterized hydromuscovite from Ogofau described by Brammall, Leech and Bannister (1937).

The most noticeable features of the analysis are that the alkalis are lower and the H_2O^+ higher than in a normal muscovite. The structural formula calculated from the analysis on the basis of a total of 24 oxygen and hydroxyl ions per structural unit gives:

$$(K, Na, Ca, Ba)_{1.72}(Al, Fe^{3+}, Fe^{2+}, Cr^{3+}, Mg)_{3.90}(Si, Al)_8O_{19.38}OH_{4.62}$$

This formula shows considerable deviation from the ideal muscovite formula in regard to the number of interlayer cations and the number of hydroxyl ions. To account for the marked deviations of hydrous micas from the ideal muscovite formula, Brown and Norrish (1952) suggested

TABLE 1. CHEMICAL ANALYSIS AND IONIC COMPOSITION OF HYDROMUSCOVITE FROM MOUNT LYELL, TASMANIA

	1	2	Atomic proportions	Atoms per structural unit on the basis of 24(O+OH) per unit	Atoms per structural unit on the basis of Twenty O & Four OH per unit
SiO_2	46.54	45.65	0.7601	Si 6.00	6.06
Al_2O_3	36.37	36.03	0.7068	Al 5.58	5.63
Fe_2O_3	0.72	1.80	0.0226	Fe^{3+} 0.18	0.18
FeO	0.36	0.13	0.0018	Fe^{2+} 0.01	0.01
Cr_2O_3	—	0.25	0.0032	Cr^{3+} 0.03	0.03
MgO	0.50	0.52	0.0129	Mg 0.10	0.10
CaO	0.22	0.23	0.0041	Ca 0.03	0.03
BaO	—	0.22	0.0014	Ba 0.01	0.01
Na_2O	0.46	1.23	0.0396	Na 0.31	0.32
K_2O	8.06	8.18	0.1736	K 1.37	1.38
$H_2O+(105°)$	6.31	5.27†	0.5850	H 4.62	$\{0.66 = 0.22\ H_3O^+$ $4.00 = 4.00$ OH
$H_2O-(105°)$	0.52	0.68†			
FeS_2	—	0.27			
	100.31*	100.46‡			
Less O=F	0.01	Less O=S 0.05			
Total	100.30	100.41			

* Includes $TiO_2 = 0.17$, $P_2O_5 = 0.06$, $F = 0.02$, Li_2O = trace.

† Water determined at plus and minus 110° C.

‡ Elements also sought include TiO_2 = trace, MnO = trace, P_2O_5 = nil, Li_2O = nil.

1. Hydromuscovite A from Ogofau, Carmarthenshire (Brammall, Leech and Bannister, 1937).
2. Hydromuscovite from Lyell Comstock Mine, Mount Lyell, Tasmania. Analyst I. M. Threadgold.

that the low alkali and the high water content are due to the replacement of interlayer potassium ions by oxonium ions (H_3O^+). The following structural formula, obtained using the method of Brown and Norrish* (1952), is in good agreement with that of a normal dioctahedral mica:

$$(K, Na, Ca, Ba, H_3O)_{1.96}(Al, Fe^{3+}, Fe^{2+}, Cr^{3+}, Mg)_{4.01}(Si, Al)_8O_{20}OH_4$$

Muñoz Taboadela and Aleixandre Ferrandis (1957), following Mackenzie's classification of the clay micas, give suggested limits for K_2O+Na_2O percentages, K^++Na^+ ionic ratios and H_3O^+ ionic ratio for muscovite and hydromuscovite. These values, quoted below, show that the mica from Mount Lyell lies outside the suggested limits of a hydromuscovite, being intermediate between muscovite and hydromuscovite.

	K_2O+Na_2O %	K^++Na^+ Ionic ratios*	H_3O^+ Ionic ratio†
Muscovite	9	1.6–2+	—
Hydromuscovite	8–9	1.3–1.6	0.4–0.6
Hydromuscovite (Mount Lyell, Tasmania)	9.41	1.68	0.22

* Values calculated on the basis of $O+OH=24$.

† Values calculated by the method of Brown and Norrish (1952).

However, it is sufficiently hydrated to warrant the name hydromuscovite, as the prefix draws attention to the hydrated nature of the mica, and it is suggested that the limits set by Mackenzie should be extended.

A semi-quantitative spectrographic analysis showed the presence of titanium, manganese and vanadium, each ranging from 0.01 to 0.001%. The following additional elements, arranged in approximate order of decreasing abundance, were detected in trace amounts: Sr, Cu, Ni, Zr, Rb. Lithium was not detected and, if present, its concentration is below 0.01%.

X-Ray Powder Data

Apart from a number of weak lines, the *x*-ray powder pattern of the hydromuscovite, the interplanar spacings of which are given in Table 2, is similar to that of the 6-layer monoclinic (6*M*) polymorph of lepidolite recorded by Levinson (1953).

Smith and Yoder (1956) have found that the 6*M* polymorph, originally described by Hendricks and Jefferson (1939), can be indexed on the basis of a 2-layer monoclinic cell. This polymorph they renamed $2M_2$

---

* There is a printer's error in the second equation of Brown and Norrish p. 931. Equation given as $24+y/n=$(Atomic proportion of oxygen) should read $24/n+y=\sum$(Atomic proportion of oxygen).

TABLE 2. *X*-RAY POWDER DATA. Cu/Ni RADIATION

$2M_2$ hydromuscovite, Lyell Comstock Mine, Mount Lyell, Tasmania				$2M_2$ ($6M$) lepidolite, Gunnison County, Colorado (Levinson, 1953)			
d (Å)	I (est.)	*d*	I	*d*	I	*d*	I
10.0	8	2.19	½	9.89	MS	2.190	VVW
5.01	4	2.14	¼	4.99	M		
4.48	9	2.08	1½	4.49	M	2.039	VW
4.39	½	2.00	3			1.985	S
4.27		1.716	¼				
3.89	3	1.691	½	3.84	W	1.684	VVW
3.66	4	1.667	½	3.61	M		
3.50	3½	1.638	½	3.47	M	1.633	VVW
3.34	6	1.619	¼	3.31	M		
3.20	4	1.586	½	3.19	M	1.572	VVW
3.06	3½	1.565	¼	3.07	M		
3.01	½	1.503	5			1.506	M
2.93	½	1.480	¼				
2.87	3	1.427	½	2.88	M		
2.81	3	—	—	2.775	M	1.393	VVW
2.58	10	1.355	¼	2.572	VS	1.355	VVW
2.46	2	1.315	¼			1.319	VVW
2.40		1.298	2	2.416	M	1.300	W
2.25	1	1.250	1	2.248	VVW	1.239	VVW

to distinguish it from the more common 2-layer monoclinic polymorph $2M_1$, which has a different stacking arrangement. *X*-ray powder photographs of a $2M_1$ muscovite and the $2M_2$ hydromuscovite, from Mount Lyell, are reproduced in Fig. 1.

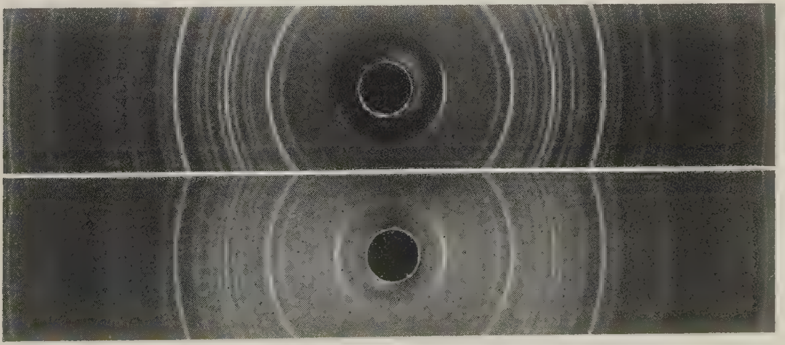

FIG. 1. Top: *X*-ray powder pattern of a fine-grained muscovite with $2M_1$ structure, from Mount Lyell, Tasmania.

Bottom: *X*-ray powder pattern of hydromuscovite with $2M_2$ structure, from No. 4 level, Lyell Comstock Mine, Mount Lyell, Tasmania.

Differences in the observed intensities of corresponding reflections, given in Table 2, are in part due to preferred orientation in the powdered specimen and the differences in the chemical compositions of the two minerals. Significant differences may be expected in the intensities of the (00*l*) reflections, in view of the replacement of a considerable part of the octahedral Al^{3+} by Li^{+} in the lepidolite.

Previously the $2M_2$ ($6M$) mica polymorph was only known to exist in lepidolites having a Li_2O content within the range 4.0–5.1% (Levinson 1953). Levinson (1955), after examining a number of illites and hydrous micas, recognized within this group the existence of $1M$, $1Md$, $3T$ polymorphs and the normal $2M_1$ polymorph, but not the $2M_2$ type described here.

Differential Thermal Analysis

The *DTA* apparatus used in this investigation was that described by Carthew and Cole (1953), modified by having a 24 -12W (chromium-tungsten) heat resistant steel sample block and a Sunvic D.C. amplifier.

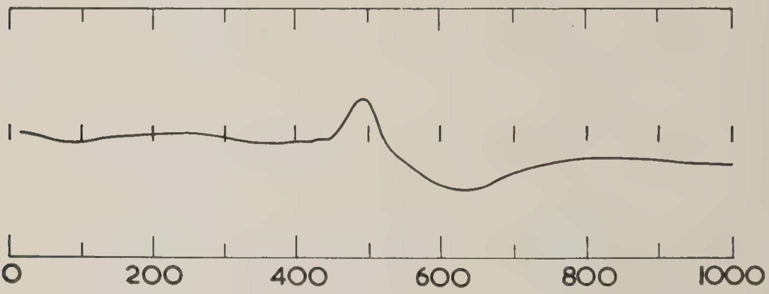

FIG. 2. DTA curve of hydromuscovite from No. 4 level, Lyell Comstock Mine, Mount Lyell, Tasmania.

The *DTA* curve shown in Fig. 2 is, except for the exotherm at 495° C., similar to the curves of a number of fine-grained muscovites from Mount Lyell. The broad, shallow, low temperature endotherm extending up to about 250° C. is associated with the loss of hygroscopic and interlayer water, presumably in the form of H_3O^{+}. Oxidation of the small amount of sulfides in the sample, chiefly pyrite, gives rise to the exotherm at 495° C. This exotherm is immediately followed by a broad endotherm, with a peak at 630° C., corresponding to the loss of hydroxyl water. Depression of the base line following this reaction can be assumed to be due to changes in the specific heat and the bulk density of the sample. As this feature has not been observed in any of the *DTA* curves of previously examined fine-grained muscovites from Mount Lyell, it is probably the result of oxidation of the sulfides.

Between 250° C. and the beginning of the exotherm at about 430° C. there is a shallow "apparent" endotherm which probably represents the commencement of the endotherm due to the loss of hydroxyl water, the smooth contour of the curve being interrupted by the oxidation of the sulfides.

Discussion

Except for the high water to alkali ratio the hydromuscovite is chemically similar to a normal muscovite. This deviation from the ideal muscovite composition may be explained by the presence of oxonium ions substituting for interlayer K^+ ions. If this is true, it is unlikely that the existence of interlayer oxonium ions is the cause of the $2M_2$ crystallization of the hydromuscovite, as the H_3O^+ and K^+ ions have approximately the same ionic radii.

Since the specimen was collected from the workings of the Lyell Comstock Mine, in which fine-grained masses of "sericite" were not uncommonly associated with the orebody, it is most probable that the hydromuscovite is a product of interaction between hydrothermal ore-forming solutions and the schistose country rocks, that consist chiefly of sericite, quartz and chlorite. This is supported to some extent by the fine grain size and the presence of sulfides.

Acknowledgments

The author is indebted to Mr. A. A. Baker, Curator, Geology Department, University of Melbourne, for the loan of the specimen described in this paper. Drs. A. B. Edwards and W. F. Cole, of the Commonwealth Scientific and Industrial Research Organization, Mineragraphic Investigations Section and Division of Building Research respectively, have critically read the manuscript. The differential thermal analysis was carried out by Miss N. Rowland, through the kindness of Dr. W. F. Cole.

References

Brammall, A., Leech, J. G. C., and Bannister, F. A. (1937), The paragenesis of cookeite and hydromuscovite associated with gold at Ogofau, Carmarthenshire: *Mineral. Mag.*, **24**, 507–520.

Brown, G., and Norrish, K. (1952), Hydrous Micas: *Mineral. Mag.*, **29**, 929–932.

Carthew, A. R., and Cole, W. F. (1953), An apparatus for differential thermal analysis: *Aust. J. Instr. Technol.*, **9**, 23–30.

Edwards, A. B. (1939), Some observations on the mineral Composition of the Mount Lyell Copper Ores, Tasmania, and their modes of occurrence: *Proc. Aus. Inst. Min. Met.*, No. **114**, 62–109.

HENDRICKS, S. B., AND JEFFERSON, M. E. (1939), Polymorphism of the micas: *Am. Mineral.*, **24**, 729–771.

LEVINSON, A. A. (1953), Studies in the mica group; Relationship between polymorphism and composition in the muscovite-lepidolite series: *Am. Mineral.*, **38**, 88–107.

LEVINSON, A. A. (1955), Studies in the mica group; Polymorphism among illites and hydrous micas: *Am. Mineral.*, **40**, 41–49.

MUÑOZ TABOADELA, M., AND ALEIXANDRE FERRANDIS, V. (1957), The mica minerals, in *The Differential Thermal Investigations of Clays* (Mackenzie: ed.), 165–190.

PETTERD, W. F. (1910), Catalogue of the Minerals of Tasmania: Mines Department, Tasmania.

SMITH, J. V. AND YODER, H. S. (1956), Experimental and theoretical studies of the mica polymorphs: *Mineral. Mag.*, **31**, 209–235.

Manuscript received July 31, 1958.

THE AMERICAN MINERALOGIST, VOL. 44, MAY–JUNE, 1959

X-RAY AND ELECTRON DIFFRACTION DATA FOR SEPIOLITE*

G. W. Brindley, *Department of Ceramic Technology, The Pennsylvania State University, University Park, Pennsylvania.*

Abstract

X-ray powder data for sepiolite are indexed on the basis of an orthorhombic cell. The mineral shows marked variations in crystallinity. Single crystal, electron diffraction diagrams confirm the *b* and *c* parameters, and in conjunction with electron microscope observations prove that the lath-like crystals develop on the (100) plane.

X-Ray Data

X-ray, dehydration, thermal, and other measurements by Caillère (1936), Migeon (1936) and Longchambon (1937) on sepiolites from various sources have established that sepiolite is a distinct mineral. The "X-Ray Powder Data File" (1958 Edition) contains data for four sepiolites additional to those given by the above investigators. There are very considerable differences among these data and none of them is indexed. Collectively they may suffice to identify the mineral, but they leave much uncertainty regarding the weaker x-ray reflections.

The crystal structure of sepiolite has been analyzed by Nagy and Bradley (1955), who showed that the mineral consists of mica-like units extending parallel to the fiber axis (c-axis); Fig. 3 shows schematically a cross-section of a sepiolite fiber based on their analysis. Nagy and Bradley indexed the $hk0$ reflections in an x-ray fiber diagram, but these do not account for all the reflections in a powder diagram. They showed that the unit cell is either orthorhombic or monoclinic and gave the cross-section of the cell as 13.4×27.0 Å. Preisinger (1957) stated that the cell is orthorhombic with parameters.

$$a = 13.4, \quad b = 26.8, \quad c = 5.26 \text{ Å}$$

in agreement with the results of Nagy and Bradley. His results have been published so far only in abstract form. The space group was suggested as probably $C2/m$ by Nagy and Bradley, and as $P2_1/n\ 2/c\ 2/n$ by Preisinger. On the basis of powder measurements it is scarcely possible to make reliable comments on the space group and it will be shown that the data can be indexed on the basis of an orthorhombic cell with $(h+k)$ even.

In the present work sepiolites have been examined from various localities including Little Cottonwood, Utah; Gouverneur, New York; Knights Quarry, Cal.; Cornwall, England; Vallecas, Spain; an unknown locality in Kenya; and Eski Chehir, Asia Minor.

---

* Contribution No. 58-6 from the College of Mineral Industries, The Pennsylvania State University, University Park, Pa.

Most of these materials appear to be pure or almost pure sepiolite as judged by the absence of unusual reflections, but the crystallinity varies considerably. Extreme cases are illustrated in Fig. 1 which shows x-ray diffractometer records of sepiolites from Little Cottonwood, Utah (the upper trace), and from Eski Chehir (the lower trace). The lattice spacings and reflected intensities for these materials, and for two others of intermediate degree of crystallinity from Vallecas, Spain, and from Kenya, are listed in Table 1, where the d-values are measured with respect to CuKα radiation (λ1.5418 Å).

The powder data are indexed in terms of the following unit cell:

$$a = 13.50 \pm 0.02, \qquad b = 26.97 \pm 0.03, \qquad c = 5.25_5 \pm 0.01 \text{ Å}$$

The indices hkl and the calculated d values are given in Table 1, and are complete down to $d = 2.40$ Å. Additional calculated values down to $d = 2.0$ Å are given which correspond to observed reflections. For $d < 2.0$ Å the calculated spacings are too numerous for reliable correlation with the observed values.

Electron Diffraction Data

It is well established that sepiolite has a fibrous lath-like morphology and this has been confirmed in the present work. However, the laths are far from being equally well developed in all specimens. In the case of the Eski Chehir material, the individual fibers are very small and poorly developed, and the single crystal diffraction patterns are also very poor. Figure 2(b) shows a typical diffraction diagram for the Eski Chehir sepiolite.

The well developed and well crystallized fibers of sepiolite from Little

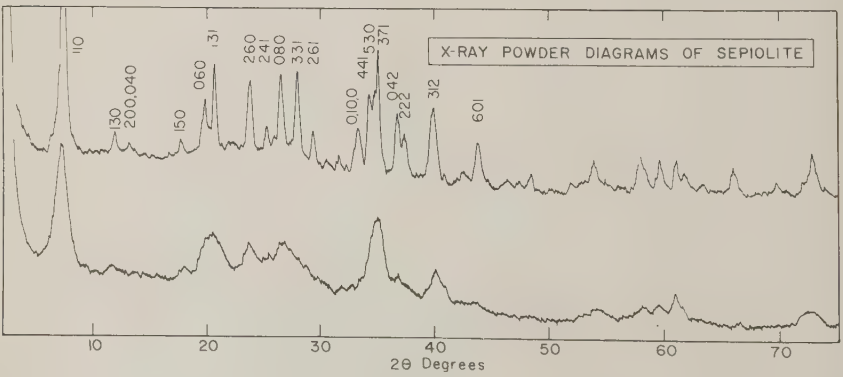

Fig. 1. X-ray diffractometer records of sepiolites from Little Cottonwood, Utah (upper curve), and Eski Chehir, Asia Minor (lower curve).

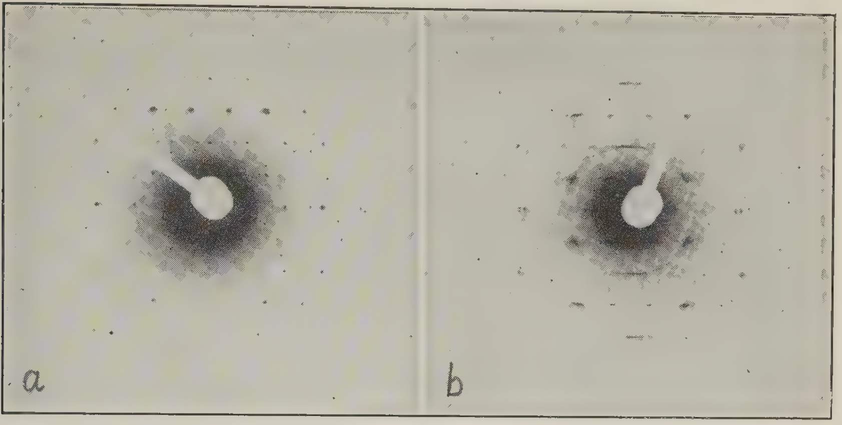

FIG. 2. Single crystal electron diffraction patterns of sepiolite from (*a*) Little Cottonwood, Utah, (*b*) Eski Chehir, Asia Minor.

Cottonwood, Utah, give excellent single crystal diagrams and a typical example is shown in Fig. 2(*a*). From enlargements of several of these patterns it is readily found that the diffraction spots lie on a rectangular net with sides about 1/5.3 Å and 1/26.8 Å to within ±1%. Therefore the lath-shaped crystals lie with their *b* and *c* axes, i.e., the (100) plane, on the stage of the instrument. The usefulness of single-crystal electron diffraction data in establishing unit cell parameters when only powder or, at the best, fiber diagrams are obtainable with *x*-rays, is well illustrated by this example

In terms of the structure described by Nagy and Bradley, it can now be said that the individual crystals develop primarily along the *c*-axis (fiber axis) and secondarily in the plane of the mica-like units composing the structural blocks. The laths are relatively thin in the direction of the *a*-axis, and the stacking of the mica-like units normal to the usual cleavage plane is the least favored growth process. Figure 3 illustrates sche-

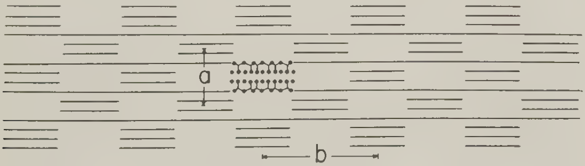

FIG. 3. Schematic representation of the cross-section of a sepiolite fiber, showing greater development in the *b* than in the *a* direction. The content of one unit cell is indicated schematically; the horizontal lines represent layers of oxygen atoms.

Table 1. Observed and Calculated *X*-Ray Powder Data for Sepiolite

hkl	*d*(Calc.) Å	*d*(Obs.) Å			
		(1)	(2)	(3)	(4)
020	13.48	—	—	—	—
110	12.07	12.05 (100)	12.1 (100)	12.1 (100)	12.3 (60)
130	7.482	7.47 (10)	7.5 (7)	7.7 (5B)	7.6 (5)
200	6.750	6.73 (5)	6.7 (4B)	6.7 (5B)	—
040	6.742				
220	6.036	—	—	—	—
001	5.255	—	—	—	—
150	5.008	5.01 (7)	5.04 (3B)	5.0 (5B)	4.9 (6B)
021	4.896	—	—	—	—
111	4.818	—	—	—	—
240	4.780	—	—	—	—
060	4.495	4.498 (25)	4.49 (25)	4.47 (18)	4.5
310	4.438	—	—	—	(20NR)
131	4.301	4.306 (40)	4.29 (35)	4.31 (25)	4.3
201	4.146	—	—	4.17 (5)	—
041	4.145	—	—	—	—
330	4.023	4.022 (7)	4.02 (7)	—	—
221	3.963	—	—	—	—
260	3.741	3.750 (30)	3.738 (25)	3.738 (20)	3.746 (20B)
170	3.705	—	—	—	—
151	3.626	—	—	—	—
241	3.532	3.533 (12)	3.506 (5)	—	3.49 (5)
350	3.455	—	—	—	—
061	3.416	—	—	—	—
311	3.391	—	—	—	—
400	3.375	—	—	—	—
080	3.370	3.366 (30)	3.339 (45)	3.339 (35)	3.34
420	3.274	—	—	—	
331	3.195	3.196 (35)	3.181 (15B)	3.187 (12)	
261	3.048	3.050 (12)	—	3.048 (5)	(20NR,B)
171	3.028	—	—	—	
440	3.018	—	—	—	
280	3.016	—	—	—	
370	2.928	2.932 (4)	2.950 (5)	—	2.98
190	2.925	—	—	—	—
351	2.887	—	—	—	—
401	2.840	—	—	—	—
081	2.837	2.825 (7)	—	—	—
421	2.778	2.771 (4)	—	2.79? (4)	—
460	2.699	—	—	—	—
0.10.0	2.697	2.691 (20)	2.66 (8NR)	2.675 (8NR)	2.67
510	2.687				
002	2.627	—	—	—	
441	2.618	2.617 (30)			
281	2.617		2.59	2.59	
530	2.586	2.586 (NR)			
022	2.580	—	(45NR)	(40NR)	2.56(40NR,B)
112	2.567	2.560 (55)			
371	2.557				
191	2.556		2.56	2.56	
2.10.0	2.505	—	—	—	
390	2.495	—	—	—	
132	2.479	2.479 (5)	—	—	2.49

TABLE 1 (*continued*)

hkl	*d*(Calc.) Å	*d*(Obs.) Å			
		(1)	(2)	(3)	(4)
202	2.448	2.449 (25)			
042	2.448		2.43 2.395 (20NR)	2.44 2.39 (15NR)	2.43 2.36 (10NR)
550	2.414				
1, 11, 0	2.412	2.406 (15)			
222	2.409				
461	2.401				
062	2.268	2.263 (30)	2.256 (20)	2.259 (18B)	2.24 (20B)
312	2.261				
2.10.1	2.260				
620	2.220	2.206 (3)	—	—	—
570	2.211				
332	2.200				
640	2.134	2.125 (7)	2.117 (4B)	2.117 (5)	—
2, 12, 0	2.130				
4, 10, 0	2.107				
402	2.073				
082	2.072	2.069 (20)	2.060 (10)	2.071 (7B)	2.08 (6B)
601	2.069				
571	2.038	2.033 (4)	—	—	—
		1.957 (4)	—	—	—
		1.921 (2)	—	—	—
		1.881 (7)	1.873 (4)	—	—
		1.818 (2)	—	—	—
		1.760 (6)	—	—	—
		1.700 (10)	1.716 (7)	1.722 (5)	—
		—	1.691 (10)	1.692 (8)	1.69 (5B)
		1.637 (3)	—	—	—
		1.592 (10)	1.598 (4)	1.583 (9B)	1.58 (7)
		1.550 (15)	1.578 (7)	1.548 (10)	1.551 (10)
			1.540 (8)		
		1.518 (15)	1.517 (15)	1.517 (15)	1.517 (14)
		1.502 (8)	—	—	—
		1.468 (4)	1.465 (3)	—	—
		1.416 (9)	1.406 (4)	1.412 (4B)	—
		1.349 (6)	—	—	—
		1.312 (6)	—	1.310 (4B)	—
		1.299 (15)	—	1.296 (10)	—

Experimental data for sepiolites from:
(1) Little Cottonwood, Utah.
(2) Vallecas, Spain.
(3) Kenya.
(4) Eski Chehir, Asia Minor.
Intensities in ( ).
B signifies "broad"; NR "not resolved."

matically a cross-section of a sepiolite fiber with greater development in the *b* than in the *a*-direction. The length of the fiber normal to the diagram may be 10–100 times greater than the cross-section.

The writer is indebted to Dr. R. C. Mackenzie, Mr. R. H. S. Robertson, Dr. R. Roy for specimens, to Dr. F. H. Gillery for assistance with

I.B.M. computations, and to Mr. J. J. Comer for assistance with electron diffraction. The work has formed part of a program of clay mineral research supported by the Gulf Research & Development Company.

Note added Oct. 1, 1958

At the time of writing the preceding article, the writer was unaware that Preisinger, in collaboration with Brauner, had already published a full account of the structure determination of sepiolite (K. Brauner and A. Preisinger, *Tschermaks min. u. pet. Mitte.*, **6**, 120–140, 1956). The abstract by Preisinger makes no reference to this publication.

REFERENCES

Caillère, S. (1936), Étude de quelques silicates magnésiens à facies asbestiforme ou papyracé n'appartenant pas au groupe de l'antigorite, Bull. Soc. Franç. Min., **59**, 353–386.

Longchambon, H. (1937), Sur certaines characteristiques de la sepiolite d'Ampandrandava, Bull. Soc. Franç. Min., **60**, 232–276.

Migeon, G. (1936), Contribution à l'étude de la définition des sepiolites, Bull. Soc. Franç. Min., **59**, 6–90; 107–134.

Nagy, B., and Bradley, W. F. (1955), The structural scheme of sepiolite, Am. Mineral., **40**, 885–892.

Preisinger, A. (1957), *X*-ray study of the structure of sepiolite, Sixth National Clay Conference, Abstracts, p. 4.

Manuscript received Aug. 2, 1958.

THE AMERICAN MINERALOGIST, VOL. 44, MAY-JUNE, 1959

ERIONITE FROM CENOZOIC TUFFACEOUS SEDIMENTS, CENTRAL NEVADA

Kenneth S. Deffeyes, *Princeton University, Princeton, N. J.*[*]

Abstract

The mineral erionite, a zeolite known previously from only one locality, has recently been identified from six different areas in Wyoming, Nevada, and South Dakota. In each case it occurs in volcanic-rich Cenozoic sediments. A re-examination of the properties of the mineral shows that the original and subsequent descriptions have been incorrect in placing the mineral in the orthorhombic system. Single-crystal x-ray photographs show that the mineral has hexagonal symmetry and the optical properties observed are consistent with an assignment to the hexagonal system.

Introduction

Erionite was defined by A. S. Eakle in 1898 from material sent to Harvard for identification from Durkee, Oregon. The mineral occurred as white wooly fibers associated with opal in cavities in rhyolite tuff. On the basis of chemical properties, Eakle placed the mineral in the zeolite family and assigned the species to the orthorhombic system because the fibers exhibited parallel extinction and, "The acute bisectrix lies parallel to the fibers, since an axial figure normal to the obtuse bisectrix can be seen in the fibers" (1898, p. 68). Since that time the mineral has been regarded as extremely rare and no additional occurrences have been noted. In 1957 Staples reported that he had found the type locality and he published optical and x-ray measurements which were consistent with orthorhombic symmetry.

In 1956 the author and F. B. Van Houten found a material from Nevada and from Wyoming which had optical properties and diffraction spacings corresponding to no known mineral. Van Houten referred some of the samples to the Geochemistry and Petrology Branch of the U. S. Geological Survey and a comparison of the x-ray powder pattern of the specimens with the U.S.G.S. collection of powder patterns was made by F. A. Hildebrand who suggested that the material was erionite (Rept. IWX 799, Feb. 21, 1957). During this time an optical and x-ray diffraction study carried out by the author showed that the material from Wyoming and Nevada did not correspond to the crystallographic properties which had been published for erionite. Through the courtesy of Dr. C. S. Hurlbut of Harvard University, a portion of the type specimen (Harvard specimen no. 86532) was made available. This material did correspond in optical properties and x-ray pattern to the materials from Nevada and Wyoming, so a redescription of the properties of erionite is necessary.

---

[*] Present address: Shell Development Company, Houston, Texas.

PHYSICAL PROPERTIES

The name erionite was derived from the Greek word for wool (ἔριον) because of the crinkly white appearance of the mineral fibers. Although this texture is duplicated in one small specimen from Nevada, more commonly the mineral occurs as fine-grained fibers or small radiating crystal groups in beds which were formed by partial or complete alteration of acidic vitric ash which fell into Cenozoic lakes. The beds composed dominantly of zeolite are thin bedded, massive, or blocky and they are white or light orange in color. In the specimens studied fine-grained mixtures of erionite and heulandite are about as common as beds of nearly pure erionite.

The measurements reported in this study were all made on crystals which were separated with heavy liquids (tetrabromethane and carbon tetrachloride) and a magnetic separator, from a sample of a tuff bed in Jersey Valley, Nevada. A full description of the outcrop is included in the discussion of localities.

The density was determined by the use of a centrifuge, heavy organic liquids, and a liquid density balance using the method described by Bass (1957). The mineral concentrate was pure except for flakes of volcanic glass which were included in about one-fourth of the grains. Since the glass is heavier than the zeolite, the density sufficient to float the first 20% of the sample is taken as the correct value: $2.070 \pm .01$ grams/cm.^{3} Eakle's original description (1898, p. 68) reported a specific gravity of 1.997.

OPTICAL PROPERTIES

Eakle's original description of erionite stated that the interference figure viewed in the direction perpendicular to the fiber axes was the obtuse bisectrix (1898, p. 68). This inference that the two optic axes were not coincident with each other and with the fiber axis has led later investigators to search for and to report variations in refractive index of about 0.002 in the directions perpendicular to the fibers (Larsen, 1921, p. 72; Staples, 1957). It is suggested that the differences reported between the least and intermediate indices has resulted from accepting the variations between grains as variations due to differences of orientation.

If the mineral were biaxial its optical behavior could be demonstrated by determinations of refractive indices of light vibrating perpendicular to the fiber axes and by locating the optic axes on the universal stage. In this study measurements of refractive index were made using a water cell for temperature control, a sodium monochromator, and a refractometer for measuring the indices of the immersion oils. The small variation from grain to grain of the least index of refraction was no greater than the corresponding variation in the greatest index. Since variations in the greatest index (vibration direction parallel to the fibers) cannot be due to differences in orientation, it is concluded that the refractive indices were not observed to depart measurably from uniaxial behavior.

By placing unusually thick mounts of loose grains in plastic on a universal stage it was possible to tilt some grains until the fiber axis was vertical. The crystals showed no birefringence when viewed along the fiber axis and in all other positions the fibers were length slow. A check on the magnitude of the birefringence was made by determining directly the thickness and retardation of grains on the universal stage using a micrometer eyepiece and a Berek compensator. The optical properties of the material from Jersey Valley, Nevada are:

n_z 1.4740 ± .0005
n_x 1.4711 ± .0005
birefringence .003
uniaxial, positive $Z=c$

These values are close to those observed by Staples (1957) but they are considerably higher than the observations quoted in standard mineralogy textbooks which were taken from the determinations of Larsen (1921, p. 72).

X-RAY STUDY

The crystal system and approximate unit cell dimensions were determined from rotation and Weissenberg photographs of a single fiber rotated parallel to the fiber axis. A rotation photograph showed a layer spacing of 15 Å and a symmetry of C_{2l}. The even layer lines have considerably greater intensities than the odd layer lines. The positions and intensities of spots on a Weissenberg photograph of the zero layer line of the same crystal indicated a symmetry of C_{6l} (Buerger, 1942, p. 483) indicating a hexagonal lattice with an a_0 spacing of 13.1 Å.

The rotation photograph was used to index peaks on diffractometer traces. The precise cell dimensions were determined with a Norelco diffractometer using a nickel filtered copper radiation and silicon metal as an internal standard. Because of the fibrous habit of the mineral the intensities observed are strongly influenced by preferred orientation. The only systematic absence noted is that peaks having the indices $hh2\bar{h}l$ are present only when l is even. The only $000l$ peak present is 0002 but the weakness of the basal series is at least partially explained by selective orientation of the fibers. The information is insufficient for the assignment to a space group but the diffraction information indicates that erionite has a primitive hexagonal lattice with $a_0 = 13.200 \pm .005$ Å and $c_0 = 15.07 \pm .01$ Å. Diffractometer traces of the type specimen from

TABLE 1. *X*-RAY DIFFRACTION DATA FOR ERIONITE FROM JERSEY VALLEY, NEVADA, OBTAINED WITH A NORELCO DIFFRACTOMETER. Cu Kα, Ni FILTER

hk.l	2θ (obs)	2θ (calc)	*d*	I
10·0	7.7	7.73	11.43	100
00·2	11.7	11.72	7.54	3
11·0	13.4	13.41	6.60	60
10·2	14.0	14.00	6.32	4
20·0	15.4	15.45	5.73	28
20·1	16.5	16.54	5.35	15
20·2	19.4	19.44	4.56	8
12·0	20.5	20.52	4.32	90
12·1	21.3	21.35	4.16	30
30·0	23.3	23.34	3.81	60
12·2	23.7	23.69	3.75	45
10·4	24.8	24.81	3.58	12
22·0	26.9	27.02	3.30	40
12·3	27.1	27.17	3.28	8
31·0	28.1	28.11	3.17	25
20·4	28.4	28.30	3.15	25
31·1	28.7	28.74	3.10	12
31·2	30.5	30.55	2.924	8
10·5		30.59	2.920	
40·0	31.2	31.27	2.858	75
12·4	31.4	31.44	2.843	25
40·1	31.8	31.84	2.808	40
40·2	33.5	33.50	2.673	14
41·0	36.0	36.00	2.493	22
32·2	36.2	36.23	2.477	12
50·0	39.4	39.39	2.287	4
33·0	41.0	40.98	2.200	12
33·2	42.8	42.77	2.112	7
42·2	43.5	43.52	2.078	4
51·1?	44.5	44.47	2.035	1
51·2	45.8	45.73	1.981	4
50·4	46.5	46.37	1.956	1
43·0	48.3	48.37	1.880	2
52·0	49.8	49.76	1.831	10
41·6	51.6	51.54	1.772	5
61.0	52.4	52.42	1.744	2
61·2	53.9	53.91	1.699	5
44·0	55.6	55.65	1.650	30
62·0	58.3	58.13	1.585	10
62·1	58.5	58.49	1.576	10
62·2	59.5	59.53	1.551	2
71·0	61.1	61.15	1.514	3
54·0	63.5	63.50	1.464	8
62·4		63.60	1.462	
80·0	65.2	65.23	1.429	4
90·0	74.6	74.65	1.270	12

Durkee, Oregon showed peaks which were broader and less distinct but otherwise the spacings and intensities were identical.

Staples (1957) reported that "The optical properties of erionite indicate that it is orthorhombic, and all *x*-ray patterns may be indexed on an orthorhombic lattice of the dimensions: $a_0=6.625$ Å, $b_0=11.53$ Å, and $c_0=15.12$ Å." His unit cell has a simple relationship to the cell selected in this study and multiplication of Staples' a_0 and b_0 dimensions by the factors shown indicates that the sizes of the cells are similar.*

Staples (1957)	This study
a_0 $6.625\times 2 \quad =13.25$	
b_0 $11.53\ \times 2/\sqrt{3}=13.31$	$a_0=13.20$
c_0 15.12	$c_0=15.07$

The *x*-ray observations can be adequately explained by a hexagonal lattice, and the following two observations indicate that there is no measureable deviation from hexagonal symmetry: (1) Certain of the diffraction peaks have one set of hexagonal indices and two independent sets of orthorhombic indices. (An example is hexagonal 20·0 which is both 020 and 110 in the orthorhombic lattice.) The splitting or broadening of these peaks on the diffractometer traces would indicate an orthorhombic symmetry, but none of the dozen peaks of this type which were observed showed any sign of broadening or splitting. (2) The intensities as well as

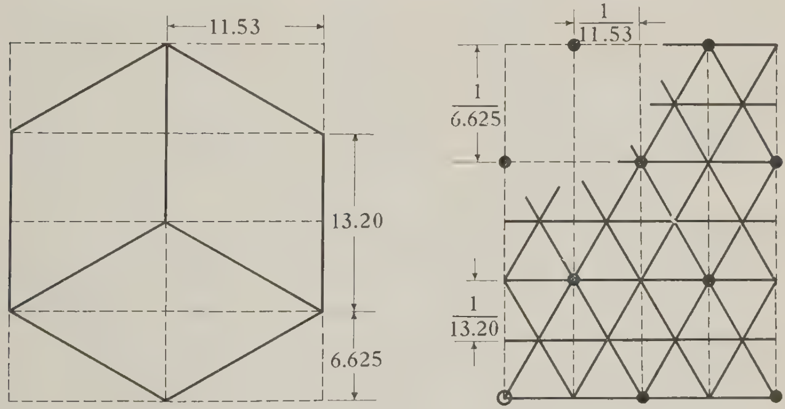

(a) (b)

FIG. 1. Comparison of orthorhombic (dashed lines) and hexagonal (solid lines) lattices for erionite. (a) Direct lattice. (b) Reciprocal lattice. Heavy dots indicate those reciprocal lattice points which have two sets of orthorhombic indices approaching the same *d* spacing.

---

* After the completion of this study, Staples and Gard stated in an abstract for the June 5, 1958 meeting of the Mineralogical Society that electron diffraction data on material from the type locality indicated a hexagonal unit cell of very nearly the same size as the one suggested in this report.

the positions of spots on the Weissenberg photograph show a sixfold symmetry which can be explained only by a hexagonal lattice or by nearly perfect pseudohexagonal twinning in which exactly equal amounts of each member of the twin is present.

Chemical Composition

Considerable labor was expended in an unsuccessful attempt to concentrate a sample of erionite of sufficient size and purity for a chemical analysis. The agreement between the mole fraction of aluminum and the mole fraction of total alkalis and alkaline earths is frequently used as a check on the quality of zeolite analyses, and since Eakle's original analysis shows an excellent agreement it has been used in the calculation of unit cell contents:

	wt. %	moles/100 grams		atoms/unit cell		
SiO_2	57.16	.953		Si	27.00	36
Al_2O_3	16.08	.158		Al	8.95	
CaO	3.50	.062	.158	Ca	1.76	
MgO	0.66	.017		Mg	0.48	
K_2O	3.51	.039		K	2.21	
Na_2O	2.47	.040		Na	2.26	
H_2O	17.30	.960		H_2O	27.2	
				O	71.9	72

The unit cell is probably composed of 36 tetrahedrally coordinated silicon and aluminum atoms linked into chains by sharing of the oxygen atoms at the corners of the tetrahedra. The alkali and alkaline earth atoms and water molecules occupy open spaces within the framework.

The unit cell composition proposed by Staples (1957) contains 16 Al and Si atoms in a cell having half the volume of the one suggested in this study. A calculation based on his unit cell dimensions and cell contents gives a density of 1.825 grams/cc., a result which seems too low to be considered reasonable.

Ion Exchange

Potassium, silver, and thallium ions were substituted for the alkali ions in erionite by heating finely ground crystals in a low melting salt of the heavy metal. The exchanged zeolites have refractive indices considerably greater than the natural product and *x*-ray diffractometer observations show that the intensities of the peaks are greatly changed but the cell dimensions remain constant, indicating a substitution which does not affect the structural framework.

OCCURRENCES

At the type locality erionite is found in association with opal in fractures in rhyolite tuff. Thus far, in addition to the type locality, erionite has been found in sediments of late Cenozoic age in Nevada and in early Cenozoic sediments from Wyoming and South Dakota.

An outcrop near the center of sec. 8, T.27N., R.40E. in northern Jersey Valley in the Sonoma Range Quadrangle, Nevada, has been the source of the material used for the mineralogical studies in this report. For this reason a relatively complete description of the outcrop is included. The outcrop is near the top of a thick sequence of Miocene and early Pliocene sediments. The nearest fossils are early Pliocene in age and are about 700 feet lower in the sequence. Figure 3 is a photograph of the tuff bed and a description is included in Fig. 2. A small quarry at this site has been a source of building stone.

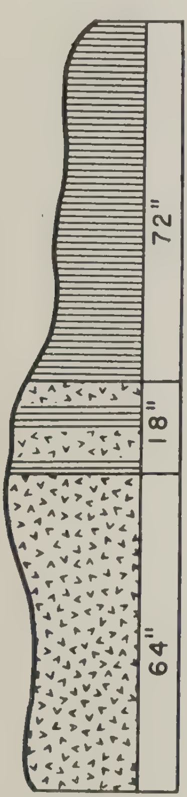

The uppermost part of the erionite bed is thin-bedded and fissile with fish fossils preserved along the bedding planes. The lower part is bedded but it is not fissile. Two well-developed sets of joints perpendicular to the bedding direction break the rock into equant blocks roughly one foot in size. Diffusion bands of orange color alternating with a gray background are present parallel to the joint surfaces and the bands are continuous across the bedding planes. The entire unit is composed of a mass of extremely fine erionite fibers with occasional grains of glass and plagioclase.

Alternating beds of tuff and erionite, similar respectively to the beds below and above.

Silver-gray rhyolite tuff, composed of well-sorted glass shards with a refractive index of 1.503. Plagioclase, zircon, quartz, and magnetite are present in very small amounts. The rock contains about 5% of radiating groups of erionite crystals about $\frac{1}{4}$ mm. long which were used for the measurements in this report. The tuff is soft but not friable. Ripple marks and disturbed bedding are occasionally present in the upper half of this unit.

FIG. 2. Section through beds composed of vitric tuff and erionite, Jersey Valley, Nevada.

In central Nevada erionite has been found in early Pliocene sediments in the Shoshone Range (T.27N., R.44E., Sec. 1) and in the valley of the Reese River (T.24N., R.43E., Sec. 26). In both localities erionite is found both as relatively pure beds and as mixtures with clinoptilolite. Erionite has been found by Regnier (personal communication) in lacustrine beds of Blancan (Plio-Pleistocene) age in Pine Valley south of Carlin, Nevada.

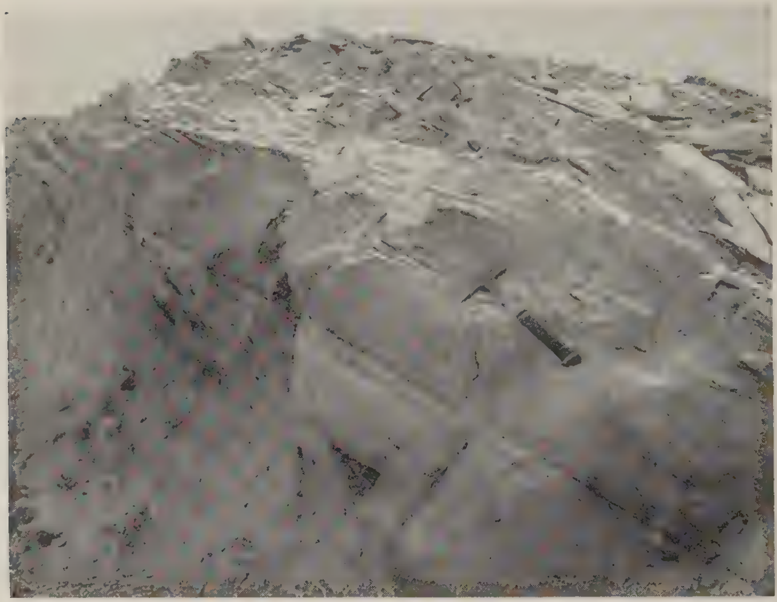

FIG. 3. Photograph of outcrop of unit described in Fig. 2. The beds composed of erionite begin about a foot above the head of the hammer.

In central Wyoming a mixture of erionite and clinoptilolite has been found by Van Houten (1954, personal communication, 1957) in thin bedded light gray altered tuff in the upper and middle Eocene rocks along the Beaver Divide east of Sand Draw. Samples of the White River (Oligocene) formation from South Dakota in the Princeton University collection which have been described by Wanless (1922) as mordenite, were re-examined by *x*-ray techniques and were found to contain a mixture of erionite and clinoptilolite.

A synthetic preparation of erionite has been reported by Breck et al. (1956).

SUMMARY

On the basis of a detailed mineralogical analysis it is concluded that erionite has erroneously been assigned to the orthorhombic system and that the optical properties and x-ray measurements are consistent with hexagonal symmetry. The mineral has the distinction of being the only known hexagonal fibrous zeolite.

Most frequently erionite has been formed by the alteration of acidic volcanic material, especially vitric ash which was deposited in lacustrine environments; moreover present knowledge of its distribution shows it is much less rare than it was formerly thought to be.

REFERENCES

BASS, M. N., 1957, Effects of gamma radiation on the physical properties of minerals: *Am. Mineral.* **42,** 100–104.

BRECK, D. W., EVERSOLE, W. G., MILTON, R. M., REED, T. B., AND THOMAS, T. L., 1956, Crystalline zeolites. I. The properties of a new synthetic zeolite, type A: *Jour. Am. Chem. Soc.*, **78,** 5963–5971.

BUERGER, M. J., 1942, *X*-Ray Crystallography, John Wiley and Sons, New York, 531 p.

EAKLE, A. S., 1898, Erionite, a new zeolite: *Am. Jour. Sci.*, 4th Ser., **6,** 66–68.

LARSEN, E. S., 1921, The microscopic determination of the nonopaque minerals: *U. S. Geol. Survey Bull.* **679.**

STAPLES, L. W., 1957, *X*-ray study of erionite, a fibrous zeolite: *Geol. Soc. Amer. Bull.*, **68,** 1847.

VAN HOUTEN, F. B., 1954, Geology of the Long Creek-Beaver Divide area, Fremont County, Wyoming: *U. S. Geol. Survey Oil and Gas Invest.* Map **OM 140.**

WANLESS, H. R., 1922, Lithology of the White River sediments: *Am. Philos. Soc., Proc.*, **61,** 184–233.

Manuscript received June 16, 1958.

THE AMERICAN MINERALOGIST, VOL. 44, MAY–JUNE, 1959

A COMPARATIVE STUDY OF TEN MONAZITES

MARTIN W. MOLLOY, *Columbia University, New York, New York.*

ABSTRACT

Optical, *x*-ray, and differential thermal methods are used to compare monazite recently discovered near Chester, New Jersey, with monazite from nine other localities. Indices of refraction, 2V and birefringence have been determined. *X*-ray diffraction patterns have been measured, indexed, and their relationships determined. Micro-camera diffraction patterns have provided information on the alteration of monazite. The application of *x*-ray fluorescence to the quantitative analysis of rare earth elements in monazite is shown to be feasible through sensitivity to minor variations caused by crystal fractionation. Theoretical factors which interfere with precise *x*-ray fluorescence, quantitative analysis of rare earth elements in monazite are examined. The effect of two types of alteration, intercrystalline and intracrystalline, upon the differential thermal pattern of monazite is observed.

INTRODUCTION

Monazite was found near Chester, Morris County, north central New Jersey during the recent, intense search for uranium. A pit in the topsoil of Mr. William Waldon's cornfield provided the first specimens. The Mineralogical Laboratory of the Department of Geology, Columbia University, received radioactive samples from this locality from Eastern Uranium, Inc.

The specimens are dense, fine-grained, reddish brown, with surficial limonite staining, and are cut by coarsely crystalline, non-radioactive quartz veins. The radioactive material is monazite with a high thorium content. Partial chemical analysis by Ledoux and Company, Teaneck, New Jersey, reports 53.36 per cent total rare earth oxide, 13.66 per cent ThO_2, 25.31 per cent P_2O_5, and 0.045 per cent U_3O_8. In thin section the specimens show numerous, euhedral monazite crystals associated with zoned zircon and quartz (Pl. 1: 1*a*, 1*b*).

About 200 pounds of high-grade monazite were recovered from the property. The monazite occurs both as soil residium and fractured blocks, associated with fractured blocks of quartz-feldspar granite. A 20 foot deep trench failed to reveal bedrock.

Specimens from this locality have been studied over a two year period. During this time the Chester monazite has been compared with specimens from nine other localities utilizing optical, *x*-ray diffraction, *x*-ray fluorescence, and differential thermal methods. Material from Chester has also been examined by Drs. E. C. T. Chao and Charles Milton of the U. S. Geological Survey (Markewicz, Chao, and Milton, 1957).

This study has been materially aided by the cooperation of the New Jersey Department of Conservation and Economic Development. Dr. Meredith Johnson and Mr. Frank Markewicz have been particularly helpful in the interpretation of field relations.

This problem was suggested, and the study guided by Dr. Paul F. Kerr, Professor of Mineralogy, Department of Geology, Columbia University. Substantial assistance has been received in the interpretation of differential thermal data from Dr. Otto Kopp, and of x-ray diffraction data from Mr. Samuel Kamhi. To these and to Miss Peggy-Kay Hamilton, Dr. Dana Kelley, and Dr. William A. Bassett of the mineralogy group at Columbia the writer wishes to express his appreciation for their kind assistance.

Monazite Localities

The monazite localities listed below are referred to in the text that follows by the simplified locality names. In the tables the Chester occurrence is listed first, followed by other localities in alphabetical order. These specimens were large, single crystals without megascopic intergrowths of foreign material, and were obtained from the Mineralogical Research Collection of the Department of Geology, Columbia University.

Locality Information	*Locality Name*
William Waldon farm, Chester, Morris County, New Jersey	Chester
Amelia, Virginia, #234C Hoadley Collection, from the D'Agostino Collection	Amelia
"Cryptolite in Apatite," N'otero, Arendal, Norway	Arendal
Augusta Court House, Virginia, Eggleston Collection	Augusta
Madison County, North Carolina; G. L. English and Company, New York	Madison
Minas Geraes, Brazil	Minas Geraes
Missoula, Montana	Missoula
South Lynne, Connecticut (Matthews, 1894)	S. Lynne
Ramsey Mine, Toledo, North Carolina	Toledo
Ural Mountains, Russia	Urals

Optical Properties

Oriented and random thin sections, as well as fragment mounts, were studied with the petrographic microscope and universal stage. Indices of refraction were determined in sodium light with high index liquids (Meyrowitz and Larsen, 1951). The optical properties are given in Table 1.

The extent of alteration is indicated by the color of the mineral, which changes from greenish yellow to opaque brown as alteration increases. Cleavage and alteration are also related. Unaltered specimens are free from cleavage, but as alteration increases, cleavage appears first in one, then in two, and finally in three directions. The most altered specimens have the lowest indices of refraction, while the least altered specimens yield the highest indices.

The associated alteration consists of limonite-stained masses or cloud-

TABLE 1. OPTICAL PROPERTIES OF TEN MONAZITES

Locality	Color	Cleavage Directions	Refractive Index (±.002) n_α n_γ	Birefringence	2V+	Degree of Opacity (Associated Alteration in per cent)
Chester	Yellow-brown	1 Good 1 Poor	1.775–1.836	.061	16°	75
Amelia	Greenish-yellow	Indistinct	1.788–1.851	.063	13°	25
Arendal	Greenish-brownish-yellow	Indistinct	1.780–1.839	.059	11.5°	37
Augusta	Greenish-yellow	Indistinct	1.774–1.849	.075	15°	65
Madison	Greenish-yellow	None	1.782–1.850	.068	16°	15
Minas Geraes	Brownish-greenish-yellow	2 Poor	1.790–1.850	.061	13°	50
Missoula	Greenish-brownish-yellow	Indistinct	1.789–1.847	.058	12°	30
S. Lynne	Greenish-brown	2 Poor	1.777–1.841	.064	15°	70
Toledo	Brown	2 Good	1.775–1.828	.053	15°	63
Urals	Brown	3 Good	1.784–1.843	.059	16°	63

like clusters of minute, opaque particles which spread through monazite crystals, sometimes following cleavage planes (Pl. 2: 2*a*, 2*b*). The degree of opacity is a measure of the degree of alteration and was determined by PhotoVolt meter readings on representative areas of oriented thin sections.

In thin section monazite is not noticeably pleochroic. The dispersion $r<v$ is weak. All specimens were biaxial positive with a small 2V. The optic angle does not show a clear relation either to the degree of associated alteration or to the chemical composition as indicated by *x*-ray fluorescence. The only example of twinning was found in the Toledo specimen, and this was of the polysynthetic type. The Madison sample consisted of rounded, placer grains, and except for this and the previously described Chester material, all specimens were large, single crystals.

DIFFERENTIAL THERMAL ANALYSIS

The monazite specimens were examined by differential thermal analysis using equipment previously described (Kerr and Kulp, 1948; Kulp and Kerr, 1949; Kulp and Perfetti, 1950). Background drift effects were removed and the corrected curves plotted (Fig. 1). In all cases sample grain size and furnace loading were duplicated as closely as possible. Despite attempts at standardization, minor variations may occur in thermal patterns produced by the same material in different furnace

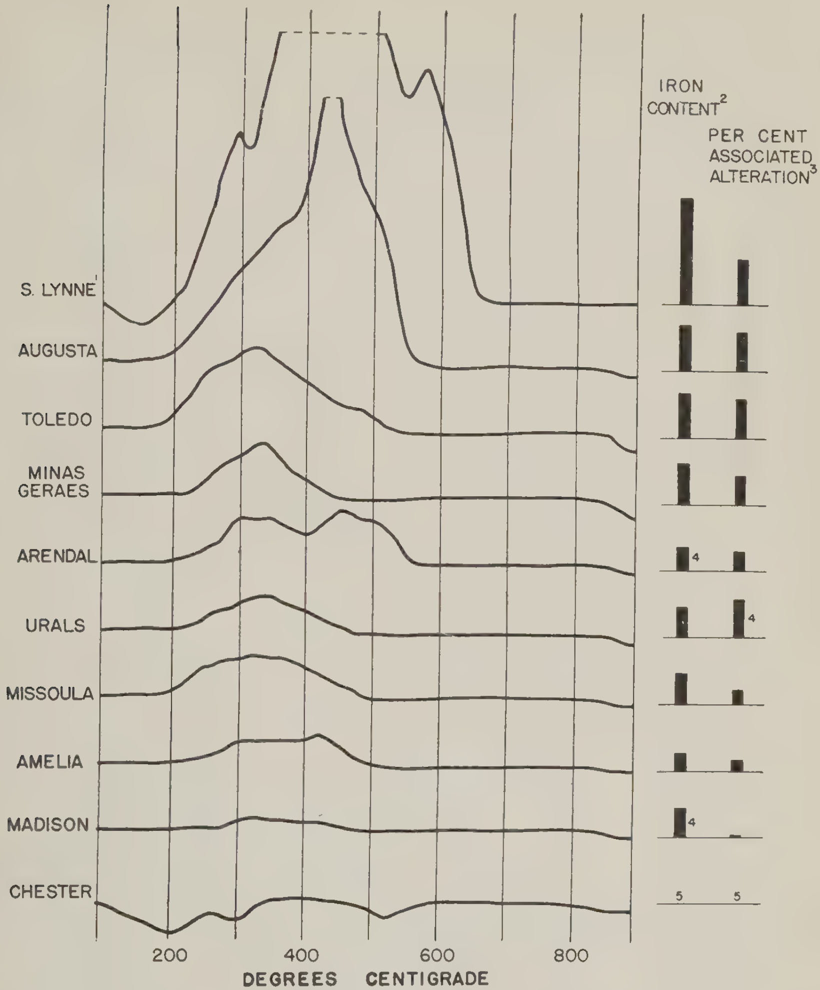

FIG. 1. Differential thermal curves of ten monazites[1] in comparison with iron content[2] and per cent alterations.[3]

[1] Arranged in order of the intensity of the 330° C. peak.

[2] From *x*-ray fluorescence analysis.

[3] Determined by PhotoVolt light meter readings on representative areas of oriented thin sections.

[4] Order inconsistent with that of thermal peaks.

[5] Interstitial limonite masks pattern from intracrystalline alteration.

runs; however, no significant variations in peak position or intensity were observed.

The exothermic reactions recorded occur in the 200–600° C. range. The

Table 2. *d* Å and Relative Intensity Diffraction Patterns of Ten Monazites

Chester		Amelia		Arendal		Augusta		Madison		Minas Geraes		Missoula		S. Lynne		Toledo		Urals	
														5.40	10				
5.23	10	5.26	16			5.25	11	5.21	12	5.22	10	5.22	6	5.21	13	5.21	17	5.22	10
5.17	10			5.17	9											5.16	14	5.16B	9
						5.05	9												
4.82	8	4.82	8							4.80	12	4.81	15			4.78	22	4.81	12
4.68	17	4.69	14	4.68	13	4.67	17	4.68	7	4.68	13	4.68	16	4.68	16	4.67	35	4.68	19
														4.42	13				
4.18	37	4.18	25	4.17	23	4.18	22	4.17	19	4.19	23	4.17	21	4.18	36	4.17	40	4.18	28
4.10	29	4.10	18	4.09B	14	4.10	11			4.10	19	4.11	18	4.11	19	4.08	23	4.10	19
3.95	10							3.95	8										
						3.85	11			3.85	9	3.84	7						
														3.53	23	3.54	27	3.53	18
3.52	29	3.52	25	3.51	44	3.49	19	3.51	44	3.51	32	3.51	28	3.51	33	3.52	31	3.51	29
3.44	15	3.48	14							3.46	13	3.46	6			3.44	48		
3.30	71	3.29	44	3.28	73	3.28	53	3.29	63	3.30	61	3.29	75	3.30	87	3.29	85	3.30	90
3.21B	11							3.21B	12			3.21	7						
						3.12	11							3.13	11	3.13	20	3.13	36
3.09	100	3.08	100	3.07	100	3.07	100	3.08	100	3.08	100	3.08	100	3.08	100	3.08	100	3.09	100
2.98	25	2.98	16	2.97	17	2.98	20	2.98	12	2.98	13	2.98	19	2.99	17	2.98	25	2.98	13
		2.96	12																
2.87	53	2.88	46	2.87	39	2.88	31	2.87	40	2.88	22	2.88	28	2.87	49	2.87	96	2.87	59
2.83	22					2.81	5					2.91	6	2.83	11				
2.79	8	2.78	7											2.79	9	2.79	17	2.78	7
2.70B	6	2.70	6	2.71B	5			2.71	7	2.71	9			2.72	7	2.72	11		
						2.67	5			2.65	6			2.65	13	2.68	7	2.68	7
2.61	19	2.62B	8	2.61B	6	2.61	12	2.61B	9	2.62B	12	2.60	10	2.61	23	2.61	15	2.61	16
2.57	5	2.57B	6	2.58	8					2.58B	5	2.58B	5						
		2.52	5	2.52	5														
2.45B	19	2.45	16	2.44B	6	2.45B	11	2.43	14	2.44	14	2.44	18	2.44	26	2.44	23	2.44	12
2.41	7			2.41	6			2.40	8			2.40	12			2.41	17		
						2.29	9												
2.21	19	2.22B	9																
2.17B	24	2.17	16	2.16	14	2.16	20	2.17	39	2.17	28	2.18	15	2.17	23	2.18	27	2.17	14
2.13	36	2.13B	21	2.13	14	2.13B	19	2.13	16	2.14	23	2.13	15	2.13	29	2.13	35	2.13	25

Chester		Amelia		Arendal		Augusta		Madison		Minas Geraes		Missoula		S. Lynne		Toledo		Urals	
2.12	39	2.12B	23	2.11B	16	2.11B	20	2.11	18	2.11	19	2.12B	18	2.11	37	2.11	27	2.11	20
2.09	24							2.09	11			2.09	6						
2.08	27							2.07	11										
2.03	15					2.02	8												
1.99	15									1.99	7								
1.98	17	1.98	25			1.98	8			1.98B	10	1.98B	13	1.98	27	1.98	25	1.98	20
1.97	14			1.97B	14			1.97B	16							1.97	12		
1.94	14			1.95	10					1.95B	10	1.95	11	1.95	14	1.95	9		
1.90B	17	1.90	14			1.90	5	1.92	10	1.91	13			1.90	13	1.91	15	1.90	12
1.88B	15	1.88	39	1.88B	13	1.88B	16			1.88B	13	1.88	21	1.88	24	1.88B	17	1.88B	20
				1.87B	16	1.87B	17	1.87B	21	1.87	26	1.86	21	1.86	27	1.85	17		
1.79	14	1.80	10	1.79	12			1.81	12							1.79	15	1.79B	10
1.78	10					1.78	12												
1.77	10	1.77	7									1.77	10	1.77	20	1.77	7		
		1.75B	14	1.75B	12					1.76	12					1.75	21	1.75B	13
1.73	20	1.73	16			1.73B	14	1.73	26	1.73	19	1.73	19	1.73	19	1.73	27		
1.72	20			1.72B	13	1.72B	13							1.72	19	1.72B	20	1.72	14
		1.69	18	1.69	11	1.69	17	1.69B	19	1.69B	14	1.69	16	1.69B	11	1.69	15	1.69	14
1.65	17	1.65	14	1.66	8	1.65	11	1.65	8	1.65B	7			1.65	11	1.65	12		
		1.62	9																
1.61	17	1.61	11			1.61	8	1.61	6	1.61	14	1.61	7	1.61	11				
1.59	15			1.59	7			1.59	5					1.59	10	1.58	13	1.59	16
1.54	12	1.55B	7							1.55	9					1.57	10		
																		1.53	6

B = broad.

broad, moderately intense peak is a composite of three exothermic reactions, which are distinctly resolved in the S. Lynne pattern. These occur about 250° C., 330° C., and 430° C. with the last peak being delayed until 570° C. in specimens with intense reactions. This indicates that the high temperature peak is due to oxidation, and is delayed by depletion of oxygen in the system by a previous oxidation reaction.

The Chester sample shows endothermic reactions at 250–300° C. and 560° C. The lower peak is distorted by the effects of the superposed 250° C. and 330° C. exothermic reactions noted above. A similar exothermic trend appears at the start of the S. Lynne pattern. The bifurcation noted in the high temperature exothermic peak of the Arendal material has not been explained.

Evaluation of the Differential Thermal Analysis

As a common placer mineral, monazite is distinguished by chemical resistance and refractivity. Madison, the sample showing the least alteration, has an almost featureless differential thermal pattern, while S. Lynne and Augusta, samples with high iron content and extensive alteration, yield pronounced exothermic reactions. The relation of iron content, degree of alteration, and intensity of the exothermic reactions is shown in each sample by the height of the 330° C. peak (Fig. 1). It seems likely that the exothermic reactions recorded are due to alteration and iron content, and that the differential thermal pattern of an alteration- and iron-free monazite would be featureless.

The alteration in the Chester monazite is predominately intercrystalline, as opposed to the almost exclusively intracrystalline nature of the alteration in the other monazites. While the monazite crystals of the Chester sample are only slightly altered, they are surrounded by large areas of reddish brown, isotropic material (Pl. 1: 1*a*, 1*b*). *X*-ray diffraction micro-camera photographs show this material to be primarily goethite. The differential thermal pattern of goethite is distinguished by a single, large endothermic reaction in the 300–400° C. region (Posnjack and Merwin, 1919). Poorly crystalline goethite gives the same reaction at 293° C. or lower (Arens, 1951). The alteration in the Chester sample yields water when heated. The effect of the endothermic reactions of goethite and water upon the exothermic pattern of monazite would be a distortion of both patterns. The Chester pattern is therefore interpreted as a composite of the 250° C., 330° C., and 430° C. exothermic reactions due to the monazite alteration superimposed on the 200–400° C. endothermic reactions of goethite and water.

Differential thermal analysis indicates that the thermal pattern of unaltered monazite is featureless, and that the reactions observed are caused by the oxidation and inversion of iron present in the alteration minerals. The associated 250° C., 330° C., and 430° C. exothermic alteration reactions are sufficiently consistent, however, to suggest the presence of monazite in differential thermal curves.

X-RAY DIFFRACTION

Except for a similarity to huttonite (Pabst and Hutton, 1951), monazite is easily distinguished by its characteristic *x*-ray powder pattern. Variation in rare earth composition causes a small range in cell dimensions among different monazites. Lines caused by significant, crystalline impurities often appear superimposed on a monazite pattern.

In the 2θ range, 10–60°, 93 reflections may be computed for monazite. This complex structure plus the variety of substitutions possible among its rare earth and thorium components, creates an intricate diffraction pattern with a few intense reflections and many that are small and overlap. In such a case the impulse counting technique of the *x*-ray diffractometer has been used in preference to the photographic method for the detection of faint reflections and in determining relative intensities.

Diffractometer charts produced by the Norelco instrument have been analyzed, and a tabulation of *d* Å spacings and relative intensity measurements prepared (Table 2). These data have been plotted graphically in Fig. 2 to show the range in intensity and position of the monazite reflections. In this plot, the data from Fig. 1 are represented as points, and vertical lines have been drawn joining points with the same (*hkl*) value. The accuracy of these *d* Å measurements increases as the spacing decreases, with the error diminishing from ±0.05 Å for the largest spacing to ±0.002 Å for the smallest.

The unit cell dimensions for monazite by Gliszczynski (1939) and Parrish (1939) are listed in Table 3. These yield the theoretical *d* Å spacings corresponding to the (*hkl*) values of monazite when substituted in the indexing equation for a monoclinic crystal (Klug and Alexander, 1954).

TABLE 3. UNIT CELL DIMENSIONS OF MONAZITE

	Gliszczynski	Parrish
a_0	6.782 kX	6.76 kX
b_0	6.993 kX	7.00 kX
c_0	6.445 kX	6.42 kX
β	76°22′	76°50′
$a:b:c$	.9686:1:.9231	.9660:1:.9167
S.G. (meas.)	—	5.173
S.G. (calc.)	5.217	5.06
Cell Volume	—	296

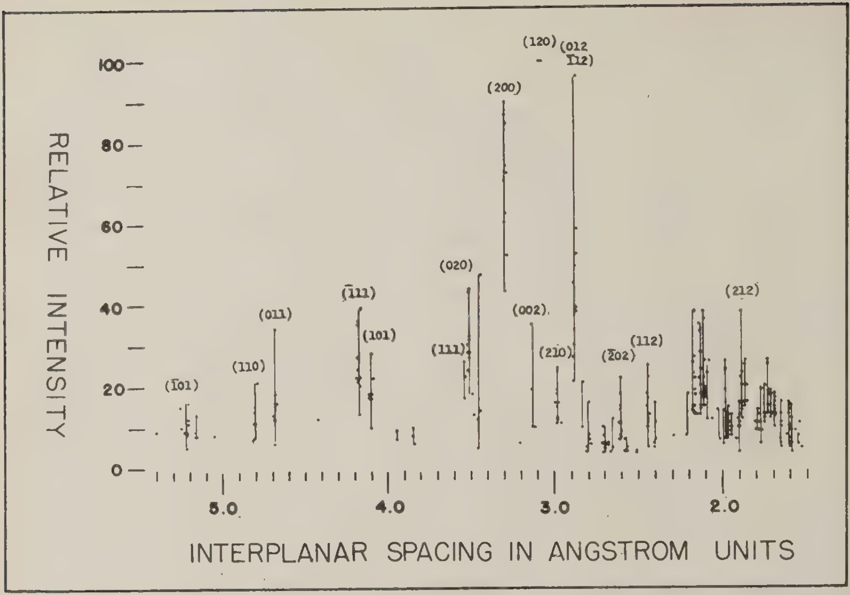

Fig. 2. Relative intensity vs *d* Å for monazite. Both the range in reflection position and intensity for any lattice plane are indicated in this diagram.

The calculations are listed in Table 4 in comparison with the ASTM monazite standard (Chochi-wan, Southern Korea; Pabst and Hutton, 1951), and the spacings obtained from the ten monazites studied (Table 2). Spacings which do not correspond to theoretical values are listed separately and are attributed to crystalline impurities. A number of spacings in the small *d* Å range may coincide with reflections caused by impurities.

The Alteration of Monazite

The nature of the alteration of monazite is of interest. *X*-ray diffraction patterns show reflections unaccounted for by the monazite structure (Table 4). However, the diffraction pattern of monazite masks that of goethite and other expectable minerals. Unless the fine alteration constituents can be concentrated to yield a pattern distinct from the host mineral, the powder method has serious limitations for identification.

It is possible to study randomly oriented crystallites as small as 50 microns (0.002 inches) in diameter, and obtain a diffraction photograph with the *x*-ray micro-camera. The technique was developed for use in synthetic fiber studies by Fankuchen and Mark (1944), and subsequently applied to mineral identification in the clay alteration studies of Kelley and Kerr (1957).

TABLE 4. *X*-RAY DIFFRACTION SPACINGS OF TEN MONAZITES FOR THE RANGE d Å $= \infty - 1.530$

hkl	$d_{calc.}$ (Å)*	Reference Monazite†		Ten Monazites $d_{obs.}$ (Å)	Impurities d Å
		d Å	I/I		
					5.40
$\bar{1}01$	5.205	5.23	40	5.21–5.26	5.16–5.18
110	4.806	4.72	40	4.78–4.82	4.05
011	4.677			4.67–4.69	4.42
$\bar{1}11$	4.178	4.17	60	4.17–4.19	3.95
101	4.090			4.08–4.11	3.84–3.85
111	3.537	3.52	50	3.53–3.54	3.48
020	3.504			3.49–3.52	3.44–3.46
200	3.299	3.31	70	3.28–3.30	3.21
002	3.143			3.12–3.13	
120	3.095	3.09	100	3.07–3.09	
021	3.060				
210	2.988	2.99	20	2.97–2.99	
$\bar{2}11$	2.953				
$\bar{1}21$	2.908				
012	2.867	2.88	70	2.87–2.88	2.81
$\bar{1}12$	2.865				
221	2.835			2.83	2.78–2.79
121	2.662			2.65–2.68	2.70–2.72
$\bar{2}02$	2.604	2.61	20	2.60–2.62	2.57–2.58
211	2.495				2.52
112	2.447	2.45‡	30B	2.43–2.45	
$\bar{2}12$	2.441			2.40–2.41	
220	2.403				
022	2.340				
$\bar{1}22$	2.338				
$\bar{3}01$	2.251				2.29
130	2.202				2.21–2.22
013	2.189	2.19	40	2.16–2.18	
$\bar{1}03$	2.148				
$\bar{3}11$	2.142	2.14	60	2.13–2.14	
131	2.131				
221	2.126			2.11–2.12	
310	2.100				
122	2.093				
$\bar{2}22$	2.090			2.09	2.07–2.08
$\bar{1}13$	2.054				
202	2.048				
131	2.029			2.02–2.03	
013	2.007				
$\bar{2}03$	1.995			1.98	
212	1.967	1.97	50	1.97	
$\bar{3}12$	1.962	1.96	10		
301	1.941			1.94–1.95	
$\bar{2}13$	1.919			1.90–1.91	
230	1.907	1.90B	20		
$\bar{2}31$	1.898				

B = broad.

* Calculations based on the unit cell dimensions of Gliszczynski (1939), see Table 3. Systematic extinction occurs when $k \neq 2n$ in $0k0$, and $h+l \neq 2n$ in $h0l$. In addition, $\overline{hkl} = hkl$; $hkl = h\bar{k}l$; and $\bar{h}kl = hk\bar{l}$.

† ASTM reference monazite, Pabst and Hutton (1951).

‡ Spacings on the ASTM card were not indexed beyond this point.

TABLE 4 (*continued*)

hkl	$d_{calc.}$ (Å)*	Reference Monazite†		Ten Monazites $d_{obs.}$ (Å)	Impurities *d* Å
		d Å	I/I		
$\bar{3}21$	1.893	1.88B	60	1.88–1.89	
032	1.875				
103	1.874			1.85–1.87	
$\bar{1}32$	1.874				
311	1.866				
320	1.864				
113	1.817			1.79–1.81	
$\bar{1}23$	1.817				
023	1.798	1.80	20		
222	1.769	1.77	40	1.77	1.78
$\bar{3}22$	1.766				
231	1.760			1.75–1.76	
040	1.752	1.75	60		
132	1.741				
$\bar{2}32$	1.739				
$\bar{3}03$	1.735				
223	1.733			1.73	1.72
321	1.697	1.70	60	1.69	
140	1.693				
$\bar{0}41$	1.687				
313	1.687				
$\bar{4}02$	1.662				
$\bar{1}41$	1.660			1.65–1.66	
123	1.657				
400	1.651	1.65	10		
$\bar{4}11$	1.650				
$\bar{3}31$	1.620	1.63	10	1.62	
$\bar{4}12$	1.618				
$\bar{1}04$	1.617				
$\bar{2}04$	1.615				
141	1.611	1.61	10	1.61	
410	1.607				
330	1.602				
312	1.589			1.58–1.59	
$\bar{1}14$	1.575				
$\bar{2}14$	1.574				
004	1.571			1.57	
213	1.565				
033	1.559				
$\bar{3}23$	1.555				
240	1.548			1.54–1.55	
241	1.543				
232	1.540	1.54	40		
$\bar{3}32$	1.537				
014	1.533			1.53	
042	1.530				
$\bar{1}42$	1.530				

Minute, reddish brown masses comprising the opaque areas between monazite crystals in the Chester monazite (Pl. 1: 1*a*, 1*b*) were removed from the thin section and photographed with the micro-camera using molybdenum filtered iron radiation to reduce the intense background. The film obtained matched that of goethite, although there were extrane-

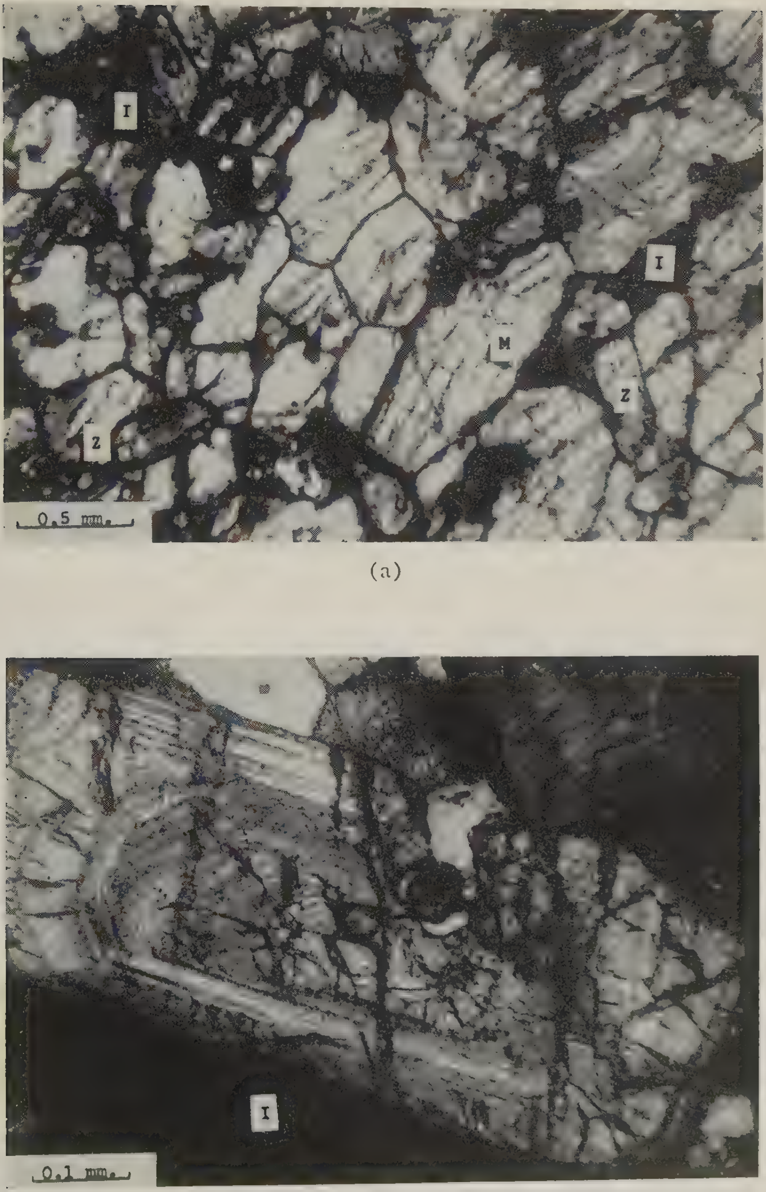

(a)

(b)

Plate 1. a. Thin section, Chester; slightly altered, euhedral monazite crystals (M) associated with zoned zircon (Z) and interstitial iron oxides (I).

b. Thin section, Chester; embayed, zoned zircon crystal partly surrounded by iron oxides (I). (× nicols.)

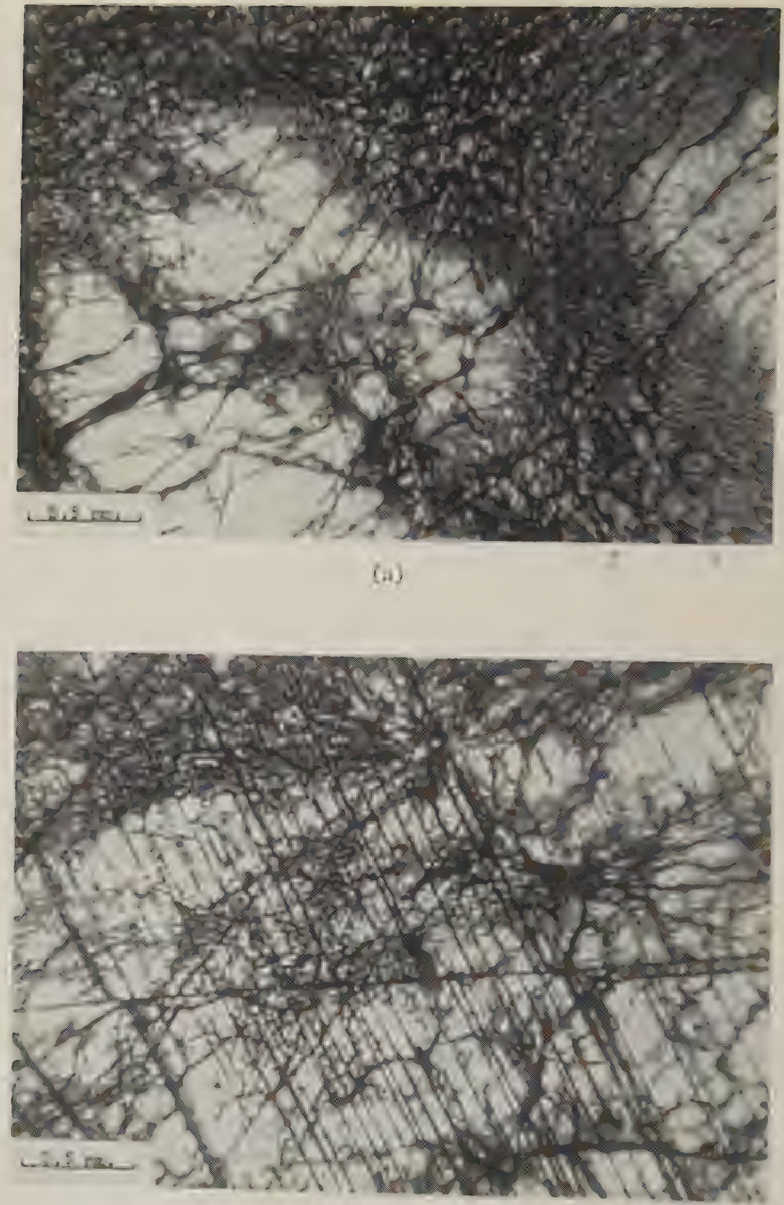

(a)

(b)

PLATE 2. a. Thin section, Minas Geraes; cloud-like alteration penetrating a single, uncleaved monazite crystal.

b. Thin section, Urals; alteration occurring both in patches and following the distinctive cleavage in this monazite crystal.

ous lines which could not be identified. Together with the high iron content from *x*-ray fluorescence and the nature of the thermal pattern, the micro-camera photographs confirm the identification of the opaque, interstitial material associated with the Chester sample as "limonite," or more specifically, goethite plus hydrous iron oxides (Mackenzie, 1957; Kulp and Trites, 1951; Blanchard, 1944).

However, limonite is not the alteration product within the monazite crystals. Thermal data indicate this to be a non-hydrous, ferrous oxide. Micro-camera photographs taken of areas of alteration in thin sections of the most altered specimens did not show any lines. Increasing the exposure of these photographs to 24 hours of Mn filtered Fe radiation produced no indication of a powder pattern due to the alteration mineral. With an exposure of this long a duration the white background continuum present even in filtered *x*-radiation is sufficient to produce a Laue photograph from the enclosing monazite crystal.

In view of the absence of any indication of crystallinity of the alteration product in the micro-camera photographs in specimens with a sufficient number of alteration particles to produce an *x*-ray diffraction pattern, the conclusion must be drawn that the material is not crystalline.

X-Ray Fluorescence Analysis

The elements from atomic number 57 to 71 (La, Ce, Pr, Nd, Sm, Eu, Gd, Tb, Dy, Ho, Er, Tm, Yb, and Lu) comprise the rare earth group. Accurate quantitative analysis for many of these elements is not possible by standard wet chemical methods. Such analysis is presently accomplished by emission spectroscopy and spectrophotometry. It is the purpose of this section to provide a basis for the extension of the *x*-ray fluorescence method (*x*-ray spectroscopy) to the quantitative analysis of rare earth elements in monazite.

X-ray spectroscopy is applicable to the detection of lithium (atomic number 3) and all heavier elements. The significant advantages of the fluorescence method are the reliability of the identification regardless of the particular element(s) involved, and the rapidity with which the analysis is made. Thus, in the case of the qualitative analysis of a complex system such as the rare earth elements in monazite, the *x*-ray fluorescence method is desirable.

The application of this method to the quantitative analysis of many of the common elements has already been done. This is dependent upon the fact that the intensity of the secondary *x*-ray spectra which an element may emit is a function of the amount of that element present in the sample. Measurement of the intensity of the secondary spectra of an element, therefore, is the means by which quantitative analysis is accomplished by x-ray fluorescence.

When it is desirable to perform the quantitative analysis of an element by x-ray fluorescence, the particular instrument must be calibrated for that element. Normally this entails preparing a series of artificial standards closely approaching the sample in composition and covering the entire range of per cent in which the element is present. Often another element not found in the sample is added so that it will reflect any unusual events which may happen. This is known as the "internal standard" method. The samples are then run on the instrument and working curves for the elements prepared.

In the case of simple systems comprised of a few common elements, such procedure is routine. As the number of elements increases, however, the problem of mutual interference in their determination becomes most serious. The mineral monazite presents just such a case.

One of the major problems in dealing with the rare earth elements is the difficulty and expense in obtaining chemically pure material for the preparation of artificial standards. The other problem is the tendency of the rare earths to occur in groups rather than alone.

Eight rare earth elements (La, Ce, Pr, Nd, Sm, Gd, Dy, and Ho) in monazite are easily detectable by x-ray fluorescence. Several other elements (Th, Y, U, Pb, and Fe) accompany the rare earths. The x-ray tube background of W, Fe, Cu, and Ni should not be overlooked. Mutual interferences between these 17 elements form the barrier to the quantitative analysis of monazite by x-ray fluorescence. To eliminate this obstacle, the following analysis of these interferences was undertaken.

As has been pointed out, quantitative analysis of an element by x-ray fluorescence depends solely upon measurement of the intensity of the secondary spectra. Any factors which affect this intensity are known as interferences, and unless taken into account will markedly decrease the accuracy of the method. To emit a secondary spectra, an element must absorb energy, which, like the emission, occurs at specific wave lengths characteristic of that element. The interferences which occur may be summarized in terms of emission and absorption interactions of the following types: Emission Absorption, Emission Enhancement, and Competitive Absorption (Fig. 3).

In Emission Absorption, the intensity of a wave length emitted by one element is decreased due to the selective absorption of that wave length by another element present in the sample. A familiar example of this interference is the use of one element to filter the radiation produced by another.

Emission Enhancement of two types occurs. Spectra may overlap causing the intensity of one line to be increased by the proximity or

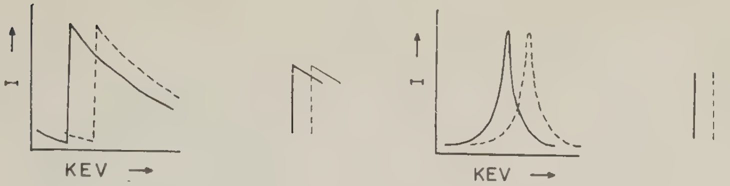

Competitive Absorption

Emission Enhancement A.

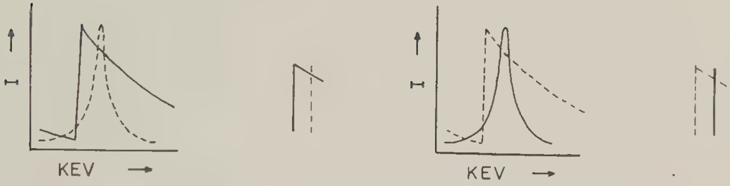

Emission Enhancement B.

Emission Absorption

FIG. 3. Diagrammatic representation of the four types of phenomena which interfere with peak intensity in x-ray fluorescence analysis.

superposition of other lines. A similar increase in line intensity may be due to the absorption of energy by one element in the range in which another is emitting. Both these difficulties are commonly encountered in rare earth analysis.

With insufficient excitation potential, a decrease in emission intensity may be noted if two or more elements absorb energy in the same range. Interference of this nature is called Competitive Absorption and may be compensated for by the use of adequate excitation potential.

The emissions and absorptions of the 17 elements detected in the fluorescence analysis of monazite are listed in Table 5. The emissions which are the most useful for quantitative work and their absorption edges are shown as solid lines in Fig. 4. All other emissions and absorptions interfere with these and are plotted as dashed lines. The interferences shown in Fig. 4 are to be interpreted in terms of the four types given in Fig. 3. Fig. 4 provides the key for evaluating the nature of the interferences encountered in the analysis of the rare earth elements in monazite. The calibration of fluorescence equipment for the quantitative determination of any or all of the 17 elements shown may be accomplished by using Fig. 4 to determine the elements which interfere (dashed lines) with the emission line and absorption edge of the selected element (solid lines). Standard mixtures of the selected element with the interfering elements may then be prepared. The data obtained from these standards on the fluorescence equipment will provide the peak height or counts per second data from which working curves for the element may be prepared. Once the instrument has been calibrated, quantitative determination of the selected element is readily achieved.

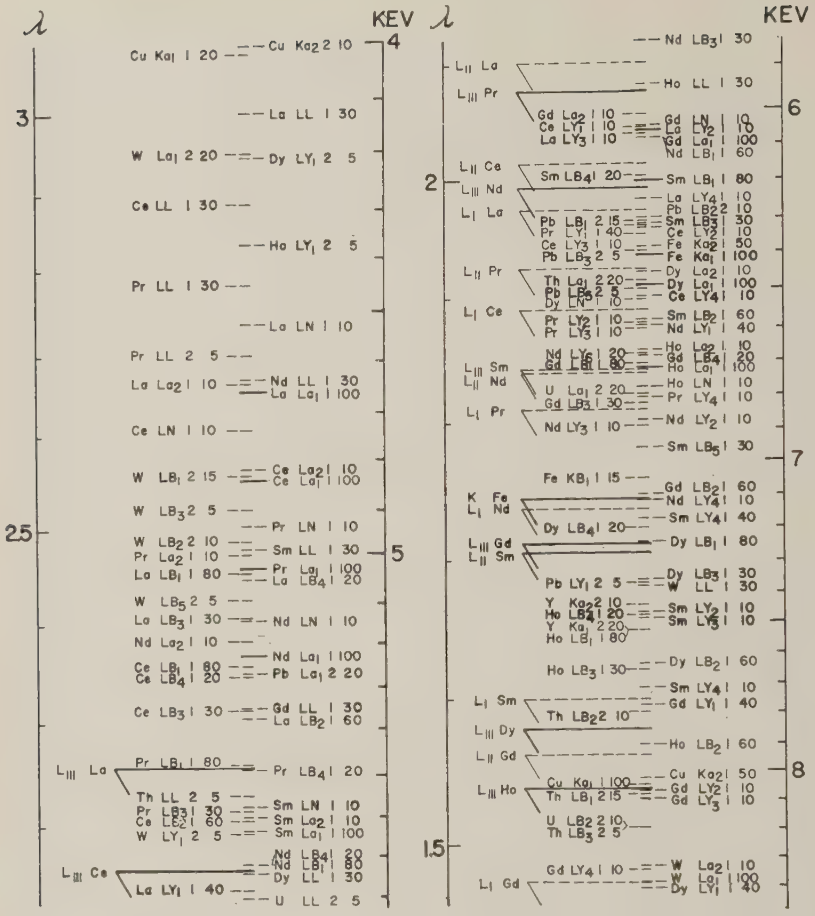

FIG. 4. Diagrammatic representation of emission lines and absorption edges (dashed lines) which interfere with accurate, quantitative analysis of the rare earth elements in monazite (solid lines).[1]

Both sample and tube background elements have been plotted. The notation used is the following: L_{III}Ce represents the III absorption edge of the L series of cerium, while Ho LB_2 1 60 stands for the beta 2 emission of the first order of the L series of holmium which has a relative intensity[2] of 60 with respect to the L alpha 1 line of that element.

1. Prepared from the tables of Fine and Hendee (1954), and Powers (1957) using the conversion equation:

$$E(\text{KEV}) = \frac{12.39644 \pm .00017}{\lambda\ \text{Å}}$$

2. Lines with relative intensity less than 5 are not represented, and the intensities of lines of orders higher than 1 have been converted from the values of Power (1957)

(*Figure and legend are continued on next page*)

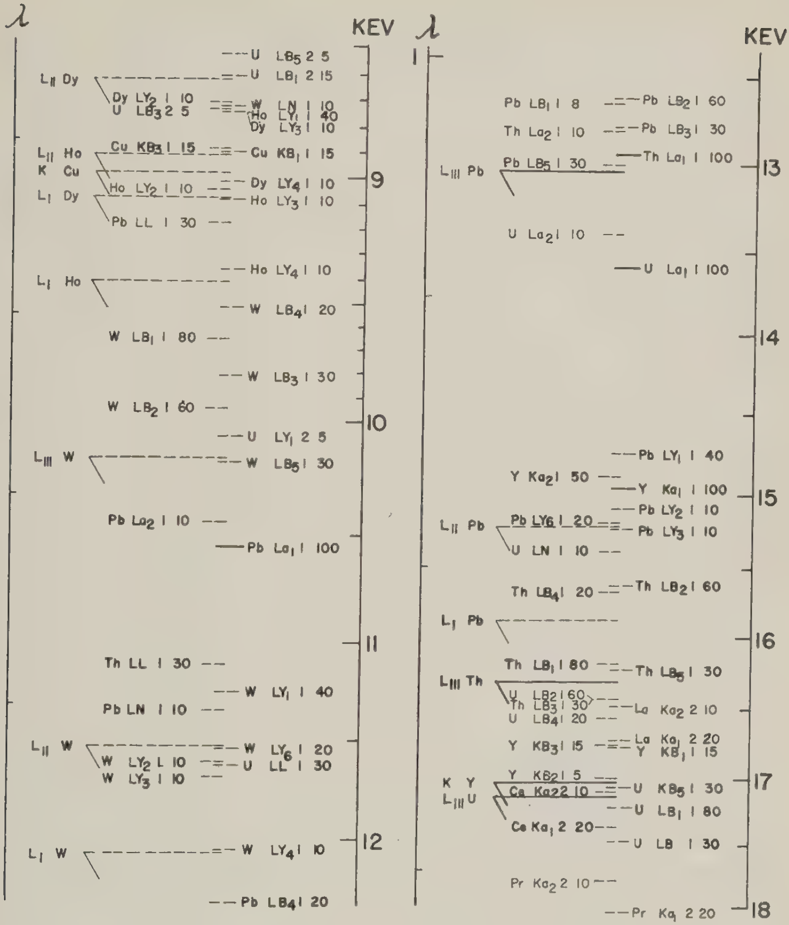

so that the intensities of all the lines of an element are directly comparable regardless of their order. For this conversion a high order line was assumed to be 1/20 the intensity of the same line in the next lowest order, and so reduced to the first order intensity. This assumption is valid for the LiF analyzing crystal which is widely used for this type of fluorescence analysis.

In the past, several workers have attempted such analysis without examining the interference problem. This is the primary limitation upon the usefulness of their work.

Goldschmidt and Thomassen (1924) were the first to attempt the quantitative analysis of the rare earths in monazite by *x*-ray spectroscopy. As was the custom of their time, the sample was made the target of the electron beam in a cathode ray tube. The primary radiation which

TABLE 5. QUANTUM MECHANICS TRANSITION RELATIONS FOR RARE EARTH *X*-RAY ENERGIES*

Emission Energies		Absorption Edges
Ka_1	=	K_{ab}–L_{III}
Ka_2	=	K_{ab}–L_{II}
Kb_1	=	K_{ab}–M_{III}
Kb_2	=	K_{ab}–N_{III}
La_1	=	L_{III}–M_V
La_2	=	L_{III}–M_{IV}
Lb_1	=	L_{II}–M_{IV}
Lb_2	=	L_{III}–M_V
$L\gamma_1$	=	L_{II}–M_{IV}

Therefore, the following absorption edges affect the corresponding emission energies of elements found in the monazite samples.

Emission Energies		Absorption Edges
La(La_1)	—	La(L_{III})
Ce(La_1)	—	Ce(L_{III})
Pr(La_1)	—	Pr(L_{III})
Nd(La_1)	—	Nd(L_{III})
Gd(La_1)	—	Gd(L_{III})
Sm(Lb_1)	—	Sm(L_{II})
Fe(Ka)	—	Fe(K_{ab})
Dy(La_1)	—	Dy(L_{III})
Ho(La_1)	—	Ho(L_{III})
Pb(La_1)	—	Pb(L_{III})
Th(La_1)	—	Th(L_{III})
U(La_1)	—	U(L_{III})
Y(Ka)	—	Y(K_{ab})

* From Fine and Hendee (1954).

it emitted was recorded on film and the line intensities determined with a photometer.

The difficulties of sample melting, segregation, volatilization, and the errors which these introduced were noted by von Hevesy (1932), and led to the abandonment of this type of analysis. In its place was employed analysis of the secondary, fluorescent *x*-radiation emitted by a sample bathed in the primary continuum from a tungsten target. The increased accuracy in angular measurement, the use of other types of radiation detectors (Parrish, 1956; Parrish and Kohler, 1956), and the recent development of the discrimination technique of Pulse Height Analysis using a proportional counter (Dowling, Hendee, Kohler, and Parrish, 1956; Miller, 1956), have provided reliable instrumentation to eliminate these errors.

Empirical investigation of the rare earth elements has been undertaken

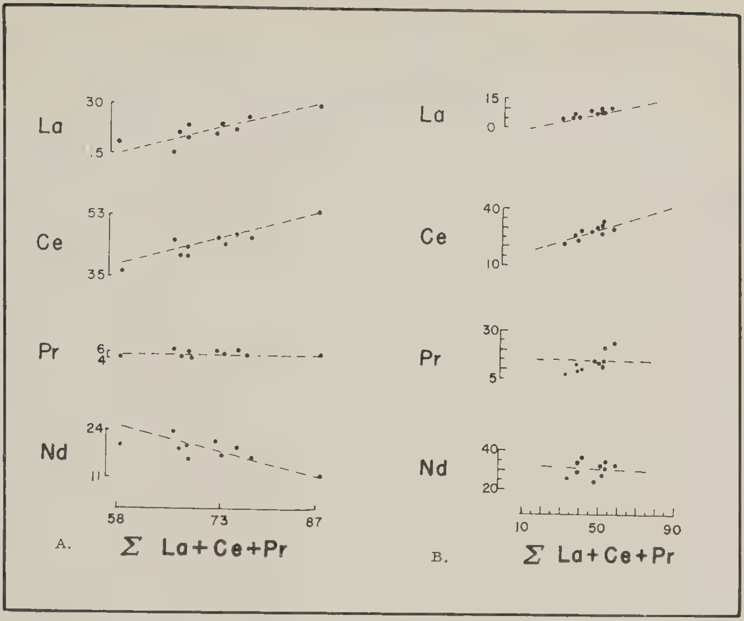

FIG. 5. Relation of the accuracy of the x-ray fluorescence method for determining rare earths in monazite to the emission spectrographic method (Murata, Rose, and Carron, 1953).

A. Atomic per cent (after Murata, Rose, and Carron, 1953). Plot of atomic percentages of rare earth elements (ordinate) versus the percentage of lanthanum group (abscissa). Dashed lines were calculated on the basis of fractional precipitation.

B. Uncorrected intensities from x-ray fluorescence. Plot of x-ray peak height (uncorrected) for rare earth elements (ordinate) versus the sum of the peak heights of the lanthanum group (abscissa). Dashed lines indicate trend of fractional precipitation.

by Dunn (1955), and Salmon and Blackledge (1955). It remains to unite such empirical work with the theoretical analysis in this paper.

While the mutual interferences preclude precise quantitative analysis at this time, in the case of several of the rare earth elements a semi-quantitative analysis is possible. This may be seen in Fig. 5 where the uncorrected peak heights from the x-ray fluorescence of the ten monazites (Table 6) have been plotted following the rules for the systematic variation of rare earths in monazite (Murata, Rose, and Carron, 1953). In the case of lanthanum and erbium the plots follow the trends they predict. On this basis, the peak heights listed in Table 6 may be used as a semi-quantitative means for comparing the rare earth content of the ten monazites. In the case of thorium, chemical analysis of the Chester monazite has shown that the recorded $L\alpha_1$ Th peak height of 74.5 corresponds to 13.66 per cent ThO_2. The complexity of this problem of

TABLE 6. *X*-RAY FLUORESCENCE PEAK INTENSITIES FOR TEN MONAZITES*

	Peak Intensity above Background											
	La($L\alpha_1$)	Ce($L\alpha_1$)	Pr($L\alpha_1$)	Nd($L\alpha_1$)	Gd($L\alpha_1$)	Sm($L\beta_1$, 4)	Fe($K\alpha_1$)†	Dy($L\alpha_1$)	Ho($L\alpha_1$)	Pb($L\alpha_1$)	Th($L\alpha_1$)	U($L\alpha_1$)	Y($K\alpha_1$)
Chester	8	26.5	14	23.5	15.5	3.5	100+	14	22	6.5	74.5	2	8
Amelia	5	25	10	28.5	21.5	12.5	17	12	6	2	72.5	0	14.5
Arendal	6.5	26.5	21.5	33.5	27.5	12.5	24	14	13	4.5	44.5	3	36
Augusta	4.5	21	8.5	26	22.5	10.5	45	18.5	8.5	4.5	65	2.5	28.5
Madison	8	28.5	23	32	20.5	5	30	6.5	5.5	1.5	35.5	2.5	12
Minas Geraes	6	23.5	10.5	33	27.5	11.5	41.5	11.5	11.5	1.5	42.5	1	29
Missoula	5	27	10	35.5	24.5	13.5	30	9.5	8	6.5	58.5	1.5	4.5
S. Lynne	8	31	14.5	27.5	16.5	2.5	100+	7.5	1	1	29.5	.5	10
Toledo	8	30	13.5	30.5	20.5	5	46.5	10.5	5	2	39	2	34
Urals.	8	32	14	31	19.5	4	30.5	7	4	1.5	38.5	0	19.5

* Norelco Spectrometer: Setting 8, 1.0, 8; 35 KV, 27 M.A.; Specimen size—120 mesh.

† Fe($K\alpha_1$) intensities include background estimated at 15.5 units.

mutual interferences precludes an attempt at this time to extend the semi-quantitative approach beyond this point.

CONCLUSIONS

Although the Chester monazite contains a considerable amount of intercrystalline goethite, it compares favorably with nine other monazite localities in physical, optical, differential thermal, and x-ray properties.

Monazite may be identified by its characteristic x-ray diffraction pattern. Dependable reflections are obtained and indexed. The range in individual (hkl) reflections among the ten specimens is shown, but does not yield any simple relation to chemical composition.

Differential thermal analysis indicates that the thermal pattern of pure monazite is featureless. The exothermic peaks obtained are considered to be caused by iron-bearing alteration minerals, and are sufficiently consistent to suggest the presence of monazite in thermal curves.

The nature of the alteration within monazite crystals is indicated by differential thermal analysis, x-ray fluorescence, and the use of the x-ray diffraction micro-camera. These point to an iron-bearing, non-hydrous, amorphous mineral or group of minerals capable of oxidation. Some form of concentration of the alteration products must be devised to continue this work.

Optical study of ten monazites does not provide a systematic relationship between index of refraction, 2V, birefringence, alteration, rare earth content, and thorium content. However, the influence of alteration on the cleavage is verified.

Qualitative chemical analysis of monazite may be accomplished by x-ray fluorescence. The method is adequate for the determination of relative amounts of rare earths among monazites, its sensitivity having been shown by the detection of predicted trends in rare earth content due to crystal fractionation. Accurate quantitative analysis is at present accomplished by emission spectroscopy of spectrophotometry. The extension of x-ray fluorescence to this field is anticipated by an analysis of the variables which now limit its use. As a step toward this end, a tabulation of the interferences encountered in the fluorescence analysis of monazite is included.

REFERENCES

ARENS, P. L. (1951), Differential thermal analysis of clays: Dissertation, Wageningen.

BLANCHARD, R. (1944), Chemical and mineralogical composition of twenty typical "limonites": *Am. Mineral.*, **29**, 111.

DOWLING, P. H., HENDEE, C. F., KOHLER, T. R., AND PARRISH, W. (1956), Counters for x-ray analysis: *Philips Tech. Rev.*, **18**, No. 9, 262–275.

DUNN, H. W. (1955), A study of x-ray fluorescence for the analysis of rare earths and other complex groups: *Oak Ridge Nat. Lab., Rept.* No. *ORNL-1917* (Aug. 4, 1955).

FANKUCHEN, I., AND MARK, H. (1944), X-ray studies of chain polymers: *Jour. App. Physics*, **15**, 367.

FINE, S., AND HENDEE, C. F. (1954), A table of x-ray K and L emission and critical absorption energies for all the elements: *Philips Tech. Rept.*, **86**.

VON GLISZCZYNSKI, S. (1939), Beitrag zur "isomorphie" von monazit und krokoit: *Zeit. Kr.*, **101**, 1–16.

GOLDSCHMIDT, V. M., AND THOMASSEN, L. (1924), Geochemische verteilungsgesetze der elemente III: *Videnskabsselskabet, Math. Naturv. Klasse, Skrifter.*, **5**, 7–58.

GRIM, R. E., AND ROWLAND, R. A. (1942), Differential thermal analysis of clay minerals and other hydrous materials: *Am. Mineral.*, **27**, 746–761, 801–818.

VON HEVESY, G. (1932), Chemical analysis by x-rays and its applications: McGraw-Hill Book Co., Inc., New York, 325 pp.

KELLEY, D. R., AND KERR, P. F. (1957), Clay alteration and ore, Temple Mountain, Utah: *Bull. Geol. Soc. Am.* **68**, 1077–1100.

KERR, P. F., AND KULP, J. L. (1948), Multiple differential thermal analysis: *Am. Mineral.*, **33**, 387–419.

KLUG, H. P., AND ALEXANDER, L. E. (1954), X-ray diffraction procedures: John Wiley & Sons, Inc., New York, p. 36.

KULP, J. L., AND KERR, P. F. (1949), Improved differential thermal analysis apparatus: *Am. Mineral.*, **34**, 839–845.

KULP, J. L., AND PERFETTI, J. N. (1950), Thermal study of manganese oxides: *Mineral. Mag.*, **29**, 239–251.

KULP, J. L., AND TRITES, A. F. (1951), Differential thermal analysis of natural hydrous ferric oxides: *Am. Mineral.*, **36**, 23–44.

MACKENZIE, R. C. (1957), The differential thermal analysis of clays: *Mineral. Soc. London.*

MARKEWICZ, F. J., CHAO, E. C. T., AND MILTON, C. (1957), Radioactive minerals of New Jersey: *Program of Annual Meeting, Geol. Soc. Ann.*, p. 93.

MATTHEWS, W. D. (1894–95), Monazite and orthoclase from South Lyme, Conn.: *Sch. Mines Quart., Columbia Univ.*, **16**, 232.

MEYROWITZ, R., AND LARSEN, E. S., JR. (1951), Immersion liquids of high refractive index: *Am. Mineral.*, **36**, 746–750.

MILLER, D. C. (1957), Some considerations in the use of Pulse Height Analysis with x-rays: *Norelco Reporter, IV*, No. 2, 37–40.

MURATA, K. J., ROSE, H. J., JR., AND CARRON, M. K. (1953), Systematic variation of rare earths in monazite: *Geochim. et Cosmochim. Acta*, **4**, 292–300.

MURATA, K. J., ROSE, H. J., JR., CARRON, M. K., AND GLASS, J. J. (1957), Systematic variation of rare earth elements in cerium earth minerals: *Geochim. et Cosmochim. Acta*, **11**, 141–161

PABST, A., AND HUTTON, C. O. (1951), Huttonite, a new monoclinic thorium silicate: *Am. Mineral.*, **36**, 60–69.

PARRISH, W. (1939), Unit cell and space group of monazite: *Am. Mineral.*, **24**, 651–652.

PARRISH, W. (1956), X-ray intensity measurements with counter tubes: *Philips Tech. Rev.*, **17**, 7–8, 206–221.

PARRISH, W., AND KOHLER, T. R. (1956), Use of counter tubes in x-ray analysis: *Rev. Sci. Inst.*, **27**, No. 10, 795–808.

POSNJACK, E., AND MERWIN, H. E. (1919), Hydrated ferric oxides: *Am. Jour. Sci.*, **47**, 311–348.

POWERS, M. C. (1957), X-ray fluorescent spectrometer conversion tables: Philips Elec tronics, Inc., New York.

SALMON, M. L., AND BLACKLEDGE, J. P. (1954), Analysis of rare earth mixtures by fluorescent x-ray spectroscopy: *Anal. Chem.*, **26**, 1667. Denver Univ., Denver Res. Inst., Progress in Research, 1–12.

Manuscript received August 15, 1958.

THE AMERICAN MINERALOGIST, VOL. 44, MAY–JUNE, 1959

HELLYERITE, A NEW NICKEL CARBONATE FROM HEAZLEWOOD, TASMANIA

K. L. Williams, I. M. Threadgold and A. W. Hounslow,
Mineragraphic Investigations, Commonwealth Scientific and Industrial Research Organization, University of Melbourne, Carlton, Victoria.

Abstract

Hellyerite, $NiCO_3 \cdot 6H_2O$, has been identified in samples from the old Lord Brassey nickel mine, at Heazlewood, Tasmania. It occurs as thin, pale blue coatings, associated with zaratite, on shear planes within a body of serpentinite. In transmitted light it is pale greenish blue in color and weakly pleochroic; its refractive indices are $\alpha = 1.455$, $\beta = 1.503$ and $\gamma = 1.549$. It is biaxial negative, with a 2V of approximately 85°. Its measured specific gravity is 1.97, and its hardness $2\frac{1}{2}$.

The x-ray powder diffraction pattern of hellyerite is similar to that of synthetic nickel carbonate hexahydrate, prepared by the method of Rossetti-François (1952). The powder diffraction pattern of the zaratite, however, cannot be indexed on the basis of published unit cell measurements.

Introduction

During a visit by one of us (K.L.W.) to the old Lord Brassey Mine, near Heazlewood in north-western Tasmania, specimens were collected from a body of serpentinite containing small amounts of a pale blue mineral and an emerald green mineral, occurring together as coatings on shear planes. Primary sulphide mineralization within the serpentinite consists of veins and segregations of heazlewoodite with a little pentlandite, intergrown with magnetite (Williams, 1958). The heazlewoodite in places is altered to millerite, and the pentlandite to violarite.

The green mineral has been described as zaratite by Petterd (1910) and Reid (1921), but the presence of the blue mineral does not appear to have been recorded. A study of this mineral shows that it is a new species, which it is proposed to name *hellyerite*, after Henry Hellyer, who was the first Surveyor-General of the Van Diemen's Land Company and who conducted surveys and exploration in north-western Tasmania in the period 1826–1830.

Hellyerite is the naturally occurring equivalent of the compound $NiCO_3 \cdot 6H_2O$, which has been prepared and described by Rossetti-François (1952). No natural occurrence of a mineral of this composition has been recorded in any of the standard sources published up to the time of writing.

Physical Properties

Hellyerite is a pale blue mineral of vitreous lustre occurring as extremely fine-grained coatings up to 1.0 mm. thick, in part coating zaratite, along shear planes in serpentinite. It has one perfect cleavage, and two good, but less perfect cleavages. The weaker cleavages are inclined at 112° to each other and are both approximately perpendicular to the strong cleavage (Figs. 1, 2). Rare crystal fragments have been observed microscopically, but none has been sufficiently large for morphological study.

The specific gravity of hellyerite, measured on a Berman microbalance, is 1.97, and its hardness is $2\frac{1}{2}$.

Hellyerite is biaxial negative, with 2V approximately 85°, and is pleochroic with X very pale greenish blue, Y very pale greenish blue and Z pale greenish blue. The refractive indices were measured in immersion oils as $\alpha = 1.455$, $\beta = 1.503$ and $\gamma = 1.549$, each ± 0.002.

The orientation of the optical directions relative to the cleavages is shown in Figs. 1 and 2. The trace of the optic plane makes an angle of 3° with the strongest cleavage on a section parallel to one of the weaker

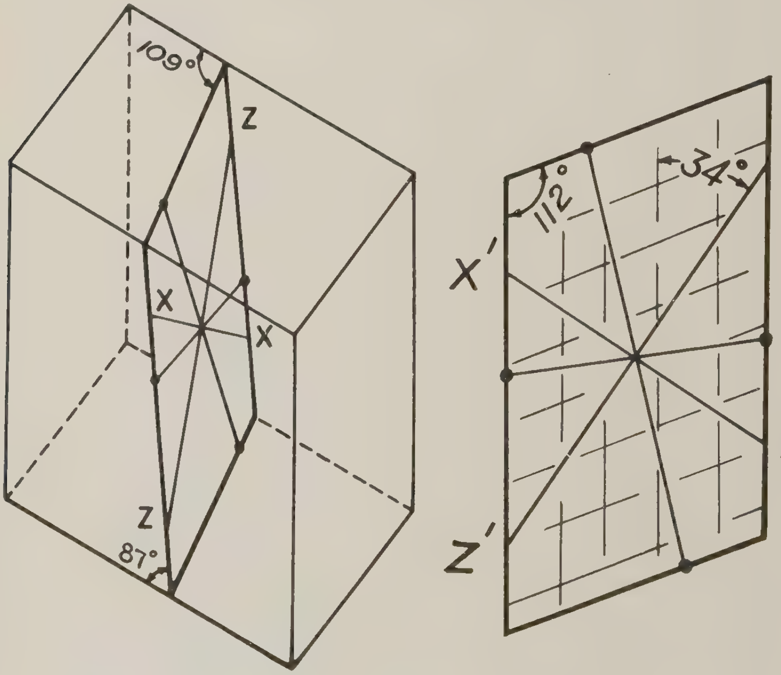

FIG. 1

FIG. 2

FIGS. 1, 2. Optical orientation of hellyerite, relative to the cleavages. Fig. 1. Isometric projection showing the orientation of the optic plane relative to the cleavages. The strongest cleavage is that cleavage almost parallel to the optic plane. Fig. 2. Position of the optic elements in a section parallel to the strong cleavage. X′X′ and Z′Z′ are the apparent positions of X and Z respectively.

cleavages; the corresponding angle on a section parallel to the other less perfect cleavage is 19° (Fig. 1). These angles were determined by extinction measurements on cleavage fragments. Each optic axis is approximately normal to one of the less perfect cleavages (Fig. 2).

Fine lamellar twinning occurs parallel to the perfect cleavage, individual twin lamellae ranging from 0.002 mm. to 0.03 mm. in width. Where the minute crystal faces are developed they commonly have a striated appearance resulting from this twinning; the effect resembles that produced by albite-type twinning of plagioclase felspars.

X-Ray Powder Pattern

The *x*-ray powder diffraction data for hellyerite are listed in Table 1, together with corresponding data for synthetic $NiCO_3 \cdot 6H_2O$ prepared by one of us (A.W.H.), using the method of Rossetti-François (1952), and with the *x*-ray data given by Rossetti-François for this compound. The table shows the close correspondence between the data for hellyerite and for our synthetic preparation. The only differences between these and the data of Rossetti-François are in two lines, given by her as 3.72 Å (in place of 3.11 Å) and 6.53 Å (in place of 6.06 Å), both errors undoubtedly arising from misprints.

Chemical Analysis

An 80 mgm. hand-picked sample of hellyerite was analyzed as follows: CO_2 was determined as loss on ignition after subtraction of water determined by the Penfield method. NiO was determined as ignition residue and independently by precipitation with dimethyl-glyoxime. Spectrographic analysis showed the presence of strong traces of Ca and Mg and a weak trace of Fe.

The results of the analysis (Table 2) show a composition close to $NiCO_3 \cdot 6H_2O$, which is in accordance with the agreement of *x*-ray powder diffraction data for hellyerite and synthetic $NiCO_3 \cdot 6H_2O$.

The analysis of the synthetic nickel carbonate hexahydrate prepared by the method described by Rossetti-François (1952) shows a nickel oxide content of 35.7 per cent (Table 2), exceeding the amount in $NiCO_3 \cdot 6H_2O$ by 2.7 per cent. This discrepancy is probably due to the presence of a proportion of a "basic" nickel carbonate which, as Rossetti-François has shown, readily forms in small amounts during the preparation of nickel carbonate hexahydrate unless very careful control of temperature and concentrations is maintained. Moreover, some decomposition may have taken place after precipitation, since Rossetti-François noted that the hexahydrate which she had synthesized was unstable, decomposing to a poorly crystalline carbonate whose composi-

TABLE 1. HELLYERITE $NiCO_3 \cdot 6H_2O$—*X*-RAY POWDER PATTERN
(Cu/Ni radiation)

Artificial $NiCO_3 \cdot 6H_2O$ (Rossetti-François, 1952)		Hellyerite, Lord Brassey Mine, Heazlewood, Tas. $CuK\alpha_1$; $\lambda = 1.5405$ Å Camera diam. 114.6 mm.		Artificial $NiCO_3 \cdot 6H_2O$ (prep. A. W. Hounslow) $CuK\alpha_1$; $\lambda = 1.5405$ Å Camera diam. 114.6 mm.	
d (Å)	I	*d* (Å)*	I (est.)	*d* (Å)*	I (est.)
9.33	10	9.4	10	9.4	9
6.53†	10	6.06	10	6.06	10
		5.69	0.2	5.71	0.2
5.33	3	5.38	2	5.40	2
5.12	2.5	5.17	2	5.19	2
		4.99	1	5.01	1
		4.81	0.5	4.83	0.5
		4.66	0.5	4.68	0.5
				4.05	<0.2
3.72	2	3.76	2	3.78	1.5
3.61	8	3.65	7	3.66	7
3.37	6	3.40	6	3.42	5
3.19	3	3.21	1.5	3.23	1.5
3.72†	4	3.11	4	3.12	4
				3.03	<0.2
2.95	2	2.98	1	3.00	1
		2.92	0.2	2.92	0.2
		2.84	0.2	2.85	0.2
2.75	4	2.78	4	2.79	4
		2.73	0.2	2.74	0.2
		2.69	1	2.70	1
2.65	2	2.62 b	2	2.64	0.5
				2.62	1.5
2.60	2	2.57	1	2.58	1
2.54	1	2.54	0.2	2.54	0.2
2.35	5	2.38	5	2.38	5
2.28	3	2.31	4	2.32	4
2.23	1	2.26	1.5	2.27	1.5
		2.21	0.5	2.21	0.5
		2.17	3	2.18	3.5
		2.11	1.5	2.11	1.5
		2.08	0.2	2.09	0.2
		2.01	1	2.02	1
		1.986	0.5	1.992	0.7
		1.965	1.5	1.973	1.5
		1.949	1.5	1.953	1.5
		1.900	0.2	1.907	0.5
		1.872	0.2	1.877	0.5
		1.845	0.2	1.847	0.2
		1.824	3.5	1.831	3.5
		1.790	1.5	1.797	1.5
		1.724 b	3	1.729 b	3
		1.700	0.2	1.704	0.2
		1.660	1	1.667	1.5
		1.634	0.5	1.638	0.7
		1.604	1	1.609	1.5
		1.577	0.2	1.580	0.2
		1.553	2	1.560	2
		1.521	0.5	1.528	0.7
		1.499	2	1.503	2

* Interplanar spacings uncorrected for film shrinkage.
† Misprint? See text.
b Denotes broad line.

TABLE 2. CHEMICAL ANALYSES

	1	2	3		4	
NiO	33.0	33.1	32.9	—	35.7	—
CO_2	19.4	19.8	22.8	—	20.0	—
H_2O	47.6	47.3	45.0	—	44.3	—
Ignition loss to 110° C.	—	—	—	39.0	—	40.7
Ignition loss 100° to 500° C.	—	—	—	23.2	—	22.2
Ignition loss 500° C. to 1000° C.	—	—	—	5.5	—	1.4
Ignition residue (NiO)	—	—	—	32.3	—	35.7
	100.0	100.2	100.7	100.0	100.0	100.0

1. Theoretical $NiCO_3 \cdot 6H_2O$.
2. Artificial $NiCO_3 \cdot 6H_2O$; Rossetti-François, 1952.
3. Hellyerite, anal. A. W. Hounslow.
4. Artificial $NiCO_3 \cdot 6H_2O$; prep. and anal. A. W. Hounslow.

tion approximated to that of a basic carbonate. A re-analysis of our synthetic product six months after preparation showed it to contain 40.3 per cent nickel oxide, an increase of 4.6 per cent over the freshly prepared material. Although clearly some further decomposition had thus occurred, an x-ray powder photograph did not show evidence of any additional phases. It appears most likely that this is due to the development of a highly disordered structure in the decomposition product. Rossetti-François, referring to the decomposition of the synthetic hexahydrate at 38° C., states that it consists in part of " . . . a continuous disorganization from the crystalline state, terminating after 188 hours . . . in a completely disorganized state. . . ." The authors observed a similar effect when hellyerite was held at 50° C. for one week.

The apparent rarity of hellyerite is in accordance with the instability of the synthetic preparation under atmospheric conditions, although it is possible that the instability of the synthetic material may have been unduly accentuated by the fact that it was obtained only in very finely divided form. The larger surface area thus obtained would aid relatively rapid dehydration. It may be expected that the more coarsely crystalline natural material would be more stable; in fact a re-analysis of hellyerite six months after the initial examination showed no change in its chemical composition.

ZARATITE

The emerald green mineral associated with the hellyerite has a chemical composition, determined by analysis, similar to zaratite from Texas, Pennsylvania (Silliman, 1848). However, it was found that the x-ray powder pattern of the Heazlewood mineral could not be indexed on the basis of the simple cubic cell, having $a_o = 6.15$ kX, attributed to zaratite by Fenoglio (1934, quoted by Palache, Berman and Frondel, 1951, p. 245).

Specimens of zaratite from Heazlewood and Trial Harbour, Tasmania, and from Texas, Pennsylvania, were obtained from several museums for comparison, and these all gave *x*-ray powder patterns similar to that of the Heazlewood mineral.

The reasons for this discrepancy are not yet known, since the authors have not had access to a copy of Fenoglio's original paper or to samples of the European material with which he evidently worked. Steps are being taken to obtain both and to institute a more complete examination of the mineral.

ACKNOWLEDGMENTS

The authors wish to acknowledge the assistance received during this investigation from Messrs. A. and F. McCormick, of Burnie, Tasmania, who provided facilities for collection of specimens. We are also indebted to Dr. A. B. Edwards and Dr. J. McAndrew for their critical reading of the manuscript, which is published by permission of the Commonwealth Scientific and Industrial Research Organization.

REFERENCES

FENOGLIO, M. (1934): Nuove ricerche sulla zaratite: zaratite sintetica—*Per. Min.*, 5, 265 (seen only in abstract form—*Min. Abstr.*, **6**, 55 (1935)).

PALACHE, C., BERMAN, H. AND FRONDEL, C. (1951): Dana's System of Mineralogy—ed. 7—New York.

PETTERD, W. F. (1910): Catalogue of the minerals of Tasmania Dept. of Mines, Tasmania.

REID, A. M. (1921): Osmiridium in Tasmania—*Geol. Surv. Tas., Bull. 32.*

ROSSETTI-FRANÇOIS, J. (1952): Etude du carbonate nickel hexahydrate—*Comptes Rendus de l'Académie des Sciences*, **234,** 840.

SILLIMAN, B. (1848): On Emerald Nickel from Texas, Lancaster Co., Pa.—*Am. J. Sci.*, **6,** 248.

WILLIAMS, K. L. (1958): Nickel mineralization in western Tasmania—*Proc. Aus. Inst. Min. Met.*, Stillwell Anniversary Volume (in press).

Manuscript received August 18, 1958.

THE AMERICAN MINERALOGIST, VOL. 44, MAY-JUNE, 1959

KYANITE-GARNET GEDRITITE NEAR OROFINO, IDAHO*

Anna Hietanen, *U. S. Geological Survey, Menlo Park, California.*

Abstract

In Clearwater County, Idaho, kyanite is found with amphibole in two rock types, (1) in kyanite-garnet gedritite near Orofino and (2) in hornblende-bearing layers of anorthosite in the Boehls Butte quadrangle. The associated rocks near Orofino are garnetiferous biotite gneisses, hornblende-biotite gneiss, garnet amphibolites, quartzites, and lime-silicate rocks of sedimentary origin. The major constituents in the kyanite-garnet gedritite are gedrite (38 per cent), quartz (26 per cent), oligoclase (16 per cent), and garnet (14 per cent). One to two per cent of kyanite in light bluish crystals is scattered throughout the rock. The formula of the gedrite calculated from the chemical analysis is

$$(K_{0.01}Na_{0.40}Ca_{0.06}Mg_{3.80}Fe^{\cdot\cdot}_{1.57}Mn^{\cdot\cdot}_{0.04}Ti^{\cdot\cdot\cdot\cdot}_{0.07}P_{0.01}Fe^{\cdot\cdot\cdot}_{0.07}Al_{1.30})_{\Sigma=7.33}$$
$$(Si_{6.33}Al_{1.67})_{\Sigma=8.00}(O_{22.10}(OH)_{1.90})_{\Sigma=24.00}.$$

The garnet consists of about 49 per cent almandite and 43 per cent pyrope with some spessartite, grossularite, and andradite. The texture suggests that gedrite and garnet crystallized later than the other minerals. The chemical analysis of the gedritite shows more than 15 per cent Al_2O_3, about 8.5 per cent each of FeO and MgO, but only 0.2 per cent K_2O and 1.7 per cent CaO.

The hornblende- and kyanite-bearing layers of the anorthosite are described briefly for comparison. The kyanite in these layers is a relict mineral, inherited from the schist that formerly occupied the area now covered by anorthosite. The occurrence of the kyanite in the anorthosite is most likely due to the slowness of reaction between the minerals of the parent rock, the schist, and the metasomatizing solutions that transformed the schist to anorthosite. For the occurrence of kyanite in the gedritite near Orofino a similar explanation is possible, but not conclusive because there are no signs of a possible disequilibrium between the fresh kyanite crystals and the enclosing gedrite. The Mg:Fe ratio of the gedrite falls within the Mg:Fe ratio possible in the cordierites, and the bulk composition of the kyanite-garnet gedritite is very close to that of cordierite gneisses and cordierite-anthophyllite rocks. Temperature and pressure during the recrystallization were close to the triple point of kyanite, andalusite, and sillimanite suggesting a somewhat lower temperature for the kyanite-gedrite assemblage than for the cordierite rocks which contain only sillimanite. The crystallization of kyanite and gedrite instead of cordierite in this rock is probably due to a stress during the recrystallization.

Introduction

Kyanite rarely occurs with amphibole in normal regionally metamorphosed rocks, as this pair of minerals is usually incompatible. As a rule, minerals like cordierite, garnet, and staurolite crystallize in the aluminous rocks rich in iron and magnesium. On some rare occasions, however, kyanite is found with amphiboles in metamorphosed sedimentary rocks as well as in metamorphosed igneous rocks. Among the sedimentary formations those occurring in the Alpine region (Garbenschiefer of the Tremola series and Quartenschiefer of the Lukmanier region) are best known (Hexner, 1908; Niggli, 1929). Kyanite with hornblende from an igneous environment was reported by Clough (1910, p.

---

* Publication authorized by the Director, U. S. Geological Survey.

35) from Lewisan gneiss in Scotland. Later, Tilley (1937) made a detailed study of these same kyanite amphibolites which are associated with eclogites and are undoubtedly of igneous origin. In some of these rocks the association of kyanite with amphiboles is probably due to the slowness of reactions during the conversion of kyanite-bearing eclogites to amphibolites. Tilley found that the content of Al_2O_3 in kyanite-garnet amphibolite in Glenelg is higher than that in its parent eclogite and concluded that migration and segregation of material takes place during the conversion.

The hornblende in the kyanite amphibolites mentioned above is a common green calcium-bearing aluminous variety. The occurrence of kyanite with an orthorhombic amphibole, aluminous anthophyllite (gedrite), has been described by Tilley (1939) from Shueretsky district in Karelia. According to Ignatiev (1934) the associated rocks there are Precambrian schist, gneisses, amphibolites, gabbro-norites, granites, and pegmatites. The garnet-gedrite-biotite rocks (gedritites) are found as narrow bands in the amphibolites in the central parts of synclines and are considered to be products of transformation after amphibolite.

A common green hornblende occurs with kyanite in some layers in anorthosite in the Boehls Butte quadrangle, Idaho. This occurrence is described in another paper[1] and only the result of the study is briefly discussed here. The kyanite is an abundant constituent in the schist around the anorthosite bodies and remnants of this schist are common in the anorthosite. The layers that are rich in hornblende and kyanite are thought to represent metasomatized remnants of this schist. The kyanite is an earlier mineral inherited from the schist, and the constituents of the amphibole were introduced during the formation of the anorthosite as were also the constituents of the plagioclase.

The kyanite-bearing garnet gedritite described in this paper was found in 1952 in the western part of Clearwater County, Idaho, in the canyon of Orofino Creek, four miles east of the town of Orofino (Fig. 1). The associated rocks there belong to a metamorphosed sedimentary series probably of Precambrian age. Quartz dioritic and tonalitic rocks of igneous and metasomatic origin occur as small masses in the metasedimentary rocks. A detailed study was made of the gedrite-bearing rocks and their minerals in the hope of throwing new light on the rare paragenesis of kyanite and amphibole.

FIELD RELATIONS

The kyanite-garnet gedritite is exposed in a southward-facing railroad cut, four miles east of the town of Orofino. The country rocks are gneisses,

---

[1] Manuscript titled "Anorthosite and associated rocks in Boehls Butte quadrangle and vicinity, Idaho."

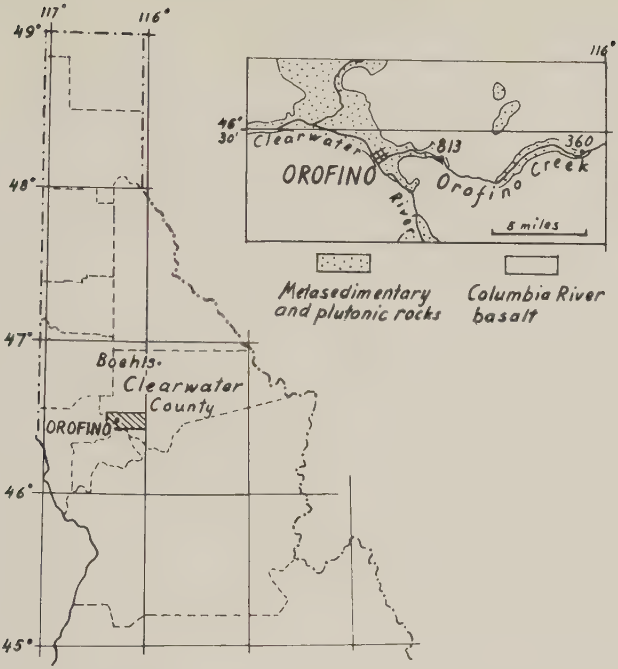

FIG. 1. Location of the kyanite-garnet gedritite. The sketch on right shows the shaded square on the map of northern Idaho (on the left). In this sketch the locations of kyanite-garnet gedritite and garnet amphibolite are indicated by numbers 813 and 360 respectively.

schists, and amphibolites, all belonging to the metasedimentary rock series that was called the Orofino series by Anderson (1930). Stratigraphy, structure, and petrology of this series has been described by the present author in another paper[2] and therefore only the layers immediately associated with gedrite-bearing rocks are described in this report. The detailed field relations are shown schematically in Fig. 2. Gedrite is found in several layers, the thickness of which ranges from 10 cm. to 15 m., in garnetiferous biotite and biotite-hornblende gneiss. In the thickest layer (813 in Fig. 2) small- to medium-size crystals of light-bluish to colorless kyanite were detected. Biotite-hornblende gneiss exposed under this thickest gedritite layer includes a few thin layers rich in gedrite (*a*, *b*, *c* just west of 812 in Fig. 2), but no kyanite was found in them. Another thick layer rich in gedrite and containing numerous large garnets, but only occasional tiny grains of kyanite, occurs lower in the series (810 in Fig. 2) under a layer of garnetiferous biotite and hornblende-biotite

---

[2] Manuscript titled "Metasomatic metamorphism along the northwest border zone of the Idaho batholith."

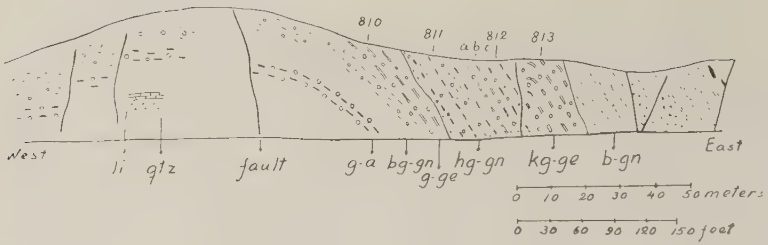

FIG. 2. Generalized geologic section in the railroad cut 4 miles east of Orofino where kyanite-garnet gedritite occurs. *kg-ge*=kyanite-garnet gedritite, *g-ge*=garnet gedritite, *b-gn*=thin-bedded biotite gneiss with lime-silicate bearing layers, *hg-gn*=hornblende-biotite-garnet gneiss, *g-a*=garnet amphibolite, *li*=limestone, *qtz*=quartzite, *bg-gn*=biotite-garnet-gneiss. Numbers 810 to 813 refer to layers from which specimens were taken.

gneiss. This layer is underlain by biotite-garnet gneiss, which in turn lies above garnet amphibolite. About 50 m. to the west the lowest part of this sequence is repeated because of folding and faulting. The strata form a gentle anticline broken by several faults. Several faults occur also on the eastern limb of the anticline east of the kyanite-garnet gedritite, where thin-bedded layers of biotite gneiss with lime-silicate-bearing layers alternate with quartzite, biotite-plagioclase gneiss, and biotite-garnet schist. Accumulations[3] of ferromagnesian minerals, mainly hornblende, occur in the quartzitic layers.

PETROGRAPHIC DESCRIPTION OF THE KYANITE-GARNET GEDRITITE AND ASSOCIATED ROCKS

Kyanite-garnet gedritite

The kyanite-garnet gedritite (813 in Fig. 2) is dark green, speckled red by garnets, medium grained, and crudely foliated. The foliation is due to a parallel arrangement of long gedrite prisms and is partly obscured by the occurrence of numerous garnets of medium size and by small, irregularly shaped clusters of quartz and feldspar. Pale-blue kyanite crystals ranging from $\frac{1}{4}$ to 1 cm. in length can be seen with the naked eye. A study under the microscope revealed numerous small kyanite crystals, most of them included in large green gedrite prisms (Fig. 3 and Pl. 1). Also, a few tiny crystals of staurolite, numerous small grains of brown rutile, and a few flakes of green, strongly pleochroic biotite are included in the gedrite. Sillimanite was found in one specimen studied. Garnet crystals ranging from 2 to 10 mm. in diameter include many fairly large quartz grains, some rutile, ilmenite, and magnetite. The major light constituent is

---

[3] See footnote 2.

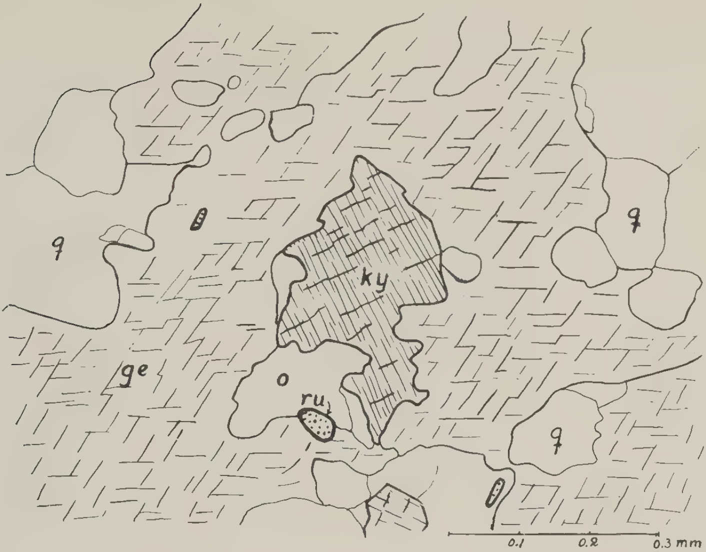

FIG. 3. Camera lucida drawing of kyanite-garnet gedritite near Orofino showing kyanite included in gedrite. *ky*=kyanite, *ge*=gedrite, *q*=quartz, *ru*=rutile.

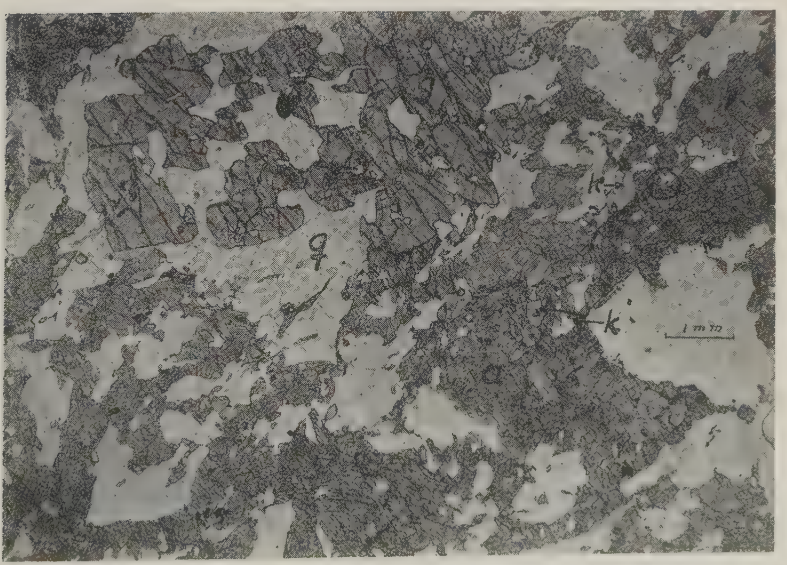

PLATE 1. Photomicrograph of kyanite-garnet-gedritite. *k*=kyanite; *g*=garnet; *a*=gedrite; *q*=quartz; small black grains are ilmenite and magnatite. Plane polarized light.

quartz, the anhedral grains of which range from 0.1 to 0.3 mm. in diameter. Plagioclase (An_{20}) occurs in anhedral grains with quartz. A few grains of magnetite, ilmenite, and apatite occur as accessories.

Garnet-gedritite

The layer of garnet gedritite (810 in Fig. 2), averaging 13 m. in thickness, is more strongly foliated that the kyanite-bearing gedritite. Weathering has changed its color to rusty brown. The garnets in this layer are much larger, ranging from 1 to 4 cm. in diameter, and show dodecahedral (110) and trapezohedral (211) faces. There is more plagioclase (An_{20}) and quartz than in the kyanite-garnet gedritite, both of these constituents showing a tendency to cluster into irregularly shaped discontinuous veinlets parallel to the foliation. The gedrite prisms are about 1 cm. long and clustered but still have their longest dimensions parallel to the lineation on the plane of foliation. Numerous small flakes of ilmenite occur between the other minerals. A few tiny grains of rutile and biotite are the additional constituents.

Hornblende-biotite-garnet gneiss

A dark-gray fairly homogeneous fine- to medium-grained rock (811 in Fig. 2) above the garnet gedritite consists of plagioclase (40 per cent), quartz (36 per cent), hornblende (19 per cent), and garnet (5 per cent) with some biotite and magnetite. Garnets in this layer are much smaller than in the gedrite-bearing layers, averaging only about 0.1 mm. in diameter. The biotite, which is found only in some layers, is a common brown variety with $\gamma = 1.617 \pm 0.002$. Hornblende is green and strongly pleochroic, as is the hornblende in garnet amphibolite. Most of the quartz and plagioclase are evenly distributed throughout the rock; only a few small clusters can be seen. Magnetite and apatite occur as accessories.

The upper part of this gneiss contains three gedrite-bearing layers (*a*, *b*, and *c* just west of 812 in Fig. 2), each ranging from 10 to 20 cm. in thickness. These three layers contain only a little biotite and garnet, but the amount of gedrite averages 30 per cent. Tourmaline, brown grains of rutile, apatite, and magnetite are the accessories.

Biotite-garnet gneiss

The gedrite-bearing layers grade over to a medium-grained gneiss in which biotite instead of gedrite occurs as a major dark constituent. This biotite-garnet gneiss (812 in Fig. 2) consists of quartz (39 per cent), plagioclase (An_{20}, 36 per cent), biotite (20 per cent), and garnet (4 per cent) with sillimanite and kyanite (together 1 per cent). Rutile and ilmenite-magnetite occur as accessories.

The texture is much like that of the nearby gedrite-bearing layers, a part of plagioclase and quartz occurring in clusters of large grains. Biotite is found in flakes of medium size with small grains of quartz and plagioclase. The diameter of large grains of quartz and plagioclase ranges from 1 to 2 mm. and that of small ones from 0.1 to 0.3 mm. Garnet crystals are 1 to 2 mm. in diameter.

Biotite in this rock is strongly pleochroic in dark and light brown with $\gamma = 1.617 \pm 0.001$. The flakes are subparallel to the foliation as is common in the gneissic rocks. A similar biotite-garnet gneiss occurs as layers in the hornblende-garnet gneiss and as a thicker layer under the garnet gedritite.

Thin-bedded biotite gneiss with lime-silicate-bearing layers

The rock east of the kyanite-garnet gedritite is medium gray, thin bedded, and fine grained. The thickness of layers ranges from $\frac{1}{2}$ to 3 cm., the thinner layers consisting of plagioclase (An_{37}), quartz, hornblende, diopside, zoisite, and garnet with some scapolite, sphene, and magnetite. Diopside is partly altered to hornblende, and scapolite to sericite. The thicker layers consist mainly of quartz, plagioclase, and biotite. Some quartzitic layers and medium-grained biotite-plagioclase gneiss layers, 5 to 20 cm. thick, are interbedded with this thin-bedded rock.

Garnet amphibolite

Garnet amphibolite is similar to the garnet amphibolite studied earlier from another locality along Orofino Creek. It consists essentially of the same minerals as the hornblende-garnet gneiss but in different quantities, the amount of hornblende being larger and that of quartz smaller. Sphene and apatite are common additional constituents. No kyanite was found in any thin-sections of garnet amphibolite in the area near Orofino.

Mineralogy of the Kyanite-Garnet Gedritite

Gedrite

The major constituent of the gedritite is a dark green amphibole that under the microscope shows only a faint pleochroism in light greenish-gray and a parallel extinction under crossed nicols. The indices of refraction, measured in immersion liquids, are α(pale) $= 1.649 \pm 0.001$; β(pale green) $= 1.656 \pm 0.001$, γ(pale green) $= 1.669 \pm 0.001$. The index of refraction of the liquid was measured by Abbé refractometer right after finding the correct value in order to avoid the influence of change of temperature. The specific gravity of 3.15 ± 0.02 was obtained from cleavage splinter by Berman balance. This mineral was separated from specimen no. 813 by R. P. Marquiss and analyzed chemically by Lucile N. Tarrant, both of the U. S. Geological Survey. Microscopic study of a sample of the analyzed material showed some tiny inclusions of rutile and quartz, a few grains of garnet, and a small flake of biotite. The result of chemical analysis (Table 1) shows that this amphibole is an aluminous magnesium-iron silicate with very little calcium belonging to the anthophyllite-gedrite group. The calculation gives the following formula with total oxygen calculated to a base of 24:

$$(K_{0.01}Na_{0.40}Ca_{0.06}Mg_{3.80}Fe^{\cdot\cdot}_{1.57}Mn^{\cdot\cdot}_{0.04}Ti^{\cdot\cdot\cdot\cdot}_{0.07}P_{0.01}Fe^{\cdot\cdot\cdot}_{0.07}Al_{1.30})_{\Sigma=7.33}$$
$$(Si_{6.33}Al_{1.67})_{\Sigma=8.00}(_{22.10}(OH)_{1.90})_{\Sigma=24.00}.$$

Aluminum substitutes for a part of the Si and also for a part of the Mg in the structure. The atomic Mg:Fe ratio is about 2:1. This chemical composition and the optical properties are close to those of the gedrite described by Tilley (1939) from a similar kyanite-gedritite in eastern Karelia. A comparison with a great number of representatives of the anthophyllite series listed by Rabbitt (1948) shows that the gedrite near Orofino is indeed chemically and optically close to the gedrite of Karelia. According to Tilley the kyanite-garnet gedritite in Karelia occurs with garnet amphibolite and garnet-gedritite in a metamorphic series that includes coarse-grained garnet and kyanite gneisses. Thus the occurrence in Karelia and that near Orofino seem petrographically and mineralogically much alike except that no sillimanite has been reported from Karelia.

TABLE 1. CHEMICAL COMPOSITION OF AMPHIBOLE (NO. 813a) IN KYANITE-GARNET GEDRITITE (NO. 813)

Lucile N. Tarrant, analyst, U. S. Geological Survey

Constituents	Weight per cent	Molecular equivalent	Number of atoms			
SiO_2	44.89	7474	Si	6.33	8.00	
Al_2O_3	17.91	1757	Al	1.67		
Fe_2O_3	0.67	42	Al	1.30	1.37	7.33
FeO	13.31	1853	$Fe^{\cdot\cdot\cdot}$	0.07		
MnO	0.37	52	$Fe^{\cdot\cdot}$	1.57	5.49	
MgO	18.09	4487	Mn	0.04		
CaO	0.40	71	Mg	3.80		
Na_2O	1.45	234	Ti	0.07		
K_2O	0.05	5	P	0.01		
TiO_2	0.67	84	Ca	0.06	0.47	
P_2O_5	0.04	3	Na	0.40		
H_2O+	2.02	1121	K	0.01		
H_2O-	0.00		H	1.90		
			O	24.00		
Total	99.87					

Garnet

Garnet in the kyanite-garnet gedritite near Orofino is pink in a fresh surface but turns brownish red during weathering. The grains are subhedral and contain large quartz inclusions which may exceed 50 per cent of the total volume of a garnet. The index of refraction is $n = 1.775 \pm 0.002$ and the specific gravity is 3.83 ± 0.02. The chemical analysis (Table 2) shows that this garnet consists of about 49 per cent almandite and 43 per cent pyrope, the rest (8 per cent) is spessartite, grossularite, and andradite. The unit cell dimension as determined by F. A. Hildebrand, U. S. Geological Survey, is $a_o = 11.526 \pm 0.006$ Å.

Kyanite

Kyanite occurs in small prisms the length of which ranges from 0.1 to 10 mm. Most crystals occur with quartz and feldspar but many are included in gedrite and a few in garnet. The kyanite crystals are light bluish or colorless, showing good cleavages parallel to the length of the prisms. The indices of refraction are $\alpha = 1.712 \pm 0.001$, $\beta = 1.723 \pm 0.001$, $\gamma = 1.728 \pm 0.001$; $-2V$ is large.

Staurolite

Some tiny grains of staurolite with pleochroism yellow to pale yellow are included in gedrite and in garnet.

TABLE 2. CHEMICAL COMPOSITION OF GARNET (NO. 813*g*) IN KYANITE-GARNET GEDRITITE

Analyst, Lucile N. Tarrant, U. S. Geological Survey
Mineral separation by R. P. Marquiss, U. S. Geological Survey

Constituent	Weight per cent	Molecular equivalent	Composition	
SiO_2	39.60	6593	Pyrope	42.69
Al_2O_3	22.45	2202	Almandite	49.13
Fe_2O_3	.62	39	Spessartite	3.46
FeO	22.77	3156	Grossularite	2.90
MnO	1.58	223	Andradite	1.82
MgO	11.05	2741		
CaO	1.70	303	$a_0 = 11.526 \pm 0.006$ Å	
Na_2O	0.00			
K_2O	0.00		$n = 1.775 \pm 0.002$	
TiO_2	0.28	35		
P_2O_5	0.04	3		
H_2O+				
H_2O-				
Total	100.09			

Sillimanite

A few clusters of fairly large prisms of a colorless mineral (Fig. 4) were found in one thin section studied. The prisms show a parallel extinction and a diagonal cleavage in their nearly square cross sections. The optic plane is parallel to this cleavage and +2V is small. These properties prove the prisms to be sillimanite.

Quartz

Quartz is the main light-colored constituent, its amount averaging 25 per cent. It occurs in elongated or rounded grains the size of which ranges from 0.1 to 15 mm. or as elongated clusters of grains between the gedrite prisms and as tiny round inclusions in garnet and in gedrite.

Plagioclase

The amount of plagioclase, $An_{20}(\gamma = 1.546 \pm 0.001)$, is less than that of quartz. This mineral occurs as anhedral grains with quartz. Most grains are twinned according to the albite law.

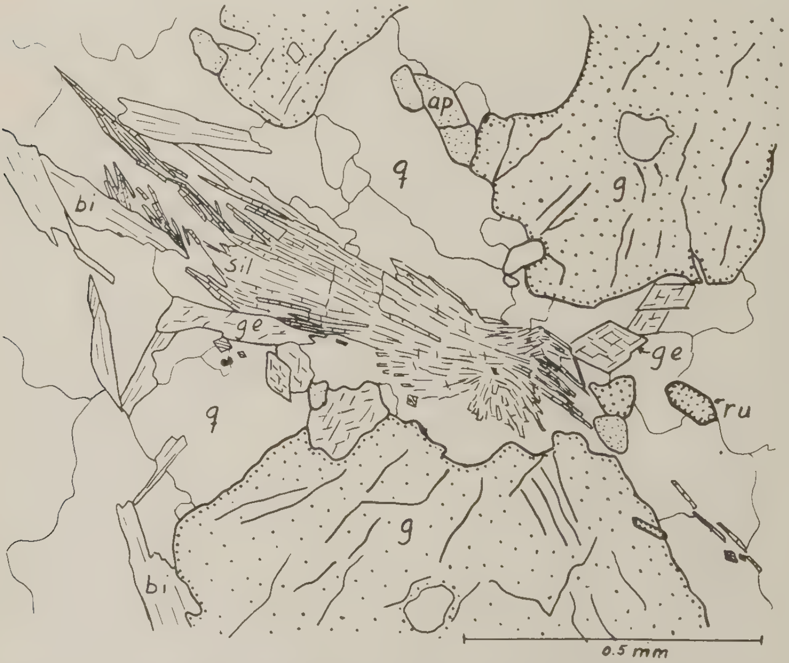

Fig. 4. Camera lucida drawing of sillimanite in kyanite-garnet gedritite near Orofino. *sil*=sillimanite, *ge*=gedrite, *g*=garnet, *q*=quartz, *bi*=biotite, *ru*=rutile, *ap*=apatite. Kyanite is found outside the field shown in the figure.

Accessories

Many small round or slightly elongated grains and small euhedral prisms of brown rutile are scattered throughout the thin sections, many being included in gedrite and in garnet. Magnetite, ilmenite, and apatite occur as tiny anhedral grains among the other minerals.

SEQUENCE OF CRYSTALLIZATION

Gedrite and garnet occur in large crystals and include the other minerals, suggesting that these two minerals crystallized late. The neighboring gneiss layers consist of quartz, plagioclase, biotite, garnet, and kyanite with some staurolite. In the gedritite, similar grains of quartz, plagioclase, kyanite, and staurolite occur, but instead of numerous small flakes of biotite, large crystals of gedrite developed and included the earlier minerals. Garnet crystals grew larger also including the other minerals.

CHEMICAL COMPOSITION

A chemical analysis made of the other half of the same hand specimen of the kyanite-garnet gedritite, from which gedrite and garnet were separated, is shown in Table 3. Compared with the neighboring metasedimentary layers this rock is rich in Al, Fe, and Mg and very poor in K. Comparison with the garnet amphibolite suggests much less Ca in the gedrite rocks. A normal garnet amphibolite in this area contains up to 10 per cent CaO[4] whereas in the kyanite-garnet gedritite the amount of CaO is less than 2 per cent, being contained in garnet and plagioclase. The scarcity of potash is, however, more striking. The chemical analysis shows only 0.2 per cent K_2O, most of which is included in biotite. The measured mode of the nearby biotite-garnet gneiss suggests that this rock contains about 1.8 per cent K_2O which is less than present in the normal mica schist. It is clear that in the presence of potash, biotite instead of gedrite would have crystallized.

More than 10 per cent corundum appears in the molecular norm, a portion of this being contained in garnet and in gedrite and the excess appearing mainly as kyanite. The total of iron and magnesium metasilicates in the norm is about 37 per cent, thus very large for a sediment. The chemical composition of the kyanite-garnet gedritite is close to that of cordierite gneiss (Hietanen 1943, Table 3) and cordierite-anthophyllite rock (Eskola 1914, Table 28).

The analyses of kyanite-garnet gedritite (No. 813), gedrite (No. 813*a*), and garnet (No. 813*g*) were plotted in ACF diagram (Fig. 5). An analysis of gedrite (No. 1a) from kyanite-garnet gedritite, Karelia (Tilley 1939, Table 1) and that of a garnet-gedritite (No. 2) from Karelia (Ignatiev 1934, Table 8, No. 1) were added for comparison. A number of analyses of other kyanite and amphibole-bearing rocks, of cordierite gneisses, and cordierite-anthophyllite rocks and their minerals are also given in Fig. 5.

---

[4] See footnote 2.

Table 3. Chemical Composition of Kyanite-Garnet Gedritite (No. 813)

Lucile N. Tarrant, analyst, U. S. Geological Survey

Weight per cent		Cation per cent		Molecular norm		Mode (calculated to correspond to the chemical analysis)	Weight per cent
SiO_2	60.29	SiO_2	56.77	Q	23.71	quartz	26.47
Al_2O_3	15.34	$AlO_{3/2}$	17.02	Or	1.20	plagioclase (An_{20})	16.45
Fe_2O_3	0.34	$FeO_{3/2}$	0.24	Ab	18.45	gedrite	38.30
FeO	8.75	FeO	6.89	An	6.65	garnet	14.65
MnO	0.41	MnO	0.33	C	10.43	kyanite	1.27
MgO	8.65	MgO	12.13	En	24.26	biotite	1.04
CaO	1.73	CaO	1.74	Fs	12.96	ilmenite	0.21
Na_2O	2.02	$NaO_{1/2}$	3.69	Ap	0.35	rutile	0.47
K_2O	0.20	$KO_{1/2}$	0.24	Il	1.24	apatite	0.35
TiO_2	0.88	TiO_2	0.62	Mt	0.36	calcite	0.34
P_2O_5	0.16	$PO_{5/2}$	0.13	Cc	0.38		——
CO_2	0.15	CO_2	0.19				99.55
F	0.03	F	(0.09)			left over	
H_2O+	0.83	H_2O+	(2.61)			$+H_2O-$	0.04
H_2O-	0.04	H_2O-	(0.12)			+CaO	0.22
Total	99.82		99.99		99.99		99.81
Less O	.01						
	——	O	161.82				
	99.81	OH	5.22				
Anions per 100 cations			167.04				

The composition of hornblende from the kyanite-garnet amphibolites from Glenelg (No. 3*h*) is very similar to that of hornblende in the kyanite-bearing anorthosite in Idaho (No. 608*h*) even though more aluminum is present in the anorthosite (compare Nos. 608 and 3 in Fig. 5). The kyanite-garnet gedritite (No. 813) contains far less calcium than the kyanite amphibolites described in literature (Tilley, 1937), coming in this respect close to the cordierite gneiss (No. 5) and cordierite-anthophyllite rocks (Nos. 6 and 7). The kyanite-hornblende layer (No. 608) in the anorthosite is richer in aluminum and calcium than the gedritite No. 813.

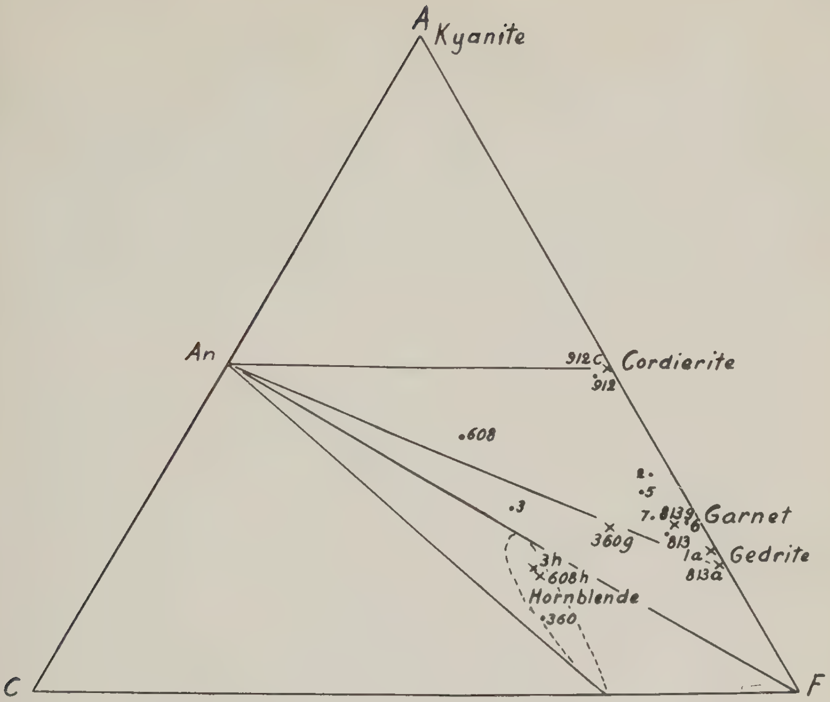

FIG. 5. ACF diagram showing the distribution of kyanite-garnet amphibolites, cordierite gneisses, and related rocks (.) and some of their minerals (x). Quartz and anorthite are stable with all assemblages given in parentheses for each rock listed below. The fields of stability for various assemblages are separated by lines connecting the plots for critical minerals.

813 = kyanite-garnet gedritite near Orofino, Idaho (kyanite-sillimanite-garnet-gedrite)
813*a* = gedrite in rock No. 813
813*g* = garnet in rock No. 813
608 = kyanite- and hornblende-bearing layer in anorthosite, Boehls Butte quadrangle, Idaho (kyanite-hornblende-bytownite-andesine)
608*h* = hornblende in rock No. 608
1*a* = gedrite from kyanite-garnet gedritite, Shuretsky, Karelia
2 = garnet gedritite, Karelia (kyanite-garnet-gedrite)
3 = kyanite-garnet amphibolite, Glenelg, Scotland (kyanite-garnet-hornblende) (Tilley 1937, p. 560)
3*h* = hornblende in rock No. 3
360 = garnet-amphibolite, Orofino Creek, Idaho (garnet-hornblende)
360*g* = garnet from rock No. 360
912 = cordierite gneiss, Boehls Butte quadrangle, Idaho (kyanite-andalusite-sillimanite-cordierite-biotite) (Hietanen 1956, Table 3)
912*c* = cordierite from rock No. 912
5 = cordierite gneiss, Kalanti, Finland (cordierite-biotite-sillimanite) (Hietanen 1943, Table 3, No 4)
6 = cordierite-anthophyllite rock, Perniö, Finland (cordierite-anthophyllite) (Eskola 1914, Table 28, p. 171)
7 = cordierite-anthophyllite gneiss, Orijärvi, Finland (cordierite anthophyllite-biotite) (Eskola 1915, Table 19, No. 50, p. 65)

Thus the gedrite seems to crystallize in the rocks poor in calcium whereas a common hornblende will appear if more calcium than needed for the formation of garnet is present. In the ACF diagram the analysis point for the gedritite No. 813 falls close to the gedrite corner of the anorthite-cordierite-gedrite triangle, into the same area as do the points for cordierite gneiss (No. 5) and the cordierite-anthophyllite rocks (Nos. 6 and 7), suggesting a disequilibrium for the kyanite. The thin-section study, however, speaks against the disequilibrium and a question arises as to whether an iron-magnesium ratio would have some bearing on the matter.

As pointed out earlier the kyanite gedritite contains very little potassium and calcium; therefore, an A′MF diagram (Fig. 6) with Al_2O_3, FeO, and MgO in the corners is particularly suitable for comparison of this mineral assemblage with that of some cordierite-bearing rocks also poor in CaO and K_2O. All cordierite-bearing rocks contain fairly little calcium but the amount of potassium varies. In the cordierite-anthophyllite rocks the amount of potassium oxide is negligible but the cordierite gneisses may carry 2 to 4 per cent of this oxide. Cordierite gneisses of the low temperature field of the amphibolite facies contain only biotite but in a somewhat higher temperature microcline also appears. In kyanite-hornblende rocks the amount of calcium is considerable as shown by the ACF diagram. However, the Fe:Mg ratio for all these rocks can be successfully studied in a modified A′MF diagram (Fig. 6) which was prepared using Eskola's (1915) method for corrections for feldspars and accessories. In Fig 6, also the amount of CaO is subtracted from the total of $Al_2O_3 + Fe_2O_3$ because much of the calcium is contained in plagioclase. For the corrections it is necessary to know the weight percentages of accessories (magnetite, ilmenite, apatite, calcite, etc.) which percentages were not available for all related assemblages given in the literature. In order to include analyses of several other kyanite-amphibole rocks and cordierite gneisses, a method of plotting, based on the molecular norm, was used in Fig. 7. As in the calculation of norm all CO_2 is calculated as calcite, all P_2O_5 as apatite, all Fe_2O_3 as magnetite, and K_2O, Na_2O, and CaO are combined with Al_2O_3 to form feldspars. The actual calculation is done in the following way: A is the number of Al ions after subtraction of the number of Al ions that is equal to the total number of combined Ca, Na, and K. F is the combined number of Fe and Mn ions after the amount to form magnetite with total of Fe_2O_3 was subtracted. M is the number of Mg ions. The total of A, M, and F is calculated to 100.

As a result of using the number of Al instead of that of Al_2O_3, all points in Fig. 7 are moved toward A corner in comparison with their positions in Fig. 6, but this change does not effect the mutual relations between the plots nor between the fields of stability which are separated by lines connecting the plots for critical minerals, such as kyanite-gedrite-garnet or cordierite-anthophyllite-garnet.

For comparison also the analyses of hornblende occurring with kyanite and that of biotite associated with cordierite are plotted even though hornblende contains a considerable amount of CaO and biotite K_2O. The A co-ordinate for these plots is modified in the similar manner as that for the other plots. As a result of this modification, the A co-ordinate is actually too small but the Fe:Mg ratio stays unchanged.

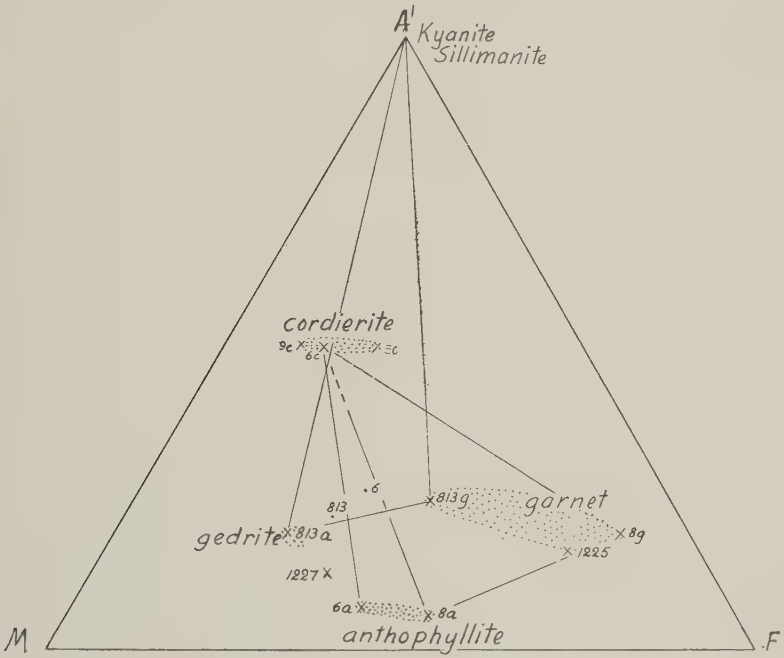

FIG. 6. A′MF diagram showing the field of stability for assemblages kyanite-garnet-gedrite (triangle 813*a*–813*g*–A′), cordierite-anthophyllite (line 6*a*–6*c*), and cordierite-anthophyllite-garnet. $A' = A - CaO = Al_2O_3 + Fe_2O_3 - Na_2O - K_2O - CaO$, $F = FeO + MnO$, $M = MgO$. 5*c*, 6*c*, and 9*c* are cordierite. 813*g*, 8*g*, and 1225 are garnet and 813*a*, 1227, 6*a*, and 8*a* are minerals of the gedrite-anthophyllite series. 813 is kyanite-garnet gedritite and 6 cordierite-anthophyllite rocks. For complete reference see explanation under Fig. 7.

Analyses points for critical minerals—garnet, anthophyllite, gedrite, and cordierite—were plotted into the same diagram. Plots for analyses of two cordierite-biotite gneisses (Nos. 5 and 912), a cordierite-garnet-biotite gneiss (No. 10), two anthophyllite-cordierite rocks (Nos. 6 and 7), and a garnet amphibolite (No. 360) were added for comparison. The

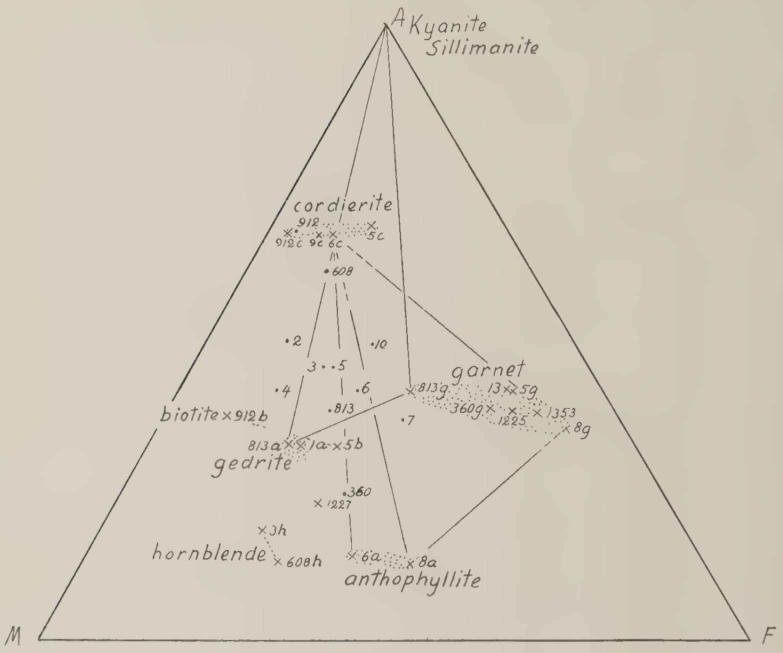

Fig. 7. AMF diagram showing the ratios of the modified numbers of Al, Fe, and Mg ions in kyanite-garnet amphibolites, garnet amphibolites, cordierite-bearing rocks (.), and in some of their minerals (x). A, M, and F refer to the number of ions calculated from chemical analyses as follows: $A = Al - (Ca + Na + K)$; $M = Mg$; $F = Fe^{\cdot\cdot} + Mn - Fe_2^{\cdot\cdot\cdot}$. Quartz and anorthite are stable with all assemblages given in parentheses for each rock listed below. The fields of stability for assemblages kyanite-garnet-gedrite, cordierite-anthophyllite, and cordierite-anthophyllite-garnet are shown. The fields of stability for any given assemblages can be easily constructed by connecting the plots for critcal minerals.

813 = kyanite-garnet gedritite, Orofino, Idaho (kyanite-sillimanite-garnet-gedrite)
813*a* = gedrite from rock No. 813
813*g* = garnet from rock No. 813
608 = kyanite-hornblende rock from anorthosite, Boehls Butte quadrangle, Idaho (kyanite-hornblende-bytownite-andesine)
608*h* = hornblende from rock No. 608
1*a* = gedrite from kyanite-garnet gedritite, Karelia (Tilley 1939, Table 1)
2 = garnet-gedritite, Karelia (Ignatiev 1934, Table 8, No. 1) (kyanite-garnet-gedrite)
3 = kyanite-garnet amphibolite, Glenelg (Tilley 1937, Table 1, No. 3) (kyanite-garnet-hornblende)
3*h* = hornblende from rock No. 3
4 = kyanite-bearing hornblende-biotite schist (Niggli 1929, Table 1, No. 32, kyanite-hornblende-biotite)
360 = garnet amphibolite, Orofino, Idaho (garnet-hornblende)
360*g* = garnet from rock No. 360

(*Continued on the next page*)

distribution of the points for the rocks carrying either cordierite (912, 10, 5), or amphibole (608, 813), or both of these minerals (6, 7), shows that either amphibole or cordierite can crystallize from the compositions that have approximately the same Fe:Mg ratio. The position of the points for Nos. 2, 3, 4, 5, 6, 7, 10, 813, and 608 shows that the amount of aluminum varies considerably but stays within the same range for the cordierite-bearing rocks, the kyanite-amphibolites, and the gedritites.

It is apparent that the fields of stability for the assemblage kyanite-garnet-gedrite (triangle 813*a*–813*g*-A) overlaps that of cordierite-anthophyllite with or without garnet and sillimanite and that of garnet-cordierite with or without sillimanite and biotite. The bulk composition in the cordierite-kyanite-andalusite-biotite gneiss No. 912 is richer in magnesium (and in potassium), the triangle 912*c*-912*b*-A being completely outside the field of stability of the kyanite-garnet-gedritite. Thus these two rocks could coexist in equilibrium in the same PT-field provided that the other factors, such as content and chemical potential of water, were the same.

Hornblende contains a considerable amount of CaO and thus has ac-

---

912 = cordierite gneiss, Boehls Butte quadrangle, Idaho (Hietanen 1956, Table 3) kyanite-andalusite-sillimanite-cordierite-biotite)
912*c* = cordierite from rock No. 912
912*b* = biotite from rock No. 912
5 = cordierite gneiss, Kalanti, Finland (Hietanen 1943, Table 3, No. 4) (cordierite-biotite-sillimanite)
5*c* = cordierite from cordierite gneiss, Rauma, Finland (Hietanen 1943, Table 1)
5*g* = garnet from cordierite gneiss, Kalanti, Finland (Hietanen 1943, Table 2)
5*b* = biotite from rock No. 5 (calculated)
6 = cordierite-anthophyllite rock, Perniö, Finland (Eskola 1914, Table 28, p. 171) (cordierite-anthophyllite)
6*a* = anthophyllite from rock No. 6 (Eskola 1914, Table 29, p. 172)
6*c* = cordierite from rock No. 6 (Eskola 1914, Table 29, p. 172)
7 = cordierite-anthophyllite gneiss, Orjärvi, Finland (Eskola 1915, Table 19, No. 50, p. 65) (cordierite-anthophyllite-biotite)
1227 = anthophyllite from garnet-anthophyllite biotite gneiss, Boehls Butte quadrangle, Idaho
1225 = garnet from garnet-anthophyllite biotite gneiss, Boehls Butte quadrangle, Idaho
1353 = garnet from anorthosite, Boehls Butte, quadrangle, Idaho
13 = almandine garnet from mica schist, Dent, Clearwater County, Idaho
8*a* = anthophyllite in garnetiferous anthophyllite-cordierite rock, Perniö, Finland (Eskola 1914, Table 30, p. 176)
8*g* = garnet in garnetiferous anthophyllite-cordierite rock, Perniö, Finland (Eskola 1914, p. 179)
9*c* = cordierite in cordierite-anthophyllite rock, Orjärvi, Finland (Eskola 1914, Table 31, p. 190)
10 = cordierite-garnet gneiss, Kalanti, Finland (Hietanen 1943, Table 3, No. 2, p. 16) (cordierite-garnet-biotite-microcline)

tually four major variables: Al, Fe, Mg, and Ca. If this mineral is plotted into a 4-component system (a tetrahedron with Al, Fe, Mg, and Ca in the corners, Fig. 8) it will lie at some distance beyond the AMF face and the stability field of the assemblage kyanite-hornblende-anorthite (such as No. 608) also would lie toward the Ca corner from the AMF face and would include the edge kyanite(A)-anorthite. However, the kyanite-garnet amphibolites (No. 3) contain garnet in addition to kyanite and hornblende and the stability field of such an assemblage would cover much of the same field as that of kyanite-garnet gedritites.

Paragenesis of Gedrite

Tilley (1939) has discussed the crystallization of gedrite and kyanite instead of cordierite and staurolite in metasedimentary formations. He remarks that, in the rocks rich in magnesium, staurolite cannot take the place of gedrite because of its ferrous character; and he raises the question as to whether the crystallization of kyanite and gedrite is linked to a magnesium-rich environment. Also in the garnet of the amphibolite facies the substitution of Mg for Fe is limited and therefore Mg-rich minerals such as cordierite and anthophyllite will crystallize. The A′MF and AMF diagrams (Fig. 6 and 7) in this paper shows that either cordierite or amphibole plus kyanite can crystallize in the rocks with the same Fe:Mg ratio. The study of the distribution of Fe, Mg, and Al in the critical minerals of all rocks concerned shows that the ratio Fe:Mg in the gedrites (Nos. 1*a* and 813*a*) falls within that in the cordierites but that the garnet takes more iron. The garnet (No. 813*g*) in the gedrite-bearing rock is richer in magnesium than the garnets common in cordierite gneisses (No. 5*g*, also compare Folinsbee, 1941). This makes the total percentage of magnesium in kyanite-garnet gedritite (No. 813) as high as is common in cordierite-garnet gneisses.

Why then does the gedrite instead of the cordierite crystallize in some rare occasions? Would a slight change in temperature or pressure or perhaps in the content of water cause the crystallization of amphibole and kyanite instead of cordierite? Or, could a shearing stress perhaps prevent the crystallization of cordierite and promote the crystallization of gedrite and kyanite? Shearing stress was suggested to be vital for the formation of kyanite in general by Tilley (1935) in his study of the rocks of the hornfels zone in Ross-shire, Scotland.

Pressure and temperature during the recrystallization

Let us first consider the pressure and temperature during the crystallization. The mineralogy of the gedrite-bearing rocks and that of the nearby layers suggests conditions of the amphibolite facies with a mod-

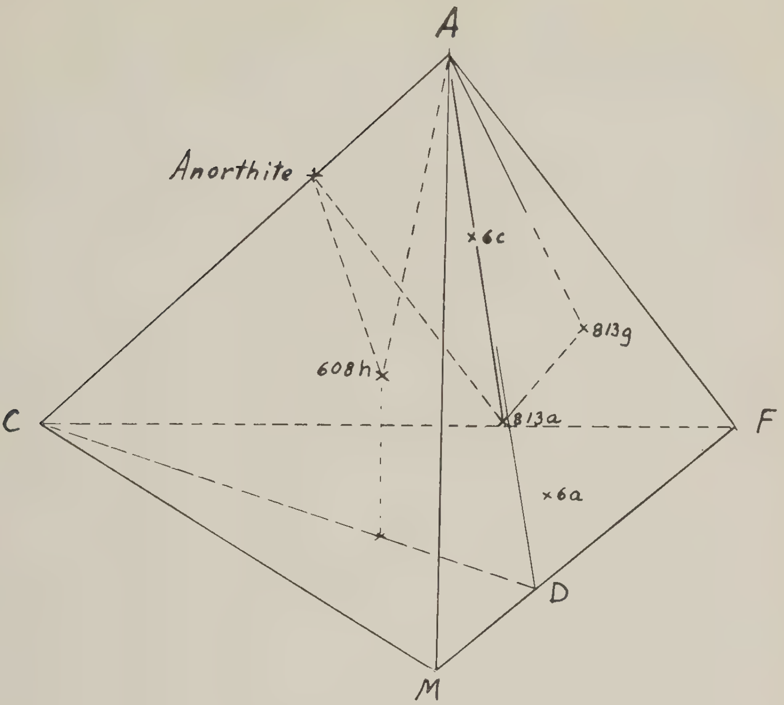

FIG. 8. 4-component system showing the relation between the stability fields of the assemblages of kyanite-garnet-gedrite-anorthite (subtetrahedron A-813*g*-813*a*-anorthite) and kyanite-hornblende-anorthite (triangle A608*h*-anorthite). The stability field of kyanite-garnet-hornblende-anorthite would be sub-tetrahedron A-813*g*-608*h*-anorthite. The point 608*h* lines on ACD plane inside the tetrahedron. The numbers refer to the same minerals as in Fig. 7.

erate temperature and high pressure. Sillimanite appears with kyanite but no andalusite was found in any of the specimens studied. Comparison with the study of the occurrence of kyanite, andalusite, and sillimanite together in the Boehls Butte quadrangle (Hietanen, 1956) suggests approximately the same temperature of crystallization for the rocks near Orofino and for those in the Boehls Butte quadrangle but the pressure was higher near Orofino. According to the suggested phase-diagram of Al_2SiO_5 (Fig. 9) andalusite would be stable only in low pressures; in higher pressures kyanite could occur with sillimanite without andalusite (Miyashiro, 1949). The occurrence of a few grains of staurolite and lack of potassium feldspar further restricts the temperature-pressure field between the PT-conditions of the crystallization of staurolite and potassium feldspar. Normally cordierite with biotite would be stable in this temperature-pressure field (cordierite-anthophyllite subfacies by Turner, 1948). In a higher temperature and pressure biotite would break down and yield cordierite and potassium feldspar, but not gedrite. In a lower temperature chlorite instead of cordierite is found in normal regionally metamorphosed rocks. It seems that the conditions under which the kyanite-garnet-gedrite assemblage crystallized were in some respect different from that of the conditions normally existing.

Comparison of the mineral assemblages of the rocks of the Orofino area with those of the cordierite gneisses of Finland (Hietanen 1943) suggests a somewhat lower temperature field for the Orofino area. Potassium feldspar is rare near Orofino and was not found with cordierite in the Boehls Butte quadrangle (Hietanen 1956). Near Orofino, sillimanite was found only in one thin section studied. The occurrence of some small crystals of staurolite, most of them included in the other minerals, suggests conditions of lower subfacies of the amphibolite facies during an earlier phase of crystallization. It is possible that near Orofino this lower temperature accompanied by a slight increase in pressure (or a stress) favored the crystallization of gedrite and kyanite instead of cordierite.

In some nearby layers epidote is found with plagioclase (An_{37-40}) suggesting, according to Barth (1952, p. 285), temperatures between 400° C. and 450° C. According to Schuiling's (1957) compilation of estimated temperatures and pressures, the triple point of the Al-silicates occurs at 540° C. in pressure of 3400 atmospheres. Both of these temperatures are in the range of that of the amphibolite facies.

Role of water

In addition to the higher pressure the content and chemical potential of water must be considered. The relation between the compositions and the specific gravities of the kyanite-gedrite assemblage and the cordierite can be shown with the following equation:

$$
\begin{array}{ccccccc}
2(\mathrm{Mg, Fe})_5\mathrm{Al_2Si_6Al_2(OH)_2O_{22}} & + & 6\mathrm{Al_2SiO_5} & + & 7\mathrm{SiO_2} & = & \\
\text{2 gedrite} & + & \text{6 kyanite} & + & \text{7 quartz} & & \\
\text{sp. gr. } 3.0 & & \text{sp. gr. } 3.6 & & \text{sp. gr. } 2.6 & & \\
\text{Mol. volume } 2\times 278.7 & + & \text{Mol. vol. } 6\times 45 & + & \text{Mol. vol. } 7\times 23 & = & 988.4 \\
5(\mathrm{Mg, Fe})_2\mathrm{Al_3Si_5AlO_{18}} & + & 2\mathrm{H_2O} & & & & \\
\text{5 cordierite} & + & \text{2 water} & & & & \\
\text{sp. gr. } 2.6 & & \text{sp. gr. } 1 & & & & \\
\text{Mol. vol. } 5\times 233 & & & & & & =1165
\end{array}
$$

Cordierite is an anhydrous mineral and could be expected to crystallize in a dry environment. As a rule, however, cordierite is found with biotite and other hydrous minerals suggesting that this point is not vital for its stability. Indeed, the experimental work by Yoder (1952, p. 583 and p. 609–612) shows that Mg cordierite can be formed hydrothermally at 490° C., but that at moderate pressures anthophyllite and pyrope are stable below 660° C. only in "water deficient" environment. The specific gravities show that the molar volume of the assemblage gedrite-kyanite-quartz is 15.2 per cent smaller than that of the cordierite on the right. The assemblage of the more tightly packed minerals could thus be expected to be stable in the higher pressure field. On the other hand, the high temperature usually causes dehydration and the crystallization of cordierite would be expected. This is in accordance with the consideration in figure 9 and together they would suggest that the crystallization of gedrite would require a higher pressure or a lower temperature than normally found for the rocks of the amphibolite facies.

Type of pressure

Verhoogen (1951) has shown that the chemical potential of a stressed solid is nearly equal to the chemical potential of the same solid, unstressed, but under a hydrostatic pressure equal to the mean hydrostatic pressure if the temperature is the same. The mean hydrostatic pressure is the mean of the three principal stresses acting upon a stressed solid. Also MacDonald (1957, p. 278) came to the conclusion that "the variation of chemical potential in the stressed solid is to a good approximation equal to the variation of chemical potential in a body under hydrostatic stress," and that "Transitions . . . involving large volume and entropy changes should not be affected by shearing stress." Accordingly, transitions such as andalusite to kyanite and crystallization of gedrite and kyanite instead of cordierite should not depend on stress and there would be no "stress" or "anti-stress" minerals in the sense Harker (1939) has suggested. However, considering the molar volumes of the minerals under discussion, we concluded that the high pressure (either hydrostatic or nonhydrostatic) during the crystallization would favor the formation of the kyanite-gedrite assemblage. At this point the geologic evidence must decide whether the pressure was hydrostatic or nonhydrostatic.

One of the main differences in the PT-conditions in nature and in the laboratory is different kinds of pressure. During the laboratory experiments the pressure is hydrostatic but in nature it is more often nonhydrostatic. In the areas where recrystallization has taken place contemporaneously with the deformation the rocks were subjected to a directed rather than to a hydrostatic pressure. It is well known that penetrative shearing has a catalytic influence on the recrystallization. Many minerals that are oriented at random in the sediments attain a preferred orientation through recrystallization or through some other mechanism during the deformation. The chemical composition of these minerals is not changed; they are in chemical equilibrium with their environment but still the penetrative shearing will cause recrystallization and reorientation of the mineral grains in order to provide a preferred position in which the mineral can better endure the shearing stress or yield by translation.

The capacity of a mineral to endure shearing varies in different directions. These directions are certain crystallographic directions, for example micas grow with their sheets of SiO_4 tetrahedra parallel to the shear plane and amphiboles their chains parallel to the direction of the shear. It is also well known that some minerals are more sensitive to the penetrative shearing than the others. These studies in the structural petrology show that the shearing stress plays an important role during the recrystallization, and it would be only natural that various minerals could endure the shearing in different proportions depending on their crystal structure. The sheet structure of the micas and the chain structure of the amphiboles endure a great amount of shearing whereas some other minerals may not have any "durable" crystallographic directions.

Kyanite is frequently found in non-stressed environments such as in pegmatites and in quartz veins. On the other hand, the anthophyllite-cordierite assemblage shows that these two minerals can crystallize under the same PT-conditions. However, cordierite is not normally found in strongly sheared schists. This suggests that Harker's (1939) concept of stress and anti-stress minerals in regard to the minerals under discussion should be modified to read as follows: The "stress" minerals may crystallize equally under hydrostatic or nonhydrostatic pressure but the anti-stress minerals cannot be formed under strong shearing stress. This modification does not contradict the theoretical considerations recently discussed by MacDonald (1957, p. 272).

Comparison of the texture of the kyanite- and gedrite-bearing rocks near Orofino with that of their neighboring layers suggests crystallization under stressed conditions for some layers, but in the other layers minerals show only a subordinate amount of orientation. The garnet gedritite layer shows signs of strongest deformation. The gedrite prisms are parallel to the axis of the folding and mark a strong *b* lineation. The deformation was apparently accompanied by a stretching parallel to the *b* axis. In the kyanite-garnet gedritite a similar lineation parallel to the *b* axis occurs even if this rock as a whole is less sheared. In the garnet gedritite the clusters of light constituents are elongated parallel to the axis whereas in the kyanite-bearing rock they are irregular in shape. The stretching parallel to the axis was probably intensified by a second fold-

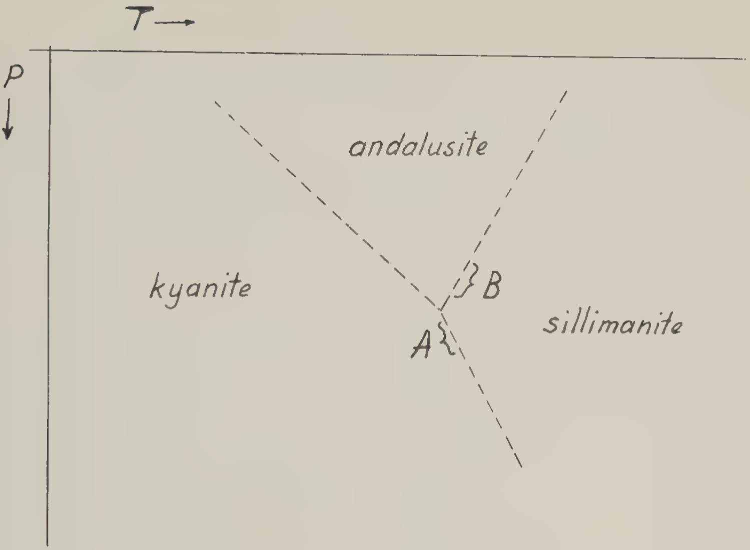

FIG. 9. Position of kyanite-garnet gedritite (region A) and cordierite-anthophyllite rocks (region B) in the suggested phase diagram of kyanite, andalusite, and sillimanite.

ing that bent the strata near Orofino to form an open drag around the axis that makes an angle of about 60° with the axis of smaller folds.

The layer of biotite-garnet gneiss that occurs between the two gedrite-bearing layers contains some staurolite and shows less sign of shearing than the gedritites. Biotite instead of gedrite crystallized in this layer, apparently owing to the presence of potash. Also, in the nearby schist the ferromagnesian minerals are garnet and biotite and the excess of aluminum, if present, crystallized as kyanite and sillimanite.

The cordierite gneisses in Finland show a fairly well developed mica orientation (Hietanen 1943) suggesting crystallization under stress. The mean hydrostatic pressure in this case, however, was probably smaller than that acting upon the kyanite-gedrite assemblage (see Fig. 9).

Comparison with kyanite-hornblende-anorthite assemblage

The occurrence of kyanite with hornblende in some layers in the anorthosite in the Boehls Butte quadrangle (Hietanen in press) is probably due to a later introduction of elements. The country rock of the anorthosite is a garnet-biotite schist rich in aluminum silicates. Some of the anorthosite contains several minerals inherited from the schist. In this case the occurrence of kyanite, andalusite, and sillimanite together in the neighboring layers fixes the temperature and pressure to the triple point of figure 9. The older rocks in this area consisted of sedimentary formation in which layers rich in aluminum and layers rich in calcium alternated.* During the metamorphism first bytownite crystallized in the limy layers and Al-silicates with micas in the aluminous layers. Later, an introduction of sodium took place and was accompanied by an extensive rearrangement of material. Bytownite reacted with sodium forming andesine, but this reaction was not completed: numerous bytownite grains were left between and in the newly formed large andesine grains giving rise to the anorthositic rock with two plagioclases. Many segregations of ferromagnesian minerals show that iron and magnesium also were mobile. During the introduction of sodium a part of Ca, Fe, and Mg were removed from the anorthositic layers. These elements migrated to the nearby schistose layers (which were rich in Al-silicates) giving rise to the crystallization of hornblende with kyanite. The layers, in which kyanite occurs with hornblende, also contain bytownite and andesine, thus two plagioclases that should have reacted to form labradorite. The relation between the kyanite and hornblende is comparable with that between the bytownite and andesine. The kyanite can be an earlier mineral inherited from the schist and the hornblende crystallized later during the formation of anorthosite. Unless new information will prove otherwise, it is not safe to assume that kyanite in this rock is in equilibrium with hornblende.

In the light of the occurrence of kyanite with hornblende in the anorthosite one might think that a similar metasomatic addition of elements may have caused the crystallization of gedrite near Orofino. This suggestion is strengthened by the occurrence of several accumulations of ferromagnesian minerals in the nearby schist and quartzite layers. During a regional study of the rocks near Orofino these accumulations were found to be metasomatic.† The sequence of crystallization in the gedrite-bearing rocks also favors the metasomatic origin of gedrite. The parent rock may have been a similar biotite-garnet gneiss as found between the two gedrite-bearing layers. An addition of Mg and possibly of some Fe and a removal of K may have changed the composition of the biotite gneiss to be suitable for the formation of gedrite. In this case kyanite could be a relict mineral as it is in the anorthosite in the Boehls Butte quadrangle. However, in contrast to the kyanite in anorthosite the kyanite in the gedritite has quite fresh borders. It is usually surrounded by gedrite and there are no signs of disequilibrium.

In the country rocks of the anorthosite in the Boehls Butte quadrangle

* See footnote 1.

† See footnote 2.

cordierite crystallized in some aluminous layers rich in magnesium and gedrite with garnet in some other layers that are richer in iron; neither of these types of layers shows signs of an exceptionally strong shearing stress. In this case the crystallization of either cordierite or gedrite is apparently due to the chemical composition of the layers. The gedrite in the Boehls Butte quadrangle (No. 1227 in Fig. 7) is only a little richer in iron than the gedrite near Orofino; the garnet (No. 1225 in Fig. 7), however, contains considerably more iron than this mineral near Orofino (No. 813*g*).

CONCLUSION

It seems that, in addition to a suitable chemical composition (an environment rich in aluminum and magnesium, containing a moderate amount of iron and only a small amount of water), a slight increase in nonhydrostatic pressure (stress) favors the formation of gedrite and kyanite instead of cordierite in that temperature field of the amphibolite facies in which staurolite is changing to kyanite and garnet and in which first crystals of sillimanite may appear. This is very close to the same temperature-pressure point in which the three aluminum silicates—kyanite, andalusite, and sillimanite—can occur together. The occurrence of kyanite with the hornblende in some layers of the anorthosite suggests that in some cases kyanite may be found with amphibole because of slowness of reactions between the minerals of the parent rock and the introduced solutions carrying magnesium and iron.

REFERENCES

ANDERSON, A. L. (1930), The geology and mineral resources of the region about Orofino, Idaho: *Idaho Bur. Mines and Geology*, Pamph. **34,** 1–63.

BARTH, T. F. W. (1952), Theoretical petrology, New York, John Wiley and Sons, Inc., 387 p.

CLOUGH, C. T. (1910), The geology of Glenelg, Lochalsh, and south-east part of Skye: *Geol. Survey Scotland, Memoir*, p. 35.

ESKOLA, PENTTI (1914), Petrology of the Orijärvi region in south-western Finland: *Comm. Geol. Finlande, Bull.* **40,** 1–277.

——— (1915), Om sambandet mellan kemisk och mineralogisk sammansättning hos Orijärvitraktens metamorfa bergarter: *Comm. Geol. Finlande, Bull.* **44,** 1–145.

FOLINSBEE, R. E. (1941), The chemical composition of garnet associated with cordierite: *Am. Mineral.*, **26,** 50–53.

HARKER, ALFRED (1939), Metamorphism; a study of the transformations of rock masses, 2d ed., rev., London, Methuen and Co., 362 p.

HEZNER, L. (1908), Petrographische Untersuchung der kristallinen Schiefer auf der Südseite des St. Gotthard (Tremolaserie): *Neues Jahrb. Beil. Band* **27,** 157–218.

HIETANEN, ANNA (1943), Über das Grundgebirge des Kalantigebietes in südwestlichen Finnland: *Ann. Acad. Sci. Fennicae A*, **III,** no. 6, 1–106.

——— (1956), Kyanite, andalusite, and sillimanite in the schist in Beehls Butte quadrangle, Idaho: *Am. Mineral.*, **41,** 1–27.

——— Anorthositization of schist and quartzite northwest of the Idaho batholith: *20th Internat. Geol. Cong., Mexico,* **1956,** *Proceedings,* (in press).

Ignatiev, N. A. (1934), Amphibolites, garnet-gedritites and micaites from outskirts of S. Shueretski: *Akad. Nauk SSSR Petrog. Inst. Trudy,* **6,** 65–82.

MacDonald, Gordon J. F. (1957), Thermodynamics of solids under nonhydrostatic stress with geologic applications: *Am. Jour. Sci.,* **255,** 266–281.

Miyashiro, Akiho (1949), The stability relation of kyanite, sillimanite, and andalusite, and the physical conditions of the metamorphic processes: *Geol. Soc. Japan, Jour.,* **55,** 218–223.

Niggli, P. (1929), Die chemisch-mineralogische Charakteristik der metamorphen Paragesteinsprovinz am Südrande des Gotthardmassivs: *Schweizer. Mineralog. Petrog. Mitt.,* **9,** 160–187.

Rabbitt, John C. (1948), A new study of the anthophyllite series: *Am. Mineral.,* **33,** 263–323.

Schuiling, R. D. (1957), A geo-experimental phase diagram of Al_2SiO_5 (Sillimanite, Kyanite, Andalusite): *Koninkl. Nederlandse Akad. Wetensch. Proc., Ser. B,* **60,** no. 3, 220–226.

Tilley, C. E. (1935), The role of kyanite in the "hornfels zone" of the Carn Chuinneag granite (Ross-shire): *Mineralog. Mag.,* **24,** 92–97.

——— (1937), The paragenesis of kyanite-amphibolites: *Mineralog. Mag.,* **24,** 555–568.

——— (1939), Kyanite-gedrite parageneses: *Geol. Mag.,* **76,** 326–330.

Turner, F. J. (1948), Mineralogical and structural evolution of the metamorphic rocks: *Geol. Soc. America, Memoir* **30,** 342 p.

Verhoogen, Jean (1951), The chemical potential of a stressed solid: *Am. Geophys. Union Trans.,* **32,** 251–258.

Yoder, H. S., Jr. (1952), The MgO-Al_2O_3-SiO_2-H_2O system and the related metamorphic facies: *Am. Jour. Sci.,* Bowen volume, 569–627.

Manuscript received August 26, 1958.

THE AMERICAN MINERALOGIST, VOL. 44, MAY-JUNE, 1959

UVAROVITE GARNET AND SOUTH AFRICAN JADE (HYDROGROSSULAR) FROM THE BUSHVELD COMPLEX, TRANSVAAL

J. J. FRANKEL, *University of Natal, Durban, South Africa.*

ABSTRACT

Uvarovite garnet is an uncommon silicate matrix in chromitite seams in the Norite body of the Bushveld Igneous Complex, Transvaal, Union of South Africa. Separated uvarovite samples were analyzed chemically, and unit cell, specific gravity and refractive index values determined. Uvarovite, grossularite and andradite are the dominant "end members." A linear relationship between chromic oxide content and physical properties is modified by titanium and iron. The deviations are discussed and estimated. The green color is tinged with brown where titanium and iron are high. The associated chromite grains have a chemical composition similar to that of nearby chromitite seams. Uvarovite-diopside layers between uvarovite-bearing chromitite seams in the Eastern belt of the Norite are described. It is considered that the uvarovite was formed in pyroxenite and chromitite where adequate chromium was available, by metamorphic metasomatic processes after the consolidation of the Norite body itself.

The pale green, fine-grained, ornamental rock known as South African Jade is found to be hydrogrossular that varies in composition over a restricted range near the grossularite end of the hydrogarnet series. Specific gravity and refractive index decrease with increase in combined water. The mineral replaces basic feldspar through zoisite, in anorthosite and feldspar-rich pyroxenite horizons near the Lower group of chromitite seams in the Western Belt of the Norite. The mineralogical changes are thought to be due to the addition of calcium in heated waters.

INTRODUCTION

Uvarovite, the bright green chromian garnet, was first reported associated with chromitite seams, from the eastern part of the Bushveld Complex (Hall, 1908, p. 60; Hall and Humphrey, 1909, p. 74). Grossularite, calcium aluminium garnet, in a massive form associated with anorthosites and pyroxenites, was described from the Brits area in the western part of the Complex (Hall, 1925). Several occurrences of green garnet, probably grossularite, and other varieties in metamorphosed dolomitic rocks at the contacts with the base of the Complex have also been recorded (Kynaston, 1909, p. 20; Wagner, 1929, p. 175). A few further details of garnet in the Complex were given by Hall (1932) and Kupferbürger (1937).

My interest in these garnets arose during an examination of chromite deposits in the Bushveld Complex with the late Dr. J. Gelletich. Professor E. Mendelssohn, Witwatersrand University, later gave me a uvarovite-bearing chromitite of remarkable grain size variation; I also received specimens from Professor B. V. Lombaard, Mrs. A. Blignaut of the Johannesburg Public Library Museum and Dr. J. D. Steyn of the Union Geological Survey Museum, Pretoria. A detailed investigation of uvarovite and of South African Jade which could add to known mineralogical data was then possible.

The localities of the specimens investigated are shown on the map (Fig. 1). In addition to these localities, several others are known.

The chromium-bearing garnet is less abundant and more restricted in its associations than other members of the garnet family. Uvarovite is usually found as a matrix to closely-packed chromite grains, in thin veins or scattered in metamorphosed sediments. The crystals are generally small and intimately associated with other minerals. This makes a clean separation of uvarovite difficult and may account for the paucity of good chemical analyses coupled with adequate physical data. Thus correlation of chemical composition and physical properties in the chrome-bearing varieties of the ugrandite series has been based upon sparse and incomplete information.

The distribution and mineral associations of uvarovite and grossularite in the Bushveld Complex are dissimilar in many respects, although they do occur more or less in the same zone above the base of the Norite body. The uvarovite is rarely associated with grossularite and vice-versa. For this there must be some fundamental reason. Aims of the present study, therefore, were to clarify the relationships between these garnets and to contribute towards an understanding of their origins in the Bushveld Complex.

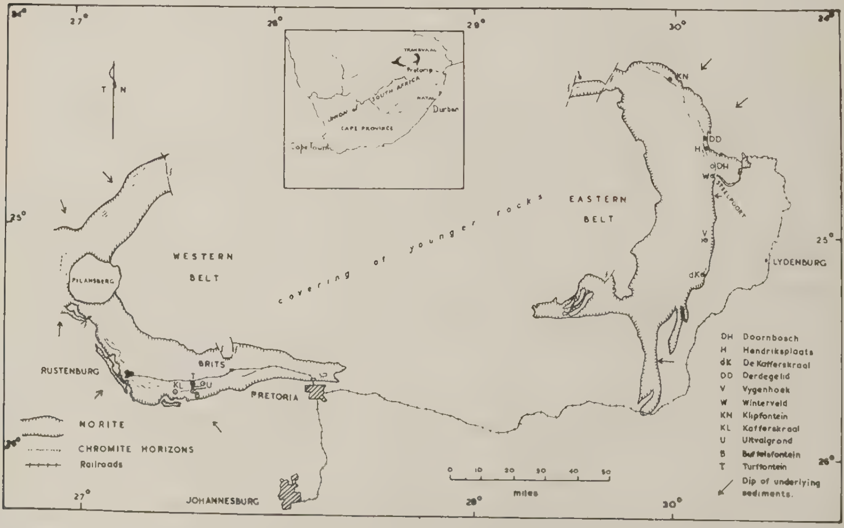

Fig. 1. Geological sketch map of the Central Transvaal, showing the extent of the Norite body of the Bushveld Complex and the localities of specimens here described. (Modified from Union Geological Survey Maps.)

THE FIELD SETTING OF THE UVAROVITE AND SOUTH AFRICAN JADE

The field occurrence of the garnetiferous rocks will be made clear from the following brief account of the Bushveld Igneous Complex. This basin-like structure occupies an area, elongated along an east-west axis, in the central part of the Transvaal Province of the Union of South Africa. The surrounding, underlying sediments dip towards the centre of the Complex of which much is covered by later formations. The main continuous exposures are preserved in two areas, known as the Eastern and Western Belts (Fig. 1).

The Complex comprises two major rock groups; an upper Red Granite overlying and bordered by a lower Norite-gabbro body. The Norite body exhibits "pseudo-stratification" or rifting which agrees in a general way with the low to moderate dip of the floor strata. It has been sub-divided into several zones, of which the Critical zone rather low down in the body, is composed of a well pseudo-stratified, diversified, layered succession of peridotite, anorthosite, pyroxenite and chromitite "seams."

The chromitite seams consist of chromite crystals with little interstitial silicate mineral. They range from thin partings to robust seams several feet thick that persist for long distances along strike and parallel to the pseudo-stratification of the enclosing rocks. Disseminations of chromite crystals are common in the pyroxenites.

There are two well-defined groups of seams in the Eastern Belt, designated Lower and Middle groups. They are well exposed in the hilly and mountainous country. There is also an Upper group in the Western Belt where the country is flat. Faulting or black turf overburden often make outcrop correlation uncertain.

The Bushveld uvarovite occurrences are all associated with chromitite seams, at the contacts with surrounding rock, as cross-cutting veins, as lenses and bands within the seams, or in lenticular bodies with disseminated chromite not far from a true chromitite seam.

In the field the uvarovite appears to take the place of pyroxene and feldspar within the chromitite seams or at the contacts with anorthositic or pyroxenitic rocks. Sometimes, masses of almost pure uvarovite associated with crystals of diopside and zoisite and only very small amounts of disseminated chromite grains, are marginal to chromitite seams. Most of the uvarovite in the Eastern Belt is associated with the Lower group chromitite seams; the examples from the Western Belt may come from the Middle or Upper groups.

The rock prized as an ornamental stone and known as South African Jade occurs in the almost featureless flat country about 40 miles due west of Pretoria. Although poorly exposed through a black turf overburden, the field relationships have been clearly revealed in trenches and pits.

Two or three bands of massive pale green rock, from a few inches to two feet thick are separated by bands of light-colored massive anorthosite. An anorthosite-norite with jade, rests on a chromitite seam below the main jade seams. Scattered thin bands or streaks of chromite crystals also lie within the jade. The jade layers and the associated rocks conform to the characteristic pseudo-stratification of the Norite body and dip at 15 to 20 degrees towards the north.

According to Hall (1932, p. 415), the jade horizon can be traced at intervals along many miles of strike, and where it leaves the chromitite horizon it is a white lime silicate hornfels. Occurrences of similar rock have also been reported from the Potgietersrust area in the northern part of the Complex and from the eastern part as well.

UVAROVITE

Experimental Procedure

The uvarovite is generally the matrix around fine chromite crystals so that separation cannot be achieved by simple hand-picking; similarity in grain size of garnet and chromite does not allow of separation by sieving. In most of the specimens garnet was only liberated from the associated minerals after crushing to minus 200 mesh Tyler. The following procedure for separating the garnet from other minerals was adopted.

Gentle crushing in a diamond mortar released larger chromite grains, so that a fair percentage could be eliminated by hand-picking and coarse sieving. The minus 200 mesh powder was gently deslimed, dried, and repeatedly centrifuged in Clerici solution S.G. 3.8 to 3.9. In this way free particles of garnet and other lighter minerals were separated from the chromite and aggregate chromite-garnet grains. The lighter minerals were removed from the garnet by centrifuge treatment in methylene iodide or suitably adjusted Clerici solution. All samples were carefully checked microscopically for purity. The minute amount of chromite in scattered aggregate grains still present after purification cannot have a significant effect on the chemical analyses of the garnet. The garnet powders were thoroughly washed to remove adhering heavy liquid and were finally oven-dried.

The determination of specific gravity on the fine powders proved difficult, but repeated measurements using Ellsworth's vitreosil pyknometers gave reasonably consistent results and all values were then calculated to 20° C. A few values were checked by suspension of grains in Clerici solution suitably diluted. The refractive index measurements were made in West's high refractive index liquids in sodium light.

The color of the garnet was measured on a Donaldson Trichromatic Colorimeter which I had previously used with some success (Frankel, 1953). Colors are also described by comparison with a standard color chart.

Full chemical analyses were not made on all specimens, mainly owing to lack of sufficient material. The accuracy of ferrous oxide determinations in garnets is often questioned and considerable attention was paid to this matter by the analysts, who used several methods, all of which gave reasonably consistent results. Mr. Schutte used Hey's method (1941), while Mr. Herdsman carried out the determination by simple solution in phosphoric acid in constant flow of carbon dioxide and checked against a blank and a standard powder. Particular attention was also paid to the determination of combined water in the uvarovite.

The National Physical Laboratory reported that the Debye-Scherrer photographs were taken in a camera of 114.59 cm. diameter according to the Straumanis principle, using either Cu K_α or iron-filtered Co radiation. Exposure times were approximately 7 and 16 hours respectively.

Chemical and Physical Data on Uvarovite

The chemical analyses (Table I) of the garnet can be recast as isomorphous mixtures of "end members"; mainly uvarovite, grossularite and andradite which, except for Specimens Nos. 1 and 2, range in approximate proportions from 5:5:1 through 4:2:1 to 2:2:1, respectively. Chromium is the dominant trivalent ion in most of the specimens which are, therefore, called "uvarovite." There are also small amounts of pyrope and almandine. In Specimen No. 1 only, is grossularite the dominant "end member."

The molecular ratios show considerable divergence from the ideal formula (3:1:3).

	RO_2	R_2O_3	RO
Analysis 4	2.91	1	3.06
5	2.89	1	3.33
6	3.48	1	3.91
7	3.09	1	3.65
10	2.97	1	3.33

The unit cell contains an "excess" of Ca ions (Table II), and recasting the composition into "end members" also gives excess CaO that makes the true proportions of "end members" difficult to estimate. Betekhtin (1946, p. 69) also found calculation of uvarovite analyses unsatisfactory.

Vermaas (1952) experienced similar difficulties with manganese-iron garnet. He suggests that near agreement between determined and calculated specific gravity values in such garnets, indicates that excess atoms occupy positions within the unit cell. Since the measured and calculated specific gravity values of the uvarovite specimens are in good agreement,

Table I. Chemical Analyses of Uvarovite

	1	2	3	4	5	6	7	8	9	10
SiO_2	38.67	—	—	33.50	34.64	36.86	33.33	35.18	35.69	34.52
TiO_2	0.38	n.d.	0.30	1.97	2.24	0.40	2.50	1.31	0.24	1.68
Al_2O_3	n.d.	—	—	9.12	9.44	8.98	7.50	n.d.	n.d.	8.05
Fe_2O_3	4.94	4.86	9.38	6.13	6.30	2.22	6.26	3.96	5.97	3.80
Cr_2O_3	3.93	9.44	10.56	11.16	11.49	11.54	11.70	11.96	13.62	14.83
FeO	1.96	2.70	—	2.73	1.72	2.92	2.51	2.55	2.34	2.53
MnO	—	—	—	0.03	n.d.	n.d.	0.02	—	—	0.03
MgO	1.51	—	—	1.67	0.78	0.62	1.28	—	—	1.86
CaO	33.97	—	—	33.70	33.26	35.93	35.12	33.11	33.07	32.81
	—	—	—	100.01	99.87	99.47	100.22	—	—	100.22

1. Lydenburg district, Eastern Belt. Partial Analysis. Analysts W. H. Herdsman (Fe_2O_3, Cr_2O_3, FeO). J. J. Frankel (SiO_2, TiO_2, MgO, CaO).
2. Klipfontein, 119, Lydenburg district, Eastern Belt. Partial Analysis. Analyst W. H. Herdsman.
3. Winterveld, 424, Lydenburg district, Eastern Belt. Analyst McLachlan & Lazar (total iron as Fe_2O_3).
4. Vygenhoek, 209, Lydenburg district, Eastern Belt. Analyst C. E. G. Schutte.
5. Uitvalgrond, 71, Brits area, Western Belt. Analyst W. H. Herdsman.
6. Derdegelid, 141, Lydenburg district, Eastern Belt. Analyst W. H. Herdsman.
7. De Kafferskraal, 359, Lydenburg district, Eastern Belt. Analyst C. E. G. Schutte.
8. Kafferskraal, 915, Rustenburg district, Western Belt. Partial Analysis. Analysts W. H. Herdsman (Fe_2O_3, Cr_2O_3, FeO). J. J. Frankel (SiO_2, TiO_2, CaO). McLachlan & Lazar ($H_2O+0.48\%$).
9. Hendriksplaats, 357, Lydenburg district, Eastern Belt. Partial Analysis. Analysts W. H. Herdsman (TiO_2, Fe_2O_3, Cr_2O_3, FeO). J. J. Frankel (SiO_2, CaO).
10. Doornbosch, 423, Lydenburg district, Eastern Belt. Total includes SrO 0.11%. Analyst W. H. Herdsman. FeO by F. J. de Wet.

the excess of RO group may also be accommodated in cavities in the garnet. Packing index is close to that given for garnets by Fairbairn (1943).

Alderman (1935) suggested that Si and Fe^{2+} ions are replaced by Al with Fe^{3+} entering the RO group. This replacement would account for excess R_2O_3 in almandine. Fleischer (1937) who showed that most garnets conform closely to the ideal ratio, thought that Alderman's observed discrepancies might be due to under-estimation of ferrous oxide, so that more iron would be reported in the R_2O_3 group. Fleischer did not, however, deal specifically with uvarovite nor with garnets containing more than 0.5 per cent TiO_2 and it is in such garnets containing much TiO_2 or FeO that deviations from the ideal ratio are found.

Although, according to Kunitz (1936), Ti replaces Si, the exact behavior of Ti in garnet is not known with certainty and Zedlitz (1933) has

Table II. Number of Atoms (O=96) in Unit Cell of Uvarovite

	4	5	6	7	10	Theoretical
O	96	96	96	96	96	96
Si	21.86	22.43	23.87	21.88	22.43	—
Ti	0.97	1.09	0.20	1.23	0.82	—
	22.83	23.52	24.07	23.11	23.25	24
Al	7.02	7.20	6.85	5.80	6.17	—
Fe^{3+}	3.01	3.07	1.06	3.09	1.86	—
Cr	5.75	5.88	5.90	6.07	7.62	—
	15.78	16.15	13.81	14.96	15.65	16
Fe^{+}	1.49	0.93	1.58	1.38	1.37	—
M^{2}n	0.02	—	—	0.01	0.02	—
Mg	1.62	0.75	0.60	1.25	1.80	—
Ca	23.55	23.06	24.92	24.69	22.83	—
Sr	—	—	—	—	0.04	—
	26.68	24.74	27.10	27.33	26.06	24

suggested that Ti may possibly be in the trivalent state and so cause a corresponding amount of Fe_2O_3 to be reported as FeO. In calculations of the molecular ratios of Bushveld uvarovite given above, all Ti has been added to Si, although all or part can occur as Ti_2O_3 and Al can replace Si. Further calculations were made in which all the Ti was assigned to the R_2O_3 group with an equivalent amount of ferric iron subtracted from the iron of the RO group, and excess Al was added to Si. These results approached the ideal formula more closely, but the RO group still showed excess Ca.

Attempts to correlate chemical composition of garnet with physical

Table III. Specific Gravity, Optical and *X*-Ray Data for Uvarovite

	1	2	3	4	5	6	7	8	9	10
S.G.$_{4^\circ}^{20^\circ}$C (± .005)	3.709	3.742	3.763	3.772	3.754	3.740	3.772	3.754	3.789	3.798
Calculated S.G.				3.767		3.758	3.767			
R.I. (Na light) (± .002)	1.783–1.786	1.817–1.820	1.824	1.833	1.830	1.801	1.832	1.828–1.830	1.830–1.833	1.837
a_0(± .001 Å)	11.915	11.946	11.955	11.973	11.961	11.923	11.989	11.955	11.969	11.975
Mol. wt.	—	—	—	490.0	485.4	482.2	493.4	—	—	488.8
Packing Index				6.2		6.3	6.2			

Table IV. *X*-Ray Powder Spacing Data for Uvarovite

4		7		10	
d Å	I	*d* Å	I	*d* Å	I
—		—		4.2187	?
2.9694	m-s	2.9751	m	2.9683	m-s
2.6541	s	2.6594	s	2.6535	s
2.5334	w	2.5351	w	2.5300	w
2.4268	m-s	2.4280	m	2.4268	m-s
2.3293	m	2.3012	m-w	2.3322	m-w
2.1708	m	2.1728	m-w	2.1701	m-w
1.9317	m-s	1.9311	m	1.9313	m
1.8768	w	1.8851	m-w	1.8841	w
1.7175	m	1.7191	m-w	1.7223	m-w
1.6515	m-s	1.6536	m	1.6529	m-s
1.5928	s	1.5943	s	1.5910	s
1.4903	m	1.4991	m-w	1.4918	m-w
1.3343	m	1.3352	m	1.3343	m-w
1.3021	m	1.3035	m	1.3023	m
1.2726	m	1.2738	m	1.2720	m-w
1.2062	w	1.2058	w	1.2063	w
1.1095	m	1.1140	m	1.1083	m
1.0905	m	1.0922	m	1.0902	m
1.0559	m	1.0575	m	1.0560	m-w
0.99601	w	0.99839	m-w	0.99564	w
0.98237	w	0.98380	w	0.98236	w
0.96985	m-s	0.97108	m	0.97010	m
0.90188	vw	—		0.9±	?
0.89156	m	0.89253	m	0.89148	m
0.88179	m-w	0.88280	m-w	0.88173	m-w
0.88137	m-w	—		—	
0.86346	m	0.86460	m-w	0.86363	m-w
0.82971	m	0.83087	m-w	0.82995	w
0.82208	m-s	0.92324	m	0.82197	m
0.81436	s	0.81582	s	0.81453	s

w=weak m=medium s=strong.

properties have been made for three "end members" (Ford, 1915), and correlation involving four "end members" has been reasonably successful. Levin (1949, 1950) has shown that five components can account for 99 per cent or more of the composition of a garnet. By means of partial chemical analysis and the three physical properties, refractive index (R.I.), specific gravity (S.G.) and unit cell dimension (a_0), the molecular proportions of the five compositional molecules can be obtained by setting up and solving five simultaneous equations. His investigation did not include garnets containing the uvarovite "end member."

von Knorring (1951) showed that a direct relationship exists between the above three physical properties and the chromic oxide content in uvarovite. This is to be expected, because the replacement of Al^{3+} (ionic radius 0.57 Å) by Cr^{3+} (0.64 Å) or Fe^{3+} (0.67 Å) must expand the lattice of grossularite as the composition approaches that of uvarovite or andradite. Although von Knorring made the first study of uvarovite in which full chemical analyses were correlated with the physical properties, he investigated three specimens only. It was hoped that the larger number of samples available in the present investigation would confirm and extend his findings.

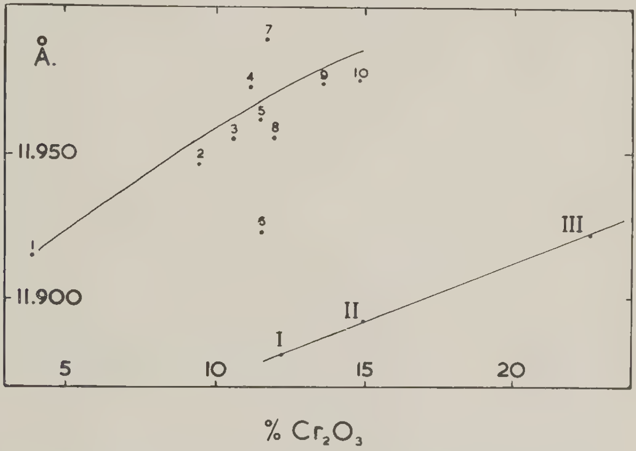

FIG. 2. Variation of unit cell with chromium content. Bushveld uvarovite specimens—Arabic numerals. von Knorring's specimens—Roman numerals.

However, when chromic oxide content was plotted against a_0, S.G., and R.I. in the manner adopted by von Knorring, the results did not show the perfect linear relationships he obtained (Figs. 2, 3, and 4). Specimens which have Cr_2O_3 contents similar to those examined by him, have larger unit cell dimensions and higher R.I. values. Only Specimen No. 6 with a Cr_2O_3 content near that of von Knorring's Sample No. 1 has similar physical properties; it is, however, low in titanium and iron. Titanium was not reported in von Knorring's analyses, so that there is, presumably, little or none.

No linear relationship exists between unit cell dimensions and Cr_2O_3 contents in Bushveld uvarovite (Fig. 2). Zedlitz (1933) found a linear increase in the lattice constant of melanite with increase in TiO_2 and he suggested (1935) that one per cent of TiO_2 increases the unit cell by 0.01 Å. This expansion is thought to be due to replacement of Si by Ti which has a larger ionic radius. When the unit cell values of the Bushveld uvarovite are adjusted using this "correction," the amount of scatter of the plotted points of Fig. 2 is not appreciably reduced. The deviations from the linear relationship between unit cell dimension and Cr_2O_3 content are not due in any degree to titanium but rather to iron.

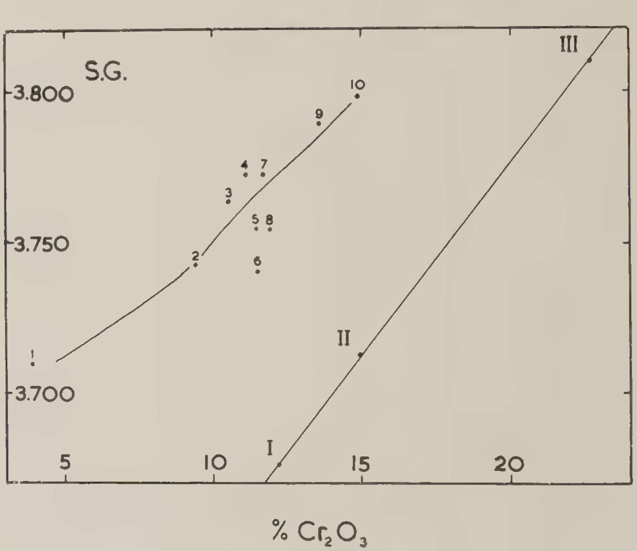

FIG. 3. Variation of specific gravity with chromium content. Bushveld uvarovite specimens—Arabic numerals. von Knorring's specimens—Roman numerals.

The effect of iron is shown by the difference between unit cell dimensions of von Knorring's low iron specimens and those of Bushveld uvarovite of similar Cr_2O_3 content. By calculation (total iron regarded as ferric oxide) one per cent of ferric oxide increases the unit cell dimension by 0.09 Å approximately.

Figure 3 shows a general increase in S.G. as Cr_2O_3 content increases. Where Cr_2O_3 contents are similar, S.G. differences are obviously due to variations in the amount of iron. In Specimen No. 9, for example, which contains only a small amount of titanium, the higher iron content offsets possible lower values of physical properties. High refractivity of iron raises the R.I., but titanium which has a low refractivity appears also to have some elevating effect on R.I. in many minerals for reasons not clearly known; as Fairbairn has remarked, other factors must be operative.

Figure 4 shows an almost linear relationship between R.I. and Cr_2O_3 content, roughly parallel to the straight line drawn by von Knorring, or the line linking pure grossularite and uvarovite. It is clear that while the TiO_2 content has modified the R.I.—Cr_2O_3 relationship, the appreciable iron content has also raised the R.I. value.

The refractivities of Fe^{3+} and Cr^{3+} ions are probably similar, so that ferric oxide can be considered equivalent to chromic oxide. Accordingly when the amounts of ferric oxide and chromic oxide are combined for each analysis, and the values of "chromic oxide" plotted against R.I., the curve so produced is nearly parallel and closer to the curve obtained by von Knorring and also to that of grossularite-uvarovite.

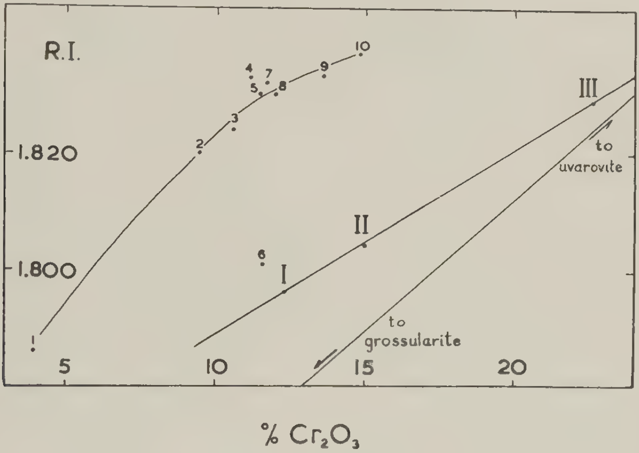

FIG. 4. Variation of refractive index with chromium content. Bushveld uvarovite specimens—Arabic numerals. von Knorring's specimens—Roman numerals.

The replacement of small by larger radius ions expands the unit cell while large ions like Ca in grossularite are surrounded by distorted polyhedra (Menzer, 1929). The present study supports the theory that the garnet structure is probably "elastic" like that of micas (Jaffe, 1951), and capable of taking up a wide range of ions.

Statistical methods of correlation of chemical composition and physical properties could not be applied to the small number of uvarovite occurrences for which both these factors are accurately known. It was not possible to use Levin's algebraic method for the calculation of chemical composition from partial analysis and physical properties.

Quantitative color measurements were made on three specimens of minus 200 mesh uvarovite powder using a Donaldson Trichromatic Colorimeter. There is a slight increase in the red component for uvarovite of higher titanium and iron contents.

	x	y	z
Specimen No. 4	0.382	0.439	0.179
No. 7	0.397	0.437	0.166
No. 10	0.375	0.452	0.173

The colors of minus 200 mesh powder of a representative number of specimens were compared with the matt surface of the British Trade Council Color Chart. The following are some of the closest color matchings.*

Specimen No. 1	Limpet green	Reference C C 97
No. 3	Georgian green	C C 249
No. 5	Bronze green	C C 84
No. 6	Leaf green	C C 92
No. 7	Woodpecker green	C C 244
No. 8	Moss green	C C 83
No. 9	Rockingham green	C C 93

Both the qualitative and quantitative measurements show that with increase in iron content the green color becomes deeper, while the uvarovite of higher titanium content has a "rusty" green color due to an increase in the amount of red or purple. The purple color of titan-augite is considered to be due to a similar effect.

The D.T.A. curve (Fig. 5, No. 1) shows that the uvarovite undergoes no change on heating to 1100° C.

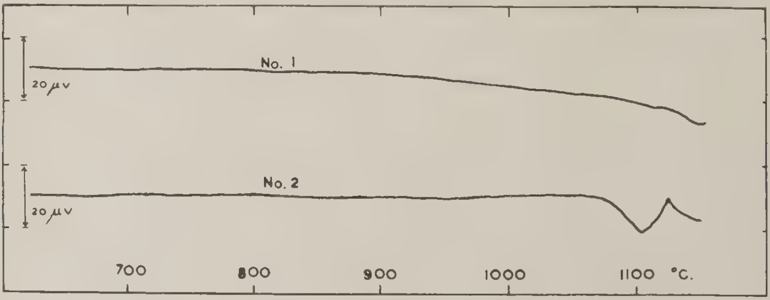

FIG. 5. Differential thermal analysis curves of (1) Uvarovite, de Kafferskraal, No. 359. Table I, Analysis No. 7). (2) South African Jade, Buffelsfontein, No. 205. (Table VI, Analysis No. 1)

THE PETROGRAPHY OF THE UVAROVITE-BEARING ROCKS

Thin section examination showed that the relationship between uvarovite and chromite is always very much the same. The following account describes the features of those rocks from which the garnet had been separated and analyzed.

---

* All the color measurements were kindly made by Mrs. P. Angus-Leppan, Paint Industries Research Institute, University of Natal.

No. 1. Lydenburg district. There is no chromite in the section which is made up of large plates (up to 1.8 mm. across) of slightly pleochroic, pale green orthopyroxene holding exsolution lamellae, and diopside ($2V_\gamma$ 58°, $c \hat{} Z$ 40°, γ 1.706). The diopside may have replaced an earlier pyroxene. Very pale green garnet grains fully isotropic, 0.4 to 0.6 mm. diameter, replace both pyroxenes which are cloudy near the garnet.

No. 2. Klipfontein, No. 119. Large plates of colorless to pale green diopside 0.9 to 1.8 mm. across ($2V_\gamma$ 58°, $c \hat{} Z$ 36°, γ 1.706), and markedly zoned orthopyroxene $2V_\gamma$ 68°, with a pale pink to green, pleochroic core rimmed by diopside, are partly replaced by uvarovite. Highly corroded chromite grains 0.07 to 0.45 mm. across, lie in the irregular patches of garnet which are also peppered by chromite granules 0.01 mm. or less. The garnet is deeper green where it surrounds chromite grains. There is also a little interstitial zoisite.

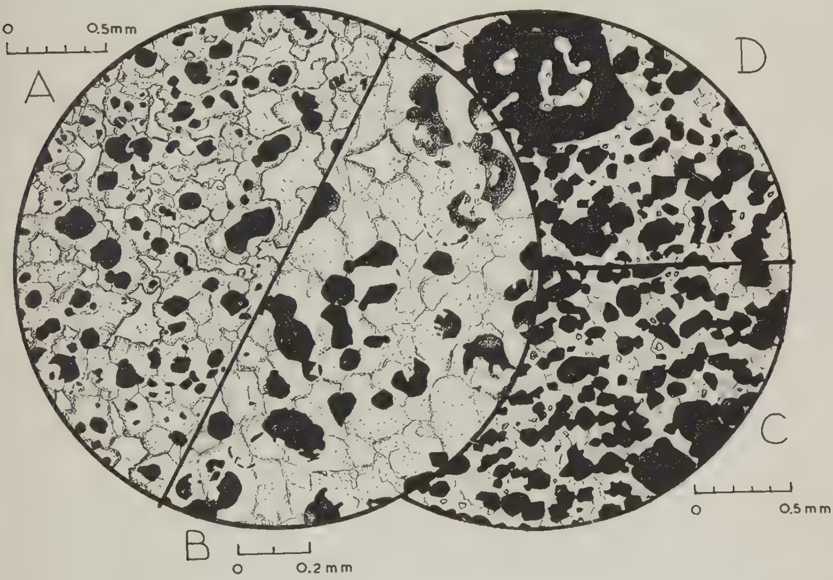

FIG. 6. A and B. Highly corroded chromite remnants (black) in uvarovite (stippled). Clear areas are mainly zoisite. Vygenhoek, No. 209. C. Chromite grains linked in short chains in uvarovite. A few small serpentinized olivine grains are present. de Kafferskraal, No. 359. D. Corroded chromite grains in uvarovite. de Kafferskraal, No. 359.

No. 4. Vygenhoek, No. 209. The chromite grains 0.15 mm. average diameter, are isolated or lie in short, straight to curved chains in the deep green, granular uvarovite. The chromite is rounded and embayed and almost completely absorbed by the garnet (Fig. 6, A and B). Patches of zoisite (0.12 mm. across) partly replace the little diopside present. Small, brown-stained inclusions 0.02 $mm.^2$ in the garnet may be serpentinized olivine.

No. 5. Uitvalgrond, No. 71. The chromite is scattered as individual slightly rounded dodecahedral or octahedral grains 0.04 to 0.3 mm. in diameter, or as small clusters in a translucent, pale olive green garnet. The subhedral uvarovite grains range from 0.08 to 0.5 mm., with an average diameter of 0.15 mm. Small irregular patches of diopside and serpentine are interstitial to, or lie within the garnet or surround the chromite grains.

No. 6. Derdegelid, No. 141. The chromite grains (0.08 to 0.45 mm. diameter) are slightly rounded and show few corrosion effects even under high power. They lie in subhedral to euhedral grains of uvarovite. Patches of a lath-like mineral, probably zoisite, and a little diopside are interstitial to the garnet. Small, serpentinized granules, probably forsterite originally, are imbedded in the garnet.

No. 7. de Kafferskraal, No. 359. In addition to isolated or small clusters of grains, the chromite crystals form short, roughly parallel chains (Fig. 6, C). Although the crystals are frequently euhedral dodecahedrons, 0.05 to 0.4 mm. in diameter, ragged grain margins demonstrate corrosion (Fig. 6, D). The dull green uvarovite of the same grain size as the chromite, contains a noticeable amount of small, elongate grains from 0.004×0.012 mm. to 0.027×0.054 mm. in size. The colorless grains generally have a brown surface stain and show low interference colors. They are considered to be serpentinized olivine. A small amount recovered during the uvarovite cleaning process gave a faint *x*-ray pattern resembling that of chrysotile and a spectrographic analysis showed magnesium and silicon as main constituents.* A few serpentine patches interstitial to garnet are present.

No. 8. Kafferskraal, No. 915. Euhedral chromite grains 0.07 to 0.25 mm. in diameter lie in curved or short, parallel chains in the green uvarovite matrix of similar grain size. There is little corrosion of the chromite grains which are sometimes surrounded by granules of diopside (?) 0.01 mm. or less in size. There are small inclusions resembling augite in the garnet and some interstitial serpentine.

No. 9. Hendriksplaats, No. 357. In the field this occurrence is vein-like and cuts through a chromitite seam (Hall, 1908, p. 60). The hand specimen is made up of patches of chromite crystals in the bright green uvarovite, and irregular, grey veins up to 5 mm. wide merge with larger aggregates of diopside crystals several cms. across.

Specimen No. 3 Winterveld, No. 424 is so similar to this material that the following account serves to describe both.

The pale green uvarovite grains average 0.1 mm. diameter and larger grains up to 0.3 mm. diameter are linked in distinct chains. Some grains which have color zoning show slight anomalous birefringence. The large garnet grains are intimately associated with colorless diopside ($2V_\gamma$ 58°, γ 1.704) in plates several mm. across. Fragments of partly replaced diopside in the garnet are in optical continuity.

Chromite is scattered throughout the garnet as residual granules of a few microns and as larger, angular and embayed grains 0.25 mm. in diameter. The margins of the larger chromite grains are bordered by brown, translucent zones of replacing garnet which still contains some of the chromite substance (Plate 1 (1)). Chromite grains within pyroxene plates are bordered by granules of uvarovite (Plate 1 (2)). Small circular areas of augite 0.01 mm. diameter lie in the chromite grains. There are also interstitial patches of serpentine.

No. 10. Doornbosch, No. 423. Within the bright green garnet matrix, large, anhedral chromite crystals from 2 to 7 mm. across are linked in chains (Fig. 7), while most of the subhedral chromite grains 0.2 to 0.4 mm. in diameter lie between the chains in haphazard fashion. A colorless mineral of low R.I. (1.450) and birefringence about 0.002, fills some interstitial areas between, or forms extremely thin borders to chromite grains. It was determined as gmelinite from an *x*-ray photograph.† A little calcite interstitial to chromite is also present. Polished section shows a few chalcopyrite particles and silvery grains of 2 microns diameter may be hematite or platinoids.

---

* Kindly determined by Dr. S. A. Hiemstra, Union Geological Survey.

† Kindly determined by Dr. H. Heystek, National Chemical Research Laboratory.

Other uvarovite-bearing rocks. In the Winterveld-Hendriksplaats area of the Eastern Belt, thin, fine-grained chromitite seams of the "hard lumpy" variety of ore are separated by irregular patches and bands of green compact rock 0.3 to 5.0 cms. thick. They are similar to South African Jade in appearance but are duller and the hardness is frequently less than 6.5.

Under the microscope the green bands and irregular patches are translucent, colorless to grey, and composed mainly of laths of stocky crystals either in stellate or haphazard arrangement. There is a faint, ghost outline suggestive of original pyroxene plates. The thin, lath-like crystals, 0.1×0.02 mm., identified as diopside,* are associated with granular zoisite. Small, almost equant, colorless patches with radiating cracks and sheaf-like aggregates may be prehnite.

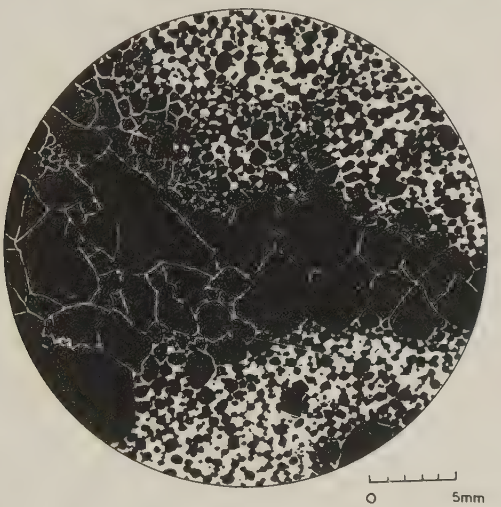

FIG. 7. Chain of large chromite grains in uvarovite-bearing chromitite. Locality Doornbosch, No. 423.

Small, pale green or yellow-green, subhedral uvarovite crystals ($n=1.830$) are scattered throughout the rock. The amount of garnet increases at the contact with the chromitite where replacement of the chromite is clearly demonstrated (Plate 1. (3A)). There is also a blue-green, anisotropic mineral of low birefringence which resembles the green uvarovite. It is probably a chromium-bearing hydrogrossular. It replaces chromite but is itself replaced by colorless chlorite and uvarovite which surround it (Fig. 8).

Chromite in individual grains or small clusters may be partly or completely replaced by the hydrogrossular, chlorite and uvarovite (Plate 1, (3B)). Occasional grey or pale cream, translucent patches of low interference color that have a ghost outline of original pyroxene are also thought to be hydrogrossular. Thin veins of later calcite and possible magnesite have partly replaced chains of uvarovite crystals and diopside matrix.

Two specimens of the green bands were partially analyzed. The material for Analysis No. 2 was treated in hot concentrated hydrochloric acid and then after water washing, strongly heated.

---

* Confirmed by an x-ray powder photograph taken by Dr. Heystek.

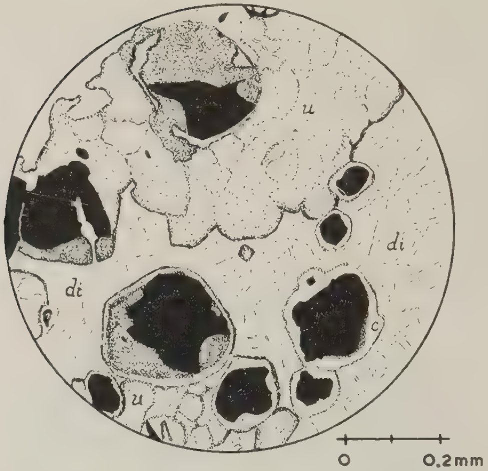

Fig. 8. Contact between diopside-rich band (di) and chromitite, showing corroded and replaced chromite (black) in green uvarovite (u), dark blue-green birefringent garnet (heavy stipple) and colorless chlorite (c).

	(1)	(2)	
SiO_2	39.8	49.2	
R_2O_3	12.0	12.4	
CaO	24.0	25.3	
MgO	17.2	13.4	Analyst J. J. Frankel.
Ignition loss	7.2	—	
	100.2	100.3	

1. Pale green band between chromitite seams, Winterveld, No. 424.
2. Acid and heat treated material from green band, Winterveld, No. 424.

Both analyses cast into "norms" give dominant diopside with zoisite, and for Analysis No. 1, some magnesium carbonate as well.

Chromite Associated with Uvarovite

The chromite crystals of the Doornbosch specimen (No. 10), have a wide grain size range known only in a few of the many chromitite outcrops. Because the crystals are not interlocked, this rock is very friable, and it disintegrates when lightly tapped with a hammer. This treatment, preliminary to the concentration of the uvarovite, fractured few of the larger crystals; any stray fragments were easily hand-picked from the finer crystals. After separation of uvarovite, the chromite was cleaned in hydrofluoric acid. The sample was sifted over Tyler sieves and four of the grades so produced were analyzed (Table V).

TABLE V. CHEMICAL ANALYSES OF CHROMITES

	1	2	3	4	5
SiO_2	2.2	2.0	2.0	1.8	0.60
TiO_2	0.18	0.25	0.22	0.10	0.70
Al_2O_3	11.95*	12.46*	13.0	13.50	13.16
Fe_2O_3	11.0	10.3	10.9	11.2	18.16
Cr_2O_3	47.85	47.05	47.10	47.25	39.92
FeO	13.2	13.95	13.35	12.45	14.72
MnO	0.05	0.04	n.d.	0.01	0.29
MgO	13.6	13.7	13.35	13.65	12.45
CaO	n.d.	n.d.	n.d.	n.d.	0.50
	100.03	99.75	99.92	99.96	100.50
S.G.$_{4^\circ}^{20^\circ C}$.	4.46	4.46	4.46	4.45	4.43

* By difference.

Chromite crystals separated from uvarovite-bearing chromitite, Doornbosch, No. 423, Eastern Belt. No. 1. +14 mesh Tyler. No. 2. −35+48 mesh. No. 3. −48+100 mesh. No. 4. −100+200 mesh. Analyst J. F. de Wet (MnO by J. J. Frankel). No. 5. Chromite separated from uvarovite-bearing chromitite, de Kafferskraal, No. 539, Eastern Belt. Analyst C. E. G. Schutte.

There is no well-defined grading in crystal size which would be expected had the chromitite been formed by crystal settling. The large crystals lie in scattered clusters or chain structures in the rock. It has been suggested on geochemical grounds that early formed chromite crystals are richer in Cr, Al and Mg, while later crystals have more Fe^{2+}, Fe^{3+} and Ti (Malhotra and Prasada, 1956). This appears to be true for some chromitite seams where crystals at the base have more Cr_2O_3 than those at the top (Frankel, 1949). Except for the very slightly higher percentage of Cr_2O_3 in the coarse crystals, there are no distinct trends in the four graded fractions. It is possible, therefore, that the chromitite crystallized slowly from a re-fused chromitite (Sampson, 1932, p. 143); the larger crystals having formed first.

The analyses Nos. 1 to 4 resemble those quoted for the Main Seam of the Lower group on adjacent farms (de Wet, 1952, p. 150), but they differ from an analysis from Doornbosch farm itself (Kupferbürger et al., 1937, p. 25).

Chromite from the de Kafferskraal uvarovite-bearing chromitite has a lower Cr_2O_3 content than the majority of seams in the two groups identified in the Eastern Belt. The field relationships of this rock are obscure—it might belong to the Middle group in which chromite generally has less Cr_2O_3 than the underlying group of seams.

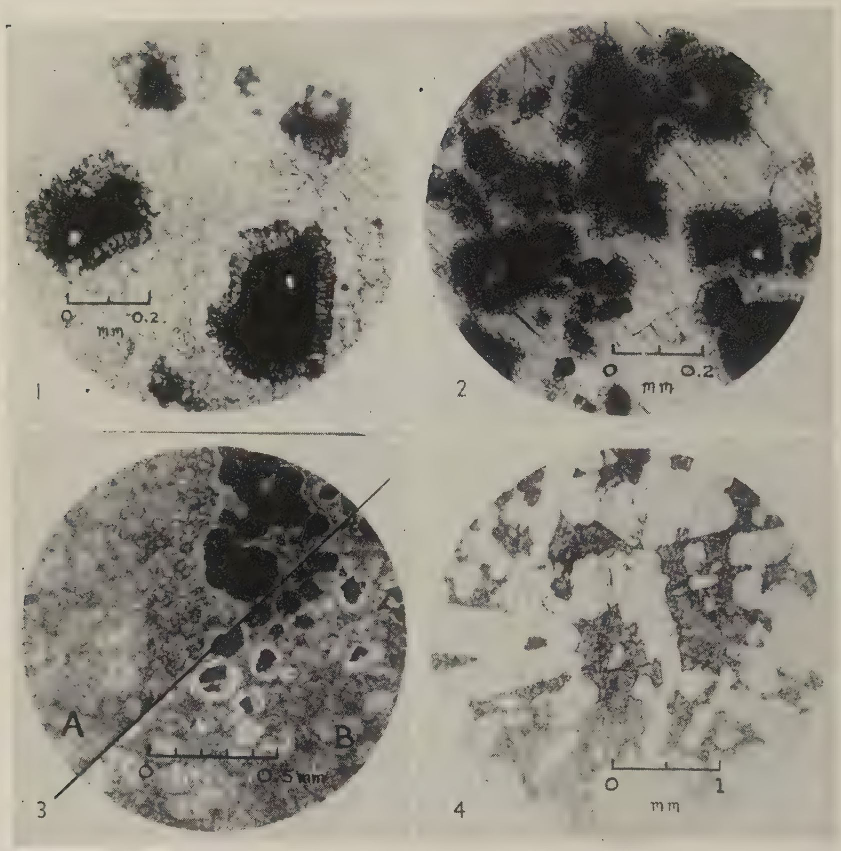

Plate 1. (1) Brown translucent zones around chromite grains in uvarovite. The zones consist of uvarovite and brown remnants of chromite. Hendriksplaats, No. 357. Plane polarized light.

(2) Uvarovite granules around corroded chromite crystals in diopside. Winterveld, No. 424. Plane polarized light.

(3A) Uvarovite crystals in fine-grained diopside rock. Slightly corroded chromite grains are bordered by uvarovite and chlorite. Winterveld, No. 424. Plane polarized light.

(3B) Chromite grains in diopside rock replaced by colorless chlorite, blue-green hydrogrossular (?) and uvarovite. Winterveld, No. 424, Plane polarized light.

(4) South African Jade. Gabbro texture as seen in plane polarized light. Between crossed nicols this slide is fully isotropic.

The Origin of the Uvarovite

Although some chromitites hold significant amounts of plagioclase, it was not the dominant constituent in any of the uvarovite-bearing chromitite specimens. Uvarovite formation, therefore, required the addition of

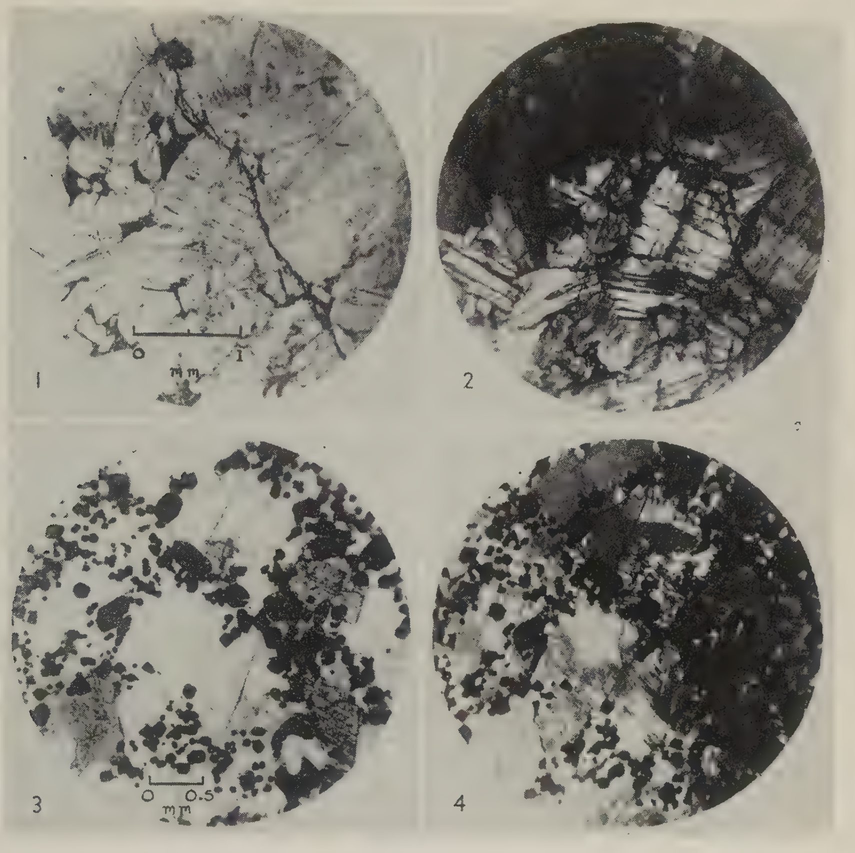

Plate 2. (1) South African Jade in plane polarized light.

(2) South African Jade between crossed nicols. Same field as fig. 1. Note anomalous birefringence and twinning effects.

(3) Partly altered chromite-bearing pyroxenite. Clear areas original feldspar with some pyroxene. A few striated orthopyroxene crystals also visible. Plane polarized light.

(4) Same field as in fig. 3. Clear areas of fig. 3 are isotropic or anomalously birefringent. The orthopyroxene is also partly altered to hydrogrossular: Crossed nicols.

lime and it is considered to be a product of lime metasomatism with attendant metamorphic effects.

Interstitial serpentine could be derived from orthopyroxene, whereas the isolated small grains of serpentinized olivine, are similar to those found in impure magnesium limestones that have undergone low grade thermal metamorphism. This suggests that some magnesium carbonate was present long before uvarovite was formed. It could have been produced by the action of carbonated waters, perhaps of deuteric origin, on enstatite. Forsterite would develop early with increase in temperature, and the introduction of calcium in heated waters and an increased metamorphic grade, would assist uvarovite formation. The moderate amount of aluminium required would be available from feldspar dissociation.

Thin bands of orthopyroxene between chromitite seams are also considered to have been partly converted to carbonate. Lime metasomatism and heat increase, assisted the formation of diopside and "grossularite," and uvarovite was a final product.

Uvarovite is also associated with diopside and zoisite in veins cutting across chromitite seams. Betekhtin (1946, p. 70) reported a similar association which he attributed to pneumatolytic-hydrothermal agencies. Fortier (1946) has also described the formation of chlorite and uvarovite from chromite, and many other examples are on record.

Synthetic uvarovite is readily produced in an anhydrous environment at 855° C. (Hummel, 1950). This temperature is obviously too high for the metamorphic/metasomatic processes outlined above for Bushveld uvarovite and associated minerals. Perhaps high pressure and the presence of water, lower the formation temperature. Nevertheless, it is clear that when chromium is available, the ugrandite garnet, uvarovite, forms relatively easily in nature in either hydrous or anhydrous environment.

It is suggested that in a magmatic body like the Bushveld Norite there would be local surges of heat coupled with slight dynamic effects, due to sagging in the body. These surges would give rise to simple metamorphic effects, contemporaneous or slightly later than the introduction of heated lime-bearing solutions.

There is also the possibility that the calcium came from small amounts of carbonate xenoliths derived from the floor of the Complex and which were completely digested in the Norite body in the vicinity of the Lower group of chromitite seams. This would account for the erratic and irregular nature of the uvarovite-bearing chromitites.

SOUTH AFRICAN JADE (HYDROGROSSULAR)

Uvarovite holding a large amount of the grossularite "end member" occurs with diopside and zoisite and a little disseminated chromite (Specimens Nos. 1 and 2 described above). Garnet, essentially grossularite, has been reported as a metamorphic mineral at the contacts of the Norite with underlying carbonate rocks from many localities in the Eastern and Western Belts (Kynaston, 1909, p. 20; Wagner, 1929, p. 175).

Hall (1925) described the rock prized as an ornamental stone, and known as South African Jade from the farms Turffontein No. 356 and Buffelsfontein No. 205 in the Western Belt, as a massive fine-grained variety of grossularite. Although it contains no nephrite or jadeite, this material will be referred to as Jade, using the term in the general sense for compact tough minerals suitable for the making of ornaments. In hand specimen the rock is pale green to grey, massive and translucent with scattered chromite grains. It is quite distinct from the sparkling crystalline granular uvarovite in chromitite.

Thin sections are mainly colorless or very pale cream-brown and faintly cloudy. Except for faint straight "cleavage" traces or crystal faces, the garnet shows no crystal outlines, and between crossed nicols is either isotropic or gives grey interference colors of anomalous birefringence. Zoning and the remarkable twinning effects described by Hall, simulate twinning of albite.

In several slides, however, outlines of stout laths arranged with somewhat cloudy interstitial patches are seen in plane polarized light; between crossed nicols the whole rock may be fully isotropic (Plate 1 (4); Plate 2 (1, 2)). This ghost texture is identical to that of the feldspar-pyroxene associations commonly seen where the noritic rocks grade into anorthosite. A particularly good comparison can be made with the anorthositic layer associated with the Merensky Reef chrome band.

Partial transformation of pyroxenite to jade at the contact of a chromitite seam was observed. The small amount of feldspar and larger areas probably of clinopyroxene, were completely replaced by isotropic jade; the remaining pyroxene, dominantly enstenitic, is fairly fresh (Plate 2 (3, 4)). Only a few of the chromite grains show green chlorite-like margins. No zoisite was seen. However, a little zoisite is common as a well distributed mineral in many specimens. It is dominant in saussuritized anorthosite where feldspar (An_{62}) shows partial or complete alteration to saussurite which grades into a more clearly defined aggregate of small garnet crystals in the zoisite. This in turn grades into clear isotropic jade, in which no trace of original minerals is preserved.

Green isotropic rims around chromite are probably a true uvarovite. Many chromite grains, however, are either slightly corroded or completely replaced by jade.

Slightly wavy thin transparent bands alternate with somewhat less cloudy zones in many specimens. In thin section the white bands are slightly darker than the rest of the isotropic jade and they lie close to the clear-cut margins of saussuritized zones. Rhythmic replacement as jade developed from saussurite may account for the banding.

Hall's Analysis No. 5, of his specimen No. 616 c5 (Slide 1128) in spite of its high total, approaches the theoretical analysis of grossularite more closely than any of his other analyses. In thin section, this rock is colorless, clear and fully isotropic with no relict structures. Variations in the other analyses may be attributed to small and variable amounts of zoisite and residual pyroxene and feldspar. The trace of chromium reported is due, either to the chromium in the garnet, or to scattered chromite grains.

Hall gave some physical data but made no comment thereon. In 1928 van der Lingen found that the transmission spectrum of the South African Jade showed the presence of OH groups in the molecule itself, and not in water of crystallization. He concluded that the material is not grossularite. Herbert Smith (1949, p. 312) stated that the specific gravity and refractive index of the jade have slightly lower values than those usually recorded for grossularite.

There is more combined water in all Hall's analyses than is required for the small amounts of zoisite. In the present investigation combined water and physical properties were determined on several different specimens. A complete chemical analysis was also carried out on clear isotropic jade which contains few scattered chromite grains and traces of zoisite.

It is concluded from the chemical analyses and physical properties that South African Jade is not true grossularite but hydrogarnet that

TABLE VI. CHEMICAL ANALYSES OF JADE

	1	2	3
SiO_2	36.55	37.60	39.30
TiO_2	0.12	0.10	nil
Al_2O_3	23.44	22.25	21.93
Fe_2O_3	1.27	0.50	0.80
Cr_2O_3	0.25	0.10	0.13
FeO	0.52	0.55	0.28
MnO	0.04	trace	nil
MgO	0.79	trace	traces
CaO	36.06	38.40	37.10
H_2O+	1.16	1.20	0.30
CO_2	none	—	nil
	100.20	100.95	99.84
S.G.	3.488	3.52	3.5062
R.I.	1.728 (±.002)	—	1.741
a_0	11.859 Å (±.001)	—	11.85 (±.01) Å

1. South African Jade, Buffelsfontein, No. 205, Dried at 105° C. Analyst J. J. Frankel (H_2O+ Messrs. McLachlan and Lazar).
2. "Green Jade," Buffelsfontein. Total includes P_2O_5 0.05%, H_2O- 0.20% (Hall, 1925).
3. Grossularite from near Georgetown, California (Pabst, 1936).

has slight variations in composition. Hutton (1943) gave data for several specimens of the grossularite-hydrogarnet series which he named "hydrogrossular." Both Hutton and Yoder (1950) have suggested that the majority of garnets described as grossularite are really hydrogarnet, and Hutton says that the usual constituent of altered gabbros and related basic intrusive rocks is a member of the garnet-hydrogarnet series near the grossularite end. The South African hydrogrossular has the same variation trends of physical properties with change in water content as the New Zealand specimens.

TABLE VII. VARIATION OF SPECIFIC GRAVITY AND REFRACTIVE INDEX WITH COMBINED WATER CONTENT IN SOUTH AFRICAN JADE

% H_2O+ (samples dried at 105° C.)	0.83	1.02	1.16	1.56	2.38	2.73
R. I.	1.731	1.730	1.728	1.725	1.712	1.708
S. G.	3.523	3.505	3.488	3.468	3.430	3.401
% SiO_2	—	—	36.55	—	—	34.82

The D.T.A. diagram (Fig. 5, No. 2) shows that no change takes place during heating until the temperature reaches 1100° C. approximately. At this temperature the mineral probably begins to decompose in the solid state (c.f. Yoder, 1950, p. 239). There is no clear indication of the temperature at which water is lost. The diagram affords no evidence of an inversion from birefringent to isotropic jade.

Hall put forward two modes of origin for the jade –(1) magmatic and (2) metamorphic.

(1) The material of the jade, derived from the norite magma, was later concentrated into bands, in a manner analogous to that of magnetite or chromite seam formation.

(2) The garnet is a metamorphic-metasomatic product resulting from intensive alteration of an original calcareous aluminous sediment (like a calcareous/dolomitic marl) upstoped from the sedimentary floor of the Complex and brought into the present position as xenoliths within the Norite body.

Alteration into massive lime garnet from an original aluminous calcareous rock implies an increase in silica and alumina, and removal of carbon dioxide. Hall suggested that carbon dioxide could be lost because the thin bands of the rock were engulfed in a great thickness of magma and the addition of other elements could be due to a metasomatic replacement caused by magmatic infiltration.

van Biljon (1955, p. 132) stated that the composition of the jade suggests that it is an intermediate product of the metasomatism which transformed sedimentary carbonate rocks to anorthosite. Thin section, however, has convincingly revealed that feldspar laths (An_{62}) are transformed progressively with crystal outlines preserved, through zoisite to hydrogrossular. If the feldspar had formed *from* the hydrogrossular it is unlikely that well-defined crystal boundaries would develop before the whole of the enclosed volume had been converted to feldspar. In any event, the palimpsest textures of anorthosite and norite do not support van Biljon's theory.

The fairly uniform thickness of the jade layers "interbedded" with anorthosites, pyroxenites and chromite horizons, points simply to their being metasomatized equivalents of such rocks *in situ;* access for calcium-bearing solutions being provided by the planes of pseudo-stratification or rifting. The dominant cations in the original minerals were Al, Ca with less of Na in the feldspar, and Mg with some Fe^{2+} in the orthopyroxene. Additional lime with a small amount of water could displace magnesia and silica. Both Yoder (1950) and Hummel (1950) stress that water acting as a catalyst may possibly assist the formation of even anhydrous grossularite in hydrothermal transformations.

Many authors have pointed out (Harker, 1939, p. 174) that saussuritization of feldspar belongs to a late stage in the cooling down of an igneous rock, so that grossularite and zoisite may have formed during this period when some stress may also have operated. This would afford a simple explanation for jade formation. However, it is difficult to understand why only certain zones of the anorthosites and pyroxenites should have been saussuritized, and a source of additional lime would still be necessary for the production of jade from pyroxenite and norite.

Several kinds of lime metasomatism are listed by Turner and Verhoogen (1951, p. 488) and the type described in the present paper has been previously recorded from New Zealand. Dykes containing diallage, prehnite and grossularite have been shown by Grange (1927) to be altered gabbros really, with grossularite and prehnite secondary after feldspar. He suggested that grossularite-diopside veins were formed by solution which took up lime, magnesia and alumina from pyroxene, but direct evidence of the transformation to grossularite was lacking.

Turner (1933) suggested that in pyroxenites the reaction products are stress minerals, and with aqueous solutions OH group minerals would form. Turner quotes Benson who thought that "rodingite" was due to the action of concentrated magmatic water under high pressure, and that lime-silicate rocks from New South Wales were transformed by calcium-rich aqueous solutions which came from a cooling peridotite mass; monoclinic pyroxene was suggested as the source of the calcium.

Carbonate rocks in the floor of the Bushveld Complex below the jade occurrence on Buffelsfontein are a nearby source for the additional calcium required in the transformation to "garnet." This calcium could have been introduced by heated waters.

It is considered, therefore, that the South African Jade is a metasomatic replacement of anorthosite, pyroxenite, and of the gangue minerals of the chromitite seams.

CONCLUSIONS

Both uvarovite and hydrogrossular have developed within the same zone of the Norite body, although the modes of occurrence differ. Uvarovite is intimately associated with chromitite and pyroxenite whereas the jade lies in anorthosite. It would appear, therefore, that the original composition of the rocks and the subsequent metasomatic/metamorphic processes have determined the variety of garnet developed.

Yoder failed to produce grossularite synthetically, however, and found as other workers had, that only hydrogrossular formed relatively easily in a hydrous environment. Hummel was able to prepare anhydrous uvarovite without difficulty. Undoubted anhydrous grossularite does exist in nature; it is possible that at high temperatures and elevated pressures hydrogrossular may be made over to grossularite.

In the formation of the jade, fairly uniform thicknesses of anorthosite have been saussuritized and converted to hydrogrossular *in situ*. The pale green tint is due to chromium from small amounts of dissolved chromite grains. In rare instances chromite is rimmed by true uvarovite which suggests local temperature increase. Jade formation is not dependent on the presence of chromium.

It is unlikely that, as suggested by Hall, the fairly uniform jade layers represent actual limestone horizons torn up from the floor of the Norite body and brought to their present position where they were transformed. Rather, it is visualized that anorthosite bands were transformed by heated calcium-bearing solutions.

Hummel found that a hydrous environment is not necessary for uvarovite formation, and none of the Bushveld uvarovite contains a significant amount of combined water. The associations show that the uvarovite formed essentially in pyroxenite and pyroxene-bearing chromitite as a result of deuteric alteration and lime metasomatism, followed by thermal metamorphism. Uvarovite formation was entirely dependent upon the presence of adequate amounts of chromium.

The chromite in the jade is relatively unattacked whereas it is generally corroded in the uvarovite-bearing rocks. It is suggested that this also points to higher temperatures at the time that the uvarovite was formed.

The complete digestion of small carbonate xenoliths within the chromitite zone may explain the irregular and erratic distribution of the uvarovite and such a possibility, of course, would allow of an additional source of lime.

ACKNOWLEDGMENTS

Considerable assistance in chemical, differential thermal and x-ray analyses was given by Dr. J. F. de Wet, National Chemical Research Laboratory, Dr. T. L. Webb, National Building Research Institute, Drs. J. N. van Niekerk and F. Herbstein and Mr. F. T. Wybenga, National Physical Research Laboratory; all of the Council for Scientific and Industrial Research, Pretoria. Through the good offices of the Director of the Union Geological Survey, some chemical analyses were carried out by the Division of Chemical Services, Pretoria. Other analyses were made possible by the Research Grant Board of the Union of South Africa and the University of Natal Staff Research Fund. The Department of Geology, Witwatersrand University made a number of Hall's original thin sections available. All other slides were prepared in this Department by Mr. C. N. Govender.

A short note by C. E. Tilley on the replacement of anorthosite by hydrogrossular appeared in *Geol. Soc. South Africa Trans.*, **60,** 15–17.

REFERENCES

ALDERMAN, R. A., 1935, Almandine from Botallack, Cornwall: *Mineralog. Mag.*, **24,** 42–48.

BETEKHTIN, A. G., 1946, On chrome-garnets from the Nizhne-Tagilsk dunite massif: D. S. Belyankin jubilee vol. *Acad. Sci. U.S.S.R.*, 68–73.

BRITISH COLOUR COUNCIL, 1949, Dictionary of colours for interior decoration: 3 vols., London.

DE WET, J. F., 1952, Chromite investigations—pt. 3: *Chem. Metall. Min. Soc. South Africa Jour.*, **52,** 143–153.

FAIRBAIRN, H. W., 1943, Packing in ionic minerals: *Geol. Soc. America Bull.*, **54,** 1305–1374.

FLEISCHER, M., 1937, The relation between chemical composition and physical properties in the garnet group: *Am. Mineral.*, **22,** 751–759.

FORD, W. E., 1915, A study of the relations existing between the chemical, optical and other physical properties of the members of the garnet group: *Am. Jour. Sci. 4th ser.*, **40,** 33–49.

FORTIER, Y. O., 1946, Some observations on chromite: *Am. Jour. Sci.*, **244,** 649–657.

FRANKEL, J. J., 1949, Bushveld chromite investigation: *South African Min. Eng. Jour.*, **60,** 417–419.

———, 1953, South African asbestos fibres: *Mining Mag.*, **89,** 73–83, 142–149.

GRANGE, L. I., 1927, On the "Rodingite" of Nelson: *New Zealand Inst. Trans.*, **58** 160–166.

HALL, A. L., 1908, Geology of the Haenertsburg goldfields and the adjoining parts of Secoecoeniland east of the Lulu Mountains: *Geol. Surv. Transvaal. Ann. Rept.*, **(1907)**, 31–60.

———, 1925, On "Jade" (massive garnet) from the Bushveld in the Western Transvaal: *Geol. Soc. South Africa Trans.*, **27** (for 1924), 39–55.

———, 1932, The Bushveld Igneous Complex of the Central Transvaal; *Geol. Surv. South Africa Mem.*, **28.**

Hall, A. L., and Humphrey, W. A., 1909, On the occurrence of chromite deposits along the southern and eastern margins of the Bushveld Plutonic Complex: *Geol. Soc. South Africa Trans.*, **11,** (for 1908), 69–77.

Harker, A., 1939, Metamorphism: London, Methuen.

Hey, M. H., 1941, Determination of ferrous iron in resistant silicates: *Mineralog. Mag.*, **26,** 116–118.

Hummel, F. A., 1950, Synthesis of uvarovite: *Am. Mineral.*, **35,** 324–325.

Hutton, C. O., 1943, Hydrogrossular, a new mineral of the garnet-hydrogarnet series: *Royal Soc. New Zealand Trans.*, **73,** 174–180.

Jaffe, H. W., 1951, Minor elements in the garnet group: *Am. Mineral.*, **36,** 133–155.

Kunitz, W., 1936, Beitrag zur Kenntnis der magmatischen Assoziationen. III. Die Rolle des Titans und Zirkoniums in den gesteins bildenden Silikaten: *Neues Jahrb., Mineral., Beilage-Band* **70,** Abt. A., 385–436.

Kupferbürger, W., Lombaard, B. V., et al., 1937, The chromite deposits of the Bushveld Igneous Complex, Transvaal: *Geol. Surv. South Africa Bull.*, No. **10.**

Kynaston, H., 1909, The geology of the country north and north-west of Potgietersrust: *Geol. Surv. Ann. Rept.*, (**1908**), 11–23.

Levin, S. B., 1949, The physical analysis of polycomponent garnet: Presented 30th Ann. Meeting. *Geol. Soc. America Bull.*, **60,** 1905.

———, 1950, Genesis of some Adirondack garnet deposits: *Geol. Soc. America Bull.*, **61,** 519–565.

Malhotra, P. D., and Prasada Rao, G. H. S. V., 1956, On the composition of some Indian chromites: *Am. Mineral.*, **41,** 460–473.

Menzer, G., 1929, Die kristallstruktur der granate: *Zeits. Krist.*, **69,** 300–396.

Pabst, A., 1938, Garnets from vesicles in rhyolite near Ely, Nevada: *Am. Mineral.*, **23,** 101–103.

Sampson, E., 1932, Magmatic chromite deposits in Southern Africa: *Econ. Geol.*, **27,** 113–144.

Smith, G. F. H., 1949, Gemstones, London, Methuen.

Turner, F. J., 1933, The metamorphic and intrusive rocks of Southern Westland, Part II: *New Zealand Inst. Trans.*, **63,** 178–284.

Turner, F. J., and Verhoogen, J., 1951, Igneous and Metamorphic Petrology: New York, McGraw-Hill Book Co.

van Biljon, S., 1955, l'Origine des structures rubanées dans le partie basique du complexe du Bushveld: Sciences de la terre, No. hors serie, one vol., Nancy. 131–148.

van der Lingen, J. S., 1928, Garnets: *South African Jour. Sci.*, **25,** 10–15.

Vermaas, F. H. S., 1952, Manganese-iron garnet from Otjosondu, South-West Africa: *Mineralog. Mag.*, **29,** 946–951.

von Knorring, O., 1951, A new occurrence of uvarovite from northern Karelia in Finland: *Mineralog. Mag.*, **29,** 594–601.

Wagner, P. A., 1929, The Platinum deposits and mines of South Africa: Edinburgh, Oliver and Boyd.

Yoder, H. S., 1950, Stability relations of grossularite: *Jour. Geol.*, **58,** 221–253.

Zedlitz, O., 1933, Ueber titanreichen Kalkeisengranat: *Centralbl. Mineralogie, Abt.* **A,** 225–239.

———, 1935, Ueber titanhaltige Kalkeisengranate: *Centralbl. Mineralogie, Abt.* **A,** 68–78.

Manuscript received July 31, 1958.

THE AMERICAN MINERALOGIST, VOL. 44, MAY-JUNE, 1959

THE IDENTIFICATION OF ORIENTED INCLUSIONS IN PYROXENE CRYSTALS

M. G. Bown* and P. Gay, *Department of Mineralogy and Petrology, University of Cambridge, Cambridge, England.*

Abstract

Simple x-ray techniques enable the identification of oriented intergrowths of minor components in "single" crystals. The methods developed have been applied to pyroxene crystals. Results are presented for the orientation and identification of augite, pigeonite and orthopyroxene in poly-phase crystals. Inclusions of ore minerals and amphibole can also be characterised.

Introduction

Not infrequently a single crystal of a mineral contains many smaller crystals of a different substance, produced for example by exsolution, alteration or partial inversion. Irrespective of the method of formation such a crystal composed of host and inclusions may be called an intergrowth. A distinction can be made between oriented intergrowths, in which there is a definite, constant, and structurally significant relationship between the axial directions of the host and inclusions, and disoriented intergrowths which have no such relationship.

Microscopic examination of an intergrowth often allows the identification of the minor components as well as the host, the determination of any fixed orientation of the optical properties and of the shape of the crystallites relative to the host, and hence their mutual axial orientations. However, should the crystallites be very small identification using the microscope may be uncertain, and in the limit the very presence of inclusions may be unsuspected. In such cases the methods of x-ray diffraction may aid the petrologist.

For identification alone the x-ray powder method may suffice, though it can never give information about orientation. It will not be successful, however, should the volume of inclusions be less than about 10% of the total volume, or should the powder patterns of the two phases be complex; for in the first case the pattern of the minor component will scarcely be seen at all, and in the second case the overlapping of the two patterns will make any identification uncertain. If the composite crystals are large enough for single crystal x-ray photography to be practicable (greater than 0.05 mm.) the resolution can be improved, for the pattern of the host crystal will be a series of spots instead of the lines given by a powder. Should the intergrowth be a disoriented one the inclusions will still give their own powder pattern, but the problem of overlapping is removed, and identification is easier. The most favourable case occurs if the inclusions are all parallel, for then the diffraction patterns of the individual crystallites superimpose on one another, giving a second "single-crystal" pattern. This concentration of intensity enables very small amounts of inclusion to be detected. If the identification can be made then the axial orientation can also be found; indeed the orientation not infrequently is helpful in the identification. Of course it is impossible by a diffraction method to determine the shape and macroscopic orientation of the crystallites, except to a limited extent in very special cases.

---

* Present address: Department of Geology and Mineralogy, University Museum, Oxford.

Thus for the study of oriented intergrowths the x-ray method is a particularly useful tool. In the rest of this paper the application of the method to many of the possible intergrowths in pyroxenes of the diopside-hedenbergite-ferrosilite-enstatite system is described. The techniques are simple and demand only slight experience in x-ray crystallography: further, it would not be difficult to apply similar methods to other oriented intergrowths.

METHOD

As the work requires a survey of the whole of reciprocal space, an oscillation photograph showing the projection of a three dimensional sample is more valuable than a Weissenberg or precession photograph showing only a two dimensional layer. For pyroxenes z-axis oscillation photographs were taken with FeKα radiation in two 15° ranges, symmetrically across the normals to (100) and (010). (CuKα radiation can be used, but fluorescent scattering from iron atoms gives a dark background.) Oscillation ranges chosen so that the photographs show some symmetry are easy to locate accurately by Laue photographs. These are desirable in that they enable diffraction spots from non-oriented crystallites, whether inclusions or adhering fragments, to be separated from the rest, for such spots will not be related by the symmetry. It should be emphasised that oriented crystallites will give spots related in position by the host symmetry, whatever their own symmetry or orientation. For example, when monoclinic augite lamellae separate from a crystal of ortho-pyroxene it is found that the two phases have the y and z crystallographic directions in common. Since $\beta \neq 90°$ for augite, there are then two possible orientations for the augite, related as by twinning about the normal to (100), which are equivalent with respect to the orthopyroxene. In the absence of disturbing factors the intergrowth should contain as many lamellae in one orientation as in the other, on the average, so that the compound crystal will have the same orthorhombic symmetry as the host. If there are only a few lamellae in the crystal the numbers in the two orientations may be quite different. In the diffraction pattern the augite spot positions, but not their intensities would be related by the orthorhombic symmetry. The principle is a general one, and in the rest of this paper is referred to as "the intergrowth symmetry principle." (The symmetry of the minor phase may, of course, be greater than that of the host.)

By comparing such photographs of composite crystals with "standard" photographs of the pure host material, taken under the same experimental conditions, the diffraction spots given by the host may be most easily separated from those due to the inclusions. From the latter the nature and orientation of the inclusions have to be found. The practice of comparing photographs is to be preferred to calculation of spot positions and intensities, as being quicker, and possible even when the cell size and crystal structure are unknown. If allowance is made for slight changes in position and intensities for different compositions, only two standard photographs (one for each oscillation range) are needed for each of the pyroxene structure types.

If from optical observation or otherwise, the nature and orientation of the inclusions can be postulated, a photograph of the pure substance taken in the suspected orientation can be compared directly with the "inclusion spots" on the photograph of the intergrowth. A good match of positions and relative intensities provides confirmation, and the intergrowth photograph can itself be used as a "standard" in further investigations.

In a more difficult case it may not be possible by microscopic examination to identify the inclusions from among several substances, or to get any information about orientation. For example, an ore mineral exsolved from a pyroxene is often difficult to characterise optically. The identification may then be carried a stage further by comparing the inclusion spots on the intergrowth photograph with powder photographs, (taken in the single-crystal camera) of each of the possible materials. If for one of the powder photographs each inclusion spot lies on one of the powder rings a tentative identification is made (of course it is not necessary for there to be a spot on every ring). The orientation of the intergrowth must next be found. This may be done (1) by measuring the layer line spacing of the intergrowth spots, if these lie on layer lines; (2) by indexing the spots from the indexed powder photograph; (3) by arguments as to structural similarity between the two phases; (4) by a combination of these approaches suited to the particular example. The identification is only completed by a satisfactory correspondence between the inclusion spots and a "standard" photograph taken in the predicted orientation.

In the most difficult circumstances there is no previous clue to the identity of the inclusions. Then measurement of the *d*-spacings of the inclusion spots on a series of oscillation photographs and use of the A.S.T.M. index may lead to a definite identification, but this procedure should only be used as a last resort; fortunately it is rare that no suggestion as to the identity can be made.

By these methods the orientations of many of the common intergrowths in pyroxene crystals have been determined; the following sections describe the results which, it is hoped, may be of use to other investigators. Discussion of the structural significance of the results is held over for a subsequent paper. It is convenient to treat separately the cases of intergrowths of pyroxenes in pyroxenes, and other inclusions in pyroxenes.

Pyroxene Intergrowths in Pyroxene Crystals

The three main pyroxene structure types may be called augite (monoclinic, $C2/c$, a 9.7 Å, b 8.9 Å, c 5.25 Å, β 106°) pigeonite (monoclinic, $P2_1/c$, a, b, and c as for augite, β 109°) and hypersthene (orthorhombic, $Pbca$, a 18.2 Å, b 8.9 Å, c 5.2 Å). Ca-rich pyroxenes such as diopside, salite, hedenbergite and augite have the augite structure, Ca-poor clinopyroxenes the pigeonite structure, and all orthopyroxenes (except protoenstatite) the hypersthene structure.

We have examined five different combinations of host and lamellae.

(1) *Augite with (001) pigeonite lamellae*

In agreement with Morimoto (1956) it is found that the directions of the x and y axes of the two minerals are the same, while the z axes are inclined at about 3° to one another, by reason of the different β angles, (Fig. 1*a*). On oscillation photographs taken with the z-axis of augite as oscillation axis the layer lines through the pigeonite spots are twisted away from the straight augite layer lines, as shown in Figs. 2 and 3.

(2) *Augite with (100) hypersthene lamellae*

The two phases share the y and z axis directions, as shown in Fig. 1*b*, so that on the standard z-axis photographs the hypersthene spots occur on the augite layer lines. As the position of the spots are different, and those due to hypersthene show more symmetry, the two sets are easily distinguished.

(3) *Augite with both pigeonite and hypersthene lamellae*

The axial arrangement is a simple combination of the previous two, and so is the resulting photograph. Fig. 4 shows the three-phase combination: the spots from the different structures are readily identified.

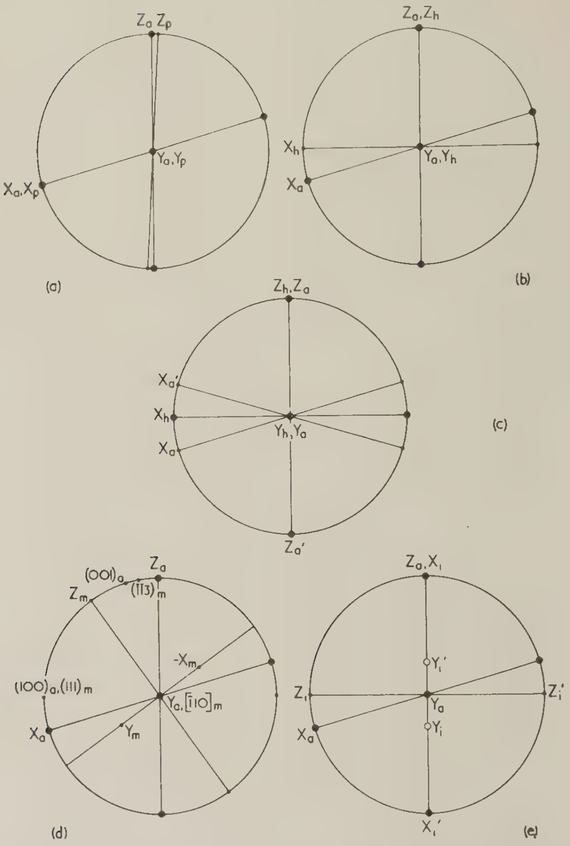

FIG. 1. Axial orientations in pyroxene intergrowths. (*a*) augite (*a*) with pigeonite lamellae (*p*). (*b*) augite (*a*) with hypersthene lamellae (*h*). (*c*) hypersthene (*h*) with "twinned" augite lamellae (*a*, *a′*). (*d*) augite (*a*) with exsolved magnetite (*m*) in the first orientation. (*e*) augite (*a*) with "twinned" ilmenite (*i*, *i′*).

(4) *Pigeonite with (001) augite lamellae*

The relative orientation is exactly the same as in (1) and the photographs are similar to Fig. 3, except that the pigeonite spots would be the stronger set, and as the pigeonite *z*-axis would have been taken as oscillation axis, the augite layer lines would be twisted and those of the pigeonite straight.

(5) *Hypersthene with (100) augite lamellae*

As in case (2) the *y* and *z* axial directions are in common, but now in accordance with the symmetry principle stated earlier, the augite lamel-

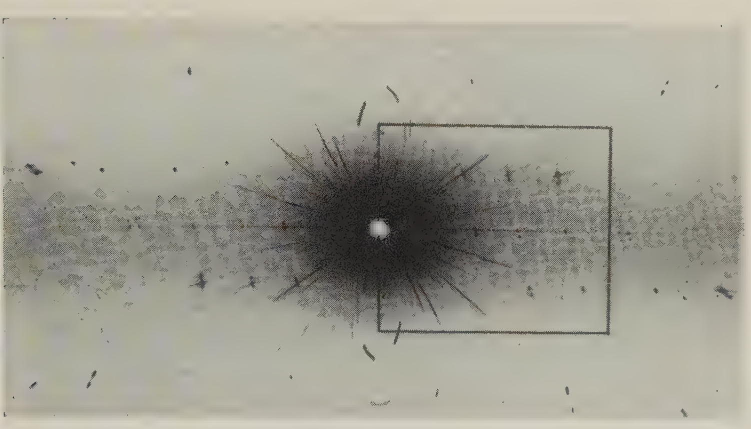

FIG. 2. Oscillation photograph about z-axis of an augite crystal containing pigeonite lamellae, taken with filtered Fe radiation. At the centre of the oscillation range the x-ray beam was parallel to the diad y-axis. The black lines indicate approximately the region illustrated for different specimens in Figs. 3 to 8. With the exception of Fig. 4, all diffraction patterns were obtained with filtered Fe radiation. [Specimen from Mt. Wellington, Tasmania.]

lae are in two orientations, as shown in Fig. 1*c*. Fig. 5 shows the type of photograph obtained: in this case there is less augite in one orientation than in the other.

Other combinations of phases and other orientations are sometimes found, but these five are the most common, and they persist even when additional phases such as ores and amphibole are present. No list of ξ, ζ coordinates for the spots of the various phases is given since it is defi-

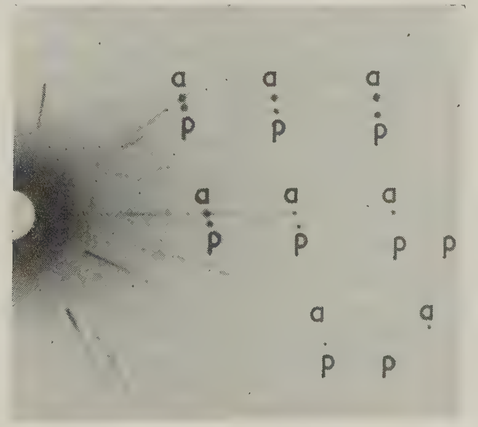

FIG. 3. Augite (*a*), with exsolved pigeonite (*p*). [Specimen from Skaergaard Intrusion, E. Greenland. No. 1691.]

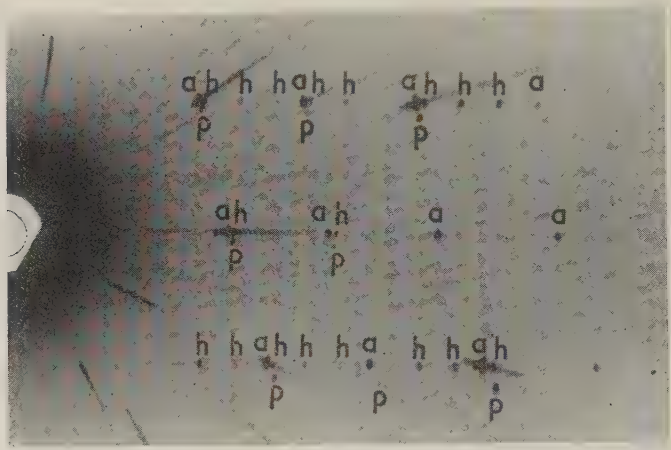

FIG. 4. Augite (*a*), with exsolved pigeonite (*p*) and hypersthene (*h*) (filtered Cu radiation). [Specimen from Skaergaard Intrusion, E. Greenland. No. 4087.]

nitely to be recommended that "standard" comparison photographs should be made by anyone using the method.

OTHER INTERGROWTHS IN PYROXENE CRYSTALS

The examples given in this section are those which the authors have encountered and examined; others are certainly to be found, and could be treated by the same methods.

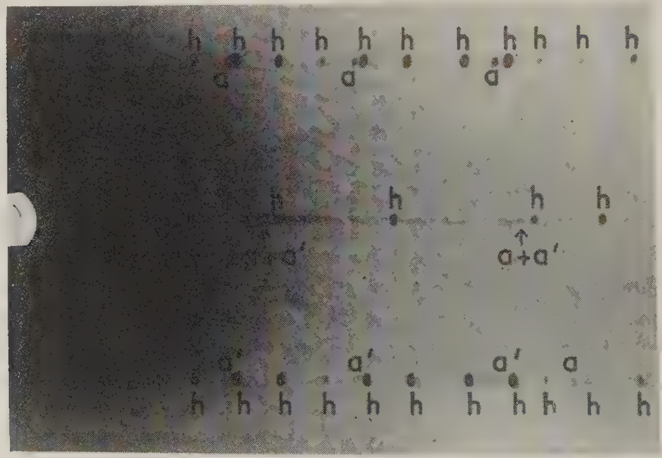

FIG. 5. Hypersthene (*h*) with unequal amounts of "twinned" augite (*a*, *a*′). [Specimen from Bushveldt Complex, S. Africa.]

(1) *Magnetite and spinel*

Magnetite may occur as thin plates or rods lying in the (100) and (001) planes of augite. Two axial orientations are found, which are thought to correspond to these two macroscopic dispositions. In the first of these the axes are arranged as in Fig. 1*d*, the (111) plane of magnetite being parallel to (100) of augite. The second orientation is the same but for a rotation of approximately 7° about the $[\bar{1}10]$ magnetite axis so as to bring $(1\bar{1}3)$ of magnetite parallel to (001) of augite. The two orientations seem to be independent, for the relative proportions present can vary in different crystals from the same specimen. Magnetite has a spinel-type crystal structure, and it would be expected that any other spinel intergrowth with augite should show the same orientation as magnetite. (Indeed without careful intensity measurements it is impossible to prove from the *x*-ray evidence alone that the phase assumed to be magnetite is not another spinel of approximately the same cell size.) Fig. 6 shows an augite host with, among other phases, both magnetite and the iron-aluminium spinel hercynite in both orientations.

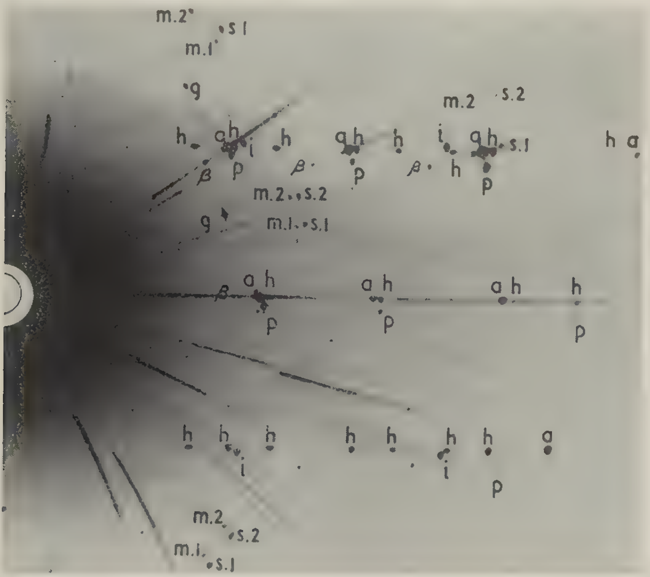

FIG. 6. Augite (*a*), with both pigeonite (*p*) and hypersthene (*h*). Other phases are ilmenite (*i*), magnetite and spinel (probably hercynite) each in two orientations (*m*.1, *m*.2, *s*.1, *s*.2). *g* indicates spots from a disoriented fragment, and β those produced by FeKβ radiation. (A few spots due to clino-amphibole are also present but are unmarked.) [Specimen from Kragerö, Norway.]

Natural hypersthenes may also contain magnetite: this is found to have the first orientation described above for augite, together with the "twin" about the normal to (111) of magnetite demanded by the intergrowth symmetry principle. When iron-bearing orthopyroxenes are heated in air magnetite is formed in the same orientations as for the natural material; an example of this is shown in Fig. 7.

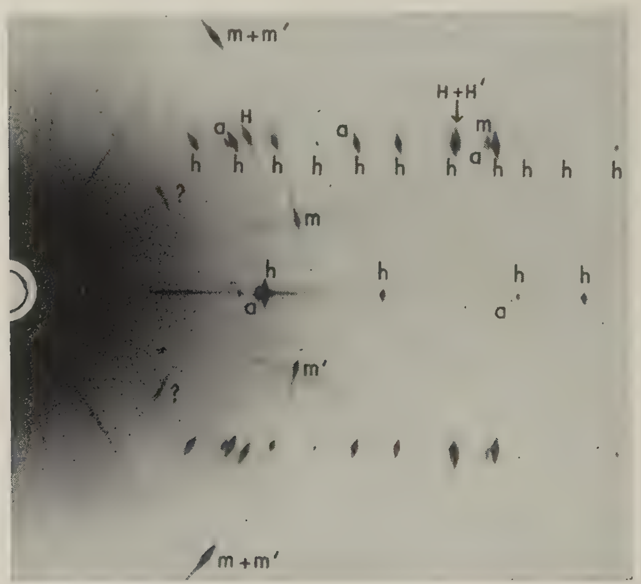

Fig. 7. Initially single-phase volcanic hypersthene (*h*), which on being heated at 1050° C. in air has exsolved "twinned" augite (*a*, *a'*), magnetite (*m*, *m'*) and haematite (*H*, *H'*). The origin of the short streaks marked ? is uncertain: they may be from an oriented form of silica. [Specimen from Koolau, Oahu.]

No naturally occurring example of an intergrowth of magnetite and pigeonite has been examined, but one of the effects of heating single-phase pigeonite in air is to form magnetite in the two orientations as described for augite.

(2) *Ilmenite and haematite*

Associations of ilmenite and augite occur naturally, and the axes of the trigonal ilmenite are arranged as shown in Fig. 1*e*, "twinned" to conform with the intergrowth symmetry principle. Fig. 6 shows the positions of the ilmenite spots.

Ilmenite is sometimes found intergrown with hypersthene: the arrangement of ilmenite in the two positions of Fig. 1*e* has effectively orthorhombic symmetry,* and the same arrangement is found in hypersthene. When hypersthenes are heated in air some haematite is formed as well as magnetite. Haematite is structurally very similar to ilmenite, and it takes up the same orientations: because of the difference in cell sizes, however, the two phases can be distinguished. Fig. 7 shows haematite spots.

Heating single-phase pigeonite in air produces haematite as well as magnetite, and the orientations found are the same as those for ilmenite in augite. Natural intergrowth of ilmenite and pigeonite was not encountered.

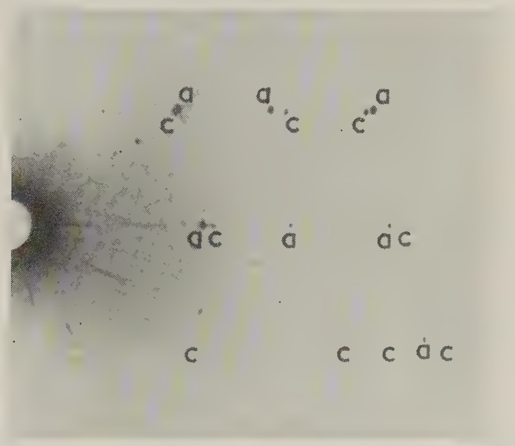

FIG. 8. Augite (*a*), with clino-amphibole (*c*). [Specimen from Ballachulish, Scotland, No. 343.]

(3) *Clino-amphibole*

Hornblende is a fairly common alteration product of augite, and is often orientated so that the x, y and z axial directions are all in common with that of the augite. (This is possible as the β angles of the two phases are virtually the same.) Fig. 8 illustrates this situation.

Hypersthene alters to twinned clino-amphibole rather than to orthorhombic amphibole. The y and z directions are common, and the amphibole is "twinned" about the normal to (100).

CONCLUSION

The fact that pyroxene crystals often contain other phases in a definite crystallographic relation enables the nature of the minor components to be established by single-crystal methods even when they are present in very small amounts. A recommended procedure for such identification has been outlined, illustrated by typical photographs.

---

* Strictly speaking ilmenite has point-group $\bar{3}$, so that four orientations are needed to give orthorhombic symmetry, but it has strong pseudo-symmetry $\bar{3}m$. Haematite has $\bar{3}m$ as point-group.

ACKNOWLEDGMENTS

We wish to thank Professor C. E. Tilley, F. R. S. for his help and encouragement, Dr. S. O. Agrell and Dr. I. D. Muir for many useful discussions and the provision of specimens, and Mr. K. Rickson for taking many of the photographs.

REFERENCE

MORIMOTO, N., 1956, *Proc. Jap. Acad.*, **32,** 750.

Manuscript received September 6, 1958.

THE AMERICAN MINERALOGIST, VOL. 44, MAY–JUNE, 1959

PERTHITE FORMED BY REORGANIZATION OF ALBITE FROM PLAGIOCLASE DURING POTASH FELDSPAR METASOMATISM

FORBES ROBERTSON, *Petrobrás CENAP, Curso de Geologia, Universidade da Bahia, Salvador, Bahia, Brasil.**

ABSTRACT

Orthoclase microperthite in quartz monzonite and alaskite in the Boulder batholith, Montana, originated by replacement of plagioclase. Orthoclase which crystallized between early-formed crystals of plagioclase late in the magmatic stage is not perthitic. The crystallization sequence leading to perthitic orthoclase was: (1) deuteric alteration of andesine to albite at the contact of invading potash feldspar; (2) replacement of albite by potash feldspar which is perthitic. An intermediate soda-rich potash-bearing feldspar, described as anorthoclase, is locally preserved and formed as an intermediate crystal phase between albite and orthoclase. The textures of the albite blebs in orthoclase resemble replacement perthite, but other evidence of late soda metasomatism is lacking. These perthites are considered to have formed by the reorganization of the albite portion of the original andesine. During potash feldspar metasomatism, albite, which formed at the advancing orthoclase front, was partly taken into solid solution in orthoclase. The remainder was in some instances, left as relic blebs, but in most cases the albite was reoriented into more orderly arranged blebs and patches resembling replacement perthite textures. Perthite of this type, although resembling replacement perthite, does not in itself constitute a criterion of late soda metasomatism.

INTRODUCTION

The perthitic textures commonly found in potash feldspars in granitic rocks have generally been attributed to one of two well established modes of occurrence, namely, exsolution or replacement. The criteria for their recognition are illustrated by Alling (1921). Exsolution perthites occur in potash feldspars which crystallized from a disordered state at elevated temperature and from which albite exsolved on cooling. Replacement perthites are much less well organized than the exsolution types and formed by partial or selective replacement of potash feldspar by albite. Such late soda metasomatism is recognized in many granites, especially those of metasomatic origin.

The perthitic feldspars described in this report are in quartz monzonite and related alaskite of the Boulder batholith in which the perthitic textures appear to have formed as a result of a specific sequence of metasomatic events at the deuteric stage of crystallization and in a chemical environment in which soda metasomatism was lacking. Similar perthites have been recognized at a number of other localities including a granogabbro which is probably related to the Boulder batholith; a granitic differentiate in diabase at Mt. Sheridan in the Wichita mountains, Oklahoma; a red granite from the Wichita mountains; and the Silvermine granite in the St. Francois mountains in Southeastern Missouri.

---

* Address after Sept. 1, 1959: The Principia College, Elsah, Illinois.

In the rocks of the Boulder batholith, and in those of the other localities mentioned, orthoclase that contains blebs or irregular patches of albite is believed to have replaced plagioclase. The albitic blebs are thought to be residual albite which was originally a part of the plagioclase that could not be taken into solid solution in orthoclase. Perthites formed in this way are neither the product of exsolution nor replacement in the sense of a late stage of soda metasomatism.

Perthites in Quartz Monzonite and Alaskite of Boulder Batholith

The Boulder batholith, located in southwestern Montana, is generally agreed to be an orthomagmatic igneous intrusive and is comprised principally of quartz monzonite with associated more mafic granodiorite and granogabbro and more felsic alaskite and aplite. In quartz monzonite and the more mafic rocks with hypautomorphic textures, the early sequence of crystallization of minerals followed the classic line. Plagioclase was the first mineral to crystallize in quantity, in part accompanied by minor amounts of pyroxene and followed by hornblende and biotite. Potash feldspar is only a minor constituent in granogabbro, is present in essential amount in granodiorite and is a major constituent in quartz monzonite in which it is nearly as abundant as plagioclase. Quartz crystallized last.

Textures in Quartz Monzonite

Although the essential mineralogy and relative proportions of the minerals are roughly the same in the varieties of quartz monzonite, there is a wide variety of textures ranging from fine grained quartz monzonite porphyry through medium grained holocrystalline rocks to coarse grained rocks which are, in some instances, porphryoblastic. The coarse grained rocks have an average grain size of a little more than 2 mm. This usage follows the practice of the U. S. Geological Survey party that is completing mapping in the batholith (Becraft 1955). The textural varieties are almost entirely due to differences in grain size and habit of potash feldspar and quartz crystals.

In quartz monzonite porphyry, euhedral plagioclase, subhedral hornblende and sometimes biotite crystallized early as phenocrysts. In some cases the groundmass contains subhedral plagioclase and biotite with anhedral potash feldspar and quartz, and in other cases, the groundmass is composed almost entirely of potash feldspar and quartz. Rarely, the groundmass consists of granophyric intergrowths of potash feldspar and quartz.

In medium grained quartz monzonite, the grains of late magmatic potash feldspar and quartz which crystallized between the earlier formed minerals, principally plagioclase, are larger than in quartz monzonite porphyry, so that the porphyritic texture is inconspicuous and both quartz and orthoclase may be recognized with the aid of a hand lens. In some of the medium grained rocks, the potash feldspar crystals which are nearly equal in size to plagioclase occur as anhedral porphyroblasts which formed by recrystallization of much finer grained orthoclase in the groundmass and by the partial replacement of plagioclase.

In coarse grained quartz monzonite, the equigranular texture is due principally to the development of mostly anhedral, but sometimes subhedral, orthoclase porphyroblasts which are about the same size as euhedral to subhedral plagioclase which crystallized early. In rare instances, potash feldspar porphyroblasts are many times larger than the original plagioclase crystals. In these rocks, plagioclase may be partly replaced by orthoclase.

The porphyroblastic growths are found in various stages of development. In quartz monzonite porphyry, the porphyroblasts are inconspicuous and are rarely distinguishable with a hand lens. In the medium and coarse grained rocks, the texture of the rock may be characterized by the size of the potash feldspar porphyroblasts. In these, most of the quartz is fine grained, equal in size to groundmass crystals in quartz monzonite porphyry or to that of some medium grained rocks. Only rarely do euhedral potash feldspar porphyroblasts form to produce a coarse grained porphyroblastic texture.

Texture of Alaskite

The alaskite is believed to be quartz monzonite that suffered extreme deuteric potash metasomatism during which the original texture was all but obliterated. The texture of alaskite is heterogeneous with respect to grain sizes. Potash feldspar and quartz predominate, having replaced large portions of the early minerals. In some instances, the crystal shape of plagioclase is preserved, in other instances, the shape is obliterated.

Mineralogy of Quartz Monzonite

Plagioclase

Plagioclase was clearly the first essential mineral to crystallize in significant amount and occurs in euhedral to subhedral crystals as large as 5 mm. Its composition is more or less uniformly a calcic andesine, about

Ab 55 An 45. It is commonly zoned in the normal habit with more calcic cores, but some rhythmic zoning is recognized. The zoning is conspicuous in sections nearly parallel to 010. Optic angles range from 70° to 75° which are somewhat smaller than the values given for plagioclase of this composition in the standard curves. Crump and Ketner (1953, p. 31) illustrate a wide range of optic angles for plagioclase of this composition, namely from 72° to 88°.

Plagioclase phenocrysts commonly have distinctive internal fractures along which, in many cases, late deuteric solutions reacted with the crystals to produce a much more albitic feldspar, normally albite-oligoclase.

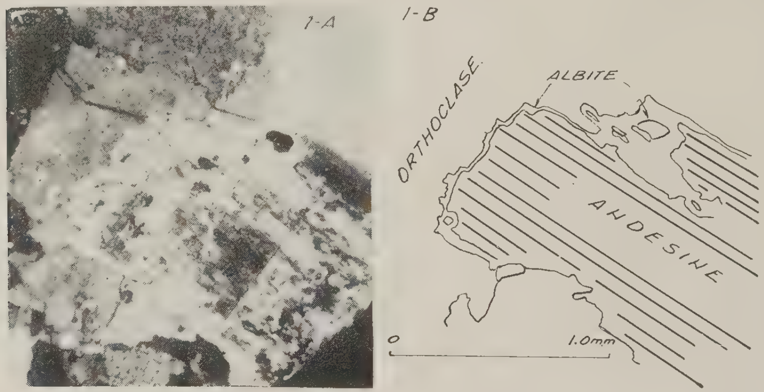

FIG. 1. Andesine plagioclase crystal in contact with and partly replaced by orthoclase. Note particularly the untwinned zone of albite between the two minerals. Figure 1 A is a photomicrograph; 1 B a line diagram which emphasizes the interpreted relationships.

A similar albitic zone is always present at the contact between plagioclase and replacing potash feldspar. Normally, the albitic zone is not twinned, as shown in Fig. 1. Figure 1 A is a photomicrograph which shows an andesine crystal, partly replaced by orthoclase, with an intervening zone of albitic feldspar. The albite twin lamellae in the andesine terminate within the albitic rim. Figure 1 B is a line diagram which emphasizes the distribution and relationships of the feldspars.

Although albitic rims are virtually always untwinned, one rim was observed to be distinctly twinned. The composition, based on its index of refraction and extinction angles, is albite. This twinned rim is on a plagioclase crystal that is partly replaced by potash feldspar and which is next to an incipient vein-like structure. Conceivably, the temperature of formation of the albite was slightly higher than the temperature of formation of most of the albite alteration products. Kohler (1948) and Laves and Chaisson (1950) suggest that such twinned plagioclase formed at a higher temperature than the untwinned product. If there is any thermal significance to the twinned rims, then much of the late potash feldspar metasomatism occurred at a temperature lower than, but only slightly lower than the high-low temperature boundary of the twinned and untwinned albite.

Orthoclase

Orthoclase has several modes of occurrence. That which crystallized with quartz in xenomorphic aggregates and in granophyric intergrowths, is not perthitic. That which is porphyroblastic where plagioclase was incorporated and that which replaced plagioclase, is commonly perthitic. The various modes of occurrence are summarized.

(1) Orthoclase occurs in small xenomorphic crystals in the fine grained groundmass of quartz monzonite porphyry, shown in Fig. 2, and interstitially between plagioclase and other early-formed minerals in some of the coarser grained rocks. It appears to have crystallized from the magma and, together with quartz, occupies the space between earlier formed phenocrysts in the clearly porphyritic rocks and the space between obviously early formed crystals in some of the more nearly equigranular rocks. Orthoclase with these relationships has not been observed to be perthitic.

(2) Orthoclase is present, locally, in micrographic intergrowth where it is dominantly interstitial between early plagioclase phenocrysts. This type of orthoclase is not perthitic.

(3) Orthoclase occurs in a variety of porphyroblastic growths, most conspicuously developed in the coarser grained rocks where xenomorphic orthoclase porphyroblasts are about equal in grain size to plagioclase. Rarely, even larger porphyroblasts, which have good crystal form, are present. The successive stages of porphyroblastic growth are similar to those noted in metamorphic rocks. The first step was the formation of optical continuity over an area of several grains in which quartz may be poikilitically enclosed. Gradual replacement of quartz and "clearing" of the core of the crystal took place, but the margins may remain ragged and poikilitic. Figure 2 illustrates an early stage of porphyroblastic growth. Note the optical continuity, marked by extinction, and the very irregular outline of the grain which is about 0.5 mm. long. Figure 2 A is a photomicrograph. Figure 2 B is a line diagram that indicates the outline of the porphyroblast. Figure 3 shows a more advanced stage with poikilitically enclosed quartz and relics of plagioclase. This crystal, only a part of which is shown, is about 3 mm. long. Orthoclase, which developed in this way, generally encountered and replaced some plagioclase and is commonly partly perthitic. In Fig. 3 A, which is a photomicro-

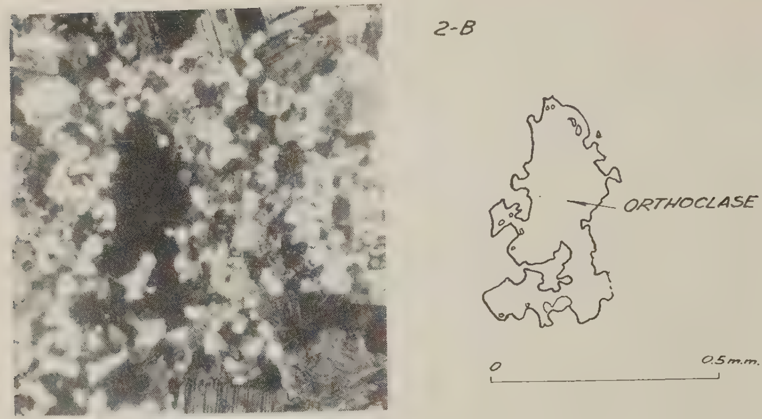

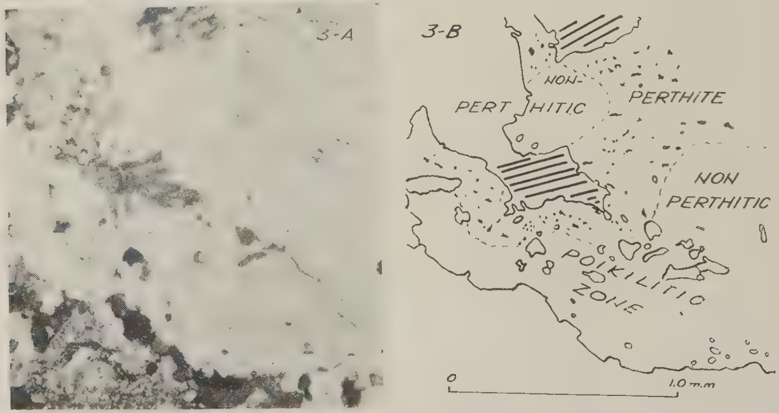

Fig. 2. (Top) Early stage of porphyroblastic orthoclase in fine grained groundmass of quartz monzonite porphyry. The photomicrograph (2 A) illustrates xenomorphic quartz and potash feldspar in the groundmass. Figure 2 B is an interpretation of the area of the porphyroblast, based on the optical continuity, marked by extinction, in 2 A.

Fig. 3. (Bottom) Advanced stage of porphyroblastic orthoclase in quartz monzonite. The groundmass quartz is only slightly coarser than that shown in Fig. 2 A. Quartz and relics of plagioclase are poikilitically enclosed. In the vicinity of plagioclase which is partly replaced by orthoclase, the orthoclase is perthitic. In the poikilitic zone, the orthoclase is dominantly non-perthitic. Figure 3 A is a photomicrograph; 3 B a line diagram of the interpreted relationships.

graph, the perthitic texture is inconspicuous but present. Figure 3 B is a line diagram showing the outline of the porphyroblast and the poikilitically enclosed minerals. The perthitic areas are indicated in the vicinity of the plagioclase relics.

(4) Orthoclase also occurs in a variety of replacement relations with plagioclase. In some instances, plagioclase crystals are deuterically al-

tered to a more albitic composition and then replaced by potash feldspar in such a way as to preserve the form of the initial plagioclase crystal. Figure 4 is a photomicrograph of such a crystal in which a relic of the original plagioclase is preserved. Figure 6 A is a photomicrograph of a crystal of orthoclase which is perthitic within that part of its area that was formerly occupied by a plagioclase crystal. Where the potash feldspar extends beyond the limits of the original plagioclase it is noticeably less perthitic. Figure 6 B is a line diagram illustrating the relationships more clearly.

In other instances, plagioclase crystals are completely replaced but the space of the original crystal is occupied by two or more grains of potash feldspars with different orientations. Figure 5 is a photomicrograph showing a plagioclase crystal, partly replaced by two grains of orthoclase. Relics of albite or reorganized blebs of albite are in orthoclase within an area formerly occupied by plagioclase. Figures 7 and 8 are photomicrographs of the same field in which a large plagioclase phenocryst was formerly present but is now occupied by three potash feldspar crystals with distinctly different orientations. In Fig. 7, relics of plagioclase throughout the area of the photograph show a common orientation of albite twinning which indicate the position and orientation of the original crystal. Figure 8, rotated about 30° counterclockwise from the position in Fig. 7, shows that the same area is occupied by three potash feldspars. The twinned plagioclase relics are white. The dark gray area represents

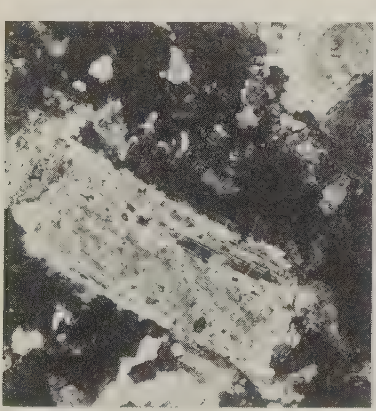

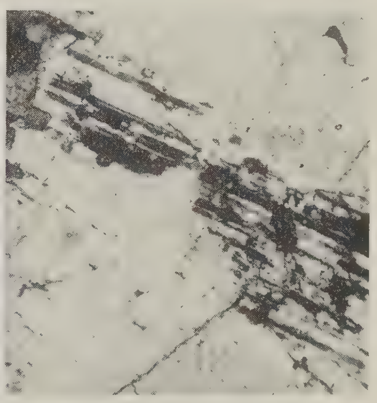

Fig. 4. (Left) A relict of andesine remains in deuterically altered phenocryst. The alteration is partly to albite (white) and a potash-bearing feldspar (light gray). The original shape is preserved. Original crystal about one mm. long.

Fig. 5. (Right) Andesine phenocryst partly replaced from two sides by orthoclase. Note concentration of albite at upper margin of plagioclase and irregular patches of albite in orthoclase within the limits of the original plagioclase crystal. In lower left hand part of photograph, the albite is in irregular strings.

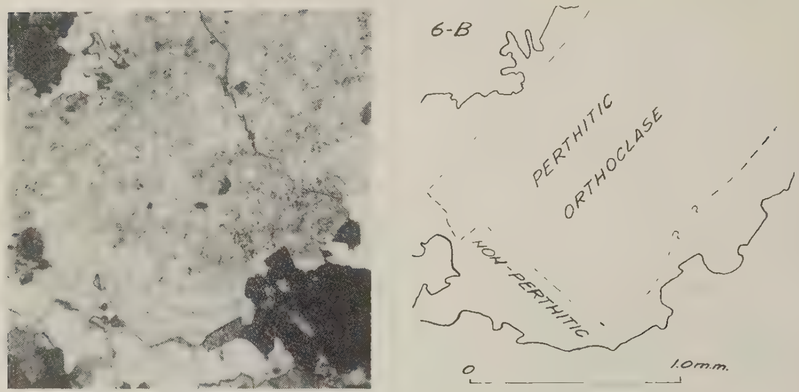

FIG. 6. The photomicrograph (6 A) shows orthoclase microperthite which has the form of a plagioclase phenocryst. The area of the original plagioclase is marked by a sub-graphic perthitic texture. The margin of the crystal, especially in the lower left hand part of the photo, appears to represent orthoclase which grew beyond the limits of the original plagioclase. This portion of the crystal is not perthitic. Figure 6 B is a line diagram of the interpretation of the area of the original plagioclase crystal and the extended, porphyroblastic growth of orthoclase.

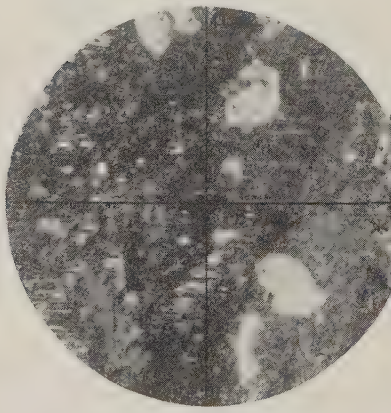

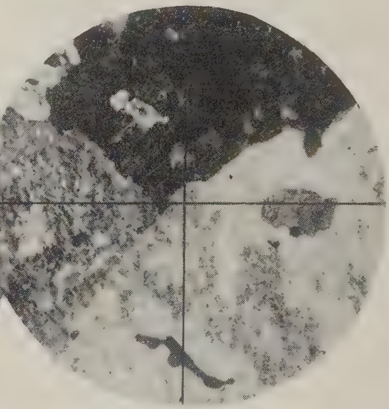

FIG. 7. (Left) Photomicrograph of field of potash feldspars in which relicts of plagioclase (marked by albite twinning) indicate the presence of a plagioclase crystal which nearly filled the field of the photo. Radius of photo about one mm.

FIG. 8 (Right) Photomicrograph of same field as shown in Fig. 7, but rotated about 30° counterclockwise revealing three distinct potash feldspar crystals. The dark gray is anorthoclase, medium gray orthoclase microperthite, light gray probably anorthoclase, white relicts of plagioclase.

anorthoclase with its distinctive inconspicuous grid twinning; the intermediate gray is orthoclase which is conspicuously perthitic; and the light gray is probably anorthoclase. This example is from an alaskite, but similar relations are found in coarser grained quartz monzonite.

Microcline

Microcline occurs in minor amounts in some of the coarser grained rocks only, and is recognized by its clearly defined grid twinning and large optic angle. The bulk of the potash feldspar which shows an indistinct grid twinning is not microcline, and where examined, has a much smaller optic angle. The mineral is anorthoclase or a potash-bearing feldspar similar to anorthoclase.

Anorthoclase

Anorthoclase apparently means different things to different petrologists and it is with some reservation that the term is applied here. There is considerable confusion in the literature about its optical properties and doubt has been cast on the validity of the species (Laves 1952, p. 568). Laves, in his summary of the literature, reports that "Anorthoklas" was first described by Rosenbusch in 1855 but the term has since been applied to a variety of minerals which have slightly different optical properties. He states, "no other mineral of importance appears to play such an ambiguous role in mineralogical and petrographic literature as 'anorthoclase.' Numerous attempts have been made to define and characterize this mineral, and virtually every publication and textbook considers it in a different way" (Laves 1952, p. 567). The principal contributors to the present knowledge of anorthoclase are: Brögger (1890, p. 539, 563; 1897, p. 12–14) who considered anorthoclase a soda-microcline, *Nathron-mikroklin;* Forstner (1884) who contributed optical data indicating variable properties; Winchell (1925, 1933, 1951) who assembled and attempted to organize the data; Alling (1926) who considered that anorthoclase may not be homogeneous and may not be triclinic; Spencer (1937, 1938) who studied the stability relations of the mineral; Oftedahl (1948) who considered that the cryptoperthitic nature of anorthoclase is an important characteristic; Laves (1950, 1952) who critically reviewed the literature and whose experiments with melts led him to use the term K-analbite for anorthoclase, indicating that the mineral is disordered and stable at high temperature; Tuttle (1952) who carefully determined the optical and chemical properties of anorthoclases from a suite of volcanic rocks; and MacKenzie and Smith (1955, 1956) who developed *x*-ray techniques for the study of the alkali feldspars, including anorthoclase.

Lacking *x*-ray equipment, the mineral herein called anorthoclase is a potash-bearing, apparently soda-rich feldspar which has the following properties: The optic angle is somewhat variable, even within an individual grain, as also noted by Tuttle (1952, p. 562), but is about 54°; is optically negative; has slightly lower birefringence than orthoclase; commonly exhibits an indistinct grid twinning; gives variable but commonly negative results when stained with sodium cobaltinitrite solution (Gabriel et al. 1929, Chayes 1952b, Rosenblum 1955). Some of the largest crystals in alaskite and in potash-rich selvage zones around segregations of tourmaline and pyrite in quartz monzonite, have an optic angle $2V = 54° \pm 2°$, based on 6 universal stage measurements. One hand picked grain has $n_\beta = 1.529 \pm .001$. From the index of refraction, the composition is estimated to be about Or 20 An 80 (Tuttle 1952, p. 559). Other anorthoclase or anorthoclase-like grains which are slightly stained with sodium cobaltinitrite may contain a larger proportion of potash.

Identification of anorthoclase in thin section is not always certain. The large crystals of orthoclase are commonly perthitic, anorthoclase is not perthitic; anorthoclase commonly exhibits an indistinct grid twinning, similar in some respects to microcline with which it may be confused. The birefringence is somewhat less than orthoclase and the relief difference is insignificant. Anorthoclase commonly lacks uniform appearance throughout the mineral, and has been described in the writer's notes as "messy." The best means of positive identification of the mineral herein called anorthoclase are its twinning and small optic angle. In stained thin sections, the distinction is usually clear. Plagioclase is unstained and twinned according to the Albite law, orthoclase stains uniformly, anorthoclase is normally not stained, but may be stained in patches.

Assuming slowly falling temperatures through the deuteric stage of crystallization, anorthoclase formed at a relatively low temperature—slightly below the albite alteration and somewhat higher than orthoclase which replaced it. In this regard, it more nearly fits the properties and presumed stage of crystallization indicated by Winchell (1951, p. 299) than any other. He does not give any specific temperature of formation, but it is indicated to be at a temperature well below 600° C. The mineral did not crystallize directly from magma and definitely did not form at the elevated temperature of K-analbite of Laves (1952, p. 561).

Other Minerals

Quartz is the last mineral to crystallize, commonly replacing plagioclase and potash feldspars, but in some instances appears to have crystallized simultaneously with orthoclase in granophyric intergrowths.

Other minerals include minor amounts of monoclinic pyroxene, normally augite, which is commonly found in the cores of actinolitic hornblende. Biotite is brown and strongly pleochroic. Magnetite and apatite are the principle minor accessory minerals. Sphene, tourmaline and zircon are present.

Minerals in Alaskite

Plagioclase in alaskite, where preserved as distinct relics of earlier larger crystals, is commonly oligoclase. Albite is abundant in well organized strings and blebs in orthoclase. The potash feldspars are the same as the replacement types in quartz monzonite. Anorthoclase is moderately abundant, and quartz may comprise as much as 20 per cent of the rock, about twice the normal content of quartz monzonite. Some shreds of muscovite represent the position of former biotite crystals. Much of the plagioclase is flecked with sericite and in some instances, individual plagioclase grains are strongly sericitized. Black tourmaline is relatively abundant at some localities.

Orthoclase Microperthite

Albite, in small, irregular patches, blebs, strings and sub-graphic textures in orthoclase occurs in quartz monzonite as shown in Figs. 8, 2, 10 and 6. Its distribution is frequently erratic and there is no obvious crystallographic control in many instances. In some cases, the albite appears to be small relics. In most quartz monzonite and in alaskite generally, albite occurs in reasonably orderly arranged blebs and strings showing a greater tendency towards crystallographic control, and indicated in Figs. 6, 11 and 12. Figure 11 A is a photomicrograph of a string-type perthite in orthoclase. At the contact with plagioclase, which appears to have been in part replaced by orthoclase, the strings are distinctly broader than in the rest of the orthoclase crystal. Figure 11 B is a line diagram showing the relationship a little more clearly. Figure 12 is a photomicrograph of a typical flame texture in which the albite appears to have become well organized in a specific crystal zone.

The non-uniform distribution of albite in orthoclase and the general absence of obvious crystallographic controls, make an exsolution origin improbable (Alling, 1921, Anderson, 1928). In many of the perthites, and particularly in Figures 11 and 12, the textures clearly resemble replacement textures described by Alling (1921), Anderson (1928) and Faessler and Tremblay (1946). The mobility of soda in the end stage of crystallization in perthites has been brought out by Gates (1953, p. 55) who found the two-fold classification of perthites, replacement and exsolution, unsuitable. Although the textures resemble replacement textures described in the literature, the absence of any other evidence of soda metasomatism, such as late albitization and the occurrence of perthitic textures only in those potash feldspars which replaced plagioclase, leads the writer to question a simple replacement origin.

SODA AND POTASH IN BOULDER BATHOLITHIC ROCKS

Chemical analyses of batholithic rocks reveal a relatively small quantity of soda generally. In the most mafic rocks, the soda content is 4 to 5 per cent; in granodiorite, the amount is somewhat less; in quartz monzonite, about 3 per cent; and in alaskite 2 to 3 per cent. These data plotted on a Larsen variation diagram (1938) yield a straight line whose slope decreases slightly from the mafic to felsic rocks.

Potash, on the other hand, increases from about one per cent in gabbroic rocks to 2 to 3 per cent in granodiorite to 4 to 5 per cent in quartz monzonite to about 6 per cent in alaskite. Similarly plotted, the curve indicates a distinct increase in slope through the range of quartz monzonites and a leveling off in alaskite.

Lime drops from nearly 10 per cent in the most mafic rocks to about 4 per cent in quartz monzonite to less than one per cent in alaskite. The elimination of plagioclase by deuteric potash metasomatism is clearly reflected in the lime and potash curves. Soda remains almost the same but is found in several different minerals at different stages. Larsen diagrams of Boulder batholithic rocks were published by the writer in notes on the chemical petrology of the batholith (Robertson, 1953).

In quartz monzonite, as more and more plagioclase was replaced by orthoclase, the lime was lost, but the soda content remained nearly constant with perhaps a slight tendency towards its reduction. In the nearly complete replacement of plagioclase in alaskite by orthoclase and anorthoclase, the soda content is only slightly lowered and potash increased.

The petrographic evidence of potash metasomatism in striking. The relative abundance of anorthoclase in alaskite suggests that insufficient potash was available to convert all of the anorthoclase to orthoclase. There is no textural evidence for late soda metasomatism in which orthoclase should be replaced by albite. Only the reverse is evident. The available chemical data support the petrographic observations.

PERTHITES FROM OTHER LOCALITIES

Orthoclase microperthites that appear to have been formed in the same manner as those of the Boulder batholith have been noted at several other localities and in a variety of rock types, all considered to be magmatic in origin, and the perthite to have formed by deuteric processes. They have not been investigated in the same detail as those in the Boulder batholith, but they are considered worthy of mention to indicate that this type of perthite may not be rare.

A granogabbro sill, located about 35 miles west of Helena, Montana on U. S. highway 10 N, contains perthitic orthoclase which formed by the replacement of plagioclase by orthoclase. Along small vein-like bodies, anorthoclase-like minerals replace plagioclase, and are in turn replaced by orthoclase, indicating the same late magmatic sequence—late potash metasomatism and absence of soda metasomatism. The amount of orthoclase microperthite is small.

A granitic differentiate formed by deuteric solutions which replaced plagioclase, pyroxene and biotite in a diabase at Mt. Sheridan in the Wichita mountains, Oklahoma, consists of plagioclase, a potash-bearing probably soda-rich feldspar (not anorthoclase), orthoclase and quartz, together with strongly altered mafic minerals (Robertson, 1954). Potash metasomatism is conspicuous in the replacement of plagioclase by orthoclase which is, in part, perthitic. The amount of perthite is small.

Orthoclase microperthite of similar origin occurs in two pre-Cambrian granites, one a red granite in the Wichita mountains, another the Silvermine granite which crops out southwest of Fredericktown, Missouri. In the granite from the Wichita mountains, perthitic orthoclase clearly replaced plagioclase. In the Silvermine granite, a conspicuously perthitic anorthoclase-like mineral is present which appears to represent an intermediate mineral stage in the replacement of plagioclase by orthoclase.

ORIGIN OF THE PERTHITE

Crystallization Sequence

The data accumulated in the study of the perthites in the Boulder batholithic rocks, and probably at the other localities cited, suggest a mode of origin different from either of the classic concepts, viz. exsolution or replacement. Orthoclase which formed by the replacement of plagioclase, and orthoclase which replaced anorthoclase which had previously replaced plagioclase, is perthitic. Gates (1953, p. 65) noted associations of anorthoclase and perthite and reported anorthoclase remnants, usually small, "in crystals which are largely perthitic." He implies that the anorthoclase formed by the alteration of albite blebs after the formation of perthite. In this investigation, anorthoclase appears to have formed at an intermediate stage in the formation of some of the orthoclase microperthite from plagioclase, and that anorthoclase occurs infrequently as relics in perthite, as illustrated in Fig. 9.

Temperature and Environment of Formation

The evidence suggests that the temperature of formation was relatively low, probably below 500° C., and that the perthite formed in essentially a static environment in contrast to a stress environment. The low temperature of formation of the perthites is postulated because of

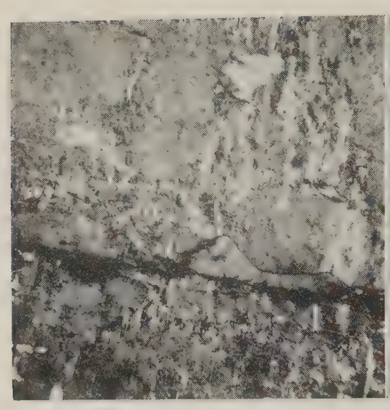

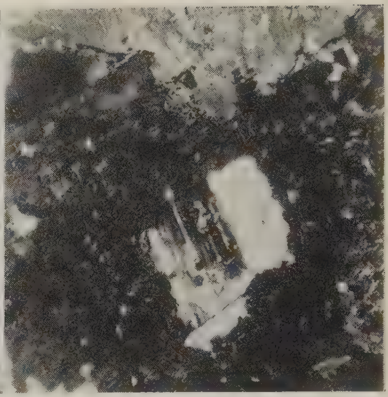

Fig. 9. (Left) Photomicrograph of orthoclase with relict patches of anorthoclase showing the indistinct grid twinning. A relict of plagioclase is shown in the upper part of the photo. The albite twinning in the plagioclase relict is parallel to one of the twin directions in the anorthoclase. The field is about one mm. wide.

Fig. 10. (Right) Photomicrograph of relict of plagioclase in anorthoclase (dark gray) with orthoclase microperthite replacing the anorthoclase. Note the string type albite in orthoclase. Diameter of field about one mm.

the sequence of mineralogical events in the deuteric stage which suggests slowly decreasing temperatures throughout crystallization from normally untwinned albitic alteration of plagioclase, to replacement of albite by anorthoclase (where formed) to replacement of anorthoclase by orthoclase which is perthitic.

Chayes (1952a) and earlier Phemister (1926) pointed out that a stress environment appears to favor the formation of perthite. Mäkinen (1913, p. 35) noted a close relationship between microcline grid twinning and perthite, and considered that the control was one of stress. The presence of granophyric intergrowths in the groundmass and the absence of any obvious directional trends in the rocks tends to favor a more nearly static state than one under stress.

Origin of Albite in Perthite

In the transformation from plagioclase (andesine in the Boulder batholith) to orthoclase microperthite, the chemical and mineralogical sequence appears to be as follows: (1) Plagioclase was altered to albite in a narrow zone between the original plagioclase crystal and the invading potash feldspar. Space was thus made for orthoclase by the expulsion of anorthite and by the greater solubility of orthoclase in albite than in the original plagioclase. (2) Albite was then replaced by orthoclase, or in some instances, anorthoclase. If the replacement proceeded directly to orthoclase, a large part, if not all, of the albite remained essentially in

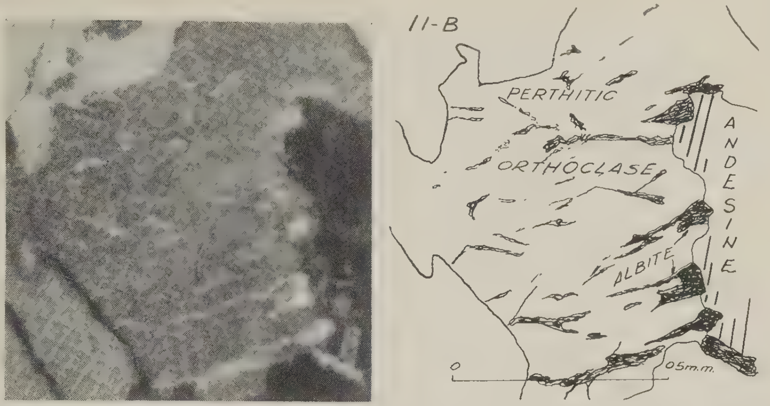

FIG. 11. Photomicrograph (11 A) of string type orthoclase microperthite in contact with plagioclase which has been at least partly replaced by orthoclase. Note that the albite strings terminate against plagioclase in much wider "heads" of albite. Figure 11 B is a line diagram emphasizing the interpreted relationships.

place, evidently within the space occupied by the original plagioclase crystal. Undoubtedly some albite was taken into solid solution in orthoclase. The excess albite which could not be taken into solid solution remained in discrete relics. The final reorganization of albite relics into blebs and strings, commonly with some tendency towards crystallographic control, attests to the mobility of the albite within orthoclase at this late stage. Where anorthoclase formed as an intermediate step, as indicated in alaskite and some quartz monzonite, the anorthoclase was in turn replaced by perthitic orthoclase. The albite originally in anortho-

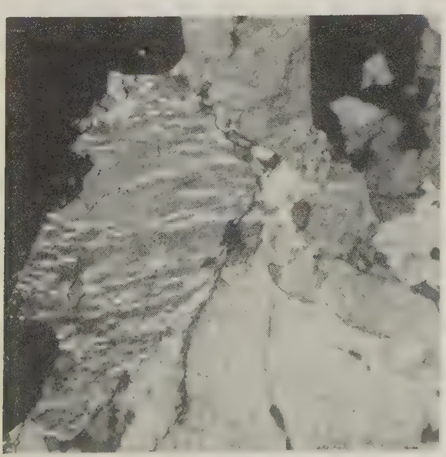

FIG. 12. Photomicrograph of flame-type orthoclase microperthite in alaskite which resembles a replacement type. Width of crystal is about 0.5 mm.

clase was reorganized into blebs in orthoclase. Since anorthoclase is a more potash rich feldspar than albite, it would seem that if anorthoclase did not form generally as a distinct mineral phase, the chemical stage represented by anorthoclase was passed through.

The abundance of anorthoclase in alaskite probably indicates that the replacement process was arrested before completion by the exhaustion of the potash available for replacement of anorthoclase to orthoclase. So far as the writer is aware, perthite which formed in this way, by the reorganization of albite as a consequence of deuteric potash metasomatism, has not been previously described.

Summary of Stages Leading to Formation of Reorganization Perthite

1. Plagioclase (calcic andesine in quartz monzonite) is attacked and altered to albite, commonly in a narrow zone between plagioclase and replacing potash feldspar. The albitic feldspar is normally untwinned, but in one instance, the albite alteration rim is distinctly twinned.
2. Albite was partly replaced by potash feldspar. In some instances there is an intermediate anorthoclase stage with anorthoclase in turn replaced by orthoclase. In orthoclase formed by this sequence of crystallization, albite blebs are found.
3. The albite blebs appear to be small relics in some instances. In most cases the albite appears to have been reorganized into discrete blebs or strings which resemble those found in replacement perthites. Some perthite formed in this way in alaskite and some quartz monzonite indicates further reorganization into crystallographically controlled zones in orthoclase.

In the formation of reorganization perthite, albite, originally in solid solution in plagioclase, remains essentially in the same area, first crystallized to albite, then part of the albite taken into solid solution in orthoclase and the remainder remaining as blebs, patches or strings, reorganized into favorable zones within orthoclase.

Orthoclase microperthite which exhibits textures similar to those found in replacement perthite of the type herein described does not necessarily constitute a criterion of late soda metasomatism.

ACKNOWLEDGMENTS

The writer wishes to express his gratitude for the criticisms offered by Dr. Cordell Durrell and for his careful editing of the manuscript.

REFERENCES

ALLING, H. L., 1921, The mineralogy of the feldspars: *Jour. Geology*, **29,** 193–294.
———, 1926, The potash-soda feldspars: *Jour. Geology*, **34,** 591–611.

ANDERSON, OLAF, 1928, The genesis of some types of feldspar from granite pegmatites: *Norsk Geologisk Tidsskr.*, **10,** 116–207.

BECRAFT, G. E., 1955, New field classification of the quartz monzonite and granodiorite of the Boulder batholith, Montana: *Geol. Soc. America Bull.*, **66,** 1642 (abs).

CHAYES, FELIX, 1952a, On the association of perthitic microcline with highly undulant or granular quartz in some calcalkaline granites: *Am. Jour. Sci.*, 5th ser., **250,** 281–296.

———, 1952b, Notes on the staining of potash feldspar with sodium cobaltinitrite in thin section: *Am. Mineral.*, **37,** 337–340.

CRUMP, R. M., AND KETNER, K. B., 1953, Feldspar optics: in Selected petrogenetic relationships of plagioclase: *Geol. Soc. America Memoir*, **52,** 23–40.

FAESSLER, CARL, AND TREMBLAY, L. P., 1946, Perthite as age indicator in Laurentian gneiss and Pine Hill intrusives: *Canadian Inst. Min. Met. Trans.*, **405,** 58–70.

FORSTNER, H., 1884, *Zeits. Kryst.*, **9,** 333.

GABRIEL, A., AND COX, E. P., 1929, A staining method for quantitative determination of certain rock minerals: *Am. Mineral.*, **14,** 290–292.

KÖHLER, ALEXANDER, 1948, Zur optik des Adulars: *Neues. Jahrb.* sect. A., No. 5–8, 49–55.

LARSEN, E. S., JR., 1938, Some new variation diagrams for groups of igneous rocks: *Jour. Geology*, **46,** 506–520.

LAVES, FRITZ, AND CHAISSEN, U., 1950, An *x*-ray investigation of the high-low albite relations: *Jour. Geology*, **58,** 584–592.

LAVES, FRITZ, 1950, The lattice and twinning of microcline and other potash feldspars: *Jour. Geology*, **58,** 548–571.

———, 1952, Phase relations of the Alkali feldspars, I Introductory remarks; II The stable and pseudo-stable phase relations in the alkali feldspar systems: *Jour. Geology*, **60,** 436–450; 549, 574.

MACKENZIE, W. S., AND J. V. SMITH, 1955, The alkali feldspars, I. Orthoclase microperthites: *Am. Mineral.*, **40,** 707–732.

MÄKINEN, EERO, 1913, Die Pegmatite von Tammela in Finlande und Ihre Minerals: *Comm. Geol. Finlande Bull.*, **35.**

OFTEDAHL, C., 1948, Studies in the igneous rock complex of the Oslo region, IX. The feldspars: *Norske vidensk. Akad. Oslo Skr. I, Math. naturu. Kl.*, **3,** 1–71.

PHEMISTER, J., 1926, The geology of Strath Oykell and lower Loch Shin (Explanation of Sheet 102): *Scotland Geol. Sur. Memoir.*

ROBERTSON, FORBES, 1953, Notes on the chemical petrology of the Boulder batholith and related rocks: *Montana Acad. Sci. Proc.*, **13,** 67–76.

———, 1954, Deuteric differentiation of gabbro at Mt. Sheridan, Wichita mountains, Oklahoma: *Geol. Soc. America Bull.*, **65,** 1349 (abs.).

ROSENBLUM, S., 1955, Improved technique for staining potash feldspars: Unpublished Manuscript, *U. S. Geological Survey, Spokane Office, Washington.*

SMITH, J. V., AND MACKENZIE, W. S., 1955, The alkali feldspars, II. A simple *x*-ray technique for the study of alkali feldspars: *Am. Mineral.* **40,** 733–747.

SPENCER, E., 1957, The potash-soda feldspars, I. Thermal stability: *Min., Mag.*, **24,** 453–494.

———, 1958, The potash-soda feldspars, II. Some applications to petrogenesis: *Min. Mag.*, **25,** 87–118.

TUTTLE, O. F., 1952, Optical studies on alkali feldspars: *Am. Jour. Sci.*, **Bowen Volume** part 2, 553–567.

WINCHELL, A. N., 1925, Studies in the feldspar group: *Jour. Geology*, **33,** 714–727.

———, 1933, 1951, Elements of optical mineralogy: Part II, Description of minerals: John Wiley & Sons, New York.

Manuscript received September 5, 1958.

THE AMERICAN MINERALOGIST, VOL. 44, MAY-JUNE, 1959

RE-EXAMINATION OF "STRUVERITE" FROM SALAK NORTH, MALAYA*

B. H. FLINTER, *Geological Survey Department, Federation of Malaya.*

ABSTRACT

Critical re-examination of the original "struverite" from Salak North, Malaya, shows that the samples contain much ilmenite and some cassiterite. As a result, the analysis given by Crook and Johnstone in their description of the mineral in 1912 (1) indicates some contamination by ilmenite and cassiterite, and the subsequent ASTM x-ray powder data card for "struverite" (2-1354) gives a mixed pattern of "struverite" and ilmenite. Furthermore, due probably to the difficulty of analysing Ta/Nb at that time, an incorrect, and very high, value of tantalum was quoted in the original analysis. The mineral is actually richer in niobium than in tantalum and should properly be termed 'ilmenorutile' and not "struverite." Neither of these terms is favoured by the present writer who prefers the terms "*niobian-rutile*" and "*tantalian-rutile*" respectively.

Using more sensitive methods of magnetic separation together with x-ray powder and polished section studies the mineral is found to be homogeneous, consisting essentially of titanium, niobium, tantalum, and iron. A definite, but complex, relationship between the composition and specific gravity and mass magnetic susceptibility is indicated. X-ray powder patterns of the most magnetic material give an apparent bi-rutile structure, which can be seen to develop from a rutile structure in the less magnetic material. As such the mineral is intermediate between rutile and tapiolite, an isomorphous series postulated by Prior in 1908 (2).

INTRODUCTION

This paper is part of a general investigation into the relationship of rutile (TiO_2) and the tetragonal tapiolite-mossite series ($Fe(Ta,Nb)_2O_6$). Methods of study include electromagnetic separation, chemical analyses, certain physical and optical determinations, examination of polished sections, and x-ray powder work.

The first discovery of "struverite" (Ta/Nb-rutile) in Malaya was made in 1909 and was described by Crook and Johnstone in a paper published in 1912 (1). It occurred as alluvial grains obtained from a tin-mining lease near Salak North in Perak. The only material available to the writer was that of three concentrates, retained in the Central Reference Collection of the Geological Survey of Malaya and registered as GS: 3140, 3141 and 4893, labelled "struverite." The total weight of each concentrate was only a few grammes.

PREPARATION OF THE MATERIAL

The three concentrates available to the writer were electromagnetically separated on a Frantz Isodynamic separator. Using a side slope of 25° and a forward slope of 15°, each sample was separated by passing

---

* Published by permission of the Director, Geological Survey with the authority of the Minister of Natural Resources, Federation of Malaya. Government copyright is reserved.

TABLE 1. ELECTROMAGNETIC DISTRIBUTION OF THE Ta/Nb RUTILE

Fraction	Magnetic at	Sample No. 3140 Wt. (gm)	3140 %	4893 Wt. (gm)	4893 %
d	0.6 amps.	—	0	—	0
e	0.7 amps.	1.35	83.9	0.57	71.3
f	0.8 amps.	0.07	4.3	0.02	2.5
g	0.9 amps.	0.09	5.6	0.10	12.5
h	1.0 amps.	0.10	6.2	0.11	13.7
		1.61	100.0	0.80	100.0

Chemical assays for $(Ta/Nb)_2O_5$ on fractions (d) and the more magnetic fractions gave a maximum value of 0.27%, an average figure for Malayan ilmenites.

through field intensities induced by current increments of 0.1 amp. Examination of the various fractions under the microscope, combined with chemical analyses for $(Ta/Nb)_2O_5$ and zinc-dish treatment for the detection of any cassiterite, gave the following approximate compositions:

	3140	3141	4893
Ta/Nb-rutile	1.61 gm.	0.25 gm.	0.80 gm.
Ilmenite	3.26	7.03	0.55
Cassiterite (some magnetic)	1.39	0.45	2.82
Xenotime and monazite	—	1.15	—
Tourmaline	—	—	0.08
	6.26 gm.	8.88 gm.	4.25 gm.

Because of the small amount of Ta/Nb-rutile in sample 3141 no further work was carried out on it. The electromagnetic distribution of the Ta/Nb-rutile in samples 3140 and 4893 is given in Table 1.

CHEMICAL COMPOSITION

Crook and Johnstone (1912, p. 226) gave the following quantitative analysis of the mineral:

TiO_2	45.74%
Ta_2O_5	35.96
Nb_2O_5	6.90
FeO	8.27
MnO	trace
SnO_2	2.67
SiO_2	0.20
H_2O at 105° C.	0.08
H_2O above 105° C.	0.42
	100.24%

They state that the SiO_2 occurs as free quartz and indicate that the SnO_2 is an impurity. The presence of magnetic cassiterite detected in the re-examined concentrate strongly supports their assumption. The mineral is therefore an oxide of iron, titanium, tantalum, and niobium. Crook and Johnstone state that "there is apparently no reasonable alternative to the view suggested by Prior that 'struverite' is a homogeneous isomorphous mixture, and it is to be regarded as consisting essentially of a solid solution of tapiolite in rutile." Ignoring the SiO_2, SnO_2 and H_2O they recalculate the analysis to give the following ratio of the two molecules:

TiO_2	41.39%
$Fe(TaNb)_2O_6$	58.61

All evidence supports their view that the "struverite" is a "homogeneous isomorphous mixture," but one that is a continuous series rather than a mixture of the rutile and tapiolite molecules.

The structural formula for Ta/Nb-rutile is given by Dana (3) as $Fe_x^2(Ta,Nb)_{2x}Ti_{1-3x}O_2$, with the condition that x must not exceed about 0.2. This can be written as $Fe_x^2(Ta,Nb)_{2x}Ti_{60-3x}O_{120}$, with x not exceeding about 12.

Recalculating the original analysis by Crook and Johnstone on a basis of 120 oxygens in the unit cell, the number of cations in the unit cell is:

38.21	Ti
10.86	Ta
3.49	Nb
7.69	Fe
60.25	

This gives a structural formula of $Fe_{7.69}(Ta,Nb)_{14.35}Ti_{38.21}O_{120}$ which fits almost perfectly, the slight excess of Fe being attributable to some iron oxide or a little ilmenite.

The high tantalum figure was a point of great interest, as no other tantalum/niobium oxide, except a euxenite, has been found in Malaya with Ta exceeding Nb. Because of the small amount of material available to the present writer it was not possible to carry out a complete analysis by wet chemical methods. A partial analysis of fraction (e), the most magnetic material, gave:

	3140(*e*)	4893(*e*)
% Nb_2O_5	17.80	15.92±0.24
% Ta_2O_5	14.18±0.18	13.90±0.26

The difference between the two results is striking. There would appear to be two possible explanations. Either the original analysis is correct and the present material is not representative of the original sample, or the original analysis is incorrect due to the great difficulty in separating the titanium, tantalum and niobium oxides at the beginning of the century. All available evidence indicates the latter possibility. It is also possible that the TiO_2 figure is too low and that the original sample contained much more ilmenite, not mentioned by Crook and Johnstone, but making up the bulk of the present material, and that the close agreement of the structural formula is fortuitous.

According to the original analysis the tantalum/niobium ratio is 81:26 and the mineral would rightly be named "struverite" (4). The recent analyses give tantalum/niobium ratios of 32:67 and 31:60 respectively. Thus the bulk, if not all, of the mineral is in fact "ilmenorutile" (4). Neither of these terms is favoured by the present writer who prefers the terms "*tantalian-rutile*" (with the presence of a variable, but subordinate, amount of niobium implied) and "*niobian-rutile*" (with the presence of a variable, but subordinate, amount of tantalum implied) respectively.

From the relationship

$$\text{mass susceptibility} = \frac{\text{magnetic susceptibility}}{\text{density}}$$

the less magnetic (i.e. lower mass susceptibility) fractions of the material might be expected to have a higher proportion of tantalum to niobium, due to a higher density. It is thus quite possible that some of the Salak North material may be tantalian-rutile. This indicates the undesirability of having specific names for the two varieties. The term Ta/Nb-rutile covers the entire sample.

Physical and Optical Characters

The mineral is black, with a metallic lustre which is usually bright but sometimes dull. The grains average 2 mm. in length and 1 mm. in width. They are usually rounded, less often sub-rounded with four or five faces showing when a prismatic habit can usually be distinguished.

Crook and Johnstone reported that the particles, when crushed, are not opaque but are either brownish-yellow (O-ray) or strongly pleochroic in brownish-yellow and dull bluish-green (E-ray). The present writer considers the brownish-yellow and the dull bluish-green to be more of an orange-brown and dark bottle-green respectively. A difference was also found in the degree of opacity according to the mass magnetic susceptibility of the mineral. In the weakly magnetic material (fraction *g*) the translucency can be seen quite easily under fairly low power. With the most magnetic material (fraction *e*), however, this can be seen only under high-power and then usually on the edge of the fragment only. Similarly the colour of the crushed powder varies from dark chocolate-brown in (*e*) to light purple-brown in (*h*), the latter closely resembling the fawn powder of pure rutile.

It was not possible to obtain an interference figure because the grains had to be crushed extremely fine to achieve translucency, but the mineral is known to be uniaxial (from *x*-ray data) and positive in sign (because the E-ray is the slower of the two). No attempt was made to obtain the refractive indices of the mineral.

Using a Berman density balance the specific gravity of three single grains of the most magnetic material (fraction *e*) was obtained. The resulting values of 4.876, 4.968 and 5.138 show considerable variation and indicate a wide range of chemical composition. A wide range of values within a magnetic fraction is to be expected, for even if there is a relationship between the chemical composition, mass magnetic susceptibility and density, it could not be a simple one. For any given composition in which the ratio of Ta to Nb remains constant the density and mass magnetic susceptibility of the mineral would be expected to increase in direct relationship to an increase in total Ta/Nb (and therefore Fe″) content. For any given composition in which the total Ta+Nb (and therefore Fe″) content remains constant, the density will be expected to behave as for the columbite-tantalite series, increasing as the Ta increases and decreasing as the Nb increases. The mass magnetic susceptibility, however, will be the reverse because of the higher density of the tantalum-high end. Thus a given density or mass magnetic susceptibility value could be due either to a high tantalum-high titanium or to a high niobium-low titanium composition.

EXAMINATION OF POLISHED SECTIONS

An examination in reflected light of polished grains of fractions (*e*) to (*h*) of sample 3140 gave the following data:

Homogeneity

The mineral is perfectly homogeneous. Both the weakly and strongly magnetic material, because of twinning, exhibit irregular small patches, sometimes constituting nearly half the area of the grain. These slightly darker patches are barely visible in plane polarized light, but with crossed nicols (Fig. 1) they are prominent because of the strong anisotropism of the mineral. These patches of twinning indicate different degrees of reflectivity according to the crystallographic orientation, and their irregularity would seem to indicate a random distribution of the replacing ions.

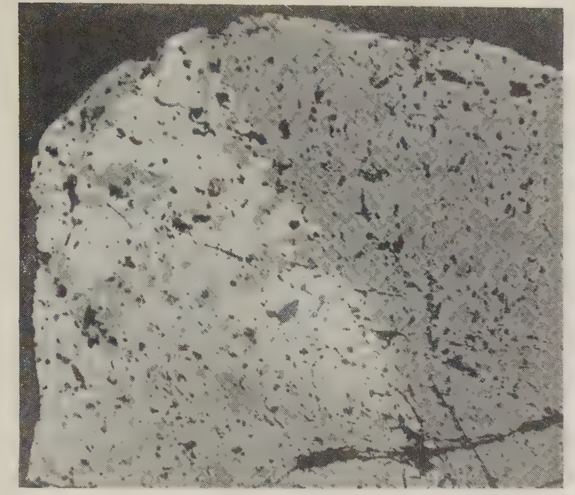

FIG. 1. Single grain of Ta/Nb rutile (sample 3140e) showing irregular patches due to different orientation. Crossed nicols. ×100.

Hardness

Using a micro-hardness tester on a Vickers Projection microscope, two series of tests were made with weights of 50 gm. and 100 gm. respectively. For each series, six readings were taken for each of three fractions, three for the main bulk of the mineral and three for the twinning "blebs." The three fractions included the most magnetic and the least magnetic material from one concentrate. Comparative tests were made on samples of pure rutile and columbite. The results are given in Table 2.

TABLE 2. HARDNESS TESTS

Sample	Weight applied in grams			
	50		100	
	*d**	HV	*d**	HV
3140*e*	4.0	927	6	824
3140*g*	4.0	927	—	—
3140*h*	4.0	927	5.5	981
Rutile	3.5	1211	5.5	981
Columbite	4.25	821	6.5	702

d = mean diameter of indentation (1 unit = 2.5 microns).

HV = Vickers hardness number.

* Mean of six readings. In samples 3140*e*, *g* and *h* the six readings were constant

With a 50 gm. load the nioban-rutile is intermediate between rutile and columbite and shows no variation. A 100 gm. load, which is probably more accurate because of the larger indentation, indicates a decrease, from a value similar to rutile to a value approaching columbite, with an increase in mass magnetic susceptibility. The readings are insufficient, however, to give this a statistical basis.

Other properties

The mineral has C/D reflectivity (5). Under crossed nicols it shows strong anisotropism with two positions, at 90°, which are light yellow-grey and dark grey, there being four maxima during each complete revolution. In addition to the random patches mentioned previously the grains show normal twinning (Fig. 1).

The internal reflection varies from a deep red, easily visible, in fraction (*g*) to none in fraction (*e*).

X-RAY POWDER DATA

The ASTM *x*-ray powder data card (2-1353) for "ilmenorutile," from the Ilmen Mts., Ural, gives a perfect rutile pattern with a slight increase in the *d*-spacings over the values for pure rutile. The ASTM powder data card (2-1354) for "struverite" is of material taken from Salak North, Malaya. The pattern is a very complex one, but closer examination shows it to be a mixture of rutile and ilmenite patterns. This is not surprising considering the high percentage of unsuspected ilmenite present in the original sample, which was thought to be pure. The relevant data are reproduced in Table 3.

The writer obtained powder photographs of the various magnetic fractions of both samples. Only one grain was used in each case. The mineral was found to exhibit two distinct patterns. The less magnetic material gave a rutile pattern with increased *d*-spacings and unit cell dimensions and a few extra faint lines due to a superlattice. The most important of these extra lines, which become stronger with an increase in magnetism, is at $d = 2.9^{+}$. This is the strongest line in the columbite pattern, but it can be indexed as (001) in the rutile pattern. One of these patterns (3140*g*) is given in Table 4.

The more strongly magnetic material gave a complex pattern. Results from two such grains (3140*e* and 4893*e*) are given in Table 4. This appears to be a combination of rutile and columbite. Alternatively it can be indexed as a single pattern of a tetragonal mineral with a_0 slightly larger than for rutile and c_0 approximately double. The mineral is homogeneous, so that it would appear to possess a structure which is either a mixture of a rutile and a columbite phase or a *bi-rutile* one. The writer is of the opinion that the latter is the correct interpretation. As such the mineral is structurally intermediate between rutile and tapiolite, with its tri-rutile structure. Plotted against the x-ray powder data of rutile (4-0551) and tapiolite (2-1341), the two bi-rutile patterns given fit perfectly. They also indicate some inaccuracies in the indexing of the tapiolite. Part of the plot is given in Fig. 2. Some extra lines, due to a tri-rutile super-lattice, are present in both patterns.

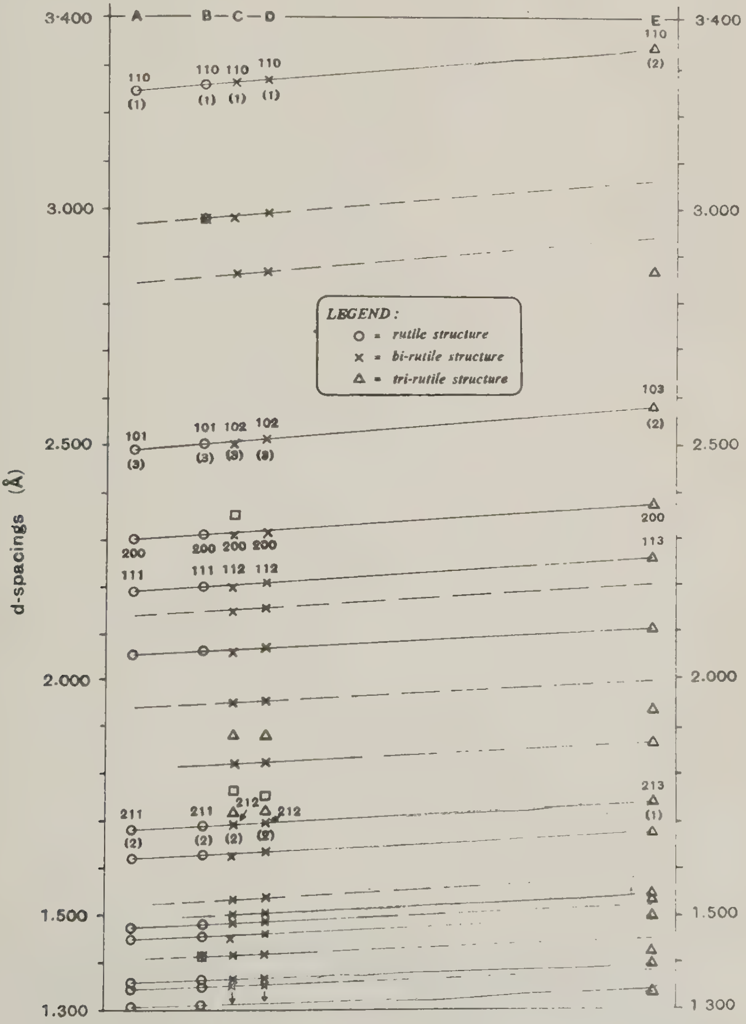

FIG. 2. Plot of a portion of the x-ray powder data to show the relationship of the rutile, bi-rutile and tri-rutile structures. For explanation, see next page.

Fig. 2 represents d spacings (for the range $d=3.400$ to 1.300 Å) which have been indexed to indicate the relationship between the rutile, tri-rutile and the proposed bi-rutile structures, as follows:

A Rutile ASTM-4-0551	B[a] Sample 3140*g*	C Sample 4893*e*	D Sample 3140*e*	E Tapiolite ASTM-2-1341
110	110	110	110	110
—	001[b]	002	002	—
—	—	111	111	N.I.[c]
101	101	102	102	103
—	—	N.I.[c]	—	—
200	200	200	200	200
111	111	112	112	113
—	—	201	n.m.[d]	—
210	210	210	210	202[e]
—	—	211	n.m.	—
—	—	t.s.	t.s.	212
—	—	202, 103	202, 103	N.I.[f]
—	—	N.I.	N.I.	—
211	211	t.s.[g] 212, 113	t.s. 212, 113	213
220	220	220	220	220
—	—	300	n.m.	—
—	—	203	n.m.	301, 214
002	002	004	004	006[h]
310	310	310	310	310, 311[j]
—	102[b]	104	n.m.	—
—	—	—	—	312
301	301	302	n.m.	303, 116[k]
112	112	114	114	—
311	311	↓	↓	313

(*a*) Values for C should be plotted coincident with B, but are separated on the diagram for clarity.

(*b*) For line B values of $d=2.981$ and $d=1.4185$ which have been indexed on the rutile lattice as 001 and 102 respectively can alternatively be due to the bi-rutile super-lattice.

(*c*) N.I. means "not indexed."

(*d*) n.m. means that a line is present on the film but it is not measurable.

(*e*) The value of $d=2.11$, indexed in E as 202, can also be indexed as 210.

(*f*) The value of $d=1.86$, unindexed in E, can be indexed as 203.

(*g*) t.s. means lines due to a tri-rutile super-lattice.

(*h*) The value for 006, given in E as 1.546, should be 1.5351.

(*j*) The indexing of $d=1.505$ as 311, in E, is incorrect. An index of 311 gives $d=1.4810$.

(*k*) The indexing of $d=1.408$ as 116, in E, is incorrect. An index of 116 gives $d=1.3960$.

Line Intensities: The three strongest lines of each pattern are shown in brackets beneath the appropriate d values.

TABLE 3. ASTM *X*-RAY DATA

'Ilmenorutile' 2-1353		'Struverite' 2-1354		Rutile 4-0551		Ilmenite 3-0781	
d Å	I	*d* Å	I	*d* Å	I	*d* Å	I
—	—	3.87	20	—	—	3.73	50
—	—	3.59	40	—	—	—	—
3.27	70	3.25	80	3.245	100	—	—
—	—	2.76	40	—	—	2.74	100
2.50	50	2.50	70	2.489	41	2.54	85
2.31	10	2.32	40	2.297	7	—	—
2.19	10	2.20	40	2.188	22	2.23	70
—	—	2.07	20	2.054	9	—	—
-	—	1.88	40	—	—	1.86	85
1.70	100	1.70	100	1.687	50	1.72	100
1.63	50	1.64	60	1.624	16	1.63	50
—	—	1.51	20	—	—	1.50	85
1.48	10	1.49	40	1.480	8	—	—
—	—	1.47	50	—	—	1.47	85
1.46	30	—	—	1.453	6	—	—
1.37	30	1.37	70	1.360	16	—	—
1.36	10	1.36	60	1.347	7	1.34	70
—	—	—	—	1.305	1	—	—
—	—	1.26	40	1.243	3	1.27	60
—	—	—	—	1.200	1	1.20	30
—	—	1.18	70	1.1700	4	1.18	60
—	—	1.16	60	1.1485	4	1.15	70
—	—	—	—	1.1329	1	—	—
—	—	1.11	70	1.0933	4	1.12	70
—	—	1.09	60	1.0827	4	—	—
1.05	50	1.05	80? 70	1.0424	5	1.07	70
—	—	1.04	60	1.0361	4	and six more lines to 0.913	
—	—	—	—	1.0273	3		
—	—	—	—	.9642	2		
—	—	—	—	.9071	3		
—	—	—	—	.9007	3		
.895	30	—	—	.8892	5		
.881	30	—	—	.8773	6		

There appears to be no direct relationship between the position on the plot and the Ta/Nb content. The bi-rutile and tri-rutile patterns seem to appear suddenly at certain values. What these values are is not known, but, from the structural formula, the values of $x=10$ and $x=15$ (i.e. $Fe_{10}(TaNb)_{20}Ti_{30}$ and $Fe_{15}(TaNb)_{30}Ti_{15}$) give a bi-rutile pattern of $(Fe(TaNb))_{30}Ti_{30}$ and $(FeTi)_{30}(TaNb)_{30}$ respectively. Whether the change is

TABLE 4. X-RAY POWDER DATA FOR LESS MAGNETIC (3140g) AND MORE MAGNETIC FRACTIONS (3140e AND 4893e). CuKα=1.5417 Å; CAMERA DIAMETER 114.83 MM. A SINGLE GRAIN WAS USED IN EACH CASE

hkl	3140 *g*			*hkl*	3140 *e*			4893 *e*		
	d (Å) (meas.)	*d* (Å) (calc.)	I (visual)		*d* (Å) (meas.)	*d* (Å) (calc.)	I (visual)	*d* (Å) (meas.)	*d* (Å) (calc.)	I (visual)
	—			001	5.903	5.973	<1	5.903	5.952	<1
—				100	4.603	4.623	<1	4.589	4.(07	<1
—	—	—	—	101	3.627	3.657	4	3.625	3.642	2
110	3.233	3.257	10	110	3.258	3.269	10	3.249	3.258	10
001[a]	2.951	2.981	<1	002	2.944	2.988	8	2.956	2.976	8
—	—	—	—	111	2.8425	2.8679	<1	2.8525	2.8579	<1
101	2.4815	2.5033	8	102	2.5000	2.5098	8	2.4905	2.4997	8
—	—	—	—	N.I.[c]	—	—	—	2.3538	—	<1
200	2.2946	2.3030	1	200	2.3048	2.3115	1	2.2963	2.3035	1
111	2.1900	2.1996	4	112	2.1918	2.2056	3	2.1919	2.1969	3
—	—	—	—	201	↓	2.1563	<1	2.1488	2.1483	<1
210	2.0512	2.0599	1	210	2.0675	2.0675	1	2.0621	2.0604	<1
	—		—	211	↓	1.9539	<1	1.9463	1.9471	<1
—			—	N.I.[d]	1.8823	—	<1	1.8834	—	<1
—		—	—	202, 103	1.8119	1.8280 1.8294	<1	1.8196	1.8217 1.8224	<1
—	—	—	—	N.I.	1.7586	—	<1	1.7640	—	<1
—		—	—	N.I.[e]	1.7243	—	<1	1.7220	—	1
—	—	—	—	N.I.	—	—	—	1.7087	—	<1
211	1.6873	1.6946	9	212, 113	1.6975	1.7002 1.7009	9	1.6908	1.6941 1.6944	9
220	1.6268	1.6287	1	220	1.6335	1.6347	4	1.6298	1.6291	2
—	—	—		300		1.5410	<1	1.5354	1.5357	<1
—		—		203	↓	1.5088	<1	1.5061	1.5033	<1
002	1.4807	1.4911	<1	004	1.4940	1.4942	1	1.4841	1.4880	<1
310	1.4540	1.4567	<1	310	1.4621	1.4620	2	1.4570	1.4570	1
102[b]	1.4234	1.4185	<1	104	↓	1.4216	<1	1.4133	1.4160	<1
301	1.3606	1.3651	2	302	—	1.3696	—	1.3669	1.3646	3
112	1.3479	1.3555	<1	114	1.3609	1.3589	4	1.3519	1.3534	1
311	1.3129	1.3089	<1							
202	1.2468	1.2516	<1	↓	↓	↓		↓	↓	
212	1.2138	1.2077	<1							
321	1.1729	1.1743	<1	Arrows indicate the presence of one or more lines too faint and diffuse to measure accurately.						
400	1.1505	1.1515	<1							
222	1.0965	1.0995	<1							
330	1.0857	1.0856	<1							
411	1.0469	1.0461	<1	412	1.0514	1.0497	2			
312	1.0409	1.0418	<1	314	1.0459	1.0450	1½			
↓	↓	↓								
402	.9107	.9114	<1							
510	.9029	.9033	<1	↓	↓	↓				
213	.8939	.8952	<1	216	.8965	.8973	<1			
N.I.	.8902	—	<1	—	—		—			
431	.8819	.8802	<1	432	.8841	.8833	1½			
332	.8784	.8777	<1							
422, 223	.8479	.8475 .8484	<1	↓	↓	↓				
303	.8331	.8344	<1	306	.8363	.8364	<1			
521	.8234	.8222	<1	522	.8270	.8251	<1			
	$a_0=b_0=4.606$ Å $c_0=2.982$ Å $a:b:c=1:1:0.6474$				$a_0=b_0=4.623$ Å $c_0=5.976$ Å $a:b:c=1:1:1.2927$ S.G. (measured): 4.968			$a_0=b_0=4.607$ Å $c_0=5.950$ Å $a:b:c=1:1:1.2915$ S.G. (measured): 4.876		

[a] Alternatively is bi-rutile super-lattice (002).
[b] Alternatively is bi-rutile super-lattice (104).
[c] Tri-rutile super-lattice (200).
[d] Tri-rutile super-lattice (212/203).
[e] Tri-rutile super-lattice (213). The strongest line.

made at these values or below and above them cannot be stated until complete analyses have been carried out on single grains for which the x-ray patterns are known.

A hypothetical consideration of the possible structural changes from the tetragonal (rutile) form of TiO_2 to the tetragonal form of $FeTa_2O_6$

(Nb being omitted for simplicity) is given schematically in Fig. 3. This disallows any limiting value on x, which theoretically can range from zero ($Ti_{60}O_{120}$) to 20 ($Fe_{20}Ta_{40}O_{120}$), in the structural formula. Taking six unit cells (in the c_0 direction) of rutile there are six Ti ions equally spaced at a value of $c_0 = r$. As Fe″ and Ta (ignoring Nb, which would go with the Ta, for simplicity) enter the formula the ions substitute randomly for Ti giving six TiTaFe positions with no change in c_0, but a super-lattice begins to form. At a certain value of Ti, which is probably above but certainly at 30 (i.e. $x = 10$ or less in the structural formula) the structure changes to a bi-rutile one, the c_0 repeat distance being $2r$ and the ion positions being taken by Ti and FeTa. Between the values of Ti = 30 and 15 (i.e. $x = 10$ & 15) Ti and Ta change places and at Ti = 15 the ion positions are occupied by FeTi and Ta. As the Ti decreases some of the Ta occupies the FeTi positions and a super-lattice begins to form until, at a certain value of Ti a tri-rutile structure obtains giving a repeat distance of $3r$. Whether the change from a bi-rutile to a tri-rutile structure does occur in nature can only be shown by studying low-titanium material, but the presence of a tapiolite super-lattice in the two bi-rutile patterns given indicates that it does.

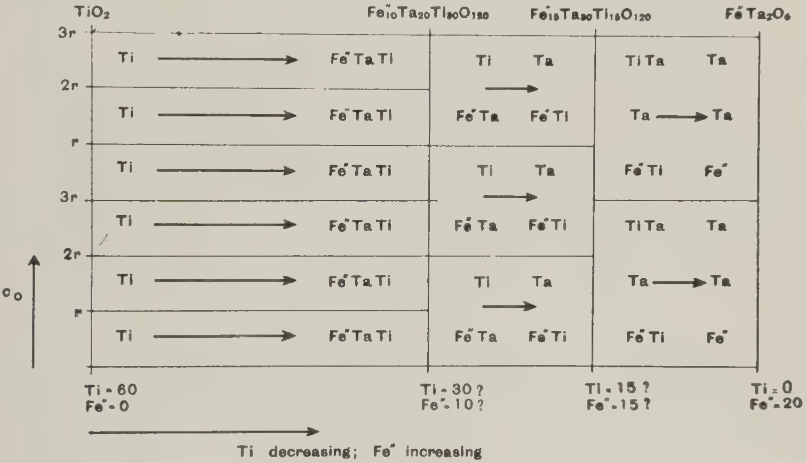

FIG. 3. Hypothetical structural changes.

CONCLUSION

Tantalian- and niobian-rutile (i.e. "struverite" and "ilmeno-rutile") have long been regarded as members of an isomorphous rutile-tapiolite series though proof of such a series is still lacking. The niobian-rutile from

Salak North is a mineral of variable composition, structurally and chemically intermediate between rutile and tapiolite and with intermediate optical and physical properties. It establishes the presence of an isomorphous series for the rutile end, the members varying from a Ta/Nb-free mineral with a rutile structure to a Ta/Nb-rich mineral possibly with a bi-rutile structure. Whether the series at the Ti-free end is complete is not known. There appears to be no valid reason for doubting its existence though it can be proved only by a continued search for its members.

ACKNOWLEDGMENTS

Grateful acknowledgment is made to the Director, Geological Survey, Federation of Malaya, for his encouragement and for permission to publish this paper; to W. A. Tooke, formerly Chief Chemist, Geological Survey of Malaya, for carrying out the chemical analyses; to my subordinates for their help in the preparation of the samples; and to the Department of Mines, Federation of Malaya for the use of their Vickers Projection microscope. My thanks are also due to Dr. C. O. Hutton of Stanford University for helpful comments and for reading the manuscript, but the author is entirely responsible for the ideas expressed herein.

REFERENCES

(1) CROOK, T., AND JOHNSTONE, S. J. (1912), On struverite from the Federated Malay States. *Mineralogical Mag.*, **XVI** No. 75, 224–231.

(2) PRIOR, G. T., AND ZAMBONINI, F. (1908), On struverite and its relation to ilmenorutile. *Mineralogical Mag.*, **XV** No. 68, pp. 78–89.

(3) DANA, System of Mineralogy 7th ed., Vol. 1, p. 557.

(4) DANA, System of Mineralogy 7th ed., Vol. 1, p. 558.

(5) SHORT, M. N., (1940), Microscopic determination of the ore minerals. *U. S. Geological Survey Bull.* **914**, 62.

Manuscript received September 9, 1958.

THE AMERICAN MINERALOGIST, VOL. 44, MAY-JUNE, 1959

NINGYOITE, A NEW URANOUS PHOSPHATE MINERAL FROM JAPAN*

Tadashi Muto,[1] Robert Meyrowitz,[2] Alfred M. Pommer,[2] and Toru Murano[1]

Abstract

Ningyoite, $U_{1-x}Ca_{1-x}R.E._{2x}(PO_4)_2 \cdot 1\text{–}2H_2O$, where x is about 0.1 to 0.2, is a new uranous mineral which occurs in an unoxidized zone of the Ningyo-toge mine, Tottori Prefecture, Japan. It coats pyrite and other minerals, or fills cavities and cracks in the ore. Ningyoite is acicular or elongated lozenge-shaped, and is very fine grained. The color is brownish green or brown in transmitted light, and faint pleochroism, darker in the Z direction, is observed. Extinction is parallel with positive elongation. The index of refraction varies and is about 1.64. Double refraction seems to be low. The x-ray pattern of the mineral resembles that of rhabdophane, $R.E.PO_4 \cdot H_2O$, but whereas rhabdophane has hexagonal symmetry, ningyoite is pseudohexagonal, orthorhombic, and the space group is probably $P222$ (D_2^1). The unit cell has dimensions $a=6.78\pm0.03$ Å, $b=12.10\pm0.05$ Å, and $c=6.38\pm0.03$ Å, and contains 3 formula weights.

A similar compound, $UCa(PO_4)_2 \cdot 1.5H_2O$, was synthesized from slurries composed of uranous phosphate and calcium phosphate in sealed glass tubes at 150° C., and 185° C. at pH 1.4 to 4.8. The synthetic compound was not obtained at 100° C. and 130° C., nor when the HCl concentration was greater than (1+10). The synthesized acicular crystals are green in transmitted light. Pleochroism is Z=green and X=pale green. Extinction is parallel, elongation positive. α is between 1.69 and 1.70, and γ is between 1.70 and 1.71, but they are variable. The x-ray powder diffraction patterns of the samples of the synthetic compound are almost the same as that of the natural ningyoite, except for slight differences in line spacings. The cell dimensions are $a=6.73\pm0.03$ Å, $b=12.13\pm0.05$ Å, and $c=6.36\pm0.03$ Å.

Upon heating at 800° to 900° C. in argon, both the natural mineral and the synthetic compound changed to a monazite-type structure which has a smaller cell size than that of natural monazite and is close to that of cheralite.

The properties of ningyoite and the synthetic mineral are compared and the effect of the presence of rare earths on the properties of the former are discussed.

The mineral was named for the locality.

Introduction

The uranium deposit in Ningyo Pass, Tottori Prefecture, Japan, was found in November 1955, by the carborne radiometric survey of the Geological Survey of Japan. Since the discovery, the area has been explored by the Atomic Fuel Corporation, Japan, and it is now the biggest uranium mine in Japan. Originally, only autunite was known as the ore mineral, but in March 1957, a more radioactive black ore was found in the unoxidized zone by members of the Atomic Fuel Corporation, Japan.

---

* Publication permitted by the President, Atomic Fuel Corporation, Japan. Publication authorized by the Director, U. S. Geological Survey.

[1] Atomic Fuel Corporation, Tokyo, Japan.

[2] U. S. Geological Survey, Washington 25, D. C.

After the discovery of this black ore, Tadashi Muto and Toru Murano were assigned to study the mineralogy of the black ore, and found that the uranium in the ore was not in known minerals. The nature of the new mineral, however, could not then be determined because of the extreme fineness of the crystals and the difficulty of obtaining a pure sample of this mineral.

In March 1958, Muto was sent to the U. S. Geological Survey where he and members of the U. S. Geological Survey resumed the study of this mineral after a purer sample was prepared. Subsequent *x*-ray, spectrographic, and microchemical analysis revealed the nature of the mineral. However, as a pure fraction of the mineral could not be separated, synthesis of the mineral was undertaken.

The new mineral, ningyoite, is named for the locality, Ningyo Pass.

Occurrence of Ningyoite

The geology of the Ningyo-toge mine was described by Katayama and Sato (1957), and Sato (1958). The Tertiary conglomerate where ningyoite occurs is called the Ningyo-toge formation, and overlies the eroded surface of Cretaceous granite. The pebbles are mainly granite and andesitic rocks. Ningyoite occurs in the unoxidized zone, usually as a thin coating on pyrite and apatite or filling cavities, especially in the matrices of the conglomerate or on the surface and along the cracks of the pebbles. Minerals associated with ningyoite are pyrite, marcasite, sphalerite, apatite, chlorite, gypsum, quartz, feldspar, hypersthene, biotite, rutile, calcite, kaolinite, montmorillonite, and traces of unidentified minerals. At least the first six minerals seem to have been brought in after the sedimentation along with ningyoite, which is apparently the last phase except for gypsum. A photomicrograph of a thin section of the ore is shown in Fig. 1.

Physical and Optical Properties of Ningyoite

The ore containing ningyoite is black or gray, and is very friable. Cavities are abundant. Because of its extreme fineness and contamination with other minerals the specific gravity and hardness of the mineral cannot be measured. It sinks in methylene iodide.

Ningyoite is acicular or elongated lozenge-shaped. The color is brownish green to brown, and slight pleochroism was observed, the color being paler in the X direction. Extinction is parallel, elongation positive. The crystals are so small (about 5μ) that the index of refraction cannot be measured exactly, but it is estimated to be about 1.64, and seems to vary a little from crystal to crystal. The double refraction seems to be low.

SEPARATION

Ningyoite is very difficult to separate because of its extremely small crystal size and intimate association with pyrite, clay minerals, and other contaminants. Radioactivity is higher in the finer-grained part than in the coarser-grained part of the ore. The ore was crushed in a ball mill for about one minute, and then passed through a 40-mesh sieve. The coarser part was discarded. The finer fraction was ground again in a ball mill for about 15 minutes, and the −100 mesh fraction was treated several times on a Wilfley table. The more radioactive black material was concentrated in the intermediate portion between pyrite and felsic minerals. The ultrasonic separator was used to remove clays from the black material. Flotation, centrifuging in methylene iodide, and magnetic separation were used repeatedly and alternately. Most of the pyrite was removed by flotation using the Mayeda cell. Quartz, calcite, and feldspar were removed by bromoform. Most of the apatite went to the nonmagnetic side of the Frantz isodynamic separator at the intensity 0.5 ampere. The final concentrate (sample no. C-1-M) seemed to be about 60 to 70 per cent ningyoite, and the remainder was found to be mostly hypersthene and organic material, but still contained very small amounts of pyrite, rutile, quartz, feldspar, and probably various phosphates of calcium, manganese, aluminum, and iron, including apatite.

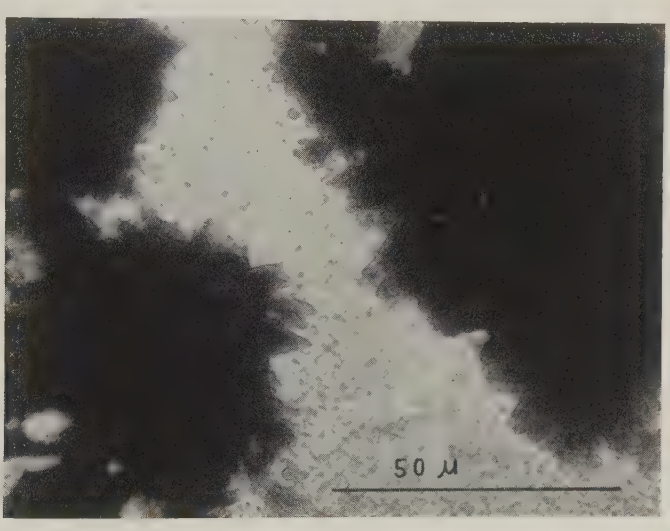

FIG. 1. Photomicrograph of a thin section of a ningyoite ore. Pyrite (black mass) is coated by ningyoite growing towards a cavity.

CHEMISTRY

As ningyoite could not be purified sufficiently, a preliminary leaching was made on a sample (sample no. N-2-W), a lower concentrate (about 30 per cent) of ore taken from another place in the mine. About 200 mg. of the sample, whose radioactivity was 1,574 counts per minute as measured by a Geiger-Müller counter, was treated with cold (1+1) HCl. After 10 minutes the green solution was filtered. The radioactivity of the residue was 96 counts per minute. By measuring the intensities of the characteristic *x*-ray diffraction lines of the contaminating minerals using an *x*-ray diffractometer, before and after the leaching, it was shown that most of these minerals were not dissolved although the ningyoite went into solution. The semiquantitative spectrographic analysis of the residue, after evaporation, of the (1+1) HCl soluble portion is shown in Table 1. It shows that the rare earths such as Y and Ce are present together with the major constituents Ca, U, and P of the dissolved fraction.

TABLE 1. SEMIQUANTITATIVE SPECTROGRAPHIC ANALYSIS OF A RESIDUE, AFTER EVAPORATION, OF THE (1+1) HCl SOLUBLE PORTION OF A CONCENTRATE OF NINGYOITE (SAMPLE NO. N-2-W)

Analyst: J. C. Hamilton, U. S. Geological Survey

Per cent[1]	Elements
>10	Ca U
7	P
3	Fe
1.5	Ce Y
0.7	La Nd
0.3	Ba Dy Er Gd Mo Pr Sr
0.15	Al Mn Pb Sc Si Sm Yb
0.07	Mg Zr
0.03	Cu
0.015	Be
0.003	Cr

[1] Figures are reported to the nearest number in the series 7, 3, 1.5, 0.7, 0.3, 0.15, etc., in per cent. These numbers represent midpoints of group data on a geometric scale.

Comparisons of this type of semiquantitative results with data obtained by quantitative method, either chemical or spectrographic, show that the assigned group includes the quantitative value about 60 per cent of the time.

The purest concentrate, C-1-M, was dried at 110° C. for about a week, in order to remove adsorbed water, before the infrared analysis The dried sample was inserted between two sodium chloride plates with a mineral oil. The curve is shown in Fig. 2. Peaks appearing at 3.4, 6.8, 7.2, and 13.8 μ are caused by the oil. Peaks at 3.0 and 6.1 μ represent water

(Hunt and others, 1950). A broad depression from 8 to 12 μ having a peak at 9.5 μ seems to indicate the presence of phosphate. There is no indication of the presence of the uranyl radical which should appear sharply at 10.6 μ (R. G. Milkey, U. S. Geological Survey, oral communication, 1958). This strongly suggests that ningyoite is a quadrivalent hydrous uranium mineral because all known sexivalent uranium minerals contain the uranyl radical.

Synthesis of Ningyoite

Various procedures for the synthesis were tried. The method by which a comparatively pure sample was obtained will be described in detail.

Fifty milliliters of a 0.5 M solution of UO_2Cl_2 was reduced in a Jones reductor to UCl_4 in the presence of excess HCl. Phosphoric acid (0.05 M) was added and the gelatinous precipitate was washed with water several times, $Ca(H_2PO_4)_2 \cdot H_2O$ (6.3 g) and water were added and mixed well. The resulting slurry was divided into three equal parts. To each of two parts were added 2.1 g. and 6.3 g. of $Ca(H_2PO_4)_2 \cdot H_2O$, none was added to the third. The resulting mixtures have U:Ca atomic ratios of 1:2, 1:4, and 1:1, respectively. Glucose (0.015 g.) was added to each part as an antioxidant. Approximately 10-ml. portions of slurry were sealed in 20-ml. glass tubes under nitrogen. Portions have the same U:Ca ratio were run in quadruplicate, two being heated at 150° C. and two at 185° C. After 18 days at 150° C. and 7 or 15 days for 185° C., the tubes were opened and the precipitates were filtered on a glass filter and washed with (1+5) HCl and then with water to remove excess calcium phosphate and uranium salts. This acid concentration was selected to minimize the solution of the synthetic compound and to remove the contaminants as completely as possible.

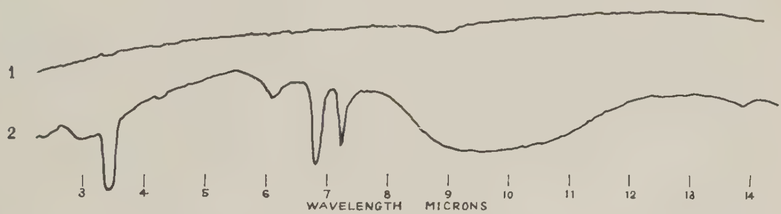

Fig. 2. Infrared analysis curve of ningyoite. 1. Blank. 2. Ningyoite with oil.

The pH of each solution before and after heating is shown in Table 2. The grayish-green precipitates were checked with an *x*-ray diffractometer for the major lines of ningyoite. These lines were almost identical with those for the natural ningyoite except for slight shifts of 2*θ*. Differences in temperature and pressure during synthesis did not seem to affect the x-ray patterns, but differences in composition of the original slurries did affect the positions and the intensity ratios of the peaks. The sample with U:Ca ratio of 1:2, formed at 150° C. (sample no. Cup-E2-150), appeared to be most similar to the natural material.

A similar procedure, in which a 1:1 U:Ca ratio was used with an initial pH of 4.8 and maintained at 100° or 130° C., failed to produce ningyoite. Under the same experimental conditions, the synthesis, however, was successful at 150° C. The precipitate formed at 100° C. was almost amorphous; that at 130° C. gave an x-ray diffraction pattern but not that of ningyoite. Ningyoite could not be synthesized using solutions containing 1:1 HCl. Under the same experimental conditions, uranyl phosphate with glucose at pH 1.4 resulted in the formation of ningyoite, but did not if the original slurry was dissolved in 1:10 HCl. In both runs, uraninite was also detected.

TABLE 2. EFFECT OF HEATING ON PH OF SLURRIES USED IN SYNTHESIS

Temperature (° C.)	Heating time (days)	pH[1]		
		U:Ca=1:1 (Cup-E1)	U:Ca=1:2 (Cup-E2)	U:Ca=1:4 (Cup-E3)
Unheated	0	1.6	1.8	2.1
185	7	1.5	1.5	1.7
185	15	1.3	1.3	1.4
150	18	1.2	1.2	1.3

[1] Measured at room temperature.

The synthesized compound is grayish green and extremely fine grained. Its specific gravity was not determined because of the extreme fineness of the material. Under the microscope, it is acicular crystalline, and green in color. Extinction is parallel, elongation positive. Pleochroism is recognized with Z = green, and X = pale green. The indices of refraction vary, but α seems to be between 1.69 and 1.70 and γ between 1.70 and 1.71. The x-ray pattern of the compound did not change after heating in air to 160° C., but the average index of refraction dropped to 1.66. This effect can be explained by the existence of zeolitic water as in rhabdophane (Mooney, 1950). The difference in the indices of refraction between natural and synthesized ningyoite seems to be caused by the presence of rare earths in the natural mineral, and probably also by the variation in the amount of zeolitic water.

Analytical Procedures

The selection of the methods used for the chemical analysis of the natural material and the synthetic compound was guided by the qualitative spectrographic analyses of the samples by K. V. Hazel and H. W. Worthing, U. S. Geological Survey. Micro- and semimicro chemical procedures were used for the various determinations. Approximately 50 mg. of the final concentrate of the natural material and 125 mg. of the synthetic compound was available for chemical analysis. Both samples were analyzed by essentially similar methods.

One portion of each sample was used for the total water and carbon determinations, another for the $H_2O(-)$, $(1+1)$ HNO_3 insoluble, total uranium, P_2O_5, CaO, and FeO determinations, and a third portion for the UO_2 determination.

The first portion, approximately 25 mg. for each sample, was dried to constant weight at 110° C. and then boiled with acid to determine the insoluble residue. An Emich microbeaker and sintered glass filter stick was used for the separation of the insoluble residue which was dried to constant weight at 110° C. The synthetic compound was boiled with $(1+1)$ HNO_3 and the residue was washed with dilute nitric acid and water before drying to constant weight. The insoluble residue in the synthetic material was found to be silica, which seems to come from glass filters used in the synthesis.

To minimize the solution of pyrite during the decomposition of the natural material for the subsequent determination of the major constituents of the mineral, the natural material was boiled with $(1+3)$ HCl instead of $(1+1)$ HCl as was done in the preliminary leaching experiment described above. The appearance of the insoluble material remaining after boiling with $(1+1)$ HCl did not seem to differ greatly from the appearance of the natural material before boiling. The solution was light yellow. To insure the solution of most of the ningyoite present, concentrated HNO_3 was added and the mixture boiled again. The boiling was continued until most of the black material was decomposed. The solution was now dark yellow and the residue contained some black dense material but the major part of the residue appeared to be fluffy and brown. The residue was mostly noncrystalline silica; hypersthene, quartz, and pyrite were present. The residue was washed with dilute nitric acid and water before drying to constant weight.

Aliquots of the filtrate from the acid insoluble determination were used for the total uranium, P_2O_5, FeO (total iron), and CaO determinations.

Total uranium was determined spectrophotometrically by the ammonium thiocyanate procedure in acetone-water medium. P_2O_5 was determined spectrophotometrically as molybdovanadophosphoric acid. A standard curve was made using known P_2O_5 solutions containing approximately the same concentration of uranium present in the aliquot of sample solution taken for the determination of P_2O_5. Total iron was determined spectrophotometrically by the o-phenanthroline procedure. CaO was determined by flame photometry (wavelength $= 554$ mμ). The solution was compared to standard calcium solutions containing approximately the same concentrations of uranium and phosphorus as present in the solution analyzed.

The UO_2 was determined volumetrically after solution of an 18-mg. portion of the synthetic compound in boiling $(1+3)$ H_2SO_4. The dissolved sample was titrated with approximately 0.03 N. standard $KMnO_4$; UO_3 was calculated by difference. Carbon and total water were determined by use of a modified microcombustion train of the type used for the determination of carbon and hydrogen in organic compounds; 30 mg. synthetic compound and 20 mg. of natural material were decomposed by ignition at 900° C. in a stream of oxygen.

ANALYTICAL RESULTS

Table 3 shows the results of spectrographic analysis of the purest concentrate of natural material, the acid soluble portion (approximately 70 per cent of original), and the acid insoluble portion. One-milligram samples were used. Table 4 shows the results of the microchemical analysis of the natural material and the synthetic compound. These results indicate that the chemical formula of the synthetic compound is $CaU(PO_4)_2 \cdot 1.5H_2O$.

From Table 3 it appears that all the phosphorus, yttrium, barium, boron, and ytterbium, and most of the calcium go into solution along with the uranium. As most of the rare earths shown in Table 1 were not detected in sample C-1-M by qualitative spectrographic analysis (Table 3) owing to the smallness of the sample and the limitations of the method (Stich, 1953), an *x*-ray fluorescence analysis was made by J. M. Axelrod, U. S. Geological Survey, on the acid soluble part of a specimen less concentrated than C-1-M. Minor amounts of Y, La, Ce, Nd, Er, Sr, Pb, Mn, and Cr, and possible minor amounts of Zn, Cu, and Gd were detected together with major amounts of U, Ca, and Fe. The total amount of rare earths seemed to be a few per cent.

It is impossible to get the exact chemical formula of ningyoite from the analysis shown in Table 4 because of the impurities. However, as discussed below, the *x*-ray data indicate a similarity of structure of ningyoite, the synthetic compound, and rhabdophane which has the ideal formula $R.E.(PO_4) \cdot H_2O$ (Palache and others, 1951). This suggests that

TABLE 3. QUALITATIVE SPECTROGRAPHIC ANALYSES (IN PER CENT) OF CONCENTRATE OF NINGYOITE
(SAMPLE NO. C-1-M)

Analyst: K. V. Hazel, U. S. Geological Survey

Substance	Elements														
	Si	P	U	Ca	Fe	Mg	Mn	Ti	Al	Na	Pb	Y	Ba	B	Yb
Original	>10	5–10	5–10	1–5	1–5	1–5	0.5–1.0	0.5–1.0	0.5–1.0	0.1–0.5	0.1–0.5	—	—	—	—
Acid soluble	0.1–0.5	>10	5–10	5–10	1–5	0.1–0.5	0.1–0.5	—	1–5	—	—	0.5–1.0	0.1–0.5	0.05–0.1	0.05–0.1
Acid insoluble	>10	—	—	0.1–0.5	1–5	0.5–1.0	0.1–0.5	0.5–1.0	0.1–0.5	—	0.05–0.1	—	—	—	

— indicates that the element was either absent or its concentration was below the limits of detection of the procedure (Stich, 1953, p. 7). Other elements were looked for but not found. Because purified material was scarce, these qualitative analyses were performed on 1-mg. samples mostly for detection of major constituents. The per cent values shown are rough estimates and cannot be compared with those in Table 1 which were derived from an extract of a 200-mg. sample.

TABLE 4. MICROCHEMICAL ANALYSES OF CONCENTRATE OF NINGYOITE (C-1-M) AND SYNTHESIZED COMPOUND (Cup-E2-150)

Analyst: Robert Meyrowitz, U. S. Geological Survey

Constituent	C-1-M	Molecular ratio	Cup-E2-150	Molecular ratio
CaO	6.1[1]	0.92	11.5	0.99
UO_2	23.3[1,2]	0.73	50.8	0.92
UO_3	N.D.[3]		0.7	
P_2O_5	16.8[1]	1.00	29.4	1.00
FeO	4.8[1,4]	0.56	N.D.[3]	
Rare earths	N.D.[3]		N.D.[3]	
Acid insoluble	30.9		1.0	
H_2O (total)	9.3	4.37	5.4	1.45
Total	91.2		98.8	
$H_2O(-)$	1.9		1.2	
C	2.3		0.1	

[1] Acid soluble.

[2] Total uranium as UO_2.

[3] Not determined.

[4] Total iron as FeO.

ningyoite has a formula close to $CaU(PO_4)_2\cdot 2H_2O$, in which the rare earths of rhabdophane are substituted for by equivalent amounts of calcium and quadrivalent uranium.

In interpreting the results in Table 4, excess calcium may come from the contaminating apatite and calcite. Iron seems to come mostly from pyrite and hypersthene and partly from the soluble phosphate minerals.

Although one cannot calculate the molecular ratio of the rare earths from the available spectrographic data, it may be estimated that the mineral contained a few per cent rare earths. This would be equivalent to a molecular ratio of a few tenths or less. Hence, excess phosphorus can be accounted for by rare earths, apatite, and possibly other soluble phosphate minerals. The high content of water seems to be derived from the organic material in which hydrogen has been oxidized to water.

There is no direct proof showing that uranium and calcium coexist with rare earths in the same mineral, but this seems reasonable, when we consider the deviations of the unit cell of the natural ningyoite and the synthetic compound from the hexagonal unit cell of rhabdophane. The comparison will be described later.

The chemical formula of ningyoite can be presented as

$$Ca_{1-x}U_{1-x}R.E._{2x}(PO_4)_2\cdot 1\text{–}2H_2O,$$

where x is about 0.1–0.2.

X-RAY POWDER DIFFRACTION PATTERNS

X-ray powder diffraction films were made on the final concentrate of ningyoite (C-1-M) and on the synthetic compound (Cup-E2-150). They resemble that of rhabdophane, a hexagonal hydrous rare earth phosphate (Hildebrand and others, 1957). Figure 3 shows films of rhabdophane (from Salisbury, Conn.), ningyoite, and the synthetic compound. The diffraction lines of the ningyoite and the synthetic compound are so broad that their crystallinity seems to be poor.

It was necessary to assume orthorhombic symmetry to index the patterns of ningyoite and the synthetic compound, though they are pseudohexagonal. The indices by the orthorhombic system for major lines were transformed from those by the hexagonal system to which rhabdophane belongs, and fairly good coincidence between the observed and the calculated *d* values were obtained as shown in Table 5. It is shown in the table that ningyoite and the synthetic mineral belong to a simple lattice as indicated by the existence of the lines such as 120, 011, etc., instead of a *C*-face centered lattice which would be that of rhabdophane, if it were regarded as of an orthorhombic system. The space group of ningyoite is presumed to be $P222$ (D_2^1), because this is the only orthorhombic space group consistent with that of rhabdophane, $P6_222$ (D_6^4). It is known that ningyoite has 3 molecules in the unit cell from the analogy with rhabdophane which has 3[R.E.$PO_4 \cdot H_2O$] in the unit cell of the hexagonal system (Mooney, 1950). The deviation from the hexagonal symmetry appears also in the ratio $a:b$ which is 0.577 in the

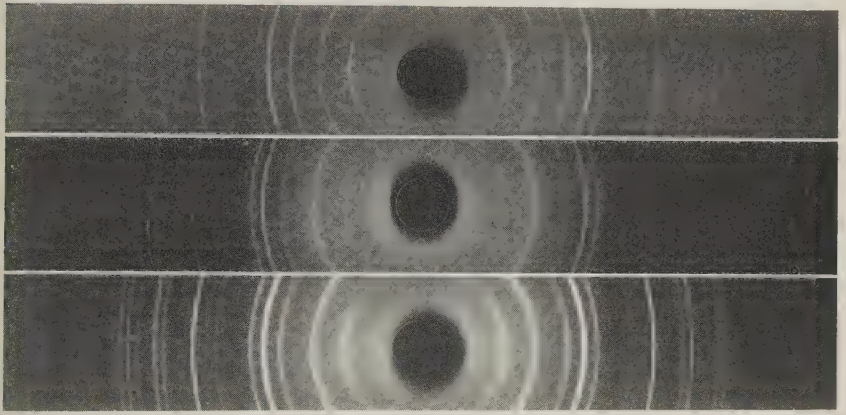

FIG. 3. X-ray powder diffraction patterns of rhabdophane, ningyoite, and synthetic compound. Camera diameter 114.6 mm., CuKα radiation. *Top:* Rhabdophane, Salisbury, Conn. *Middle:* Ningyoite (C-1-M). *Bottom:* Synthetic compound (Cup-E2-150).

TABLE 5. *X*-RAY POWDER DIFFRACTION DATA, IN Å, FOR RHABDOPHANE, NINGYOITE, AND THE SYNTHETIC COMPOUND

Rhabdophane (Salisbury, Conn.)				Ningyoite (C-1-M)				Synthetic compound (Cup-E2-150)		
d(obs.)[1]	I	*d*(calc.)	*hk.l*[2]	*hkl*[3]	*d*(obs.)[4]	I	*d*(calc.)	*d*(obs.)[4]	I	*d*(calc.)
				010	12	f	12.10	12	f	12.13
				100	6.8	f	6.78	6.8	f	6.73
				001	6.35	vw	6.38	6.33	f	6.36
6.07	m	6.05	10.0	020	5.99	wb	6.05	6.03	wb	6.07
				110			5.92			5.89
				011	5.65	vw	5.64	5.68	vw	5.64
				120	4.49	vw	4.51	4.48	vw	4.50
4.40	s	4.39	10.1	021			4.39			4.39
				111	4.33	m	4.34	4.30	s	4.32
				030	4.02	f	4.03	4.04	f	4.03
3.49	m	3.49	11.0	130	3.45	w	3.47	3.46	vw	3.47
				200	3.38	mb	3.39	3.36	mb	3.36
				002	3.19	f	3.19	3.18	f	3.18
		3.06	11.1	131			3.05			3.03
				201	3.02	vsb	3.00	3.02	vsb	2.97
3.02	vsb	3.02	20.0	040			3.02			3.03
				220			2.96			2.92
2.83	s	2.82	10.2	022			2.82			2.82
				112	2.81	s	2.81	2.80	s	2.80
		2.73	20.1	041	2.73	vw	2.73			2.74
				221	2.69	vw	2.69			2.63
2.36	w	2.36	11.2	132	2.35	w	2.35	2.35	vw	2.34
				202	2.33	f	2.32	2.30	f	2.31

Order of decreasing intensities: vs, s, m, w, vw, f; b = broad.

[1] Measured on *x*-ray powder diffraction film, camera diameter 114.6 mm. CuKα radiation, $\lambda = 1.5418$ Å; d(obs.) cut-off at 12 Å.

[2] Indices of the hexagonal system.

[3] Indices of the orthorhombic system.

[4] Measured with *x*-ray diffractometer, using CuKα radiation, $\lambda = 1.5418$ Å, 1°/min., time constant 4 sec., scale factor 2.

(*Continued on next page*)

TABLE 5 (*continued*)

Rhabdophane (Salisbury, Conn.)				Ningyoite (C-1-M)				Synthetic compound (Cup-E2-150)		
d(obs.)[1]	I	*d*(calc.)	*hk.l*[2]	*hkl*[3]	*d*(obs.)[4]	I	*d*(calc.)	*d*(obs.)[4]	I	*d*(calc.)
				150			2.28			2.28
2.28	vw	2.29	21.0	240	2.26	f	2.26	2.25	f	2.25
				310	2.22	f	2.22			2.20
				151			2.15			2.15
2.15	s	2.15	21.1	241	2.13	s	2.13	2.12	s	2.12
				311			2.10	2.08	f	2.08
		2.13	00.3	003			2.13			2.12
2.02	f	2.02	30.0	060	2.01	f	2.02	2.01	f	2.02
				330			1.973			1.961
1.920	w	1.923	30.1	061	1.926	f	1.923	1.926	f	1.926
				331	1.903	vw	1.885	1.899	vw	1.875
				152			1.853			1.844
1.859	m	1.859	21.2	242	1.845	wb	1.842	1.842	wb	1.838
				312			1.824			1.814
		1.741	20.3	043	1.740	w	1.739	1.740	vw	1.737
1.743	vwb			223	1.728	f	1.727	1.722	f	1.720
		1.746	22.0	260			1.733			1.733
				400	1.692	w	1.696	1.688	w	1.682
1.704	vw	1.705	30.2	062			1.704			1.706
				332	1.681	vw	1.678	1.669	f	1.669
				170			1.675			1.678
1.675	vw	1.678	31.0	350	1.653	vw	1.652	1.647	vw	1.646
				420	1.634	f	1.633			1.621
					1.547	vw		1.542	f	
					1.505	f		1.506	f	
					1.451	f		1.449	f	
					1.343	vw		1.346	vw	
					1.307	vw		1.304	vw	
					1.262	f		1.262	f	
					1.247	f		1.246	f	

ideal hexagonal system. Table 6 shows that the deviation of the ratio is greater in the synthetic mineral than in ningyoite.

Phase Changes on Heating

Both ningyoite and the synthetic compound were heated at various temperatures. Ningyoite ignited at 800° C. for 15 minutes and the synthetic compound ignited at 900° C. for 10 minutes (both in argon) changed to a monazite-type structure as indicated by their *x*-ray powder patterns. Table 7 shows their *x*-ray diffraction patterns together with those of natural monazite and the synthetic cheralite, $CaTh(PO_4)_2$, one of the monazite-type minerals (Bowie and Horne, 1953). Very weak lines of uraninite in the film of the ignited ningyoite and a few additional lines presumably of an unknown phase, are omitted in Table 7.

Table 6. Cell Dimensions of Rhabdophane, Ningyoite, and the Synthetic Compound

CuKα radiation, λ = 1.5418 Å

Rhabdophane (Salisbury, Conn.) $R.E.PO_4 \cdot H_2O$ (generalized formula) Hexagonal unit cell	Ningyoite (C-1-M) $Ca_{1-x}U_{1-x}R.E._{2x}(PO_4)_2 \cdot 1\text{–}2H_2O$ Orthorhombic unit cell	Synthetic compound (Cup-E2-150) $CaU(PO_4)_2 \cdot 1.5H_2O$ Orthorhombic unit cell
$a = 6.98 \pm 0.03$ Å	$a = 6.78 \pm 0.03$ Å	$a = 6.73 \pm 0.03$ Å
($b = 12.10 \pm 0.05$ Å)*	$b = 12.10 \pm 0.05$ Å	$b = 12.13 \pm 0.05$ Å
$c = 6.39 \pm 0.03$ Å	$c = 6.38 \pm 0.03$ Å	$c = 6.36 \pm 0.03$ Å
($a:b:c = 0.577:1:0.528$)*	$a:b:c = 0.560:1:0.527$	$a:b:c = 0.555:1:0.524$
V = 269.4 Å³, (539.7 Å³)*	V = 523.4 Å³	V = 519.2 Å³
		Sp. gr. (calc.) = 4.75

* The figures in parentheses show those of the orthorhombic lattice which were transformed from the hexagonal lattice.

The cell size of synthetic cheralite is most similar to that of the ignited ningyoite among the minerals having a monazite-type structure. The cheralite cell is slightly larger than the cell of the ignited ningyoite. This seems to be a result of the ionic radii of the elements involved, given in Table 8. The ionic radii of U^{+4}, Th^{+4}, Ca^{+2}, and rare earths are given in Table 8. The fairly good similarity of the *x*-ray patterns of the ignited ningyoite and synthetic compound may indicate that the average ionic radius of the rare earths contained in natural ningyoite approaches the average ionic radius of quadrivalent uranium and calcium, where as natural cheralite from Travancore, South India, has a larger cell size than that of the synthetic cheralite because natural cheralite has large

TABLE 7. *X*-RAY POWDER DIFFRACTION DATA, IN Å, OF MONAZITE, A SYNTHETIC CHERALITE, IGNITED NINGYOITE, AND IGNITED SYNTHETIC COMPOUND

CuKα radiation, $\lambda = 1.5418$ Å, camera diameter = 114.6 mm; *d*(obs.) cut-off at 12 Å

	Monazite[1] (from Magnet Cove, Ark.)		Synthetic cheralite[2] ($CaTh(PO_4)_2$)		Ignited ningyoite (C-1-M)		Ignited synthetic compound (Cup-E2-150)	
hkl	*d*(obs.)	I	*d*(obs.)	I[3]	*d*(obs.)	I[4]	*d*(obs.)	I[4]
$\bar{1}01$	5.20	13	5.18	vvw	5.18	f	5.16	vw
110	4.82	6	4.67	vw	4.75	f	4.75	vw
011	4.66	18			4.62	vwb	4.62	w
111	4.17	25	4.12	mw	4.15	m	4.13	m
101	4.08	9			4.02	f	4.04	w
$\bar{1}11$	3.51	25	3.47	w	3.45	vwb	3.47	wb
200	3.30	50	3.24	s	3.25	s	3.25	s
120	3.09	100	3.05	vs	3.04	vs	3.04	vs
210	2.99	18	2.94	vvw	2.93	fb	2.94	vw
$\bar{1}12$, 012	2.87	71	2.83	vs	2.82	vs	2.83	s
$\bar{2}02$	2.61	18	2.58	w	2.59	vw	2.58	w
211	2.44	18	2.41	w	2.41	w	2.42	m
$\bar{2}12$, 112	2.40	4			2.36	f	2.36	vw
	2.34	4			2.31	f	2.32	f
	2.25	2					2.22	f
	2.19	18	2.16	v	2.15	w	2.16	m
	2.15	25	2.11	mb	2.11	w	2.12	m
	2.13	25			2.08	w	2.08	m
	2.02	2					1.989	fb
	1.961	25	1.941	ms	1.933	s	1.929	s
	1.933	6					1.907	f
	1.895	13	1.872	vvw	1.870	f	1.870	w
	1.870	18	1.846	msb	1.841	wb	1.845	m
	1.859	18					1.834	m
	1.797	9	1.778	vw	1.774	f	1.774	vw
	1.762	18	1.740	vw	1.740	vw	1.743	w
	1.737	25	1.718	ms	1.710	w	1.713	m
	1.689	13	1.667	mw	1.658	vw	1.664	w
	1.645	6	1.629	vvw	1.603	f	1.608	vw
	1.600	6	1.583	vvw	1.578	f	1.580	vw
			1.556	vvw				
	1.535	13	1.517	mw	1.517	vw	1.519	w
	1.463	4					1.444	f
	1.386	3						
	1.368	4			1.347	f	1.347	fb
	1.339	9			1.323	f	1.323	vw
	1.329	9			1.313	vw	1.313	w
	1.307	2						
	1.280	6					1.268	f
	1.261	2			1.254	f	1.259	vw
	1.245	3					1.232	f
	1.233	9			1.217	f	1.216	vwb
	1.189	3					1.172	fb
	1.168	6					1.151	f
	1.153	3					1.133	f

---

[1] From Carron and others, 1958, p. 264–265.

[2] From Bowie and Horne, 1953, p. 97.

[3] Order of decreasing intensities: vs, s, ms, m, mw, w, vw, vvw; b = broad.

[4] Order of decreasing intensities: vs, s, m, w, vw, f; b = broad.

TABLE 8. IONIC RADII, IN Å, OF U^{+4}, Th^{+4}, Ca^{+2}, AND RARE EARTHS, INCLUDING AVERAGE IONIC RADII IN NINGYOITE AND CHERALITE

	Ahrens (1952, p. 168–169)	Gold-schmidt (1954, p. 89)		Ahrens (1952, p. 168–169)	Gold schmidt (1954, p. 89)
Elements			Er[2]	0.89	1.03
U	0.97	1.05	Tm[2]	0.87	1.01
Th	1.02	1.10	Yb[2]	0.86	1.00
Ca	0.99	1.06	Lu[2]	0.85	0.99
La[1]	1.14	1.22			
Ce[1]	1.07	1.18	Minerals		
Pr[1]	1.06	1.16	Ningyoite		
Nd[1]	1.04	1.15	$\left(\frac{U+Ca}{2}\right)$[1]	0.98[3]	1.06[4]
Sm[1]	1.00	1.13			
Eu[1]	0.98	1.12			
Gd[1]	0.97	1.11	Cheralite		
Tb	0.93	1.09	$\left(\frac{Th+Ca}{2}\right)$[1]	1.01[3]	1.08[4]
Dy[2]	0.92	1.07			
Ho[2]	0.91	1.05			

[1] Forms the monazite structure on heating (Carron and others, 1958).

[2] Forms the xenotime structure on heating (Carron and others, 1958).

[3] $>Tb=0.93$ (Ahrens, 1952). Should form monazite structure. Agrees with experiment.

[4] $<Tb=1.09$ (Goldschmidt, 1954). Should form xenotime structure. Does not agree with experiment.

amounts of rare earths such as lanthanum and cerium, which have comparatively larger ionic radii.

The similarity between rhabdophane and ningyoite is demonstrated in the fact that rhabdophane (from Salisbury, Conn.) was converted to monazite by sealing the mineral in a silver crucible containing water and heating at 300° C. for 5 days (Carron and others, 1958, p. 273). Carron and others (1958, pp. 263–269) have also shown that the rare earths having ionic radii larger than that of terbium form the monazite structure when they react with phosphate in a sealed glass ampoule or silver crucible, and those having ionic radii smaller than that of terbium form the xenotime structure. This principle is applicable for cheralite and the ignited ningyoite when Ahrens' data (1952) are taken, but is not if Goldschmidt's data (1954) are taken, as shown in Table 8.

Ningyoite ignited at 950° C. for 15 minutes in argon gave the *x*-ray patterns of uraninite and a small amount of monazite. The uraninite pattern of the ignited ningyoite seems to indicate the decomposition of the phosphate. There is no line of uraninite in the ignited synthetic ningyoite at 900° C., indicating that the rare earths in natural ningyoite possibly lowered the temperature of the decomposition of the monazite-type structure.

The synthetic ningyoite ignited at 600° C. in air for 5–10 minutes still retained the original orthorhombic structure without measurable change of the cell size. Both the ningyoite and the synthetic compound when ignited at 900° C. in oxygen changed in color and gave unidentified x-ray patterns which are different from each other. They seem to have been oxidized.

Comparison with Lermontovite

Ningyoite resembles lermontovite, $(U,Ca,R.E.)_3(PO_4)_4\cdot 6H_2O$, (Soboleva and Pudovkina, 1956, pp. 181–182) in color, chemical components, and some optical properties, but differs in the ratio of the elements and birefringence. Lermontovite has a U:Ca ratio of 10:1, whereas ningyoite has 1:1. The ratio of cations to phosphorus is 3:4 in the former and 1:1 in the latter. The birefringence of lermontovite is described as 0.14–0.15 and is much greater than that of natural ningyoite. No x-ray data are available for lermontovite.

Acknowledgments

Most of this work was done while Tadashi Muto was a participant in the training program with the U. S. Geological Survey under the auspices of the Division of Raw Materials of the U. S. Atomic Energy Commission. The authors are indebted to a number of people in the U. S. Geological Survey. Sincere thanks are given especially to D. R. Ross for preparing x-ray films, K. V. Hazel, H. W. Worthing, and J. C. Hamilton for the spectrographic analyses, R. G. Milkey for the infrared analysis, J. C. Chandler for his help in the synthesis work, J. M. Axelrod for x-ray fluorescence analysis, A. D. Weeks and Z. S. Altschuler for their advice throughout this study, and M. K. Carron for the information and the discussion on the phosphates of rare earths. We are also indebted to N. Morimoto, Geophysical Laboratory of the Carnegie Institution of Washington, for his advice on the x-ray investigation.

The early work of the study was done in the Mining Research Institute of the Mitsubishi Metal Mining Company, Japan. The authors wish to express their sincere thanks to T. Kawamura and his associates who offered their facilities and aid.

References

Ahrens, L. H. (1952), The use of ionization potentials. Part 1, Ionic radii of the elements: *Geochim. et Cosmochim. Acta*, **2**, 168–169.

Bowie, S. H. U. and Horne, J. E. T. (1953), Cheralite, a new mineral of monazite group: *Mineralog. Mag.*, **30,** 97.

Carron, M. K., Naeser, C. R., Rose, H. J., Jr., and Hildebrand, F. A. (1958), Fractional precipitation of rare earths with phosphoric acid: *U. S. Geol. Survey Bull.* **1036-N,** 253–275.

Goldschmidt, V. M. (1954), Geochemistry: London, Oxford Univ. Press.

Hildebrand, F. A., Carron, M. K., and Rose, H. J. (1957), Re-examination of rhabdophane (scovillite) from Salisbury, Connecticut (abs.): *Geol. Soc. America Bull.*, **68,** 1744.

Hunt, J. M., Wisherd, M. P., and Bonham, L. C. (1950), Infrared absorption spectra of minerals and other inorganic compounds: *Anal. Chem.*, **22,** 1487.

Katayama, N., and Sato, Y. (1957), Sedimentary environment of the uraniferous bed of the Ningyo Pass: *Sci. Papers College of General Education, Univ. Tokyo*, **7,** 131–144.

Mooney, R. C. L. (1950), *X*-ray diffraction study of cerous phosphate and related crystals. I. Hexagonal modification: *Acta Cryst.*, **3,** 337–340.

Palache, C., Berman, H., and Frondel, C. (1951), Dana's system of mineralogy, 7th ed., v. 2: New York, John Wiley and Sons, Inc., 774.

Sato, Motoo (1958), On the results of prospecting for the promising uranium deposits of Japan: Presented at the Second International Conference on Peaceful Uses of Atomic Energy, Geneva, Switzerland, September 1–13, 1958.

Soboleva, M. V., and Pudovkina, I. A. (1956), Mineraly Urana, Spravochnik (Uranium Minerals Handbook), Moscow, from *Am. Mineral.*, **43,** 379 (1958).

Stich, J. N. (1953), Spectrographic identification of mineral grains: *U. S. Geol. Survey Circ.* **234.**

Manuscript received September 22, 1958.

THE AMERICAN MINERALOGIST, VOL. 44, MAY–JUNE, 1959

NOTES AND NEWS

CHROMIAN ANTIGORITE FROM THE WOOD'S MINE, LANCASTER COUNTY, PENNSYLVANIA*

Jewell J. Glass, Angelina C. Vlisidis, and Nancy C. Pearre,
U. S. Geological Survey, Washington 25, D. C.

Introduction

The Wood's chromite mine in Little Britain Township, Lancaster County, Pennsylvania, is 2 miles southeast of Wrightsdale, and about 0.6 of a mile north of the Pennsylvania-Maryland State Line, within a large bend of Octoraro Creek. It is the largest of many mines in the State Line chromite district, and was in operation continually from about 1828 until 1868 and again between 1873 and 1880, producing more than 95,000 tons of high-grade ore. The Wood's deposit was the largest body of massive chromite ever found in North America, and before the Civil War it was the largest source of chromite in the world.

During active years the mine was also world-famous for its fine specimens of comparatively rare minerals, particularly of brucite, genthite, the chlorite kämmererite, and the antigorite variety williamsite. Although much of the dump material has been removed and the large dumps that remain have been combed frequently by mineral collectors, samples of most of the minerals for which the mine was justly famous can still be found. A lavender-colored mineral, collected in 1955 by Nancy C. Pearre and Allen V. Heyl from the dump south of the larger mine opening, is a hitherto undescribed chromian variety of antigorite.

General Geology

The Wood's deposit is in a belt of serpentinized ultramafic rocks about 30 miles long and averaging half a mile to a mile in width. The rocks trend eastward and northeastward parallel to the surrounding schists which they intrude. The Wood's mine is near the northern contact of the serpentine and schist; in the vicinity of the mine this contact dips steeply southward. The chromite occurs in irregular sack form (Sampson, 1942, pp. 124–125) and is commonly sheathed by a light yellowish-green serpentine, in some places associated with crosscutting veins of coarsely crystalline magnesite. The country rock near the mine is dark, massive serpentinized dunite that consists essentially of olivine and green antigorite with accessory chromite and magnetite (T. P. Thayer, 1956, oral communication); it characteristically weathers brown.

Numerous minerals, some of them rare, have been reported from the

---

* Publication authorized by the Director, U. S. Geological Survey.

Wood's mine (Genth, 1875; Gordon, 1922; Beck, 1952). One of the commonest of these is the pink-to-lavender chrome chlorite, kämmererite, characteristically a close associate of the high-grade chromite deposits in the area. Foliated masses and large white crystals of brucite, and apple-green to yellowish-green incrustations of the nickel mineral genthite, were common associates with the ore. Other minerals from the mine include emerald green zaratite and the chlorite penninite, white to brown deweylite, acicular crystals of hydromagnesite, and veins of chalklike magnesite; also ripidolite, enstatite, aragonite, calcite, dolomite, chalcedony, drusy quartz, and jasper. Chalcocite, millerite, hematite, ilmenite, idocrase, and uvarovite or green chromian grossularite have been found very rarely associated with the chromite.

Several varieties of serpentine are common on the mine dumps. These include the varieties williamsite, picrolite, and marmolite, and green antigorite. The lavender chromian antigorite here described bears a superficial resemblance, especially in color, to the more platy kämmererite, one of the minerals for which the mine was famous, and has probably been passed over by mineral collectors for that reason. Garrett (1853) mentions "fibrous kämmererite" at the Wood's and Line mines.

Purification of Chromian Antigorite

Material was carefully prepared for the various studies in the following manner. A 120-gram sample of the chromian antigorite was crushed gently on a steel plate with a hand roller in order to break away the interstitial dolomite grains. The finer fraction (−100) was screened off. The light-weight mineral, chromian antigorite, could not be removed satisfactorily by flotation with bromoform (specific gravity 2.8) because the contaminating mineral, dolomite, has approximately the same specific gravity as bromoform. Therefore, the fragments of chromian antigorite were selectively hand picked and ground to a powder from which the remaining magnetite grains were removed with a hand magnet, and then finally with a magnetized needle. Microscopic examination of the sample thus prepared showed no visible magnetite, but approximately one half of one per cent of dolomite was observed as impurity.

Physical and Optical Properties

Chromian antigorite from the Wood's mine occurs as an aggregate of lavender-colored, long, thin laths, some of which are more than two inches long. The slender laths are easily separated from one another. The laths are striated parallel to the elongation and are easily split into brittle columnar or needlelike rods. Cleavage is perfect in two directions parallel to the elongation of the crystals, but poor, frequently splintery, transverse to the elongation. The structure is somewhat similar to that of the variety "picrolite." The hardness is slightly greater than 4. The luster is waxy. Thin fragments are translucent to transparent. Small fragments fuse with difficulty to white opaque beads. This chromian antigorite is not noticeably attacked by either cold or warm hydrochloric or dilute sulfuric acid.

The mineral is optically biaxial negative; the axial angle is $58° \pm 3°$ and is constant in all grains observed. Dispersion of the axes is moderately strong, $v > r$; the abnormal interference color is blue. The axial plane is parallel to the elongation {100}, and the acute bisectrix X is normal to the best cleavage {010}, assuming the mineral is orthorhombic. Extinction is parallel. The pleochroism is very weak; X and Y are pinkish lavender and Z is purplish lavender. The indices of refraction measured by the immersion method in white light are: $\alpha = 1.567$, $\beta = 1.577$, $\gamma = 1.578$, $B = 0.011$. The indices and birefringence are somewhat higher than for antigorites described by Selfridge (1936), but some serpentines have even greater birefringence. The higher indices of refraction may be attributed to the presence of chromium.

The chromian antigorite sample was prepared for examination with the electron microscope by grinding lightly in distilled water, placing a droplet of the dispersed material on a collodion mount, and then drying in air. The electron micrograph (Fig. 1) shows thin angular plates and laths. The sample appears to be homogeneous. The electron microscope studies were made by Malcolm Ross, U. S. Geological Survey, who is making further studies of the mineral.

X-ray powder-diffraction studies by Fred A. Hildebrand, U. S. Geological Survey, show this lavender-colored mineral to be isostructural with antigorite.

CHEMICAL STUDIES

The chief constituents of the sample were determined by means of usual gravimetric procedures for silicate rocks. The presence of nickel made a triple precipitation of the R_2O_3 group necessary. Nickel was then determined by the dimethylglyoxime method on the combined filtrates. In the determination of chromium the sample was fused with sodium carbonate-potassium nitrate, leached with water, and filtered, and the chromium determined by a colorimetric method on the filtrate. The total water was determined by the Penfield method using anhydrous sodium tungstate (Na_2WO_4) as a flux. The analysis is given in Table 1.

Calculated on the basis of the structural formula the analysis yields:

$$[Mg_{5.32}Cr_{.33}\overset{+3}{Fe}_{.04}\overset{+2}{Fe}_{.04}Ni_{.03}Al_{.24}][Si_{3.40}Al_{.60}]O_{10}(OH)_8.$$

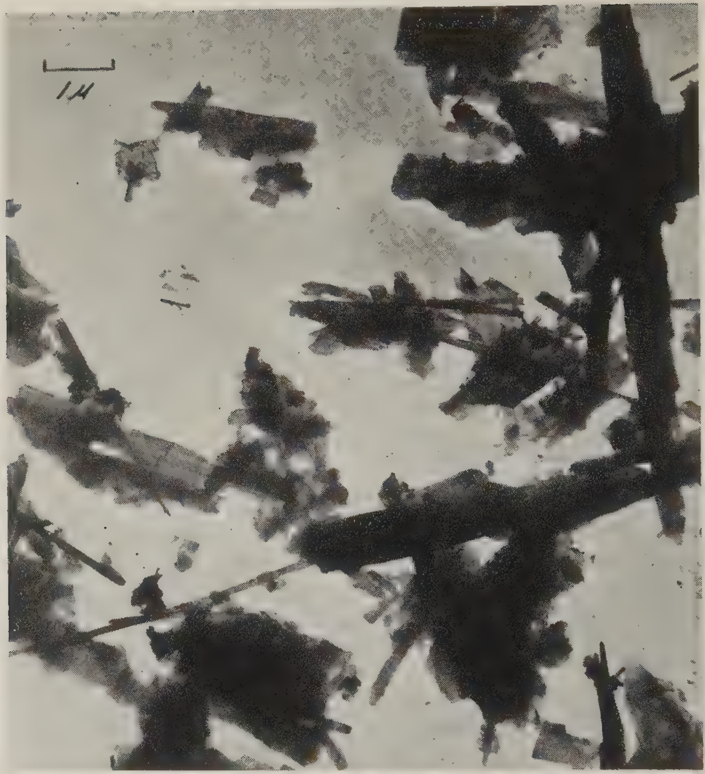

FIG. 1. Electron photomicrograph showing lath-like structure of chromian antigorite from the Wood's mine, Lancaster County, Pennsylvania.

The chemical analysis shows a higher percentage (7 per cent) of Al_2O_3 than for most antigorites; however, Bates and Mink (1950) gave a compilation of analyses in their discussion of the morphology and structure of the serpentine minerals in which some of the antigorites are shown to contain a notable amount of Al_2O_3. On the other hand, recent analyses of some antigorites by Hess and others (1952), Brindley and von Knorring (1954), and Nagy and Faust (1956) show low Al_2O_3 content

The authors have assumed that some of the magnesium in the mineral described above has been replaced by aluminum and chromium. Although the analysis agrees with some of the kämmererites, the morphology, physical properties, x-ray pattern, and the optical properties correspond closely to antigorite.

X-ray fluorescence determinations by J. M. Axelrod, U. S. Geological Survey, show 4.3 per cent Cr_2O_3.

TABLE 1. CHEMICAL ANALYSIS OF CHROMIAN ANTIGORITE

(Analyst: A. C. Vlisidis)

	Per Cent	Corrected[1]	Molecular ratios
SiO_2	36.00	36.00	0.5991
Al_2O_3	7.51	7.51	.0737
Fe_2O_3	.56	.56	.0035
FeO	.45	.45	.0063
MgO	37.87	37.75[2]	.9392
CaO[3]	.16	.00	
H_2O^- [4]	.24	.24	
H_2O^+	13.16	13.16	.7311
TiO_2	.05	.05	.0006
Cr_2O_3	4.36	4.36	.0287
NiO	.35	.35	.0047
MnO	.01	.01	.0001
CO_2 [5]	.26	.00	
	100.98	100.44	
Sp. gr.	2.62		

[1] Analysis corrected for 0.54 per cent dolomite based on 0.16 per cent CaO.

[2] Corrected for 0.12 per cent MgO present as dolomite.

[3] Not included in formula because it is present as dolomite, an impurity.

[4] Not water of composition.

[5] CO_2 calculated.

Semiquantitative spectrographic analysis by Harry Bastron, U. S. Geological Survey, gave the following results:

Mg	Si	Al	Cr	Fe	Ca	Ni	Ti	V	Mn	Cu	B	Sc
M	M	X.$^+$	X.	X.$^-$	.X	.X	.OX	.OX	.OOX$^+$	.OOX	.OOX$^-$	.OOOX

Looked for but not found: Ag, Au, Hg, Ru, Rh, Pd, Ir, Pt, Mo, W, Re, Ge, Sn, Pb, As, Sb, Bi, Zn, Cd, Tl, In, Co, Ga, Ce, Y, Yb, La, Zr, Hf, Th, Nb, Ta, U, Be, Sr, Ba, K, P.

The minor-element content of this antigorite is consistent with the theory of Faust, Murata, and Fahey (1956), as to the relation of minor elements of the serpentines to their geologic origin, in that this serpentine derived from ultrabasic rock contains Ni, Cr, Sc, and probably a trace of Co in a concentration below the limit of detectability by this method.

ACKNOWLEDGMENT

Grateful acknowledgment is made to George T. Faust of the U. S. Geological Survey for his helpful suggestions.

References

Bates, T. F., and Mink, J. S., 1950, Morphology and structure of serpentine minerals: *Pennsylvania State College School of Mineral Industries, Tech. Rept.*, no. **3**, State College, Pa.

Beck, H. H., 1952, The minerals of Lancaster County, [Pa.], 3d ed.: Lancaster, Pa., Science Press, 13 p.

Brindley, G. W., and von Knorring, O., 1954, A new variety of antigorite (orthoantigorite) from Unst, Shetland Islands: *Am. Mineral.*, **39**, 794–804.

Faust, G. T., Murata, K. J., and Fahey, J. J., 1956, Relation of minor-element content of serpentines to their geological origin: *Geochim. et Cosmochim. Acta*, **10**, 316–320.

Garrett, T. N., 1853, On minerals accompanying chromic iron: *Am. Jour. Sci.*, 2d ser., **15**, 332–334.

Genth, F. A., 1875, Preliminary report on the mineralogy of Pennsylvania: *Pennsylvania Second Geological Survey, Rept.* **B** (1874).

Gordon, S. G., 1922, The mineralogy of Pennsylvania: *Acad. Nat. Sci. Philadelphia, Special Pub.* No. **1**, 255 p.

Hess, H. H., Smith, R. J., and Dengo, G., 1952, Antigorite from the vicinity of Caracas, Venezuela: *Am. Mineral.*, **37**, 68–75.

Nagy, B., and Faust, G. T., 1956, Serpentines: Natural mixtures of chrysotile and antigorite: *Am. Mineral.*, **41**, 817–837.

Sampson, Edward, 1942, Chromite deposits, *in* Newhouse, W. H., ed., Ore deposits as related to structural features: Princeton, N. J., Princeton Univ. Press, p. 124–125.

Selfridge, G. C., Jr., 1936, An *x*-ray and optical investigation of the serpentine minerals: *Am. Mineral.*, **21**, 463–503.

THE AMERICAN MINERALOGIST, VOL. 44, MAY-JUNE, 1959

MAGMATIC DIFFERENTIATION AT AMBOY CRATER, CALIFORNIA

Ronald B. Parker, *University of California, Berkeley, California.*

Amboy Crater, a recent group of nested cinder cones near Highway 66, approximately 75 miles east of Barstow, San Bernardino County, affords an excellent example of magmatic differentiation of basaltic magma. The general geology of the area will be described elsewhere (Parker, Calif. Div. Mines, to be published). The suite of rocks selected for this discussion are from the cones themselves. The surrounding flows are not suitable for such a study due to the uncertainty of their relative ages. The absolute age of none of these rocks is known, but the relative ages of those from the cones can be judged with a high degree of certainty. All of the samples are from nested cones built around a single, central conduit with the exception of No. 4 which comes from a short intracrater-flow which breached the older cones from which specimens Nos. 1, 2, and 3 were collected.

All of the specimens are olivine basalts. In general they are composed of a groundmass of glass, plagioclase, clinopyroxene, and magnetite with phenocrysts of olivine and plagioclase. Plagioclase phenocrysts are not present in all specimens, hence were not studied for comparative purposes. Pyroxenes could not be determined due to small grain size. Olivine was determined from optic angle measurements and the curve of Tröger (1956, p. 37). Plagioclase microlites were determined by the method of Emmons and Gates (1948, p. 617). Artificial glasses were prepared from powdered samples by the method of Mathews (1951). Chemical factors after the convention of Niggli (1954, pp. 12–14) were calculated from chemical analyses of three of the specimens, Table 1. All of the above data are combined in Fig. 1.

Several features are of interest. The younger the basalt the higher is the

Table 1. Chemical Analyses

	1		3		6	
	Wt. %	Mol. %	Wt. %	Mol. %	Wt. %	Mol. %
SiO_2	45.91	51.43	48.04	53.00	46.80	56.00
Al_2O_3	16.14	10.65	17.13	11.17	16.82	11.85
FeO	5.89	5.46	5.96	5.46	4.28	4.29
Fe_2O_3	4.88	2.04	4.24	1.77	5.67	2.59
TiO_2	2.32	1.97	2.33	1.97	2.32	2.04
MnO	0.20	0.20	0.19	0.20	0.17	0.20
CaO	9.14	9.07	8.34	9.33	9.73	8.17
MgO	8.68	14.52	7.48	12.35	5.54	9.94
K_2O	1.72	1.25	1.72	1.18	1.53	1.16
Na_2O	2.96	3.15	3.27	3.48	3.18	3.68
H_2O-	0.38	—	0.30	—	0.49	—
H_2O+	0.64	—	0.54	—	1.37	—
CO_2	0.95	—	0.27	—	2.03	—
P_2O_5	0.36	0.20	0.26	0.13	0.15	0.07
	100.17	99.94	100.07	100.04	100.08	99.97
al	22.0		23.9		26.2	
fm	49.9		46.0		45.0	
c	18.9		20.1		18.1	
alk	9.1		10.0		10.6	
si	107.5		114.0		124.0	
k	.28		.25		.24	
mg	.60		.57		.51	
Qz	−28.9		−26.0		−18.4	

Analyst: W. H. Herdsman.

Mole per cent values were recast eliminating water and carbon dioxide plus lime to make calcite with the carbon dioxide present. Values for CaO and *c* are of low reliability as a result of these adjustments, and the fact that the hydrous minerals in these rocks are of unknown nature.

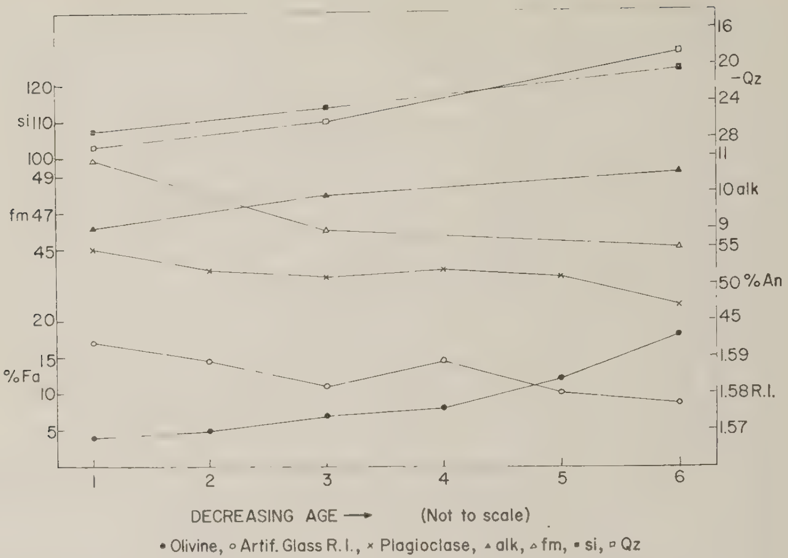

FIG. 1. Comparison of composition and refractive indices with age.

fayalite content of its olivine. While variations in the plagioclase microlites and refractive index of artificial glasses are slight compared to inherent errors in determinative methods, it is significant that the curves have the same form. The mineralogical and chemical changes observed in this sequence are precisely what would be predicted on experimental grounds in the case of a magma being "sampled" at intervals during a differentiation course of crystallization. In brief, the liquids are successively enriched in silica and alkalies, and impoverished in magnesia and alumina. Total iron diminishes slightly with decreasing age. The mechanism of differentiation must remain speculative, but perhaps removal of plagioclase and olivine by crystal settling was the major factor. Similar changes in composition of effusive material from Parícutin were observed in the early history of the volcano's eruptions (Wilcox, 1954, pp. 316–317).

REFERENCES

EMMONS, R. C., AND GATES, R. M. (1948), The use of Becke line colors in refractive index determinations: *Am. Mineral.*, **79**, 612–617.

MATHEWS, W. H. (1951), A useful method for determining approximate composition of fine-grained igneous rocks: *Am. Mineral.*, **36**, 92–101.

NIGGLI, PAUL, Rocks and Mineral Deposits: San Francisco; W. N. Freeman and Co., R. L. Parker translation from the German, 1954.

TRÖGER, W. E., Optische Bestimmung der gesteinbildenden Minerale, Teil 1, Bestimmungstabellen; Stuttgart, E. Schweizerbart'sche verlagsbuchhandlung, 1956.

WILCOX, R. E. (1954), Petrology of Parícutin Volcano, Mexico: *U. S. Geol. Survey Bull.*, **956-C.**

THE AMERICAN MINERALOGIST, VOL. 44, MAY–JUNE, 1959

THE OLIVINE-SPINEL INVERSION IN FAYALITE[1]

A. E. RINGWOOD,[2] *Dunbar Laboratory, Harvard University, Cambridge, Massachussetts.*

The author has previously described the synthesis under high pressure of a spinel polymorph of fayalite (Ringwood, 1958*a*, *b*). The early work on the transition was essentially of an exploratory nature. It revealed that fayalite was stable at pressures below 30,000 bars in the temperature range 400–600° C., while the spinel was stable above 40,000 bars in the same temperature range. Within the pressure range 30,000–40,000 bars, conflicting results were obtained. These may have been caused by metastability or by insufficient experimental accuracy. In an attempt to resolve the conflict, further runs have been carried out. The position of the transition has been approximately located at 600° C. and 500° C., but the accuracy is not sufficient to provide a reliable slope (dp/dt). It is clear that many additional runs would be required in order to find the slope. Since the author has now ceased working on this problem, it seemed advisable to record the results of runs carried out (Table 1).

Charges were prepared by weighing out ferric oxide, metallic iron powder, and Mallinckrodt silicic acid in the proportions required to give the fayalite composition plus a 10–20% excess of iron. These components were then intimately mixed together by grinding under acetone. The purpose of the excess iron was to maintain oxidized iron in the divalent state. The charges were subjected to the desired temperature and pressure in a "squeezer" apparatus (Griggs and Kennedy, 1956) which was frequently calibrated for temperature and checked for piston distortion.

After completion of a run, temperature and pressure were swiftly lowered. The transition is sluggish and no difficulty was experienced in quenching the high pressure form to atmospheric pressure. Products were examined by *x*-ray and optical methods. Identification of the spinel form of fayalite was based upon its optical properties and powder pattern, which have been previously described (Ringwood, 1958*b*).

Appearance of the charges under the microscope varied from opaque, indefinite aggregates to completely crystallized, colorless to green masses of fayalite or spinel crystals. The powder patterns showed that the opacity and darkness of samples was due principally to the presence

---

[1] Paper No. 173, published under the auspices of the Committee on Experimental Geology and Geophysics and the Division of Geological Sciences at Harvard University.

[2] Present address: Department of Geophysics, Australian National University, Canberra, A.C.T., Australia.

TABLE 1. SUMMARY OF EXPERIMENTAL RESULTS

No.	Temperature ° C.	Pressure (bars)	Time of run (hours)	Phases present (*a*) (*b*)	Notes
F3	500	20,000	7	magnetite (fayalite?)	
F6	500	20,000	24	fayalite, magnetite	(*c*)
F11	500	20,000	14	fayalite, (magnetite)	
F14	500	25,000		fayalite, (magnetite)	
F2	500	30,000	16	magnetite, spinel	(*e*)
F5	500	30,000	24	spinel, magnetite	(*c*)
F15	500	30,000		fayalite, magnetite	
F16	500	35,000	12	fayalite	
F1	500	40,000	8	spinel, ((magnetite))	
F4	500	40,000	24	spinel, (magnetite)	
F13	600	25,000	3	fayalite, magnetite	
F8	600	30,000	3	fayalite	
F9	600	35,000	3	fayalite	
F10	600	40,000	3	spinel, ((fayalite))	
F12	600	45,000	3	spinel, (magnetite)	
F7	600	45,000	4	spinel	(*c*)
F17	600	70,000	1	spinel, ((fayalite))	(*d*)

(*a*) In all runs, some unreacted iron remained in the product. This has not been recorded in the above table.

(*b*) Phases are recorded in order of abundance. Single brackets denote rarity, double brackets denote extreme rarity.

(*c*) In these runs, thermocouple behaved irregularly, preceding a corrosion break. Temperature could have been as much as 20° *higher* than that recorded.

(*d*) Starting charge was moistened Rockport fayalite.

(*e*) "Spinel" refers to the spinel polymorph of fayalite.

of magnetite. It was noticed that little or no magnetite was present when the charges had been prepared shortly before using. However if charges had been mixed more than one day, before being run, appreciable quantities of magnetite were likely to be found in the product. This may be due to oxidation of metallic iron in the charge by water from the silicic acid.

From Table 1 it is seen that the position of the transition at 600° C. is close to 38,000 bars. At 500° C. there appears to be a region of indifference where equilibrium is not always attained, with the transition probably between 30,000 and 35,000 bars.

A sample of moistened Rockport fayalite was run at 600° C. and 70,000 bars for one hour. Almost complete conversion to spinel was obtained.

REFERENCES

GRIGGS, D. T., AND KENNEDY, G. C. (1956), *Am. J. Sci.* **254,** 722.
RINGWOOD, A. E. (1958*a*), *Bull. Geol. Soc. Am.* **69,** 129.
——— (1958*b*), *Geochim. et cosmochim. acta* **15,** 18.

THE AMERICAN MINERALOGIST, VOL. 44, MAY–JUNE, 1959

CORRELATION BETWEEN *X*-RAY EMISSION AND FLAME PHOTOMETER DETERMINATION OF THE K_2O CONTENT OF POTASH FELDSPARS

DONALD O. EMERSON, *Department of Geological Sciences, University of California, Davis, California.*

Using *x*-ray emission spectroscopy in the quantitative determination of chemical composition is still in the developmental stages. As a test of its accuracy the K_2O content of potash feldspars from granitic rocks of the Inyo batholith was determined both by flame photometry and by *x*-ray emission techniques. Comparison of the results shows that the simpler and non-destructive *x*-ray emission technique gives satisfactory estimates of K_2O values.

To prepare each sample, 0.3–0.4 gram of the feldspar separate was powdered in a Wig-l-bug by shaking 0.1- to 0.2-mm. grains for five minutes in a steel capsule with steel balls. These powders were tightly packed into the wells (3/4×1/2×1/16 inch) of aluminum slides that fit the sample holder of the *x*-ray spectrophotometer.

A General Electric XRD-5 *x*-ray spectrophotometer with a lithium fluoride analyzing crystal was used. The tungsten tube was operated at 50 kilovolts and 50 milliamperes. Helium was used in the optical path, and a gas-flow proportional counter was the detector. The analytical line used was $K\alpha$. Background intensity variations of the different samples were insignificant in relation to the peak heights. Intensities were measured during a constant counting time of ten seconds. With a constant helium flow of eight cubic feet per hour the flushing time required to clear the system of air after the introduction of each sample was 120 seconds.

The standards used to establish a working curve were the chemically analyzed G-1 granite (Fairbairn *et al.*, 1951) and a potash feldspar megacryst of the Aiken facies of the McAfee adamellite (Emerson, 1959). The use of standards in a similar matrix, together with a narrow range in composition of samples, avoids significant deviations from the proportionality between analytical-line intensity and weight-fraction of the element being determined (Liebhafsky and Winslow, 1958).

Eighty-nine samples of potash feldspar were analyzed by both x-ray emission and flame photometer techniques. The flame photometer values were averaged from duplicate analyses that agreed within four per cent. The values, ranging from 9.5 to 15.2 per cent K_2O, are plotted in Fig. 1. Comparison of the values obtained with both methods show that those obtained by x-ray are unbiased, with an average error of estimate (Snedecor, 1956, p. 491) of only 0.03 per cent K_2O. The standard deviation of the difference between corresponding values from both techniques, or standard error of estimate, is 0.100 per cent. The sample correlation coefficient (Snedecor, 1956, p. 162) is 0.979, a nearly perfect correlation. The sample regression coefficient (Snedecor, 1956, p. 123) is 1.011, using the flame photometer results as the independent variable.

The high correlation, which is also reflected as a small standard error of estimate, shows that the much simpler and non-destructive x-ray

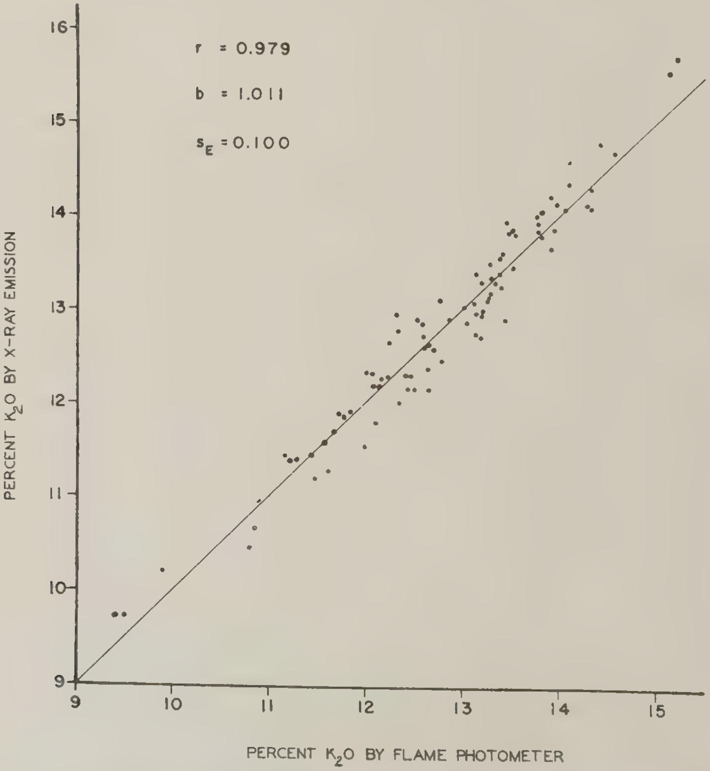

FIG. 1. Comparison of 89 K_2O values from x-ray emission and flame photometer techniques, showing a 1:1 line, correlation coefficient (r), regression coefficient (b) and standard error of estimate (S_E).

technique is as accurate a method of feldspar K_2O determination as is the conventional flame photometer technique.

REFERENCES

Emerson, D. O., 1959, Granitic rocks of the northern portion of the Inyo batholith. Ph.D. dissertation, The Pennsylvania State University, University Park, Pennsylvania.

Fairbairn, H. W., *et al.*, 1951, A cooperative investigation of precision and accuracy in chemical, spectrochemical and modal analysis of silicate rocks. *U. S. Geol. Surv., Bull.* **980.**

Liebhafsky, H. A., and Winslow, E. H., *X*-ray adsorption and emission. *Analytical Chem.*, **30,** 580–589.

Snedecor, G. W., 1956, Statistical methods. Iowa State College Press, Ames, Iowa.

THE AMERICAN MINERALOGIST, VOL. 44, MAY–JUNE, 1959

THE UNIT CELL OF CARMINITE

Abraham Rosenzweig and Joseph J. Finney, *University of New Mexico, Albuquerque, New Mexico.*

The mineral carminite was described by Sandberger (1958) from Horhausen, Rhine Province, Germany. On the basis of an approximate chemical analysis he gave the composition as $Pb_3Fe_{10}(AsO_4)_{12}$, and the specific gravity as 4.10. Foshag (1937) reported the composition of carminite as approximating $PbFe_2(AsO_4)_2(OH)_2$ for carminite from Mapimi, Durango, Mexico and from an unstated locality in Colorado, but makes no mention of the specific gravity of his material. Le Mesurier (1939) described carminite from the Ashburton District, Western Australia which agreed in composition with Foshag's formula, and for which he reported a specific gravity of 5.22. The original papers of Sandberger and Le Mesurier were not available to the authors, the reported specific gravities having been noted in Dana's System of Mineralogy (1951), page 912.

Samples of carminite from Mapimi, Durango were examined for their suitability for specific gravity determination. These samples consisted of aggregates of minute (<0.5 mm. long) lath-shaped crystals very similar to those described by Foshag. Clusters of carminite crystals were used

Table 1. Unit Cell Data for Carminite

$a_0=12.25\pm0.04$ Å
$b_0=16.52\pm0.04$ Å
$c_0=7.64\pm0.04$ Å
$a_0:b_0:c_0=0.741:1:0.456$

space group: *Amaa* or *A2aa*
cell volume: 1528 Å^3
cell formula: $Pb_8Fe_{16}(AsO_4)_{16}(OH)_{16}$
cell weight: 5046

TABLE 2. *X*-RAY POWDER DATA FOR CARMINITE

Obtained with FeK$_\alpha$ radiation in a 114.6 mm. diameter camera

d_{obs} Å	I_{obs}	d_{calc} Å	*hkl*	d_{obs} Å	I_{obs}	d_{calc} Å	*hkl*
6.73	1	6.87	011	1.888	2	1.888	004
6.05	1	6.13	200	1.834	1	1.833	433
5.94	4	5.99	111	1.816	<1	1.815	471
4.88	1	4.92	220	1.799	8	1.804	204
4.54	6	4.58	211			1.800	462
4.41	2	4.45	031			1.797	353
4.16	3	4.18	131			1.796	602
4.10	3	4.13	040	1.768	1	1.765	191
3.57	<1	3.599	231	1.743	<1		
3.50	7	3.509	311	1.719	6		
3.29	<1	3.304	122	1.694	1		
3.20	10	3.212	202	1.678	4		
3.05	5	3.062	400	1.649	2		
3.01	5	3.027	051	1.636	3		
		3.008	331	1.610	3		
2.929	8	2.939	151	1.598	1		
2.784	5	2.797	411	1.553	1		
2.705	7	2.714	251	1.543	1		
2.622	1	2.627	322	1.532	2		
2.580	9	2.595	242	1.517	4		
2.510	2	2.511	260	1.488	<1		
2.481	1	2.488	013	1.477	<1		
2.456	4	2.460	440	1.465	1		
2.429	4	2.432	351	1.446	3		
2.307	2	2.308	511	1.434	2		
2.283	3	2.285	422	1.396	<1		
2.229	<1	2.225	062	1.378	<1		
2.190	1	2.188	162	1.369	2		
2.154	7	2.153	451	1.361	5		
2.067	3	2.066	271	1.346	2		
		2.065	080	1.338	1		
2.000	2	2.002	053	1.321	1		
1.978	3	1.976	153	1.307	2		
		1.972	371	1.287	2		
1.954	2	1.956	611	1.273	1		
		1.953	362	1.258	1		
1.907	5	1.905	551	1.244	1		
		1.903	253	1.236	1		

for a rough specific gravity determination with the Berman balance. Since these clusters were very porous and the heaviest of them weighed less than ten milligrams, no great degree of accuracy could be expected. The measured specific gravity ranged from 5.03 to 5.18. Although this is not in very good agreement with Le Mesurier's data, it clearly indicates that a specific gravity of 4.10 is too low.

Single crystal *x*-ray diffraction patterns of carminite were obtained by both the precession and Weissenberg methods using CuK$_\alpha$ radiation. The levels $h0l$, $h1l$, $0kl$, and $1kl$ were recorded by the precession method, and $hk0$, $hk1$, and $hk2$ by the Weissenberg method. The crystallographic axes were assigned according to the convention $b>a>c$, yielding axes which corresponded in orientation and ratio to those reported by Foshag on the basis of the morphology. Systematic extinctions indicate that the space group is either A*maa* or A2*aa* (C_{2v}^{13} or D_{2h}^{20}). A*maa* is the more likely, since no piezoelectric effect could be detected by the Geibe-Schiebe method and the morphology is holohedral. The unit cell data is given in Table 1. Powder diffraction data, using FeK$_\alpha$ radiation, is given in Table 2. All intensities were estimated visually.

On the basis of the unit cell data obtained and the composition $PbFe_2(AsO_4)_2(OH)_2$, the number of formula weights per cell were calculated using both reported values of the specific gravity. For specific gravity 4.10, $Z=5.99$, and for specific gravity 5.22, $Z=7.64$. Examination of the two possible space groups shows that crystallographically equivalent atoms must lie in four-, eight-, or sixteen-fold positions. These positions provide no arrangement which would accommodate six lead atoms per unit cell. On the basis of the space group, it seems reasonable to assume that eight formula weights per cell is the correct figure. The calculated specific gravity for $Z=8$ is 5.46, a 4.5% deviation from Le Mesurier's value and a 5% deviation from the maximum value obtained for the Mapimi material.

REFERENCES

FOSHAG, W. F. (1937), Carminite and associated minerals from Mapimi, Mexico: *Am. Mineral.*, **22,** 479.

LEMESURIER (1939), *J. Roy. Soc. Western Australia*, **25,** 137.

PALACHE, C., BERMAN, H., AND FRONDEL, C. (1951), Dana's system of mineralogy, Vol. II: John Wiley and Sons, Inc., 1124 p.

SANDBERGER (1858), *Ann. Phys.*, **103,** 343.

THE AMERICAN MINERALOGIST, VOL. 44, MAY–JUNE, 1959

SUBSTITUTION OF Fe^{3+} FOR Al^{3+} IN SYNTHETIC SPESSARTITE

S. GELLER AND C. E. MILLER, *Bell Telephone Laboratories, Murray Hill, New Jersey.*

With a view toward producing garnets with magnetic ions in only the dodecahedral and octahedral sites (see Refs. 1 and 2), we have attempted to synthesize, at atmospheric pressure, the garnets $Mn_3Fe_2(SiO_4)_3$* and $Mn_3Cr_2(SiO_4)_3$ by means similar to those used to synthesize spessartite (4, 5) and uvarovite (6, 7). The latter are the only two silicate garnets which, to date, have been rather directly synthesized. In these experiments, garnets were not produced. We usually obtained spinel-type structures; in some cases, $MnSiO_3$ (rhodonite) was obtained. Also, in some cases, the devitrification of the silica to tridymite occurred.

Numerous experiments were carried out to determine to what extent Fe^{3+} could be made to replace Al^{3+} in $Mn_3Al_2(SiO_4)_3$. Many difficulties were encountered, especially in the formation of more than one phase and the segregation of phases. The experiment which led to the highest substitution for Al^{3+} by Fe^{3+} involved the mixing of ingredients such that 30 atomic per cent of the Al^{3+} would be replaced by Fe^{3+}. The thoroughly mixed and compacted reactants were kept at 1250° C. for 20 hours and furnace cooled. It was obvious from the powder pattern that all of the Fe^{3+} had not replaced the Al^{3+}. However, the garnet phase formed has a lattice constant of 11.658 Å or 0.043 Å larger than that of the pure synthetic spessartite.

It has been shown that when partial substitution is made for Fe^{3+} in yttrium-iron garnet by other trivalent ions (8) the solid solutions very nearly follow a linear lattice constant law. We may assume that solid solutions between $Mn_3Fe_2(SiO_4)_3$ and $Mn_3Al_2(SiO_4)_3$ would also very nearly follow a linear lattice constant law.† Now the difference in lattice constant between synthetic andradite and grossularite (9) is 0.20 Å. Then, if the lattice constant of $Mn_3Fe_2(SiO_4)_3$ were 11.82 Å (that is, 0.20 Å greater than that of spessartite), it would appear that in our experiments at atmospheric pressure, a maximum of about 20% of the Al^{3+} was replaced by Fe^{3+}.

The Cr^{3+} ions prefer the octahedral sites in the garnets (see Ref. 8), but attempts to substitute Cr^{3+} for Al^{3+} in spessaritite were unsuccessful. The substitution of Co^{3+} for Al^{3+} was also attempted, but as expected, positive results were not obtained.

REFERENCES

1. GILLEO, M. A., AND GELLER, S., *A.I.E.E. Conference on Magnetism and Magnetic Materials, November 1958, Paper No. 131.* Also *J. Appl. Phys.*, **30**, 2975 (1959).

---

* Coes (3) has reported the high pressure synthesis of $Mn_3Fe_2(SiO_4)_3$ garnet. A sample of this garnet obtained from Mr. Coes, after this note was written, has a lattice constant of 11.82 Å, as obtained from a Buerger precession photograph.

† However, solid solutions between silicate garnets and the garnets in which all metal ions are trivalent do not follow a linear composition vs. lattice constant law (see, for example, Ref. 5).

2. Geller, S., and Miller, C. E., "New Synthetic Garnets," to be published.
3. Coes, L., *Jour. Amer. Ceram. Soc.*, **38,** 298 (1955).
4. Snow, R. B., *Jour. Amer. Ceram. Soc.*, **26,** 11 (1943).
5. Yoder, H. S., and Keith, M. L., *Am. Mineral.*, **36,** 324 (1950).
6. Hummel, F. A., *Am. Mineral.*, **35,** 324 (1950).
7. Geller, S., and Miller, C. E., *Amer. Mineral.*, **44,** 445 (1959).
8. Gilleo, M. A., and Geller, S., *Phys. Rev.*, **110,** 73 (1958).
9. Skinner, B. J., *Amer. Mineral.*, **41,** 428 (1956).

THE AMERICAN MINERALOGIST, VOL. 44, MAY–JUNE, 1959

MACRO POINT COUNTING

Frank J. Fitch, *Department of Geology, Birkbeck College, University of London, England.*

Macro point counting, and a stage to facilitate its application to hand specimens, has recently been discussed by Emerson (1958, p. 1000). In 1953 the author exhibited a method of macro point counting before the Mineralogical Society of London. Five years experience confirms the value of this method, which is considered to be both simpler and superior to that described by Emerson.

The method is based on a graticule prepared by the author and his senior colleague, Dr. A. T. J. Dollar, for a variety of petrological uses. The graticule (Fig. 1) has 676 equally spaced points, and a co-ordinate reference system. It can be reproduced photographically on any scale to suit the requirements of the task. When used for modal analysis the scale is varied to suit the grain-size and porphyritic character of the rock to be analysed. For routine hand specimen analysis the graticule is printed on high resolution photographic plates, but for field use it can be prepared on plastic film. Point counting requires the identification of the mineral grains that occur at each of the equally spaced points. For this purpose the graticule is superior to the use of Zip-E-Tone, suggested by Jackson and Ross (1956), which obscures the mineral to be identified. In most cases there is no difficulty in deciding which mineral occurs at the exact centre of the circle, but when doubt arises, this is resolved by the use of a cross-wire (or transparent protractor in the field) aligned on the graticule.

It has been found by experience that porphyritic and coarse-grained rocks are not adequately sampled by micro analysis alone. Often a combination of macro and micro point count analysis is found to produce the most satisfactory results. If the object of the point count is to

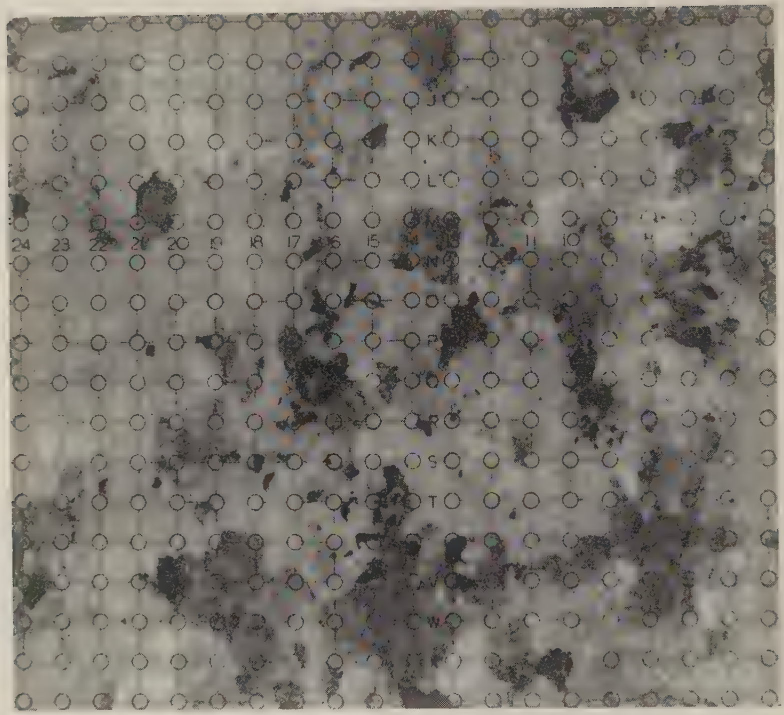

FIG. 1. Graticule on photographic plate, for use in macro point counting.

produce a true bulk modal analysis, the author agrees with Emerson that the stratified-random sampling method described by Chayes (1956, p. 29), is the most suitable. The value of point count analysis in petrofabric studies, however, is based on carefully oriented specimens. Macro point count analysis of three mutually perpendicular surfaces can confirm or deny a suspected grain- or particle-shape fabric. For example, this method has been found particularly useful in confirming poorly developed primary flow structure in porphyritic granites.

Very coarse-grained rocks, and rocks with extremely large phenocrysts require large macro-grids, but it is found that a grid prepared on a glass slip 2½ to 3 inches square is suitable for the average rock. The specimen to be analysed is cut into a parallel-sided slab and one surface smooth ground by the usual methods. Staining of some minerals at this stage may assist in their identification. The macro-grid is cemented to the smooth ground surface with glycerin jelly. To do this the specimen is placed face-downwards on a hot-plate for about a minute. This warms the surface sufficiently to melt a small lump of the jelly now placed on it. Once the glycerin is melted, the macro-grid, which has also been warmed on the hot-plate is firmly mounted and the air bubbles pressed out as in thin section making. When cold the glycerin sets firm. The advantage of using glycerin jelly for this purpose is that, when the analysis is completed, the grid can be removed, and the specimen washed clean, simply by immersing in hot water. The author uses a binocular microscope fitted with one cross-wire ocular for routine macro analysis, but a standard petrological microscope can be used if a binocular is not available. A tabulator can be used to collate the results as in micro analysis. Each circle of the graticule is viewed in turn, the rock slab being moved by hand on the microscope stage. The circles are not accurately centred on the microscope cross-wires unless there is doubt as to which mineral grain lies at the exact centre. With a little practice the 676 points can be counted in fifteen to twenty minutes. Moving the macro-grid to another position on the cut surface, or to further cut surfaces, enables any number of points to be counted, as may be required.

The principal advantage of this method is that it does not require any special apparatus other than a cheaply prepared photographic plate. Its simplicity enables it to be used by students as a routine. The use of a binocular microscope is superior to the use of a magnifying lens. Strong illumination is required if the high power objectives are to be used, but the use of a microscope enables the majority of minerals to be identified.

REFERENCES

1. CHAYES, FELIX (1956), Petrographic Modal Analysis: J. Wiley and Sons, N. Y.
2. EMERSON, D. O. (1958), A stage for macro point counting: *Am. Mineral.*, **43,** 1000–1003.
3. JACKSON, E. D., AND ROSS, D. C. (1956), A technique for model analyses of medium- and coarse-grained (3–10 mm.) rocks: *Am. Mineral.*, **41,** 648–651.

THE AMERICAN MINERALOGIST, VOL. 44, MAY–JUNE, 1959

THE RHOMBIC AMPHIBOLE HOLMQUISTITE

NILS SUNDIUS, *Mineralogical Department, Natural History Museum, Stockholm, Sweden.*

In a recent note, Vogt, Bastiansen and Skancke (1), as a result of *x*-ray studies, made the statement that the amphibole holmquistite is rhombic, and not monoclinic, as earlier supposed. Thus the amphibole species glaucophane is dimorphic.

The formula of glaucophane can be derived from that of anthophyllite. As is well known the latter often contains essential amounts of trivalent atoms Al and Fe, and at the same time alkalies, chiefly Na. The corresponding varieties have been named gedrites. The relevant substitution may be Na(Al, Fe‴) for MgMg. If $Mg_7Si_8O_{22}(OH)_2$ is accepted as the formula of anthophyllite, we can perform this substitution twice, thus $Na_2(Al_2, Fe_2''')$ for Mg_4 and we get the formula $Na_2Mg_3(Al_2, Fe''')_2 Si_8O_{22}(OH)_2$ as in glaucophane. If more alkali were to be introduced it would have to enter the vacant spaces in the structure and the substitution would be of another kind, Na(Al, Fe''') for Si. Therefore the glaucophane formula can be regarded that of an end member.

The same substitution in anthophyllite is also possible in the case of holmquistite, except that we are here concerned with LiAl instead of NaAl. Logically it seems most correct to designate holmquisite as a lithium gedrite.

Geologically the determination of the rhombic character of holmquistite is of interest, because the glaucophane is a typical stress-mineral, occurring in folded schists and crystallizing during metamorphism, whereas holmquistite has long been regarded as an exception because it is formed through contact influence from pegmatite without notable influence from stress.

Reference

1. Vogt, T., Bastiansen, O., and Skancke, P. (1958), Holmquistite as a rhombic amphibole: *Am. Mineral.* **43,** 981–982.

THE AMERICAN MINERALOGIST, VOL. 44, MAY–JUNE, 1959

AN INEQUILIBRIUM MODIFICATION OF THE CORUNDUM STRUCTURE

Davis M. Lapham, *Pennsylvania Geological Survey, Harrisburg, Pa.*

During the investigation of Devonian K-bentonite and associated Marcellus Shale from Bixler, Perry County, Pennsylvania, it was noted that samples of the shale yielded a 1050° C. endotherm and a post DTA *x*-ray pattern. The *x*-ray spacings resemble corundum but are distinct from it and other published alumina polymorph patterns.

Samples of 1) the Devonian K-bentonite containing illite, mixed layer montmorillonite-illite, chlorite, kaolinite, and gibbsite, 2) Marcellus Shale, 3) 2*M* pegmatitic muscovite, and 4) a mixture of 2*M* muscovite and hydrated alumina were subjected to DTA and *x*-ray diffraction analyses to determine the nature of the material which yielded the observed 1050° C. endotherm and the alumina type *x*-ray pattern.

Post DTA *x*-ray diffraction patterns are compared in Table 1 with a corundum reference pattern by Swanson and Fuyat (1953). The pattern designated as μ_1 was taken from the top two-thirds of the DTA sample well, and μ_2 from the bottom third. The patterns represent a gradual approach toward the corundum structure with increasing time during

TABLE 1. COMPARISON OF POST-DTA SHALE AND 2M MUSCOVITE REFLECTIONS AFTER SUBTRACTION OF QUARTZ, HEMATITE AND MULLITE SPACINGS WITH CORUNDUM REFLECTIONS

Post DTA						Corundum ASTM Index Swanson & Fuyat (1953)		
Marcellus Shale		*2M* Muscovite						
		μ_1		μ_2				
d Å	I	*d* Å	I	*d* Å	I	*d* Å	I	(*hkl*)
3.6_{B}	(?)	3.51	20	3.495	35	3.479	74	(102)
3.024	1 (?)							
2.913	1							
2.882*	6	2.847	20	2.797	10			
2.518	4	2.570	20	2.560	85	2.552	92	(014)
2.427*	12	2.424	100	2.410	60	2.379	42	(110)
						2.165	<1	(006)
2.100	3	2.101	25	2.090	60	2.085	100	(113)
2.003	1	2.009	10	2.002	1			
		1.755	8	1.744	15	1.740	43	(204)
1.615	1	1.611	18	1.601	50	1.601	81	(116)
1.530	1	1.549	12	1.543	2	1.546	3	(121)
1.419	3	1.419	50	1.419	20	1.510	7	(108)
				1.406	8	1.404	32	(124)
1.385	1	1.388	10	1.382	8			
				1.376	15	1.374	48	(300)

B = Broad reflection.

* Lines also present in K-bentonite clay samples.

which the sample was maintained at elevated temperatures. It is expected that had equilibrium been attained, corundum would have resulted.

The μ patterns illustrate a general contaction of the corundum lattice and an increase in intensity of the reflecting planes common to both μ alumina and corundum. The spacings and intensities of the shale sample did not show any significant variation with sample well depth. Many of the reflections in Table 1 are also present in kappa, gamma, theta, and other alumina polymorphs (eg., a 1.38 to 1.39 Å spacing) but with different relative intensities and with the presence of other major d values not present in this material.

For the four samples analyzed, all except the K-bentonite evidence both a 1050° C. endotherm and a μ alumina *x*-ray pattern. Since the major distinction between the shale and the K-bentonite is the presence of *2M* muscovite in the shale as contrasted with *1Md* illite in the K-bentonite, and since 2*M* pegmatitic muscovite does yield a post DTA μ pattern, it is suggested that the presence of a well crystallized mica may govern the appearance of a metastable alumina polymorph immediately previous to the formation of corundum, and having a structure approaching that of corundum. This metastable alumina polymorph has been designated μ alumina for reference convenience, and is an equilibrium modification not to be expected in natural materials.

REFERENCE

SWANSON AND FUYAT, 1953, *NBS Circular No. 559*, **II**, p. 20.

THE AMERICAN MINERALOGIST, VOL. 44, MAY–JUNE, 1959

MAGNETITE IN MICROCRYSTALLINE QUARTZ, LANCASTER COUNTY, PA.

DAVIS M. LAPHAM, *Pennsylvania Geological Survey, Harrisburg, Pa.*

During a research project on the chromites and serpentines of southeastern Pennsylvania, blebs of magnetite were observed in the silicified contact zone between a serpentinized ultramafic and a later quartz pegmatite dike. The unusual occurrence and non-crystalline, vitreous appearance of the magnetite are of interest.

The magnetite occurs near the Red Pit, two-thirds of a mile southwest of Rock Springs Church near Pennsylvania Route 222 in Lancaster County, Pennsylvania. The magnetite blebs are highly magnetic. It is restricted to hematitic microcrystalline quartz replacing bastite at a quartz pegmatite-chromiferous serpentine contact (Fig. 1).

X-ray powder diffraction patterns indicate that at least some of the magnetite is crystalline with crystallites exceeding 1000 Å. Electron photomicrographs (Fig. 2) indicate that some of the material may be amorphous, since no crystal outlines or cleavage directions are visible.

Composition, determined from a unit cell spacing of $a_0 = 8.352$ Å $\pm .006$ Å and from emission spectrographic analyses, corresponding to one magnesioferrite, one magnetite, and two ferrochromite molecules, is $(Fe_{1.7}Mg_{1.0})(Cr_{30}Fe_{1.3}Al_{0.7})O_{10}$.

Evidence bearing upon the paragenesis and genesis of this magnetite may be summarized as follows:

1. Microcrystalline quartz and chalcedony replace serpentine textures.
2. Silicification increases toward pegmatitic quartz while serpentinization textures and minerals are gradually obliterated.
3. Magnetite is restricted to microcystalline chert which is the chilled contact zone of a quartz pegmatite intrusive into serpentine.

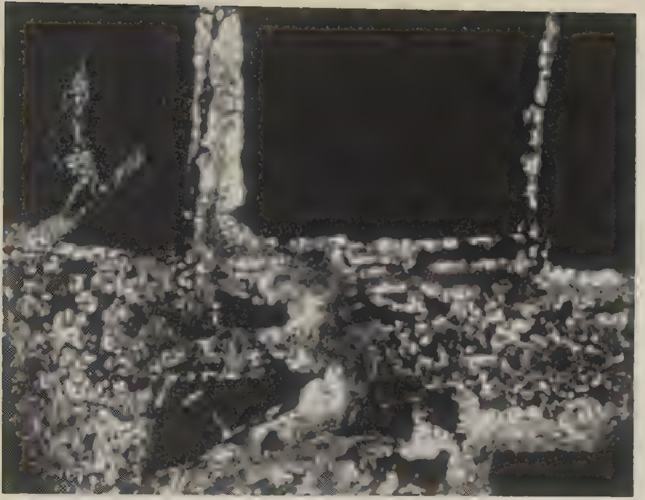

FIG. 1. Photomicrograph of magnetite in microcrystalline quartz. Crossed nicols. ×30.

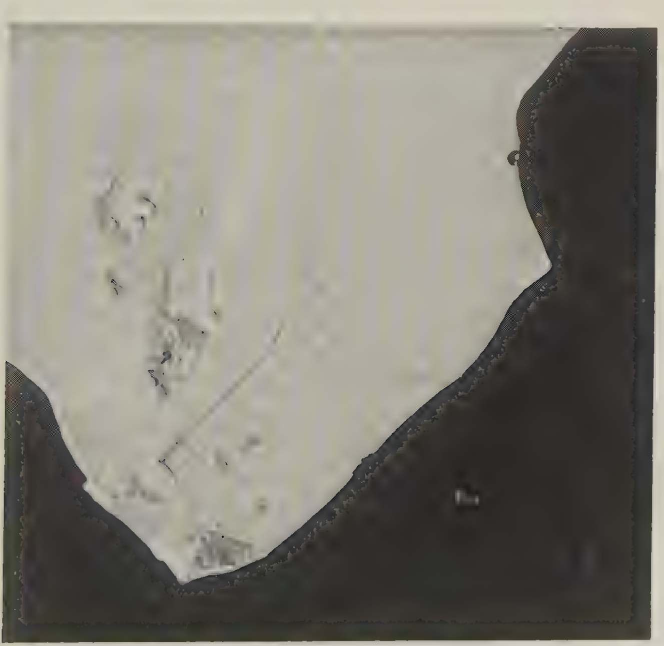

FIG. 2. Electron micrograph of magnetite. ×11400.

4. Microcrystalline quartz, and magnetite textures and crystallite sizes indicate rapid cooling and growth by multiple nucleation.

5. This serpentinized ultramafic contains sufficient Mg, Fe, Cr, and Al to have been the source of the magnetite.

These points indicate that the glassy appearing magnetite originated from pre-existing iron-magnesium silicates by alteration and remobilization of a serpentinized ultramafic along the contact of a quartz pegmatite intrusion. Crystallization was rapid, producing microcrystalline quartz, crystallites of magnetite as small as a few thousand angstroms, and possibly a magnetite glass phase. The magnetite represents a complete recrystallization rather than simply alteration of a pre-existing spinel. Silicification by granitic pegmatite intrusion may be genetically related to similar granitic intrusives in this region commonly spatially associated with serpentinized ultramafics.

ACKNOWLEDGMENTS

The author expresses his gratitude to Professor Thomas Bates and Mr. Joseph J. Comer of Pennsylvania State University for preparing electron photomicrographs of the magnetite.

THE AMERICAN MINERALOGIST, VOL. 44, MAY–JUNE, 1959

DIFFERENTIAL THERMAL ANALYSIS OF EVAPORITES

OTTO C. KOPP[1] AND PAUL F. KERR[2]

In view of the recent interest shown by petroleum geologists in the thermal history of evaporite minerals, a new development in the application of differential thermal analysis (D.T.A.) to this group may be of interest. Improved D.T.A. technique has made possible the analysis of minerals containing corrosive sulfur and arsenic (Kopp and Kerr, 1957, 1958) formerly beyond the scope of the method. More recently several evaporite minerals have been analyzed which contain elements of the halogen family, and the borate and nitrate radicals.

Difficulties ordinarily encountered in applying D.T.A. to a number of these minerals include the fluxing action of the molten material upon the metal thermocouples, corrosive gases released at some stage during the heating process, and the difficulty of sample removal upon cooling. Minerals for which difficulties have been reported include: cryolite, atacamite, borax, nitre, gypsum, polyhalite and others. Current procedure appears to consist of heating the mineral to a point somewhat below its melting point with no attempt to determine reactions above this temperature. For example, Kauffman and Dilling (1950) illustrate a differential thermal curve for cryolite and state, "The curve for cryolite shows the endothermic peak at 570° C. representing the change to the isometric modification. This reaction is reversible. The heating of this sample was stopped before the melting point was reached." Allen (1957), who analyzed thirteen borate minerals states, "Preliminary investigations confirmed these views and showed the inadvisability of heating borate minerals to temperatures approaching 1000° C." To avoid these difficulties runs were terminated at temperatures of 650° C. or less.

---

[1] Assistant Professor of Geology, The University of Tennessee.

[2] Professor of Geology, Columbia University.

Apparatus previously described (Kopp and Kerr, 1957) involves protecting the metal head and thermocouples of the equipment with concentric alundum cylinders. This technique with some modification has been found suitable for examining evaporite minerals. Early in this investigation it became apparent that molten minerals would often percolate through the relatively coarse alumina filler and pass into the space between the inner alundum cylinder and the thermal head itself. This tended to contaminate the apparatus and made sample removal difficult. It was found necessary to prepare an impermeable base for the sample well.

This was done by placing the inner and outer alundum cylinders on a

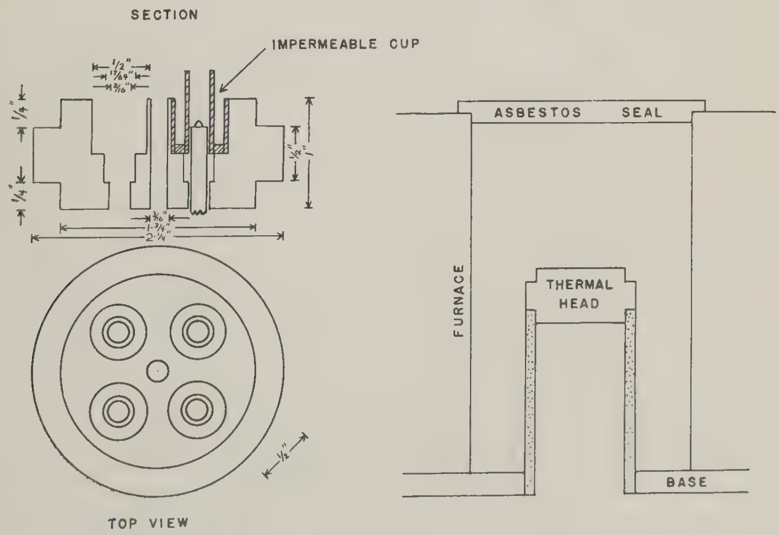

Fig. 1. Modified D.T.A. equipment for the analysis of evaporites.

suitable holder and pouring a base of alundum cement about $\frac{1}{8}$ inch thick. When dry, these cups are fired to 1000° C., hence they undergo no thermal reactions during the heating process. The cups are tested with water to be certain that they are completely sealed. Similar cups are used for both the sample and standard wells to avoid differences in heat flow characteristics. It is possible to salvage the sample cup if the reaction product is soluble, but ordinarily it is discarded after use. The apparatus is illustrated in Fig. 1.

Mineral samples were selected from the mineral collection at Columbia University and include halite, cryolite, borax, kernite, nitre, soda nitre, colemanite and sylvite. The samples were crushed and sieved and that portion passing a No. 100 sieve, but caught on a No. 120 sieve was analyzed. Samples were mixed with No. 60 alumina and tamped in the space between the inner and outer alundum cylinders. A heating rate from 12–14° C. per minute was employed. A preamplifier was used to amplify the curves 10×. Sample data are listed in Table 1 and the thermal curves obtained are presented in Fig. 2.

Discussion

The reaction products obtained during the analysis have not as yet been studied. However, in the light of melting point data and the investigations of other workers, it is possible to briefly describe the nature of the reactions observed for each sample. It should be noted that the possibility of reaction between the molten material and the alumina filler exists, and that these reactions would be recorded in the D.T.A. curve. However, this does not eliminate the utility of the method since these reactions would be related to the composition of the mineral involved.

Halite ·Only one reaction at 810° C. (endothermic) was observed for halite. This corresponds closely to the melting point given for pure NaCl (804° C.).

Cryolite—Two endothermic reactions at 565° C. and 972° C. respectively are noted in the curve for cryolite. The first corresponds to the inversion from monoclinic to isometric (570° C. according to Kauffman and Dilling, 1950). The second represents the melting point (about 1000° C.) and may also be related to the attack of the molten material upon the alumina present.

Borax—The borax used in this run has probably been converted to tincalconite by dehydration. Peaks are observed at 158° C., 343° C., 609° C. and 642° C. According to Allen (1957) tincalconite exhibits an endothermic peak at 160° C. The nature of the other peaks has not been determined.

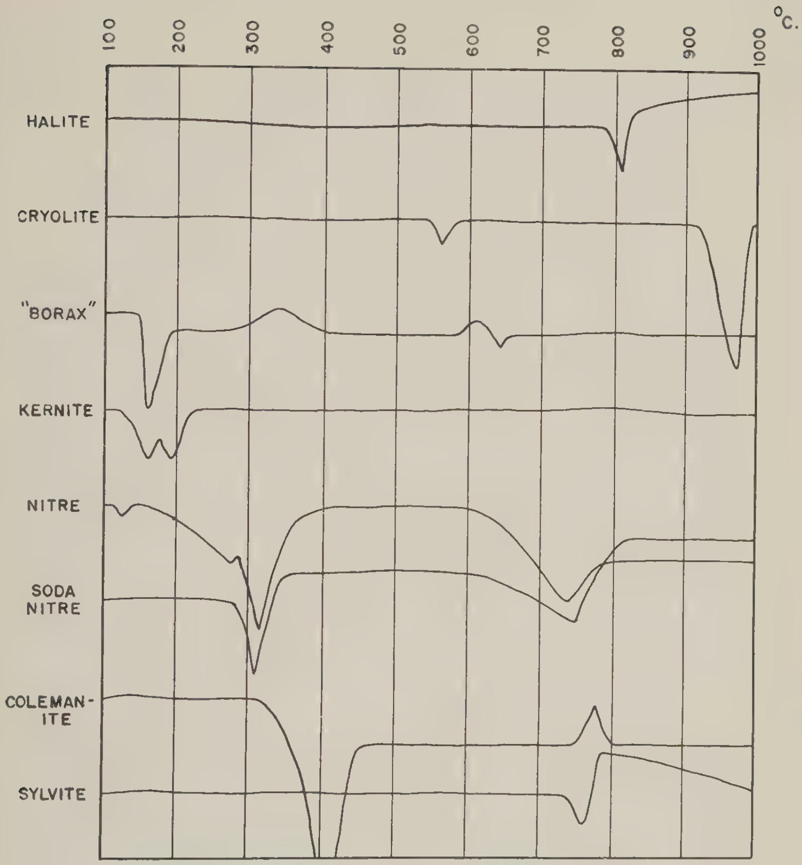

FIG. 2. D.T.A. curves for selected evaporite minerals.

Kernite—Two endothermic peaks, at 160° C. and 188° C. are observed. The endothermic peak temperature noted by Allen (1957) for kernite is 185° C. The peak at 160° C. probably reflects the presence of some tincalconite which may result from partial hydration of the kernite.

Nitre—The first endothermic reaction at 125° C. corresponds closely to the inversion temperature (129° C.) determined for nitre. The endotermic peak at 315° C. may represent the melting point (given as 334° C. in the Handbook of Chemistry and Physics, 35th edition). The other peaks are uncertain and the sample may be impure.

Soda Nitre—The initial endothermic peak at 308° C. agrees with the melting point of pure material which is also 308° C. The final endothermic peak at 754° C. is similar to the endothermic reaction recorded for nitre

Table 1. Sample Data

Mineral	Melting Temp. ° C.[1]	Locality	Weight (mg.)	Peaks (° C. ±3° C.)
Halite NaCl	804	Minas de Zipaquira, Colombia, S. A.	50	810 ↓
Cryolite Na_3AlF_6	~1000	Ivigtut, Greenland	100	565 ↓ 972 ↓
Borax[2] $Na_2B_4O_7 \cdot 10H_2O$	75	Tibet, China	50	158 ↓ 343 ↑ 609 ↑ 642 ↓
Kernite $Na_2B_4O_7 \cdot 4H_2O$	—	Kern Co., California	50	160 ↓ 188 ↓
Nitre KNO_3	129[3]	Humboldt, Nevada	100	125 ↓ 275 ↓ 288 ↑ ? 315 ↓ 733 ↓
Soda Nitre $NaNO_3$	308	Tarapaca, Chile	100	308 ↓ 754 ↓
Colemanite $Ca_2B_6O_{11} \cdot 5H_2O$	decomp.	Mojave area, California	100	410 ↓ 782 ↑
Sylvite KCl	776	Kalusz, Poland	100	763 ↓

↓ Endothermic; ↑ Exothermic; (?) May result from the overlap of two consecutive peaks in the same direction.

[1] Melting point data obtained from International Critical Tables of Numerical Data, Physics, Chemistry and Technology, Vol. I, 1926.

[2] Probably tincalconite ($Na_2B_4O_7 \cdot 5H_2O$); see discussion.

[3] Inversion temperature (orthorhombic to trigonal).

at 733° C. While the nature of these peaks is uncertain they may represent the decomposition of the molten material or its boiling point.

Colemanite—Two reactions, one at 410° C. (endothermic), and a second at 782° C. (exothermic) are noted. Allen (1957) reports a peak temperature between 370–375° C. for colemanite from Death Valley, California. The value obtained for this sample shows the greatest divergence from reported values. The reactions are uncertain, but the initial endothermic reaction may represent the melting point of the mineral.

Sylvite—The melting point recorded at 763° C. is slightly lower than the melting point for the pure compound (776° C.) and may indicate that the mineral is not pure KCl.

CONCLUSION

It appears possible through the use of the method described to extend the observable D.T.A. range beyond the melting point of a mineral without encountering the difficulties noted for analyses made with unprotected thermocouples. This offers the possibility of widespread application of the D.T.A. method to a considerable group of minerals not previously amenable to the method. The few analyses mentioned constitute a small sample of the applications which are conceivable.

REFERENCES

ALLEN, ROBERT D., 1957, "Differential Thermal Analysis of Selected Borate Minerals," *Geol. Surv. Bull.* **1036-K.**

KAUFFMAN, A. J., JR. AND DILLING, E. D., 1950, "Differential Thermal Curves of Certain Hydrous and Anhydrous Minerals, With a Description of the Apparatus Used," *Econ. Geol.*, **45,** 222–244.

KOPP, O. C. AND KERR, P. F., 1957, "Differential Thermal Analysis of Sulfides and Arsenides," *Am. Mineral.*, **42,** 445–454.

———, 1958, "Differential Thermal Analysis of Sphalerite," *Am. Mineral.*, **43,** 732–748.

———, 1958, "Differential Thermal Analysis of Pyrite and Marcasite," *Am. Mineral.*, **43,** 1079–1097.

THE AMERICAN MINERALOGIST, VOL. 44, MAY–JUNE, 1959

REFINEMENT OF THE CRYSTAL STRUCTURE OF DOLOMITE*

H. STEINFINK AND F. J. SANS, *Houston, Texas*

The mineral dolomite was one of the early substances to be investigated by *x*-ray diffraction methods (Wyckoff and Merwin, 1924). Dolomite, $CaMg(CO_3)_2$, was considered by some to be a solid solution of the simple carbonates calcite and magnesite and by others as a definite compound, distinct from the two simpler carbonates. This early investigation established, with the use of Laue photographs, that the symmetry of the atomic arrangment of dolomite was lower than that of calcite and, therefore, it was a distinct chemical compound. It also established the unit cell dimensions and showed that four atomic parameters needed to be evaluated to determine the structure. At that time no attempt was made to determine the exact positions of the atoms of the carbonate group. The atomic parameters of dolomite were not investigated until Bradley *et al.* (1953) determined the four necessary parameters from powder data. Because the dolomite structure is of such importance in mineralogy it was felt that the parameters should be redetermined from single crystal data and that the thermal anistropy of the atoms should also be investigated.

---

* Publication No. 160, Exploration and Production Research Division, Shell Development Company, Houston, Texas.

EXPERIMENTAL

A rhomb of dolomite, 0.12 mm. thick, 0.12 mm. wide, and 0.23 mm. long was rotated about an *a* axis and three-dimensional data were collected with the Weissenberg camera. Multiple films interleaved with brass foil were taken with Mo $K\alpha$ radiation and the intensities were estimated in the usual way with the aid of a calibrated intensity scale. Equivalent reflections appearing on different films were used to bring all films to the same scale. Altogether 501 reflections were observed. The indices and coordinates used in this investigation refer to the hexagonal unit cell whose lattice constants are $a=4.815$, $c=16.119$ Å. The atoms were placed in space group $R\bar{3}$ as follows: Ca in $3(a)$, Mg in $3(b)$, C in $6(c)$, and O in $18(f)$.

REFINEMENT OF PARAMETERS

Structure factors were first calculated with the parameters given by Bradley *et al.* (1953), and the signs were used to evaluate the bounded projection

$$\rho(xy) = c\int_0^{1/6} \rho(xyz)dz.$$

This projection was refined and backshift corrections on the oxygen parameters were made. The z parameter for the carbon atom was determined from a line synthesis $\rho(00z)$ and the z parameter for the oxygen atom was obtained from a line synthesis passing through the (x, y) coordinates which had been obtained previously from the bounded projection.

The coordinates thus obtained were used as the starting values in a least-squares refinement, making use of all 501 observed reflections. Two iterations on the four coordinate parameters were made using an isotropic temperature factor, and the new atomic coordinates were then used in two separate least-squares iterations which determined anisotropic temperature parameters for each atom in the structure. The available computing equipment limited the evaluation of temperature parameters to two for each atom, one parallel to the c axis and one in the plane perpendicular to the c axis. After the second temperature least-squares iteration the anisotropic parameters together with the previously obtained coordinate parameters were used in another least-squares refinement of the coordinates, and since all changes were smaller than the standard deviations, the refinement was ended. The value of R de-misprint should read "0.2474" S.G.

TABLE 1. PARAMETERS FOR DOLOMITE

	Oxygen	σ	Bradley *et al.*	Carbon	σ	Bradley *et al.*
x	0.2~~3~~474	0.00068	0.257	0	—	0
y	−0.0347	0.00068	−0.028	0	—	0
z	0.2440	0.00017	0.243	0.2435	0.00031	0.243

creased from 0.134 to 0.0925, and $\Sigma\omega(\Delta F)^2$ decreased from 9.986 to 6.270. Table 1 lists the final parameters and their standard deviations and compares the values obtained in this investigation with those reported by Bradley *et al.* (1953).

The temperature factors for the four atoms were obtained by the least-squares refinement of the expression $F(hkl)=\sum_i f_i \exp\left[-\beta_i r(h^2+k^2+hk)-A_i s l^2\right]$ where $r=\frac{1}{3}a^2$, $s=\frac{1}{4}c^2$, B_i is the temperature factor of the ith atom in the plane perpendicular to the c axis and A_i is the temperature factor parallel to the c axis. These temperature factors are listed in Table 2.

TABLE 2. TEMPERATURE FACTORS AND RMS DISPLACEMENT OF ATOMS IN DOLOMITE

Atom	B	A	$\bar{\mu}\parallel c_0$	$\bar{\mu}\perp c_0$
Ca	0.37 A^2	0.30 A^2	.062 Å	.068 Å
Mg	0.20	0.21	.050	.050
C	0.62	0.36	.067	.088
O	0.59	0.77	.099	.086

DISCUSSION

The parameters of Table 1 lead to the following interatomic distances: C—O = 1.283 Å, Mg—O = 2.095 Å, Ca—O = 2.390 Å, with standard deviations of 0.004 Å. The value of the C—O bond is in good agreement with the predicted length for this bond, 1.288 Å, and with the value 1.294 Å reported by Sass *et al.* (1957) for $CaCO_3$. The Ca—O bond length is equal to the sum of the ionic radii.

The temperature parameters determined for the cations show that they vibrate isotropically while the atoms of the carbonate group have a considerable anisotropy in their thermal motion. The carbon atom bonded to three oxygen atoms vibrates with a smaller amplitude parallel to the c axis than in the (001) plane where the amplitude of vibration is the same as for the three oxygens (Table 2). Thus the carbonate group vibrates as a unit in the plane perpendicular to the c axis. The oxygen atoms are less restricted and their vibrations parallel to the *c* axis are bigger than those in the (001) plane. Sass *et al.* (1957) reports a rms displacement for oxygen in $CaCO_3$ of about 0.09 Å parallel to *c* which is in good agreement with the value reported in this investigation. Their two anisotropic displacements in the (001) plane, 0.06 Å and 0.11 Å, respectively parallel and perpendicular to the *a* axis, bracket the value of 0.086 Å of Table 2.

ACKNOWLEDGMENTS

The writers wish to express their appreciation to Dr. A. S. Ginzbarg and Miss E. E. Allen who wrote the programs for the three-dimensional Fourier and least-squares computations and to Dr. R. A. Rowland for his critical reading of the manuscript.

REFERENCES

Bradley, W. F., Burst, J. F., and Graf, D. I. (1953), Crystal Chemistry and Differential Thermal Effects of Dolomite: *Amer. Mineral.*, **38,** 207.

Sass, R. L., Vidale, R., and Donohue, J. (1957), Interatomic Distances and Thermal Anisotropy in Sodium Nitrate and Calcite: *Acta Cryst.*, **10,** 567.

Wyckoff, W. G., and Merwin, H. E. (1924), The Crystal Structure of Dolomite: *Amer. J. Sci.*, **8,** 447.

THE AMERICAN MINERALOGIST, VOL. 44, MAY–JUNE, 1959

OCCURRENCE OF JORDANITE IN THE OTAVI MOUNTAINS, SOUTH WEST AFRICA

N. L. Markham, *Grootfontein, South West Africa*

An interesting occurrence of jordanite ($Pb_{14}As_7S_{24}$?) has recently been found at Kupferberg in the Otavi Mountains of South West Africa. The following brief note describes its mode of occurrence and chemical composition.

The Kupferberg copper prospect lies in the Otavi Valley about 40 miles South West of Grootfontein. Dolomites of the Lower (?) Tsumeb Stage of the Otavi System make up the country rock which is characterised at Kupferberg and elsewhere by widespread and intense calcite replacement. Such calcite may be fine-grained, in which case the original grain size and texture of the dolomite is largely preserved, or coarsely-crystalline with cleavage rhombohedrons up to several centimetres in dimension. Sulphide mineralisation is restricted to the coarse-grained variety of calcite.

Description

Primary sulfide minerals at Kupferberg include sphalerite, tennantite, pyrite, galena, enargite and jordanite with but trace amounts of chalcopyrite, bornite and digenite. Chalcocite and covellite are present as secondary sulfides. The associated minerals are malachite, conichalcite, duftite, mottramite, descloizite, dioptase, plancheite, smithsonite and cerussite. The mineralisation has many similarities to that of the nearby Tsumeb Mine, the sulfide ores being characterised by an abundance of arsenic.

Jordanite itself occurs in irregular masses up to 1 cm. in width, intimately associated with other sulphide minerals. It shows no trace of crystal form. Polished section study reveals three prominent mineral assemblages

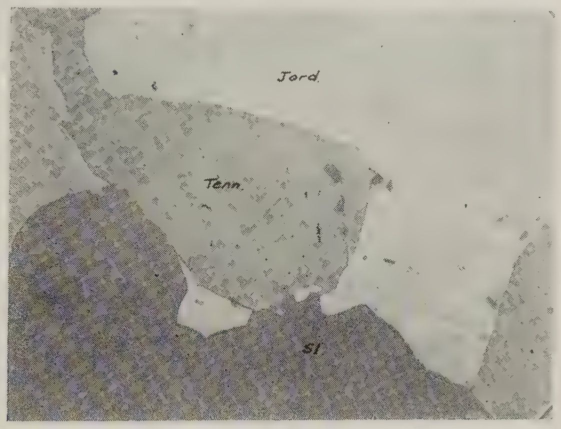

FIG. 1. The assemblage jordanite-tennantite-sphalerite. ×80.

1. Jordanite-tennantite-sphalerite.
2. Jordanite-galena-tennantite.
3. Jordanite-galena-enargite.

Pyrite may accompany these three assemblages, though many of the pyrite crystals are seen to have suffered partial replacement by tennantite and jordanite. Assemblage 1 is perhaps the most commonly observed. The three minerals show quite broad textural outlines (Fig. 1) and no evidence of replacement or the development of fine-grained intergrowths has been observed. Assemblage 2 is similar and between jordanite and galena there is again a broad textural contact (Fig. 2). Assemblage 3 is characterised by narrow veinlets of galena, frequently accompanied by enargite, that intersect masses of jordanite. The textural

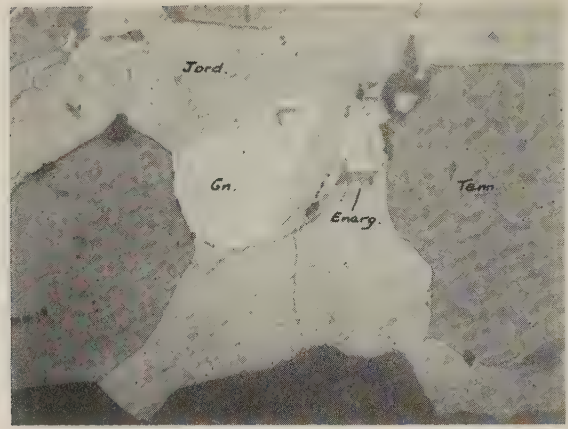

FIG. 2. The assemblage jordanite-galena-tennantite with veinlet of enargite. ×80.

evidence suggests later replacement of jordanite by galena and enargite. A similar texture may be observed in neighbouring tennantite grains wherein cross-cutting enargite veinlets are present. The optical properties of Kupferberg jordanite are in full agreement with those listed by Ramdohr (1955).

CHEMICAL COMPOSITION

A sample of jordanite was carefully hand-picked from crushed ore fragments and submitted for analysis. The results are as follows:

Pb	=68.34%
As	=12.75%
Sb	= 0.02%
S	=18.47%
Total	99.58%

Analysts: Gold Fields Laboratories, Johannesburg.

The remainder, determined spectrographically, includes Fe (0.05%) Cu (0.04%), Ag (0.007%), Mn (0.002%) and Al (0.002%).

The results indicate that Kupferberg jordanite is essentially antimony-free, its composition agreeing closely with that of jordanite from the Binnental, Valais, Switzerland (Palache, Berman and Frondel, 1944).

X-RAY DATA

Powder photographs of Kupferberg jordanite have been taken using Co Kα radiation. The *d*-spacings and line intensities agree fairly well with those listed by Douglass, Murphy and Pabst (1954) for jordanite from Wiesloch, Baden. Spacings and intensities of the strongest lines are 2.23 (10), 1.822 (8), 3.17 (7), 2.98 (7) and 2.10 (6).

ADDITIONAL LOCALITIES

Jordanite has also been noted in sphalerite-rich sulphide ores from the nearby Abenab West and Berg Aukas Mines but it is of rare occurrence and only visible microscopically. The mineral association is again with galena, tennantite, sphalerite and enargite.

ACKNOWLEDGMENT

The author is indebted to the Management of The South West Africa Company for permission to publish this note.

REFERENCES

Douglass, R. M., Murphy, M. J., and Pabst, A. (1954), Geocronite. *Am. Mineral.*, **39**, 908–928.

Palache, C., Berman, H., and Frondel, C. (1944), The System of Mineralogy. Seventh Edition, Vol. 1, Wiley & Sons, New York.

Ramdohr, P. (1955), Die Erzmineralien und ihre Verwachsungen. Akademie Verlag, Berlin.

THE AMERICAN MINERALOGIST, VOL 44, MAY-JUNE, 1959

THE PYRITE-MARCASITE RELATION—A BELATED COMMENT

A. Pabst, *University of California, Berkeley 4, Calif.*

Twenty five years ago M. J. Buerger (1934) wrote:—"The control of the precipitation of pyrite and marcasite by chemical environment suggests that these two minerals are not a dimorphous pair in the usual sense of the term, but rather that they are chemically distinct compounds. A critical study of all available analyses indicates that pyrite corresponds closely to an ideal FeS_2, but that marcasite is definitely sulfur-low." This statement was recently quoted by Kopp and Kerr (1958) without comment.

Buerger tabulated 20 analyses of pyrite and 8 of marcasite. After critical consideration there remained 7 superior analyses of pyrite and 4 of marcasite. The S/Fe ratios for these are plotted in Fig. 1A in a fashion similar to that of Buerger. He concluded that these figures indicate that marcasite is "definitely sulfur-low." Considering the density of marcasite, Buerger decided that the departure from a simple S/Fe ratio is due to "proxy solution" and that the composition is best expressed by $Fe(Fe_x, S_{2-x})$, where x is a small fraction in the neighborhood of .004. This value of x corresponds to an S/Fe ratio of 1.988. Buerger gives this as 1.985 "or thereabouts." Hiller and Probsthain (1956) give it as 1.885 (probably a misprint for 1.985) and consider this to be "within the range of homogeneity of pyrite."

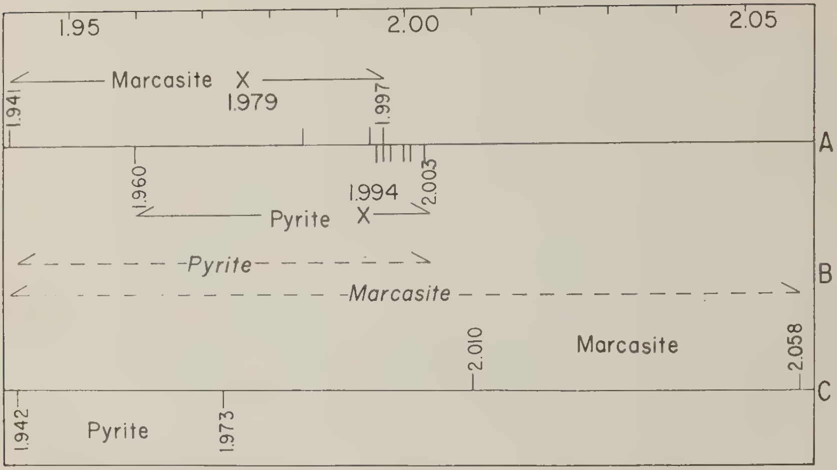

FIG. 1. Scale at top is for S/Fe ratios.

A. Ratios of Buerger's (1934) superior analyses. Ranges and means for marcasite and pyrite shown by arrows and crosses.

B. Dashed arrows show total ranges of S/Fe for marcasite and pyrite, including all analyses plotted along A and C.

C. Analyses reported by Edwards and Baker (1951).

Along both A and C marks above line are for marcasite analyses and those below line for pyrite analyses.

Buerger (1934, p. 53) stated that "One may conclude, therefore, that not only does the statistical study of the pyrite and marcasite analyses give practically unanimous support to a higher iron:sulfur ratio in marcasite than in pyrite, but that the most carefully made individual determinations, using identical methods on both minerals, bear out the same thesis," but did not explain the nature of the "statistical study." The data used by Buerger are a bit scanty for the application of statistical tests and this in itself should lead one to regard the conclusion with caution. However, to test whether the data used by Buerger and represented in Fig. 1A are adequate to support a conclusion as to systematic differences in pyrite and marcasite composition it is necessary to consider the significance of the difference of two means which are based on known data. The following test for significance was suggested to me by Dr. W. C. Krumbein in 1940.

The S/Fe ratios used by Buerger are listed below together with the mean values and the standard deviations, σ_P and σ_M, for the two sets of figures:

Pyrite S/Fe		Marcasite S/Fe	
2.000		1.995	
2.001	mean		mean

1.960	1.994	1.985	1.979
1.998			
1.997	σ_P	1.941	σ_M
1.996	0.0138		0.0226.
2.003		1.997	

The standard error of the difference between two means, σ_D, is given by the relation

$$\sigma_D = \sqrt{\frac{\sigma_1^2}{N_1} + \frac{\sigma_2^2}{N_2}}$$

(Arkin and Colton, 1939, p. 121) where σ_1 is the standard deviation of the first sample, σ_2 that of the second, N_1 the number of items in the first sample and N_2 the number in the second. Substituting one obtains:

$$\sigma_D = \sqrt{\frac{(0.0138)^2}{7} + \frac{(0.0226)^2}{4}} = 0.0126.$$

It is commonly stated that differences as much as $3\sigma_D$ may arise due to the accidents of sampling. In this case the actual difference of the means, 0.015, is 1.19 times the standard error of the difference. Formally this corresponds to about a 23% probability that the observed difference of the means is accidental (Arkin and Colton, 1939, p. 118), but such a statement is hardly meaningful when the omission of just one of the marcasite analyses would reduce the difference in the means to one sixth of the value being tested.

Edwards and Baker (1951) have published analyses of two pyrites from marine clays and of two marcasites from coal seams in Victoria, Australia, representing slightly alkaline and slightly acid environments respectively. The S/Fe ratios of the pyrites are 1.974 and 1.942 and those of the marcasites 2.058 and 2.010 (see Fig. 1C). Edwards and Baker (1951, pages 35 and 42) emphasize these differences but make no reference to Buerger's conclusions according to which one would have expected another result. If these analyses are included with those chosen by Buerger the following results are obtained:

	Pyrite		Marcasite
mean S/Fe	1.986		1.998
σ	0.021		0.044
difference of the means		0.012	
σ_D		0.019.	

The probability that the observed difference of the means arises by chance is over 50 per cent (see Fig. 1B).

No opinion is offered as to a possible connection of compositional variations with stability of marcasite and pyrite, but calculations based on the analyses used by Buerger suggest that the statistical basis for his conclusion was slim. If the analyses published by Edwards and Baker are included, indications are that the differences in the calculated means of the S/Fe ratios in pyrite and in marcasite arise from the accidents of sampling and analysis.

REFERENCES

ARKIN, HERBERT, AND COLTON, RAYMOND R. (1939), An Outline of Statistical Methods. 4th ed., 224 pages, Barnes and Noble, New York.

BUERGER, M. J. (1934), The pyrite-marcasite relation. *Am. Mineral.*, **19,** 37–61.

EDWARDS, A. B., AND BAKER, G. (1951), Some occurrences of supergene iron sulphides in relation to their environments of deposition. *Journ. of Sed. Pet.*, **21,** 34–46.

HILLER, J. E., AND PROBSTHAIN, K. (1956), Differentialthermoanalyse von Sulfidmineralien. *Geologie*, **5,** 607–616.

KOPP, OTTO C., AND KERR, PAUL F. (1958), Differential thermal analysis of pyrite and marcasite. *Am. Mineral.*, **43,** 1079–1097.

Dr. Leonard James Spencer, ScD., F.R.S., Foreign Secretary of the Mineralogical Society, and for many years editor of the Mineralogical Magazine, died on April 14, 1959.

SYMPOSIUM ON GEOCHEMISTRY

A symposium on geochemistry organized by the Commission on Geochemistry of the International Union of Pure and Applied Chemistry, will be held in Göttingen, Germany, on August 21st and 22nd, 1959, to be followed by two days' field excursions. The topics for discussion at the Symposium are:

1. Stable nuclides in Geochemistry
2. Long lived radionuclides in natural systems
3. Geochemistry of the halogens
4. Geochemical aspects of life on earth.

Introductory lectures will be held as follows: for 1) Rankama, 2) Harrison Brown, 3) Correns, 4) Oparin and Urey, who will extend invitations for further contributions.

The excursions will comprise a day's visit to the Harz and another one to the Zechstein salt deposits along the Werra.

The local chairman of the Symposium is Professor C. W. Correns, Sedimentpetrographisches Institut, Göttingen, Lotzestrasse 13.

WHEATLEY MINERAL COLLECTION

Union College, Schenectady, N. Y., recently observed the 100th anniversary of the gift of the Wheatley Collection of 7000 mineral specimens. This ranks as one of the best small college collections in the country, and contains many specimens which are no longer obtainable. Courses in mineralogy were taught at Union College as early as 1820.

ERRATUM

In the article of Sassolite in the November–December issue of *The American Mineralogist* (page 1068), the senior author was George I. Smith, and not George L. Smith, as printed. The same error occurred in the annual index.

FIFTY-PLUS COMMITTEE

The M.S.A. Fifty-plus Committee has been formed to enable members and friends of our society to help build up our endowment fund by making a pledge to this cause of not less than $10 a year for five years. Prior to this time our society had received but one gift for its endowment fund, that of $45,000 by Colonel Washington A. Roebling in 1926. Through the efforts of some 20 volunteers about 200 members of our society were canvassed; their responses were so favorable that an advertisement of this committee appeared in the March–April number of the *Journal.* Opportunity to join this committee will be held open for the remainder of this year. As of May 27 we have $10,735 from 134 pledges. The members of the committee now include the following:

Philip H. Abelson
John W. Adams
Harold L. Alling
Charles S. Bacon
Mark C. Bandy
Paul B. Barton, Jr.
Carl W. Beck
Joseph Berman
James E. Bever
Francis R. Boyd, Jr.
William F. Bradley
John S. Brown
Arthur F. Buddington
Newton W. Buerger
Bennett F. Buie
Eugene N. Cameron
Charles D. Campbell
Ralph S. Cannon, Jr.
Ralph P. Cargille
Dorothy Carroll
Charles W. Chesterman
Alfred H. Chidester
Stephen E. Clabaugh
Frank Cuttitta
Gabrielle Donnay
Joseph D. H. Donnay
James W. Earley
Edwin B. Eckel
Wilhelm Eitel
R. B. Ellestad
Richard C. Emmons
Albert E. J. Engel
Edwin S. Erickson, Jr.
Joseph J. Fahey
Harold W. Fairbairn
George T. Faust
Russell Filer
D. Jerome Fisher
Margaret D. Foster
Wilfrid R. Foster
Clifford Frondel
Richard E. Fuller
Frederick W. Galbraith
A. M. Gaudin
Joseph L. Gillson
Jewell J. Glass
Samuel S. Goldich
Julian R. Goldsmith
Oliver R. Grawe
Robert S. Green
Robert M. Grogan
John W. Gruner
James K. Grunig
John C. Haff
Michel T. Halbouty
Edward P. Henderson
Harold D. Hess
Harry H. Hess
Donnel F. Hewett
Ralph J. Holmes
Marjorie Hooker
Arthur L. Howland
Walter F. Hunt
Cornelius S. Hurlbut, Jr.
C. Osborne Hutton
Herbert Insley
John B. Jago
Richard H. Jahns
Albert J. Kauffman
Walter D. Keller
George C. Kennedy
Paul F. Kerr
Adolph Knopf
Charles Koebel
Edward H. Kraus
Esper S. Larsen, Jr.
Esper S. Larsen, 3d
Benjamin F. Leonard
Alfred A. Levinson
John B. Lyons
Brian H. Mason
Duncan McConnell
Clifford A. Merritt
Robert Meyrowitz
Richard C. Mielenz
Harry M. Mikami
Charles Milton
Berlen C. Moneymaker
Arthur Montgomery
Kiguma J. Murata
Howard K. Nason
George J. Neuerburg
James A. Noble
E. F. Osborn
Adolf Pabst
Lincoln R. Page
Frederick H. Pough
Lewis S. Ramsdell
Laura Reichen
Edwin W. Roedder
Richards A. Rowland
Joseph J. Runner
Edward Sampson
E. L. Sampter
Waldemar T. Schaller
Robert G. Schmidt
Harrison A. Schmitt
Schortmann's Minerals
Marie Siegrist
Chester B. Slawson
Joseph V. Smith
Sprague and Henwood
Lloyd W. Staples
Thomas W. Stern
David B. Stewart
Duncan Stewart, Jr.
Richard E. Stoiber
Robert L. Stone
Bronson Stringham
Ming-Shan Sun
Stephen Taber
Carl Toman
George Tunell

O. Frank Tuttle
Angelina Vlisidis
William A. Waldschmidt
Charles E. Weaver
Robert W. Webb
Alice D. Weeks
E. Joseph Weiss
Edgar T. Wherry
Horace Winchell
Alfred O. Woodford
Theodore O. Yntema

BOOK REVIEW

ELEMENTARY MATRIX ALGEBRA, by Franz E. Hohn. The Macmillan Co., New York, 1958, xi+305 pp., 6×9½ in. Price $7.50.

The methods of matrix algebra furnish a convenient and practical scheme for the rapid calculation, by desk computer or high-speed digital computer, of many quantities of interest in crystallography, of both the classical and modern varieties. The excellent papers of W. L. Bond (1946, 1948), and H. T. Evans, Jr. (1948) amply demonstrate the simplicity and power of matrix methods in this regard.

The book under review was developed for students of the junior, senior, and graduate levels "whose interests have included such diverse subjects as aeronautical engineering, agricultural economics, chemistry, econometrics, education, electrical engineering, high speed computation, mechanical engineering, metallurgy, physics, psychology, sociology, statistics, and pure mathematics." It does not treat crystallographic topics explicitly, but should be very useful to crystallographers, among others, as an introductory text or as a reference book.

A good idea of the topics treated in the book is gained from the chapter and appendix headings which are:

Chapter I. Introduction to Matrix Algebra (25 pp.)
II. Determinants (39 pp.)
III. The Inverse of a Matrix (23 pp.)
IV. Rank and Equivalence (23 pp.)
V. Linear Equations and Linear Dependence (39 pp.)
VI. Vector Spaces and Linear Transformations (40 pp.)
VII. Unitary and Orthogonal Transformations (18 pp.)
VIII. The Characteristic Equation of a Matrix (26 pp.)
IX. Bilinear, Quadratic, and Hermitian Forms (37 pp.)

Appendix I. The Notations Σ and Π (11 pp.)
II. The Algebra of Complex Numbers (6 pp.)
III. The General Concept of Isomorphism (3 pp.)

A very useful feature of this book is a selective bibliography of seven pages listing books on vector spaces, matrices, determinants, and their applications. A large number of exercises is included. The physical makeup of the book is excellent; in particular, the choice of type face amply meets the involved requirements for readable mathematical text.

References

Bond, W. L. (1946), Computation of interfacial angles, interzonal angles, and clinographic projection by matrix methods: *Am. Mineral.*, **31,** 31.

Bond, W. L. (1948), Transformation of axes: *Am. Mineral.*, **33,** 703.

Evans, H. T., Jr. (1948), Relations among crystallographic elements: *Am. Mineral.*, **33,** 60.

C. L. Christ
U. S. Geological Survey
Washington 25, D. C.

NEW MINERAL NAMES

Bilibinite

E. Z. Bur'yanova. A new hydrous uranium silicate—bilibinite. *Zapiski Vses. Mineralog. Obshch.*, v. **87**, No. 6, 667–674 (in Russian).

Analysis by E. A. Isaeva of material selected under the binoculars gave soluble silica 14.80, UO_2 5.07, UO_3 45.89, ThO_2 1.48, rare earth oxides 3.19, CaO 1.70, BaO 0.25, PbO 3.60, H_2O^+ 3.23, H_2O^- 4.90, insol. (quartz and feldspar) 16.33, sum 100.44%, corresponding to the formula

$$3(\mathrm{Ca, Pb, TR})\mathrm{O}\cdot(\mathrm{U, Th})\mathrm{O_2}\cdot 7\mathrm{UO_3}\cdot 10\mathrm{SiO_2}\cdot 19\mathrm{H_2O}.$$

Spectrographic analysis by L. I. Denisenko showed also Al 0.1–0.03, Mg less than 0.003, Fe and Mn about 0.001, Ti 0.01–0.001, V 0.01–0.1%.

The mineral is black, streak gray, opaque, but translucent bottle-green on thin edges. Isotropic with n above 1.782, less than 1.820. Shows transitions to greenish-brown, brown, and amber-yellow isotropic material with n lower, down to 1.683 for amber-yellow. Decomposed by HCl or HNO_3 with separation of gelatinous silica. Infusible. Sp. gr. of impure material 3.5.

Bilibinite is amorphous to x-rays. Material heated at 980° gives a sharp x-ray pattern of U_3O_8. A D.T.A. curve shows a large endothermal break at 80–160° and a very small endothermal break at 550–600°.

The mineral is considered to be the amorphous analogue of the crystalline mineral coffinite and the U analogue of thorogummite. It occurs as a cement in sandstones, associated with the secondary U minerals kasolite, β-uranotile, sklodowskite, autunite, and uranocircite. No locality is given, as usual.

The name is for Yu. A. Bilibin, Russian geologist.

Discussion.—Data insufficient to prove homogeneity.

Michael Fleischer

Mangan-uralite

Sripadrao Kalpady and A. S. Dave. On mangan-uralite from Ponia, Balaghat District, Madhya Pradesh. *J. Univ. Geol. Soc. Nagpur,* **1,** 4–7 (1955–56) (Published 1958).

The name mangan-uralite is given to a pink amphibole formed by the alteration of the manganese pyroxene blanfordite in a pegmatite containing microcline, albite, and apatite. Analysis by A. S. D. gave SiO_2 55.35, Al_2O_3 3.52, Fe_2O_3 12.21, MgO 14.54, MnO 3.08, CaO 2.17, Na_2O 7.44, K_2O trace, H_2O 2.90, total 101.21% (given as 99.85%). (Nothing is said as to whether FeO was determined. M.F.) This gives the formula

$$\mathrm{Na_{1.92}(Ca_{0.31}Mn_{0.35}Mg_{2.93}Fe_{1.24}Al_{0.08})(Si_{7.53}Al_{0.47})O_{22}(OH)_2}.$$

The mineral occurs as radiating aggregates of needles and fibers projecting out from embayed proxene. Monoclinic, cleavage prismatic, color pink to pinkish violet (?), pale pink in thin-section. Optically negative, α 1.65–1.66, β 1.66–1.67, γ 1.66–1.67, 2 V large, birefringence variable, $=0.014$. Pleochroic, X light pink, Y pale brown to yellow, Z faint blue; absorption $X>Y=Z$.

Discussion.—An unnecessary name. The composition is close to that of a manganoan magnesioarfvedsonite in the classification of Miyashiro (see *Am. Mineral.*, **43,** 797–798 (1958)). The name is also somewhat inappropriate, because uralite is generally understood to be an amphibole of the actinolite group, low in alkali, that has been formed from pyroxene. The described transformation of the pyroxene blandfordite to this amphibole is somewhat surprising in the chemical changes involved; analysis of the blandfordite shows a composition close to that of the amphibole except for Fe_2O_3 18.29, CaO 8.41, MgO 4.74, which implies a large loss of Fe and Ca and a large gain in Mg.

M. F.

AMERICAN MINERALOGIST

Price Information

Back issues of the AMERICAN MINERALOGIST can be purchased at the prices given below, but certain issues as listed are available only in microtext edition. The microtext edition is on 3 x 5 inch cards, each card containing 48 pages of text material, with a heading in regular type to indicate the volume, number, pages and date. Microtext will be furnished on all orders where necessary, unless specific instructions are received to the contrary. Prices apply to both the regular and microtext editions, and postage is charged except on indexes. Agents and dealers are allowed the usual 10% discount on orders. Subscriptions for the current volume (calendar year) are available to libraries, colleges, and other organizations at $6.00, postpaid. Individuals can receive the current volume by becoming members of the Mineralogical Society of America.

Volume	Year	Price per volume	Price per issue (except special issues)
1-9	1916-1924	$3.00	$ .50
10-19	1925-1934	4.00	.50
20-28	1935-1943	6.00	.80 (monthly issue)
29-42	1944-1957	6.00	1.60 (bimonthly issue)

Microtext Edition

Vol.	No.	Year
1-5	Complete	1916-1920
7	2	1922
9	3	1924
10	3	1925
11	3	1926
25	5	1940
26	1-3, 6-9, 12	1941
27	1-12	1942
28	1-8	1943
29	1-8	1944
30	1-4, 7-8	1945
31	1-4	1946
32	1-4	1947

Special Issues

Year	Issue	Vol.	No.	Price
1925	Michigan	10	9	$1.00
1925	Harvard	10	11	1.00
1927	Harvard	12	4	1.00
1928	Harvard	13	7	1.00
1930	Harvard	15	8	1.00
1932	Harvard	17	7	1.00
1937	Palache	22	7	3.00
1938	Harvard	23	11	1.50
1945	Quartz Symposium	30	5-6	$3.00
1950	Larsen	35	9-10	2.50
1953	Hunt	38	1-2	2.00
1953	Ross-Schaller	38	11-12	3.00
1955	Kraus	40	11-12	2.00
1957	Harvard	42	11-12	2.00

Indexes

Vols. 1-20 (1916-1935) $2.00; $1.00 to members; postpaid
21-30 (1936-1945) 3.00; 2.00 to members; postpaid
31-40 (1946-1955) 5.00; 3.00 to members; postpaid

Send all orders to

MINERALOGICAL SOCIETY OF AMERICA
Marjorie Hooker, Treasurer
c/o U. S. Geological Survey, Washington 25, D.C.

RECENT ACQUISITIONS IN BULK MINERALS AND ROCKS

These are just a few of the many new items that we have acquired in recent months in order to better serve the growing demand for the best in bulk minerals and rocks for teaching, laboratory instruction or research work. (For the complete listing to supplement catalog 583, write for "Ward's Mineral Department Specimen Specials"—Spring 1959)

	Price per lb.
Analcime. Calif. Small xls in rock	$1.50
Ancylite. Montana. Crystalline	4.20
Atacamite. Australia. Crystalline	4.20
Cancrinite. Ontario. Crystalline pink	1.50
Cancrinite. Maine. Yellow in syenite	3.00
Cassiterite. Wash. Massive in andalusite	1.20
Corundum. Transvaal. Massive, nearly pure	1.00
Cryolite. Greenland. Pure white masses	1.80
Dumortierite. Nevada. Lilac colored masses	.60
Gadolinite. Norway. Black massive in feldspar	8.50
Garnet. (Andradite). Ariz. Greenish crystallized	2.50
Helvite. N.M. Yellow-brown in rock	3.50
Hemimorphite. Penna. Brown xline	3.50
Idocrase. (Vesuvianite). Me. Brown xline	1.50
Illite. N.Y. Shale containing 85% illite	1.00
Petalite. Rhodesia. White cleavable	1.00
Pyroxene. (Hedenbergite). Mont. Green xline	1.20
Rutile. Norway or Mexico. Nearly pure, red brown	7.00
Basalt. Lintz, Germany. Dense, black, some olivine aggregates	.70
Chert breccia. Okla. Gray chert in dark matrix	.70
Graywacke. Ontario. Dark colored	.70

REFERENCE CLAY MINERALS

An excellent suite of reference samples of important clays which can serve for purposes of comparison in the general field of clay mineralogy. Included in the suite are: halloysite, kaolinite, dickite, montmorillonite, metabentonite, illite and pyrophyllite.

Write for GN 15.

All prices are list at Rochester, N.Y.

WARD'S *NATURAL SCIENCE ESTABLISHMENT, INC.*
P.O. BOX 1712 ROCHESTER 3, N.Y.

GEORGE BANTA COMPANY, INC., MENASHA, WISCONSIN, U.S.A.